Université Catholique de Louvain
Secteur des Sciences de la Santé
Louvain Drug Research Institute

MECHANISMS OF RETENTION OF PEGYLATED RECOMBINANT HUMAN DEOXYRIBONUCLEASE I (rhDNASE) IN THE LUNGS

Sohaib Mahri

Thesis presented in fulfilment of the requirements for the degree of
Doctor of Philosophy in Biomedical and Pharmaceutical Sciences

2020

Directors: Professor Rita Vanbever
Dr Cynthia Bosquillon

Acknowledgements

This work could not have been accomplished without the support of numerous people, both at scientific and personal levels throughout my PhD journey and earlier studies leading up to this achievement. I want to thank all of them and apologise if I have forgotten some.

I first thank Rita Vanbever and Cynthia Bosquillon for initiating and managing this project smoothly and efficiently. Rita has given me her undivided attention and has been generous with time and thoughts. I have always appreciated her deep insights, patience, and excellent management. Cynthia has introduced me to a different research environment at the University of Nottingham. Cynthia is a keen observer, thorough, agreeable, and always cheerful. Both Rita and Cynthia are talented scientists who exude kindness and confidence. They have given me trust and independence and prevented me from succumbing to the wrong conclusions. I am glad to have worked with people of such a high calibre, clear visions, and ambitious goals. I hope they succeeded in harnessing my potentials.

When I come first to the pulmonary lab, I was introduced to the work related to my PhD by Marie-Julie and Cécile, both amicable colleagues from whom I learnt a lot. I thank Bernard, Kevin, and Nathalie, for being always available and for being the glue of the social life and the reservoir of lab collective skills. They have never failed to have a hint on how things can be done. Thank you very much, Murielle, for being kind, diligent, and reliable. You are a true saviour.

I appreciate the very valuable contribution of Eléonore Hardy. I could not have progressed this far without the data she managed to put together. I am particularly grateful to Xiao for the great spirit and skills she brought to our team, and for all the pleasant moments we spent together. Thank you Tobias, for making work easier and more productive, Wilfried *mon pote*, and Soumaya. Thank you, Jessica, Yuan, and Aurélie for being so friendly and for sharing lots of fun and work tips. You are all unique, and together, we shared wonderful times as members of the *PEGylators* family.

A big thank you to the ADDB heads, Véronique Préat, Anne des Rieux, and Anna Beloqui for cultivating a warm and productive environment and for devoting extra efforts to make the ADDB the fantastic team it is.

I am grateful to members of the steering committee, Professors Bernard Gallez, Sophie Gohy, and Snow Stolnik for the friendly discussions, constructive feedback, and ample advice. You shed light on my blind spots and helped me see beyond the technicalities of the experiments. I am thankful to Professors Otmar Schmid and Koen Raemdonck for accepting to assess my work and to challenge it for the best.

I appreciate the help of Herlinde De Keersmaecker, Kevin Braeckmans, and Stefaan de Smedt from Ghent University for offering their expertise and platform. I also thank Donatienne Tyteca, Patrick Van Der Smissen, Nicolas Dauguet, and Nicolas Joudiou for providing tips and training.
Thanks to Nikos, Thibaut, Alessandra, Mengnan, Pallavi, Laure, and Yining for being real-life examples of how consistent work and focus pay off. I thank very much Chiara, Valentina, Dario, Gaëlle, Cristina, Fabienne, Luc, John, Neha, Kifah, Yoann, Carmen, Yasmine, Ariane, Viridiane, Aristote, Mathilde, Elia, Mingchao, Philippe, Jérôme, Floriane, Ilaria, Cecilia, Raquel, Laura, Mandeep, Hafiz, and others from the LDRI institute for all the good time we have had together and for sharing the ups and downs of research and life in general inside and outside the lab.
My life in Nottingham turned out to be enjoyable in the presence of Thata, Bhanu, Abdolelah, Waleed, and Mohamed. I thank you for being wonderful, selfless, and excellent ambassadors of your respective cultures and cuisines. Thank you Awaji, Safar, Fatou, Olu, Rachael, Claudia, Mohamed, Rayan, Dana, Akmal, Litty, Valentina, Esmé, Steph, Lucy, Paul, Amy, and Emanuele. Many thanks to NanoFar students, especially Natalija, Audrey, Mohamed, Ulung, Mathie, Janske, Raneem, Shabnam, and Paul.
I am indebted to NanoFar program and to Frank Boury and Marion Toucheteau for keeping an impeccable organisation of the program and to Sandrine Wollanders for managing the doctorate school at the UCLouvain. I am grateful to the "Bourse de Patrimoine" for the complementary scholarship that gave an extra breath. I do not forget to thank the EMMC-ChIR program which allowed me to go abroad and fulfil my academic dreams. Special thanks to my former mentors Azzouz, Alamir, Mona, David, and Helinor.
I am immensely thankful to Lama, my soulmate for sharing every moment of my journey with all its ebbs and flows, anguish and joy. You could not have been more supportive.
I am eternally grateful to my parents Louiza and Rabah for the unfailing faith and love, and I am blessed for having wonderful sisters Nouha, Soumia, Chafika, and Nada and amazing brothers Mohammed and Selmane. You have always been there for me despite the distance. I know how much this meant for you, and I am proud of you as much as you are proud of me. I know that you all have big dreams and I am excited to see them come true. Soumia, I want to see you a doctor next, you are up to the challenge. Special thanks to Nouha, my younger sister and the joy of our family; it has been my delight to see you flourish and excel.

To Louiza and Rabah, to whom I owe everything I have achieved and will.

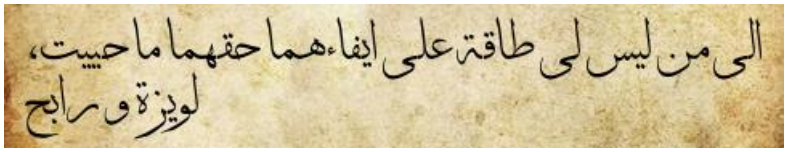

ABBREVIATIONS

AAT	Alpha-1-antitrypsin
AM	Alveolar macrophage
APC	Antigen-presenting cell
ARDS	Acute respiratory distress syndrome
AUC	Area under the curve
BAL	Bronchoalveolar lavage
BALT	Bronchus associated lymphoid tissue
BSA	Bovine serum albumin
CF	Cystic fibrosis
COPD	Chronic obstructive pulmonary disease
DC	Dendritic cell
DMEM	Dulbecco's Modified Eagle Medium
DOL	Degree of labelling
DPBS	Dulbecco's phosphate-buffered saline
DPIs	Dry powder inhalers
EPO	Erythropoietin
FcRn	Neonatal Fc receptor
FDA	Food and Drug Administration
GI	Gastrointestinal
HBSS	Hank's Balanced Salt Solution
HEPES	4-(2hydroxyethyl)-1-piperazineethanesulfonic acid
hGH	Human growth hormones
HRP	Horseradish peroxidase
IM	Intramuscular
IPF	Idiopathic pulmonary fibrosis
IV	Intravenous
LDH	Lactate dehydrogenase
mAb	Monoclonal antibody
MG	Methyl green
MW	Molecular weight
NIR	Near-infrared
NIRF	Near-infrared fluorescence

OD	Optical density
PBA	DPBS with 1% BSA
PBS	Phosphate buffer saline
PCL	Periciliary liquid
PEG	Polyethylene glycol
PEG20	Linear 20 kDa polyethylene glycol
PEG30	Linear 30 kDa polyethylene glycol
PEG40	Two-armed 40 kDa polyethylene glycol
pI	Isoelectric point
PK	Pharmacokinetics
pMDI	Pressurised metered-dose inhaler
PTH	Parathyroid hormone
rhDNase	Recombinant human deoxyribonuclease I
ROI	Region of interest
SC	Subcutaneous
SDS-PAGE	Sodium dodecyl sulfate polyacrylamide gel electrophoresis
SEC	Size exclusion chromatography
SEM	Standard error of the mean
TEER	Transepithelial electrical resistance
VIP	Vasoactive intestinal peptide
VT750	VivoTag-S ® 750 dye

Conjugation to high molecular weight (MW) polyethylene glycol (PEG) was previously shown to prolong the lung residence time of recombinant human deoxyribonuclease I (rhDNase) and improve its therapeutic efficacy following pulmonary delivery in mice. In this thesis, we investigated the mechanisms of the extended retention of rhDNase conjugates to linear 20 kDa, linear 30 kDa, and branched 40 kDa PEGs *in vivo* and *in vitro*. *In vivo* fluorescence imaging revealed that PEG30 kDa-conjugated rhDNase (PEG30-rhDNase) was retained in mouse lungs for a significantly longer period of time than native rhDNase (12 days vs 5 days). Confocal microscopy confirmed the presence of PEGylated rhDNase in lung airspaces for at least 7 days. In contrast, the unconjugated rhDNase was cleared from the lung lumina within 24 hours and was only found in the lung parenchyma and alveolar macrophages thereafter. Systemic absorption *in vivo* in mice and *in vitro* across monolayers of Calu-3 cells cultured at air-liquid interface was shown to be significantly lower for PEG30-rhDNase compared with rhDNase. The absorption was accompanied by the local degradation of both proteins; however, it was more extensive for rhDNase. Further degradation of both proteins occurred after absorption likely in the blood and/or liver and was followed by renal excretion. PEGylation decreased the uptake of rhDNase by macrophages *in vitro* whatever the PEG size as well as *in vivo* 4 h following intratracheal instillation. The reverse was observed *in vivo* at 24 h. The uptake of rhDNase by macrophages was saturable and dependent on energy, time, and concentration which is indicative of adsorptive endocytosis. Mucociliary clearance equally contributed to the clearance of native and PEGylated rhDNase from the lungs, suggesting that the mucociliary clearance might not be the main cause for the longer retention of PEGylated rhDNase. Moreover, the diffusion of PEGylated rhDNase in porcine tracheal mucus and cystic fibrosis sputa was slower compared with that of rhDNase. Nevertheless, no significant binding of PEGylated rhDNase to both media was observed. Finally, PEGylation did not significantly protect rhDNase against aggregation and loss of activity in contact with the bronchoalveolar lavage fluid. In conclusion, reduction in systemic absorption and macrophage and epithelial cell uptake seemed to play a significant role in the extended retention of PEGylated rhDNase in the lungs. Mucociliary clearance, as well as aggregation in the lungs, were involved in the clearance of both forms of rhDNase, however, unlikely to have a very significant impact on their differential retention in the lungs.

CHAPTER I

INTRODUCTION

TABLE OF CONTENTS

I. DELIVERY OF THERAPEUTIC PROTEINS TO THE LUNGS

Therapeutic proteins represent a large share of biopharmaceuticals, along with peptides, nucleic acids, and cellular therapies [1, 2]. At present, dozens of peptides and proteins are approved for human clinical use by the US Food and Drug Administration (FDA) and many more are at different stages of clinical development [2, 3]. Compared to traditional small drugs, therapeutic proteins are endowed with higher potency and specificity, reduced toxicity, lower organ accumulation and limited interaction with other drugs [3-6]. They are also more versatile as they can be designed to target numerous diseases, be multifunctional, or used as platforms to conjugate or incorporate other drugs [6].

All therapeutic proteins, with a few exceptions, are administered by parenteral routes either by intravenous (IV) infusion or subcutaneously (SC). Nonetheless, increasing efforts to exploit other routes of administration are being deployed. Despite the enormous potential of the pulmonary route, its exploitation is suboptimal at best, especially for the local treatment of lung diseases, which appears to be an easier target [7, 8].

I.1. DEFINITIONS AND SCOPE

There is no consensus on the distinction between "protein" and "peptide". However, the common usage reserves the term "protein" to chains of 51 amino acid or higher with peptide being smaller than this [9]. The organization of secondary structures into 3-dimensional domains elements gives rise to tertiary structure which is reserved to proteins [9]. Human insulin (51 amino acid, 5.8 kDa) for instance, is generally referred to as peptide, but also as protein by some authors [9].

According to their functions, different therapeutic protein categories could be distinguished such as monoclonal antibodies (mAbs), cytokines, enzymes, growth factors, antigens, hormones, fusion proteins, clotting factors, and others [7, 10, 11]. Most of the therapeutic proteins are recombinant and mAbs are the dominant category [1, 2, 11].

The scope of this introduction is limited to proteins larger than insulin (~5.8 kDa), although relevant information about insulin and smaller peptides is presented when deemed pertinent. Proteins of molecular weight (MW) less than 40 kDa are referred to as "small proteins" while the term "large protein" is reserved to proteins of MW 40 kDa or higher. This distinction is approximate and based on the shift in absorption and systemic bioavailability pattern occurring around this MW [12-14].

I.2. PULMONARY DELIVERY OF PROTEINS

Currently, recombinant human deoxyribonuclease I (rhDNase, dornase alfa) is the only protein delivered by inhalation on the market for symptomatic treatment of cystic fibrosis (CF). Likewise, insulin is the only marketed peptide for systemic action by inhalation. Due to the scarcity of approved proteins and peptides by inhalation, the discussion in this section will be limited to the most promising candidates in clinical trials.

I.2.1. *Pulmonary delivery for local therapy*

Inhaled proteins are particularly attractive for the local treatment of respiratory diseases [15]. Local pulmonary delivery allows higher concentrations of the proteins at the target site, allows rapid onset of action, requires smaller doses, and therefore, causing less side effects [16]. It is non-invasive, therefore, more convenient and accessible for ambulatory patients [16, 17].

rhDNase (Pulmozyme®) is a mucolytic agent, it improves the clearance of mucus secretions in patients with CF through cleaving the DNA leading to a reduced viscosity in the lungs [18, 19]. Another protein-containing mixture is the bovine pulmonary surfactant (surfactant proteins SP-B and SP-C, phospholipids, triglycerides, and fatty acids); it is administered by intratracheal instillation for the treatment of acute respiratory distress syndrome (ARDS) [16]. Other proteins are under investigation for the treatment of asthma, chronic obstructive pulmonary disease (COPD), infections, and cancer (Table 1).

Human alpha-1-antitrypsin (ATT, 52 kDa) is the most abundant serine protease inhibitor in the lungs. Its primary role is to neutralise neutrophil elastase and proteinase 3 [20, 21]. Inhaled AAT has potential benefits in patients with AAT deficiency [22, 23]. It entered phase III clinical trial in December 2019 after having proven more convenient to patients with congenital AAT deficiency and showed a three-fold increase of AAT in the lungs by inhalation compared with IV infusion (NCT04204252).

Pitrakinra, an IL-4 mutein which inhibits both IL-4 and IL-13, has shown promising results in the prevention of late-phase asthmatic responses to allergens both subcutaneously and by inhalation [24]. A phase IIb study has identified a subgroup of potential asthmatic responders by genotype [25]. More interest was given to targeting the IL-13 pathway considering its pivotal role in asthma. Pieris and AstraZeneca are developing anticalin PRS-060/AZD1402 (anti-IL4-Rα) for the treatment of moderate to severe asthma that does not respond to conventional therapy [17]. This drug is very stable to nebulisation and dry powder inhalation [26]. Recently completed first-in-

human phase I study has shown favourable results [27]. Inhaled IFN-β was shown to prevent symptom exacerbations during the first week of viral infection in asthmatic subjects [16]. Inhaled IFN- γ was shown to improve the clinical response when combined with standard tuberculosis therapy [16]. It reverses the declining total lung capacity in patients with idiopathic pulmonary fibrosis (IPF); however, no palpable effects were reported for the treatment of CF presumably due to the low delivered doses to the lungs [16, 28]. Inhaled IL-2 could improve the survival and delay the progression of pulmonary metastases in patients with renal cell carcinoma, however, contrary to IV therapy, no durable complete responses were registered [16].

Inhaled antigens

Vaccines are another potential application of therapeutic proteins, as many antigens are proteins in nature [29]. Inhaled vaccines are attractive, especially against infection originating in the airways such as influenza, tuberculosis, and measles [16]. A strong case for the pulmonary delivery of vaccines over parenteral immunisation is the ability to elicit a local mucosal response in the respiratory tract, preventing thus the initial pathogen-host interaction at the port of entry [30]. Beside the serum IgG, local secretory IgAs are not easily obtained by other routes of administration such as SC or intramuscular (IM) particularly for infections originating in the lungs such as influenza and tuberculosis [16]. The high density of antigen-presenting cells (APCs) such as alveolar macrophages (AM), dendritic cells (DCs), and B cells is optimal to elicit appropriate mucosal and systemic immune responses [31]. In the case of influenza, the standard IM vaccines induce only IgG response which is effective against lower respiratory tract infection, however, less effective in preventing the initial infection of the upper airways where antibody induction is absent [32]. Development of inhaled vaccines especially as dry powders is important especially for developing countries as these formulations are more stable during transport and storage and do not require sterility or special health care professionals for administration [32-34]. As an example, inhaled measles virus vaccine was shown to be more effective in humans compared to parenteral immunisation [35-37]. Inhaled influenza vaccine is efficacious in animal studies; however, no data are available for inhaled influenza vaccine in humans [32].

I.2.2. *Pulmonary delivery for systemic therapy*

Pulmonary delivery of proteins for remote systemic action could provide a less invasive alternative to other parenteral routes of administration [38]. Due to the smaller size of peptides, their bioavailability from the lungs is generally higher than that of proteins. The bioavailability of proteins by this route is limited; however, higher than after oral delivery and in some cases, nasal and transdermal delivery [16]. Advantages of pulmonary delivery compared to nasal delivery

include significantly larger surface area for absorption (100 m^2 *vs* 170 cm^2), slower mucociliary clearance, and lower metabolic activity of the pulmonary mucosa [39, 40]. Despite the advantages of the pulmonary route over the nasal route, there are more approved peptides by the latter (e.g. desmopressin, salmon calcitonin, and buserelin). Advantages of nasal over pulmonary delivery includes easier formulation and administration by the nose, more reproducible dosing, and less expensive devices compared with pulmonary delivery. Nasal delivery is also safer and more cost effective.

Satisfactory absorption after pulmonary administration could be achieved for proteins such as human growth hormones (hGH, MW 22 kDa), which had a bioavailability ranging from 5% to 45% in animals studies [16]. The availability of Fc-fusion proteins such as interferon α-Fc, interferon β-Fc, and follicle-stimulating hormone-Fc by inhalation was 20–50% in non-human primates [41, 42]. Even larger proteins such as Erythropoietin-Fc fusion protein (EPO-Fc, MW ~ 112 kDa) was shown to be absorbed in non-human primates and humans after pulmonary delivery through naturally occurring neonatal Fc receptor (FcRn) [41, 43]. Currently, no mAb by inhalation is under development for systemic delivery; this could be explained by their slow absorption, low bioavailability (< 10%), instability to aerosolisation, and the lack of data on their deposition and immunogenicity in the respiratory tract [44, 45].

Table 1.Inhaled proteins in clinical trials for topical treatments. Adapted from [16].

Drug	MW	**Clinical application**	**Clinical status (sponsor)**	**Form**	**Ref /Trial ***
rhDNase AIR DNase™/ Alidornase alfa/ PRX-110 rhDNase	37 kDa	Cystic fibrosis	II, 2017 (Protalix)	Nebulisation	NCT02722122
		ARDS	III, ongoing (University Hospital, Strasbourg, France)		NCT03368092
		ARDS in COVID-19	III, ongoing (Fondation Ophtalmologique Adolphe de Rothschild)		NCT04355364
		Neutrophilic asthma	I/II ongoing (National Jewish Health)		NCT03994380
α1-Antitrypsin (AAT)	52 kDa	AAT deficiency (Emphysema)	III, ongoing (Kamada)	Nebulisation	NCT04204252
			II/III, 2015 (Kamada)		NCT01217671
					NCT00486837
		Cystic fibrosis	II, 2004 (Talecris Biotherap)		[46]
		Lung transplant	I, 2011 (CSL Behring)		NCT01347190
			II, unknown status (Rabin MC)	IV/ Nebulisation	NCT01394835
		SARS-CoV-2	I, ongoing (Ministry of Health, KSA)		NCT04385836
Tissue Plasminogen Activator Alteplase/Activase	70 kDa	Acute Plastic Bronchitis	II, ongoing (Umich)	Nebulisation	NCT02315898
ALX-009 Hypothiocyanite + bovine lactoferrin	lactoferrin 80 kDa	Cystic fibrosis/ Bronchiectasis	I, ongoing (Alaxia SAS)	Nebulisation	NCT02598999
IL-4 mutein (pitrakinra)	15 kDa	Asthma (moderate to severe)	II, 2011 (Aerovance)	Dry powder	NCT00801853
rhGM-CSF (Sargramostim/ Leukine®) Molgramostim	14 kDa	Autoimmune Pulmonary Alveolar Proteinosis	Phase I ongoing (Cincinnati)		NCT03006146
			II/III unknown (IRCCS Policlinico S. Matteo)	Nebulisation	NCT00901511
			II, ongoing (Dai Huaping)		NCT03316651
		Nontuberculous Mycobacterial infections	III, ongoing (Savara Inc)		NCT03482752
			II, ongoing (Savara Inc)		NCT03597347

		ARDS	II, ongoing (University of Giessin)		NCT02595060
CSJ117 anti –human SLP) mAb fragment (Fab)	46 kDa	Asthma	I, 2019 (Novartis Pharmaceuticals)	Nebulisation	NCT03138811
Anti-IL4-Rα (PRS-060 /AZD1402)	18 kDa	Asthma	I, 2019 (AstraZeneca)	Dry powder/Nebulisation	NCT03921268
Recombinant soluble IL-4Rα (anti-IL-4Rα)	-	Asthma (mild to moderate persistent asthma)	II, 2000 (Immunex Corp.) II, 2008 (NIAID)	Nebulisation	NCT00017693 NCT00001909
Recombinant sialidase (DAS181)	46 kDa	Parainfluenza infection/ COVID-19 COVID-19 Influenza/SADRV (including COVID-19)	III, ongoing (Ansun Biopharma) II/III, ongoing (Ansun Biopharma) II, ongoing (Ansun Biopharma)	Nebulisation	NCT03808922 NCT04354389 NCT04298060
IFN-β (SNG001)	22 kDa	Asthma patients Viruses in COPD SARS-CoV-2 Asthma	II, 2012 (Synairgen Res.) II, ongoing (Synairgen Res.) II, ongoing (Synairgen Res.) II, 2016 AstraZeneca	Nebulisation	NCT01126177 [47] NCT03570359 NCT04385095 NCT02491684
IFN-γ	19 kDa	Pulmonary fibrosis	I, 2018 (NY Univ. School of Med)	Nebulisation	NCT00563212
IL-2 (Aldesleukin)	15 kDa	Metastatic cancer	I/II, ongoing (M.D. Anderson Cancer Center)	-	NCT01590069

* ClinicalTrials.gov; TSLP, thymic stromal lymphopoietin; COPD, chronic obstructive pulmonary disease; ARDS, acute respiratory distress syndrome

I.2.3. *Systemic delivery for local lung therapy*

Local respiratory diseases could be treated by parenteral administrations even though the lung availability of proteins by systemic route is minimal [48, 49]. Good examples of this strategy are mAbs for the treatment of severe asthma. A few drugs are already in the market such as Omalizumab (an anti-IgE), mepolizumab, reslizumab, benralizumab which target IL-5 or its receptor IL-5Ra, and dupilumab targeting IL-4 and IL-13 through blocking IL-4Ra [17, 44].

I.3. ADVANTAGES, LIMITATIONS, AND CHALLENGES OF PROTEIN DELIVERY TO THE LUNGS

I.3.1. *Advantages*

The pulmonary route is suitable for both local and systemic delivery of proteins (Table 2). Like all drugs, proteins take advantage of the large surface area of the lungs. Proteins are absorbed more effectively in the alveolar region than in the central airways because of the large surface area in alveolar surface ~ 100 m^2 *vs* 2-3 m^2 in the conducting airways [12, 50, 51]. The alveolar epithelium is particularly thin (0.1 − 0.2 μm) and covered with thin surface fluids; the mucociliary clearance in the lung periphery is slow and the short path between epithelial cells and capillary endothelium and the high blood throughput favour a rapid and high absorption of drugs into the bloodstream [52-56]. Aerosol particles with the right aerodynamic properties are highly dispersed in nature, allowing the coverage of a large area and making, thus, full advantage of this route of administration [53]. Compared to oral delivery, the bioavailability of proteins after lung delivery is much higher because of the more hospitable environment (near neutral pH and abundant antiproteases) and the avoidance of the hepatic first-pass metabolism [10, 56-59].

Table 2. Advantages and limitations of the pulmonary delivery of proteins*.

	Local delivery	**Systemic delivery**
Advantages	- Direct delivery to the disease site - Requires less dosage compared to other routes - Rapid clinical response - Low risk of systemic side-effects - **Low absorption of large proteins**	- Large surface area (100 m^2) - Higher blood throughput - Thin alveolar epithelium (0.1 – 0.2 μm) - Thin surface fluids - **Slow mucociliary clearance in the lung periphery** - **Higher absorption of small proteins compared to the GI tract and other non-invasive routes**
	Non-invasive (needle-free), Compared to the GI tract:	

	- **Less hostile environment**: near-neutral pH, less extracellular enzymes, and no hepatic first-pass - No dietary complications and less variable absorption	
Limitations	- Fast clearance - Potential **immunogenicity**	- **Low bioavailability of large proteins** - **Potential degradation in epithelial cells before absorption**
	- Potential local toxicity - **Mucociliary clearance, enzymatic degradation, and uptake by macrophages** # - **Aggregation** - **Difficulty in delivering high doses** - High costs - Special devices and patient education - Variations due to breathing patterns, anatomy, and disease status	

GI, gastrointestinal
* Elements in bold affect more proteins, others are common to most drugs
# Advantageous for the treatment of intracellular infections and activation of AMs [60]

Pulmonary delivery, whenever feasible, could provide better treatment of lung diseases such as asthma, lung infections, CF, alpha-1 antitrypsin deficiency, and lung malignancies [15]. High local concentrations could be achieved, which allows better targeting of the disease and rapid onset of therapeutic effect while avoiding the potential systemic side effects of the parenteral routes [61, 62]. This is particularly true for large proteins (MW ≥ 40 kDa) which have very limited lung penetration by other parenteral routes of administration, and on the other hand, are absorbed sparingly and slowly through the lungs (usually < 5%) allowing longer availability at the target site [12, 14, 49]. Other practical considerations that can improve patients' compliance are the non-invasiveness (needle-free, no specialised training or involvement of professional health carer) and the possibility to develop dry powder formulations for remote locations (more stable for storage and transport) [16, 62].

I.3.2. *Limitations and challenges*

Proteins for inhalation face two significant obstacles to successful clinical use, pharmaceutical and biological.

Most of the pharmaceutical challenges at the level of production, purification, characterisation, and storage of proteins are common to all routes of administration. Most proteins are unstable to extreme physical and chemical stresses such as high temperatures, shear stress, surface adsorption, freezing and thawing cycles, light, metals, organic solvents, and extreme pH [63-67]. Protein instability can be categorised into two general classes chemical and physical [68, 69]. Chemical

damage involves breaking or making covalent bonds. Deamination, oxidation, and hydrolysis are the most encountered chemical instabilities [70]. Physical damage, on the other hand, only affects the physical state of the protein without altering its chemical composition [69]. Physical damage can occur independently, but also as a consequence of chemical damage, and they include aggregation, precipitation, denaturation, and adsorption [69]. Instabilities at the pharmaceutical level (production to storage) are extensively reviewed elsewhere [64, 69-73].

Delivery to the lungs requires an unavoidable aerosolisation step using either nebulisers or pressurised metered-dose inhalers (pMDIs) for liquid formulations or dry powder inhalers (DPIs) for solid formulations [16, 74]. Nebulisers are the preferred first choice and the most used method of delivery in the clinical development of products because of the relatively high doses that can be delivered and the avoidance of further drying steps (therefore more stress) used for powder inhalers [75, 76]. Moreover, powder formulations are mostly device-specific and need to be physically stable and readily dispersible and should not compromise the biochemical stability of the protein [77]. Liquid formulations must be serile and are easier to develop; however, they tend to have a short shelf-life with the risk of protein degradation during the nebulisation process. Using preservatives to prevent contaminations and improve the stability during storage could help, however, the number of approved preservatives for inhalation is limited and their use is generally discouraged especially in patients with asthma [77].

The process of converting liquid into aerosol during nebulisation introduces other stresses such as a sudden expansion of air-liquid interface, *in-situ* heating (ultrasonic nebulisers), aerosol recycling (jet nebulisers), and solvent evaporation which might lead to further degradation/aggregation and thereby a partial or total loss of activity [76, 78, 79]. For instance, lactate dehydrogenase (LDH) could lose up to 60% or 100% of is activity upon jet or ultrasonic nebulisation, respectively [79, 80]. Dornase alfa remains unaltered upon jet or vibrating-mesh nebulisation, whereas ultrasonic nebulisation causes a 40% loss of activity [76, 81, 82]. Therefore, it is only available for nebulisation using jet nebulisers (initially) and recently mesh nebulisers [15, 83]. The instability of proteins to nebulisation could be reduced significantly using alternative nebulisation devices or strategies such as cooling, adding surfactants and polyethylene glycol (PEG), adjusting protein concentrations, and shortening nebulisation time [79, 84-86].

The deposition of proteins in the lungs (or any other drug for that matter) depends on the aerodynamic properties of the carrying aerosol particles. Particles of aerodynamic diameter higher than 5 μm have more chances to be either filtered by impaction on the walls of the upper airways

failing thus to reach their target in most cases [15, 52]. Therefore, generating aerosols of the right particle size is crucial for the successful delivery of any inhaled drug.

Once delivered to the site of action, most proteins are cleared from the lungs within 24 hours due to the combination of effective clearance mechanisms, i.e., mucociliary transport, absorption across lung epithelia into the systemic circulation, degradation processes, and uptake by lung cells [52, 87-89]. These clearing mechanisms will be explored in more details in the following section.

Other general shortcomings and challenges of pulmonary delivery are also applicable to therapeutic proteins and include variabilities related to patients (breathing patterns, anatomy, and disease status), the need for high doses to reach clinically significant local or systemic delivery and therefore a poor cost/benefit ratio, relatively long delivery time by nebulisation, high losses during the delivery step, and technological and regulatory barriers related to using specialised devices [15, 16].

II. MECHANISMS OF CLEARANCE OF PROTEINS FROM THE LUNGS

II.1. OVERVIEW

The lungs possess several physiological barriers to prevent the invasion and persistence of foreign substances and particles. The first hurdle encountered by aerosol particles is the peculiar architecture of the respiratory tract, which in combination with particle aerodynamic properties, dictates the deposition pattern in the lungs. Particles of an aerodynamic size larger than 5 μm are filtered in the upper airways by inertial impaction while particles smaller than 3 μm are more likely to deposit in the deep lungs [90].

The first surface aerosol particles come into contact with is the mucus (mainly in the conducting airways) or lung surfactant (mostly in the alveolar region) of varying thickness and composition depending on the region of the lungs. Large, solid, hydrophobic, and positively charged particles are more likely to be trapped in the mucus then be carried along by the beating cilia to the upper airways to be expelled to the pharynx then swallowed or coughed. Proteins that firmly adhere to the mucus will suffer the same consequence. This outcome is not desirable for either local or systemic delivery unless the mucus itself is targeted (i.e. mucolytics). Adherence to the mucus could also result in longer residence time in the lungs provided aerosol particles are delivered to distal airways and alveolar region where the mucociliary clearance is less effective. This is also true if the mucociliary clearance is impaired in some diseases.

Nano-sized particles (< 200 nm) and large proteins (≥ 40 kDa, 6 nm) can traverse cells by transcytosis (carrier-mediated or non-specific endocytosis) and might suffer degradation through the process. Their absorption rate is low, which expose them to uptake and metabolisation in AMs. On the other hand, smaller proteins (≤ 40 kDa, < 6 nm) can pass between cells by paracellular transport directly to the interstitium then endothelial cells to the bloodstream. Small proteins and peptides are more prone to degradation by peptidases on the surface of epithelial cells and the airspaces. Large proteins are more resistant to peptidases and slowly absorbed and can dwell longer in the lungs, which makes them more susceptible to aggregation/degradation in the airspaces and uptake by AMs.

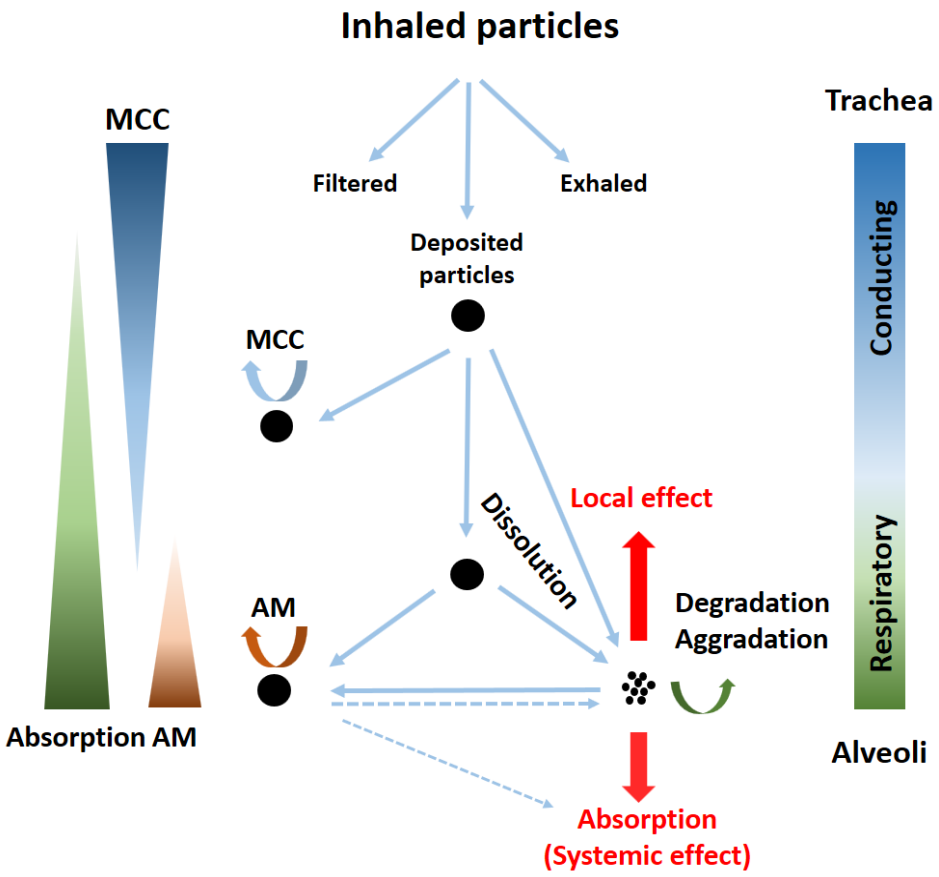

Figure 1. Fate of deposited drug particles and protein drugs in the lungs. Adapted from [34, 91]. MCC, mucociliary clearance, AM, alveolar macrophage.

All the processes mentioned above are dynamic and occur at the same time. The fate of proteins is influenced by the properties of their carriers (particles or drug system) and their size, charge (pI), nature (presence of specific receptors), modifications, stability, etc.

II.2. LUNG ANATOMY

The lungs can be divided structurally and functionally into two distinct zones, conducting zone and respiratory zone. In humans, the conducting zone from top to bottom consists of trachea, bronchi, and bronchioles. The primary function of this zone is to transport gases in and out but also to clear pathogens, humidify, and adjust the temperature of the inhaled air [92, 93]. The respiratory zone is where gases are exchanged between airspaces and blood capillaries. It consists of lung parenchyma represented by respiratory bronchioles, alveolar ducts, alveolar sacs, and alveoli [94]. Many anatomical and physiological differences exist among species, some of which are compensatory for different sizes and metabolic rates in these species (Table 3) [94].

Table 3. Interspecies anatomical differences relevant to the pulmonary drug delivery. Adapted from [95, 96].

Characteristics	Human (70 kg)	Rabbit (3.0 ± 0.5 kg)	Rat (0.30 ± 0.05 kg)	Mouse (25 ± 5 g)
Turbinate complexity	Simple	Complex scroll	Complex scroll	Complex scroll
Branching pattern	Dichotomous	Monopodial	Monopodial	Monopodial
Respiratory bronchioles	Present	Present	Rare	Very rare
Lung lobes	3 right, 2 left	4 right, 2 left [97]	4 right, 1 left	4 right, 1 left
Lung weight, g (% bw *)	1000 (**1.43**)	18 (**0.6**)	1.5 (**0.5**)	0.12 (**0.4**)
Lung volume, ml (% bw #)	4350 (4.3)	80 (4.4)	9 (5.7)	0.7 (6.2)
Airway generations	23	22	-	15
Alveolar surface area (m^2)	100	5.8	0.4	0.07
Diameter of alveoli (μm)	220	90	70	47
Alveoli number ($\times 10^6$)	950	135	43	18
Lining fluid volume, ml	30 ± 10	1.22	0.050 ± 0.005	0. 010 ± 0.005

* organ index =100 x (organ weight /body weight); # Lung volume (ml)/ lung weight (g)

The nose is more developed and complex in rodents which are obligatory nose breathers [98], on the contrary, humans have a relatively simpler nose and can breathe both from nose and mouth [99]. Moreover, nasal turbinates in rodents have a relative surface area five times higher than in humans offering more protection to the rest of the respiratory tract [94]. These variations can cause higher large particles retention in nasal cavities in small rodents [95].

Other major differences among species are related to the branching pattern of airways. In humans and non-human primates, the branching is highly symmetric bipodial (or tripodial) in contrast with a predominantly simple monopodial pattern in dogs, rabbits, and most laboratory rodents [100, 101]. In humans, the trachea undergoes on average 22 bifurcations (18 to 29) [102] before reaching the alveolar sacs, 16 of which are conducting airways compared with mice which have less than 15 airway generations and no respiratory bronchioles [87, 103].

Table 4. Respiratory parameters in mammals. Adapted from [95].

Parameters	**Human (70 kg)**	**Rabbit (3.0 ± 0.5 kg)**	**Rat (0.30 ± 0.05 kg)**	**Mouse (25 ± 5 g)**
Breathing	Nose/mouth	Nose	Nose	Nose
Respiratory rate (per min)	12-16	50	85	160
Tidal volume (ml)	400 – 616	15.8	0.87 – 2.08	**0.15 – 0.18**
Total ventilation (l/min) *	5-8	0.8	0.12	0.025
Particle size for alveolar deposition (μm)	1 – 5	-	3.5	3

* also known as RMV for respiratory minute volume

Smaller mammals have relatively larger airways lumina; therefore, a decreased ventilatory dead space but compensate with higher breathing frequency (Table 4) [104]. Despite the significant differences between species, the optimal size of aerosol particles for alveolar deposition is not significantly influenced [95].

The deposition of particles is influenced primarily by their charge and aerodynamic properties (size, shape, density, hygroscopicity, charge, velocity) and the pathophysiology of the lungs (age, sex, anatomy, disease, lung functions) [105]. Deposition of aerosols (solid or liquid particles suspended in air) in the airways occurs by inertial impaction, gravitational settling (sedimentation), Brownian diffusion, interception (e.g. elongated particles), and electrostatic precipitation (positively charged particles) (Figure 2) [90, 93, 106, 107].

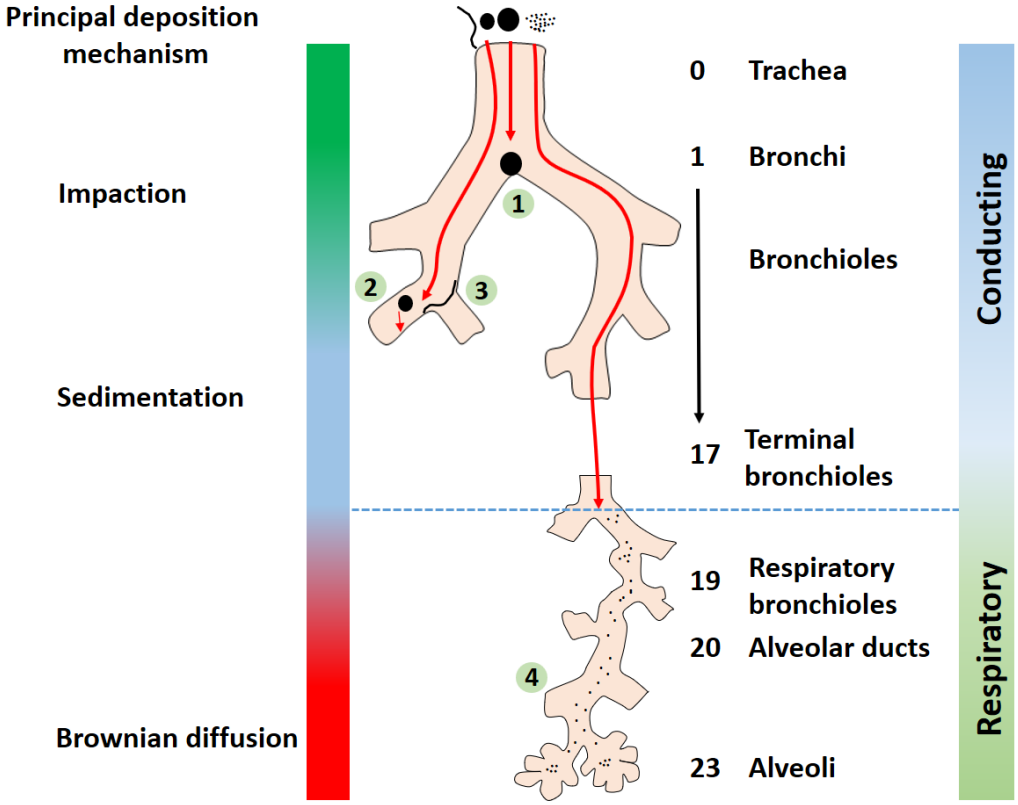

Figure 2. Deposition mechanisms of inhaled particles in the lungs. Adapted from [12]. Impaction (1), particles have enough momentum to keep their trajectory despite changes in the direction of the air stream; (2) Sedimentation, particles settle due to gravity forces; (3) Interception, dominantly for fibres in small airways without deviation from the streamlines; (4) Diffusion, random motion of very small particles.

Figure 3 shows deposition data in healthy male subjects, however, these predictions might not very accurate as they are based on monodisperse environmental aerosols rather than pharmaceutical aerosols which are more polydisperse and have higher densities.

Particle size of 1-5 μm and lung flow rates of 15–30 l/min are considered optimal for particles deposition in the respiratory tract, and it is maximal for particles of 2–4 μm diameter (40% deposition) [108]. The successive branching filters particles with large aerodynamic diameters (> 5 μm) by impaction, this latter is promoted by the hygroscopic growth of particles in airspaces due to the relative internal humidity approaching 90% [95]. Impaction in the upper airway impedes the particles from reaching the main absorptive alveolar surface and lead to early mucociliary clearance [93].

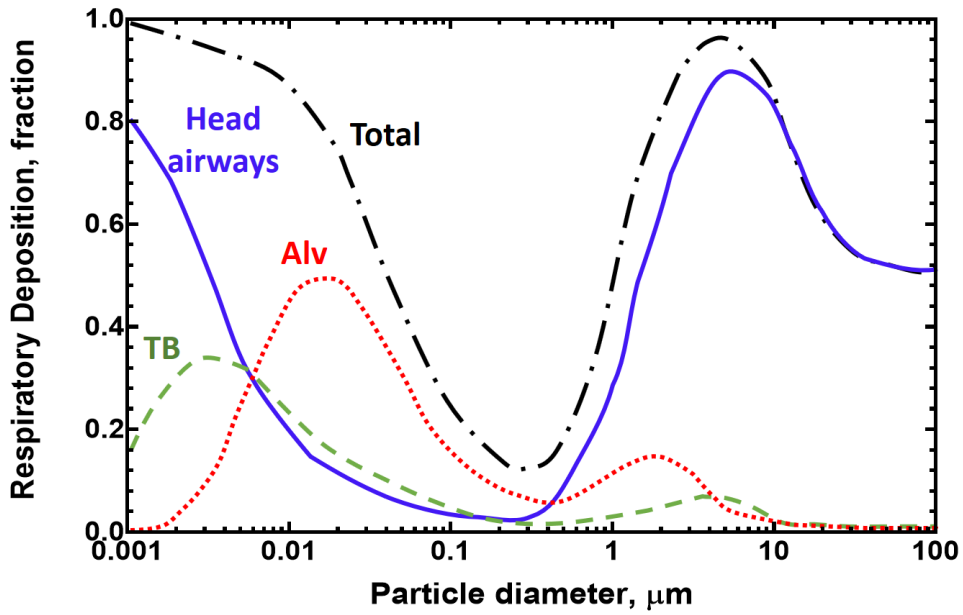

Figure 3. Predicted lung deposition of particles in different regions of the lung [90]. Alv, alveolar region; TB, tracheobronchial region.

II.3. LUNG HISTOLOGY

The conducting airways are covered by the respiratory epithelium. It has many cell types whose abundance and structure change significantly throughout the respiratory tract [50]. Most of the airway epithelium is a ciliated pseudostratified columnar epithelium [109]. The main cells in this region are ciliated, goblet, basal, brush (in rats), and neuroendocrine cells (Figure 4 and Table 5). Ciliated cells are the most abundant; they are responsible for the mucociliary escalator. They are covered by mucus produced by goblet cells (goblet-shaped cells laden with mucin granules) and submucosal glands. Goblet cells' number decreases towards the respiratory bronchioles, where they eventually get replaced by club cells [109]. Basal cells are the stem cells of the airway epithelium (ciliated and goblet cells); they provide the attachment layer to the basement membrane. Brush cells are described in rats and they get their name from the short microvilli covering their apical side; they are dispersed in all areas of the respiratory mucosa and have no identified role [109]. Finally, smalls cluster of neuroendocrine cells play the role of airway sensors and are also involved in immune responses and tissue remodelling. They secrete catecholamine and polypeptide hormones, such as serotonin, calcitonin, and gastrin-releasing factors (bombesin), among others [109].

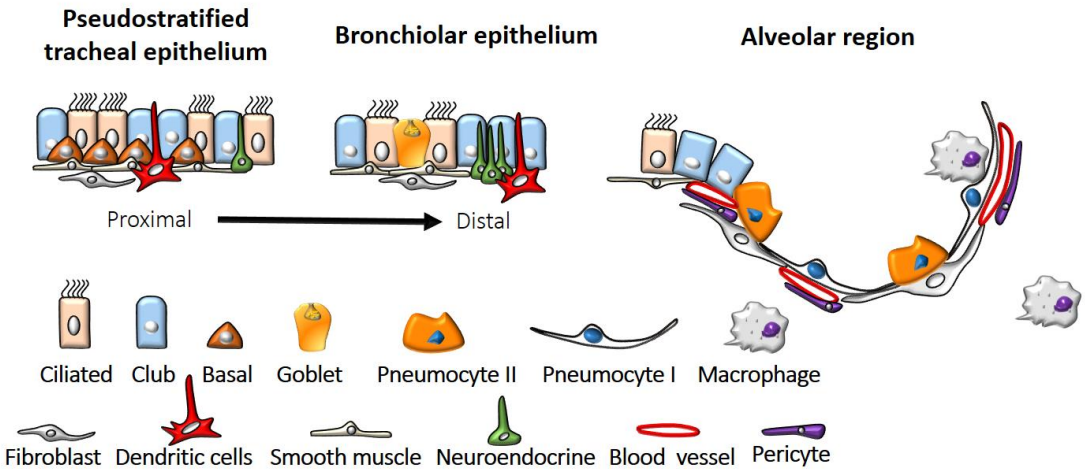

Figure 4. Major cell types in different regions of the lungs. Adapted from [110].

Serous and mucinous cells are organised in submucosal glands, and they secrete mucus and other substances into ducts and then on the bronchial mucosa [111]. The alveoli are the structural and functional unit of the lungs where gas exchange takes place. They are specialised air-sacs of roughly 200 μm diameter. In humans, millions of alveoli are responsible for the large surface area of the lungs (~ 100 m^2).

Table 5. Main cells in the lungs [94, 112]

Cells	Main role(s)
Columnar epithelial cells (ciliated)	Mucociliary clearance
Serous cells (preferentially in the rat trachea)	Secretion (e.g. liquid, mucus) and host defence (antimicrobial proteins)
Goblet cells (mucous cells)	
Basal Cells	Stem cells for epithelial tissue repair
Brush cells (in rats, type III Pneumocytes)	Unknown (chemoreceptor!)
Neuroendocrine cells (Kulchitsky cells)	airway sensors, immune responses, and tissue remodelling [113]
Club cells* (non-ciliated)	Epithelial barrier maintenance, secretion, and metabolism. [114]
Type I Pneumocytes	Gas exchange
Type II Pneumocytes	Secret surfactant, Reserve cells for the alveolar epithelium.
Macrophages	Immune response

*previously known as Clara cells

The alveolar epithelium is composed of only two cell types, type I pneumocytes and type II pneumocytes. The surface epithelium, the supporting tissue, and the network of capillaries underneath constitute the alveolar wall or septum. Type I pneumocytes are flattened squamous cells that cover most of the alveoli surface area (> 90 %) [50]; their very thin cytoplasm facilitates the air-blood gas exchange. Adjacent cells are connected by tight junctions to prevent the leakage of fluids into the alveolar lumen. Type II pneumocytes are smaller cuboidal cells (progenitor of type I cells) which mostly sit along with the alveolar openings [94]. They are more numerous than type I cells (~ 3 to 2); however, occupy less than 10% of the surface area of alveoli [50, 91]. They are endowed with a more developed cellular machinery and the presence of lamellar bodies [109]. Their primary role is the production and secretion of surfactant and regeneration of type I pneumocytes. Their functions also include xenobiotic metabolism and transepithelial movement of water [91]. Both types I and II pneumocytes can ingest particles up to 200 nm by endocytosis [115].

Immune cells at the level of alveoli consist almost entirely of AMs (discussed later). Dendritic cells are not localised in the airspaces but have projections in the airway lumen [116]. Neutrophils and rare mast cells could be recruited into airspaces when needed. Bronchus associated lymphoid tissue (BALT) in airway submucosa consists of lymphocytes T and B, organised preferentially into follicles, but also dendritic cells, plasma cells, and macrophages [94, 117]. Rodents kept in specific-pathogen-free conditions exhibit less BALT-like structures than those exposed to pathogens/foreign antigens leading to the term inducible BALT [50, 94]. Likewise, lymphoid tissue is present in human healthy lungs and mice but can be induced by antigens, infection or inflammation [117].

II.4. MUCUS AND MUCOCILIARY CLEARANCE

II.4.1. *Mucus*

The mucus is the outermost gel layer lining the airways epithelium; therefore, the first barrier foreign invaders encounter in the respiratory tract [118]. It is an extracellular viscoelastic gel which varies in thickness and composition throughout the respiratory tract. Its thickness ranges from 2 µm to 55 µm in healthy lungs to more than 250 µm in some diseases such as CF and COPD [38, 52, 119]. It is thin to absent in the alveolar region and distal airways and thicker in the upper airways due to the transport and accumulation from the lower airways and the local production of mucins in the upper airways [120]. Normal mucus is composed of 97% of water and 1-3% of mucin, proteins, salts, cellular debris, lipids, and other substances [120, 121]. Mucin is a highly glycosylated

large protein (MW up to 10^3 kDa) containing from 50 to 90% carbohydrates with terminal sugars containing mostly sulfate or carboxyl groups conferring the mucin its highly anionic nature [120, 122]. Mucins are secreted by goblet cells and mucous and serous cells of the submucosal gland [123].

Mucins in the airways can be divided into three categories, secreted mucins that polymerise to form gels (MUC5AC, MUC5B, and MUC2), secreted mucins that do not polymerise (MUC7), and cell surface-tethered mucins (monomeric) bathed in the periciliary liquid (PCL) layer (MUC1, MUC4, MUC16, MUC20) (Figure 4) [124-126]. Mucins of the first category form large oligomeric structures responsible for most of the viscoelastic properties of the mucus [123].

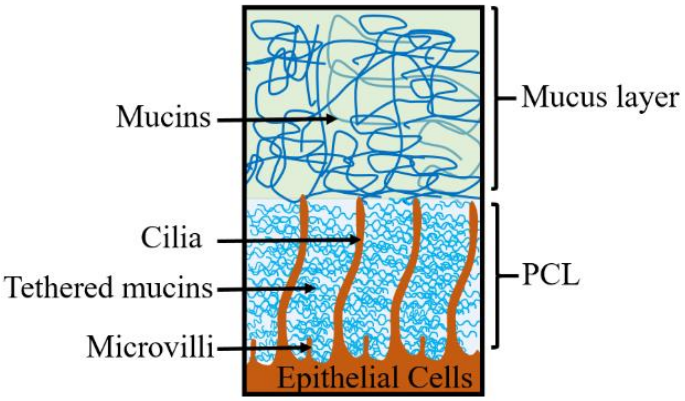

Figure 5. Mucus layer from airway epithelia. PCL, periciliary liquid [127]

Mucus plays a central role in maintaining healthy lungs. The cell-attached mucins preserve the periciliary layer and coordinated ciliary motility [124] while the secreted mucus prevents dehydration of the PCL layer by donating water [128]. Mucus acts as a trap for endogenous and exogenous substances and particles such as inflammatory cells, pathogens, pollutants, and particles facilitating, thus, their elimination by mucociliary or cough clearance [92, 124]. Other roles in innate immunity beyond the mucociliary clearance are also suggested, including direct interactions with dendritic cells and goblet cells [124].

II.4.2. *Mucociliary clearance*

Mucus is transported by the beating cilia and the expiratory airflow from the distal airways to the large airways where it encounters additional mucus produced locally [120]. Mucus is then swept upwards and propelled to the larynx then enters the pharynx, meets the mucus descending the nasal cavities, then is swallowed. Around 30 ml of the airway mucus is swallowed daily [120]. In humans, mucus turnover occurs within 24 h [129, 130], 2 to 3 times longer than in rodents [96]. The mucus velocity is relatively fast in the trachea (4 –5 mm/min) and much slower in distal airways

(≤ 1 mm/min) suggesting the existence of two phases, a fast phase corresponding to the mucociliary clearance of the tracheobronchial tree and a slower phase in the small airways and alveoli where clearance could be dominated by non-ciliated mechanisms (Table 6) [129]. The slower mucociliary clearance in the smaller airways is in correlation with the lower number of ciliated cells, shorter cilia, and lower number of secretory cells [129].

Table 6. Clearance rates of human mucus in airways. From [131]

Mucus	Clearance rate (mm/min)	Reference
Nasal	5-11	[132]
	5	[133] [134]
Tracheal	4.1 ±1.9	[135]
	4.7 (3.5 - 6)	[135] [136]
	15.5 (4.5 - 30)*	[137] [138]
Bronchial	2.4±0.5	[139]
Small airways	1	[140]

* Measured using a bronchoscopic or roentgenographic method, known to give higher measured rates

The mucus acts as a multiple barrier to the diffusion and penetration of drugs from the lumen to the epithelium where drugs are absorbed into the systemic circulation [141]. The barrier properties are mechanical (dynamic and steric) and chemical. The dynamic barrier is represented by the continuous secretion of the mucus (replaced every 20 min [125]) and the peristalsis from both a vertical and horizontal flow against the penetration of drugs. The steric barrier consists of the network organisation of mucus fibres acting as a filter for large particles and creating a tortuous pathway for their diffusion [141]. The steric barrier is enhanced by the relatively high viscosity of the mucus [141]. The chemical barrier is represented primarily by the low-affinity interactions of proteins and particles with the naked protein core of mucin, mucin carbohydrates, lipids, and other constituents *via* hydrogen bonding and ionic interactions (carboxyl or sulfate groups) [52, 141]. Proteases secreted into the airspaces and present in the mucus are another type of chemical barrier to the delivery of proteins and peptides to the lungs [142].

Drugs and particles have to traverse the mucus layer rapidly enough to be able to exert their intended pharmacological action [143]. Drugs strongly bound to the mucus are mostly eliminated by the mucociliary escalator before being absorbed or reaching their local targets. Therefore, strong binding to the mucus is undesirable for both local and systemic delivery. Nonetheless, retention or

adherence to the mucus could be beneficial for drugs targeting the mucus such as mucolytics. The hydrophilicity and viscosity of the mucus do not favour the diffusion of the hydrophobic drugs which bind non-specifically to mucus glycoproteins and end up eliminated rapidly [144].
Many studies are available on the interaction of proteins and peptides in cervical, gastric, intestinal and respiratory mucus. The overall mucin concentration and viscoelastic properties of different types of mucus are similar [145]. The mucus mesh size of mucus ranges from 20 nm in the PCL to several micrometres for the mucus gel (Table 7) [127, 146].

Table 7. Mesh size of mucus

Mucus	**Size (nm)**	**Reference**
human cervical mucus	500-800	[147]
	20-100	[148]
	100	[149]
	340 ±70 (50-1800)	[150]
Native respiratory mucus (horse)	100 to micrometres	[146]
CF sputum	140 ± 50 (60–300)	[151]
Periciliary liquid *	20-40	[127]
* From primary human bronchial epithelial (HBE) cell cultures		

Prolonging the residence time of particles in the respiratory airways could be achieved by designing particles that can cross the rapidly-cleared superficial luminal mucus layer (min to hours) and reach the adherent mucus in the PCL underneath which is cleared more slowly (hours to days) [52, 131]. This mechanism was suggested to explain the more rapid clearance of insoluble particles of radiolabelled sulfur colloid (220 nm) compared with human serum albumin after intrabronchial deposition in dogs [152]. Studies on the diffusion of viruses in the mucus showed that viruses of large size such as herpes simplex virus (HSV, 180 nm) were almost completely immobilised in cervicovaginal mucus whereas smaller mobile viruses (< 100 nm) diffused 100 to 1000 times slower than the expected rates in water [148]. Similar results were reproduced by Lai *et al.* however virus immobilisation was attributed to its mucoadhesiveness rather than to its size as the measured pore size was 340 nm on average, and the diffusion of non-mucoadhesive 200-nm nanoparticles was unhindered [150]. Particles that could penetrate the mucus were expected to have smaller sizes (100 nm or less) [131]. Nevertheless, densely coated polystyrene particles (200 and 500 nm in diameter) with short 2 kDa PEGs were, unexpectedly, shown to diffuse in the mucus rather rapidly, hundreds of times faster than uncoated hydrophobic nanoparticles [145].

Contrary to this, particles coated with PEGs of 10 kDa lost their mucus penetrating properties acquired when coated with smaller PEGs of 5 kDa, which was explained by the change in behaviour for the larger PEGs from mucoinert to mucoadhesive due to the entanglement and hydrogen bonding with mucin fibres [52].
Conjugation to PEGs of 40 kDa conferred mucoadhesive properties to anti-17A F(ab') 2 and anti-IL-13 Fab' [153]. Patil *et al.* showed that PEGylated Fab' binds to human airway mucus more than non-PEGylated Fab' [154]. The diffusion of proteins in cervical mucus was found largely unhindered compared to saline [148, 149]. Olmsted *et al.* found that antibodies diffuse more slowly in mucus through low-affinity bonds between Fc moieties and mucin fibres [148]. Impeding the electrostatic interactions with the negatively charged mucin fibres was achieved for the cationic Poly-L-ornithine (PLO, 45 kDa) upon conjugation to 8-9 units of 10 kDa PEG which enhanced its transnasal absorption [155].

II.5. ABSORPTION THROUGH LUNG EPITHELIAL CELLS

II.5.1. *Mechanisms of transport across epithelial cells*

Absorption occurs virtually throughout all lung epithelia; however, it is more effective in the alveolar region; hence, macromolecules delivered to the deep lungs are more absorbed than those deposited in central airways [52, 53]. This is due to the thin epithelium and surface fluids, large surface area and higher blood throughput and the shorter path between epithelial and capillary endothelium [52, 56]. Crossing the respiratory epithelia is the most limiting factor to the absorption of proteins as the interstitium and the capillary endothelium are easier to cross [50]. In some areas, the interstitium is absent altogether, and the basement membranes of the capillary endothelium are in direct contact with the epithelium of alveoli for optimal exchange of gases [111].

The absorption of proteins and macromolecules in the lungs is primarily dependent on their MW and nature [12, 51, 153]. Many authors have reported the existence of an inverse relationship between the MW of macromolecules and the rate of absorption from the lungs into the blood (Table **8**) [14, 50, 52, 156, 157]. Proteins of MW ≥ 40 kDa (≥ 5-6 nm in diameter) are slowly absorbed from the airspaces to the blood (hours to days) and have low bioavailability (≤ 5%). In comparison, smaller proteins and peptides of MW ≤ 40 kDa (≤ 5 nm in diameter) are more rapidly absorbed (min to hours) and have high bioavailability after inhalation or instillation into the airways.

Table 8. Pharmacokinetic parameters for some therapeutic proteins and peptides. Adapted from [50, 55]

Molecule	MW (kDa)	Diameter (nm)	Animal	Tmax, h	F%
Glucagon	3.5	-	rat		<1
Insulin	5.8	2.2	rat	0.33	14
IFN-α	19	3-4	rat	4.5	37.5 (19–56)
hGH	22	-	rat	6.0	19.5 (3–36)
GCSF	18,6	-	rat	2.5	12
rhDNase [a]	37	4.8 [b]	rat	-	15
			monkey	-	< 2
Albumin	68	7-7.2	rat	20	4.5
IgG	150	11	rat	16	1.65

F%, Bioavailability; [a] [158]; [b], measured in our lab, G-CSF, Granulocyte Colony Stimulating Factor

Based on these observations, pores in airway epithelium presumably corresponding to cell junctions were suggested. The estimated pore size for the alveolar epithelium and lung epithelial cell monolayers is ~ 6 nm [159-161]. Proteins in a solution can cross the lungs to the blood epithelial cells by two main mechanisms: through the cells (transcellular) or between the cells (paracellular) (Figure 6).

Koussoroplis *et al.* found a significant difference in lung residence time between PEGylated Fab' and dextran of similar MW, highlighting the importance of macromolecule nature in their fate in the lungs [153]. Bur *et al.* studied the transport of a series of homologous proteins in human alveolar epithelial cells *in vitro* and found no apparent size-dependent transport, consistent with paracellular diffusion [162]. They justified their unexpected results by the use of homogenous proteins, unlike other studies where proteins from other species were used in *in vivo* and *in vitro* experiments.

Transcellular transport can occur through receptor-mediated transport or receptor-independent pinocytosis (fluid phase or adsorptive endocytosis). Paracellular transport is thought to take place through junctional complexes between two or three cells and less frequently through temporary holes created by dead or injured cells before these are replaced or repaired [50].

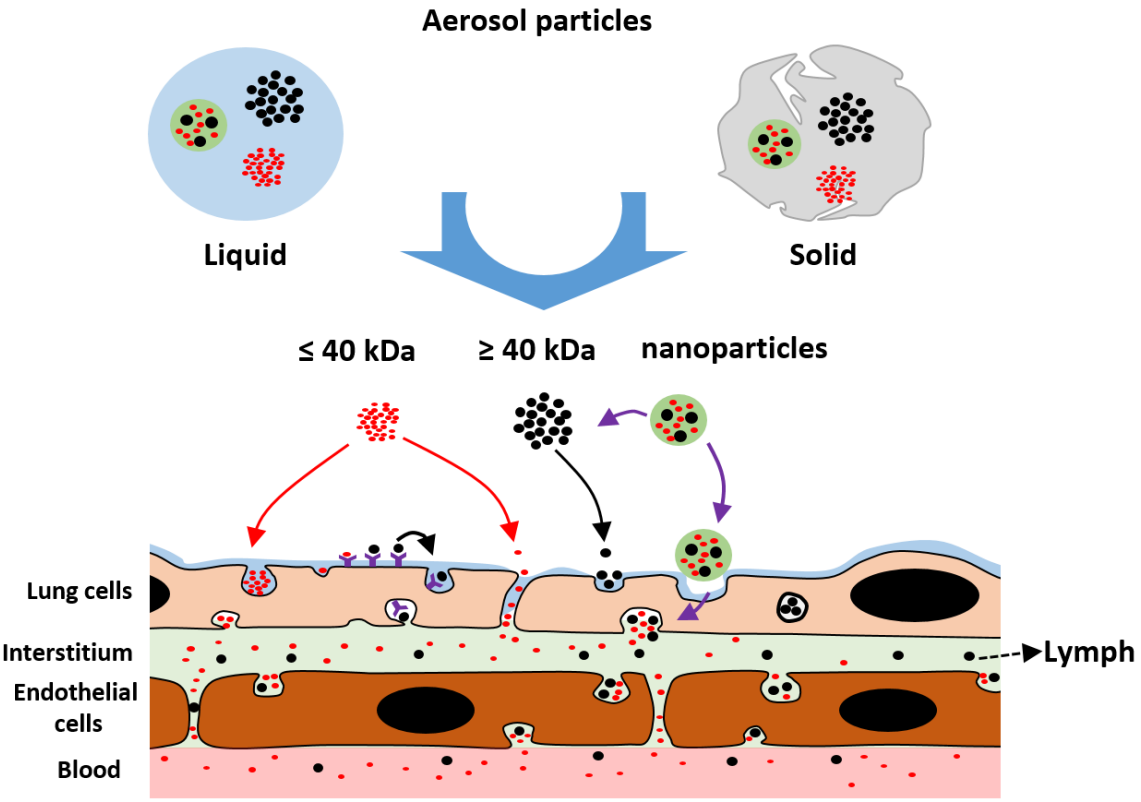

Figure 6. Mechanisms of absorption of macromolecules and nanoparticles across lung epithelial cells. Adapted from [50, 91, 163]. Solid aerosol particles should be dissolved and release their content in contact with lung fluids. Large proteins (≥ 40 kDa) might be absorbed by transcytosis (nonspecific or receptor-mediated) then enter the blood *via* transcytosis in endothelial cells, leaky capillaries or drainage into the lymph. Small proteins (≤ 40 kDa) might follow the same pathways but can also enter the blood faster *via* tight junctions (paracellular transport). Nanoparticles could release their content or be internalised as such by endocytosis.

Proteins normally occurring in the lung lining fluids such as albumin (68 kDa), transferrin (80 kDa), and immunoglobulins (IgG, 150 kDa) are thought to have receptors on the surface of epithelial cells. The absorption rates of these proteins are higher than expected based on their MW [50]. Their transport has also been shown to be directional as it occurs at higher rates from the apical to the basolateral side than the reverse [162].

Albumin is endocytosed through the clathrin-mediated pathway into both types I and II alveolar epithelial cells; however, more efficiently (> 70%) into the latter [164]. Megalin/cubilin and gp60 (60 kDa albumin-binding glycoprotein) are also possible candidates for the receptor-mediated transport of albumin [164]. Antibodies are transported *via* the neonatal Fc receptor (FcRn); this receptor is more abundant in the upper and central airways of the lungs [43]. For this reason, FcRn-dependent absorption of EPO-Fc fusion protein (MW ~ 112 kDa) was higher when deposited in those regions with a bioavailability up to 35% in monkeys [43]. Proteins or macromolecules of large size with no specific receptors can cross the respiratory epithelia *via* non-specific pinocytosis (fluid-phase or adsorptive endocytosis). Horseradish peroxidase (HRP, 40 kDa) and dextrans of

MW ≥ 40 kDa are two examples of macromolecules transported by fluid-phase endocytosis through epithelial cells [159, 165]. Fluid-phase endocytosis is a slow process, non-saturable at high concentrations, and non-inhibited by an excess of competing substrates [166-168]. Adsorptive endocytosis, on the other hand, occurs at higher rates than fluid-phase endocytosis and requires the non-specific adsorption of the proteins on the cell membrane or the glycocalyx mainly by electrostatic interactions but also hydrophobic interactions before the formation of the endocytic vesicles. This process is saturable at very high concentrations [169-171].

Smaller proteins such as growth hormone (22 kDa), dextran of MW < 40 kDa are transported *via* paracellular diffusion [159, 162]. Most small proteins such as cytokines (18-22 kDa) and peptides such as insulin (5.8 kDa) are absorbed rapidly in humans and animals likely by paracellular transport [50, 56]. Receptor-mediated (caveoli) transcytosis has been reported for insulin [53, 169, 172].

II.6. LUNG MACROPHAGES

II.6.1. *ORIGIN AND TYPES*

Macrophages in the lungs and associated tissues are called pulmonary or lung macrophages. Depending on their anatomical locations at least three different subpopulations are distinguished (1) alveolar macrophages (AMs) present on the epithelial surfaces of alveoli, (2) airway macrophages in the epithelial lining of the conducting airways (3), and interstitial macrophages in the interstitium (Figure 7) [173-176]. The first two are recoverable by bronchoalveolar lavage (BAL) and usually referred to as AMs [175, 177, 178]. Other subpopulations are also reported although less studied, such as pleural and intravascular macrophages [179]. We limit the discussion to AMs because of their direct involvement in the clearance of inhaled proteins and particles.

AMs represent the majority of cells in the BAL (> 95%) [180] and only 3-5% of all lung cells [179]. They are 3-4 times more abundant than interstitial macrophages [181, 182] and have a relatively long turnover rate of 40% yearly making them long-lived cells [183]. An extensive BAL could recover up to a third of AMs [173]. Resident macrophages firmly adhering to the alveolar epithelium and not recoverable by BAL are also called SAMs for sessile (immobile) AMs [184].

AMs are distinct form interstitial or those in blood vessels suggesting further specialisation of macrophage populations in the lungs [177]. AMs can travel freely upwards along the airways to the pharynx or downward into the terminal airways or the interstitium [175]. Every day, around one hundred million macrophages migrate to the bronchi [111].

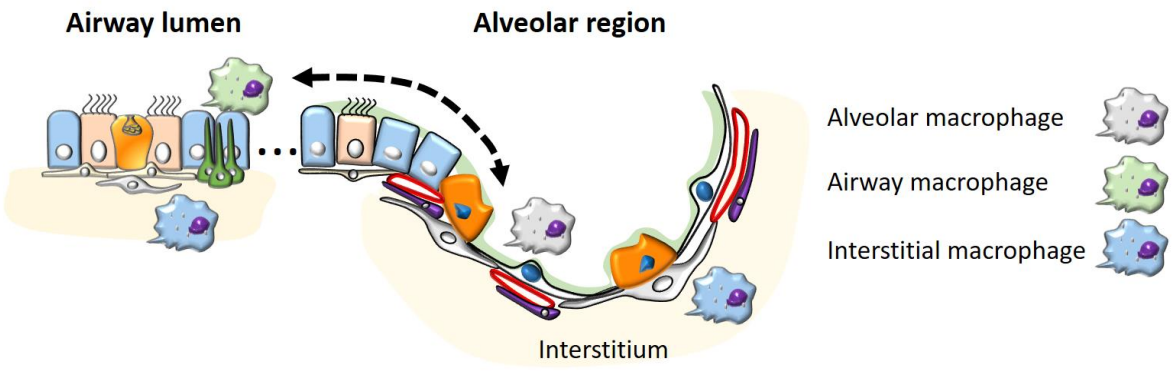

Figure 7. Main types of pulmonary macrophages.

The long-held hypothesis was that AMs originate from blood monocytes and bone marrow precursors that have matured to AMs in the interstitial compartment [179]; however, recent studies have shown that circulating monocytes contribute to the pool of AM-depleted animals or humans but not significantly to the normal lungs [179]. Shortly after birth, pulmonary macrophages differentiate from hematopoietic precursors that have populated the lungs during embryogenesis [179]. In normal conditions, lung macrophages are quiescent; however, they can proliferate locally following injury or infection [179].

Different mammals do not appear to present similar AM morphometry. The size and number of macrophages are significantly larger in humans than in rats (Table 9). An increase in the diameter of AMs from rodents to humans could translate into several folds more voluminous macrophages which could have a direct implication on the number and size of particles phagocytised [185].

Table 9. Alveolar macrophages in different mammalian species. From [95].

Characteristics	Human	Dog	Rabbit	Rat	Mouse
Size (diameter µm)	21 (15–22) [185, 186]	-	-	13.1 [185]	7-15 [a] (15.9) [187]
Alveoli number (× 10^6)	950	1040	135	43	18
AM (x 10^6)	5990	3940	142	29.1	2.9
AM per alveolus [b]	6.3 (12 [c])	3.8	1.05	0.68	0.16 (> 0.33 [d])

[a] measured in our lab; [b] Calculated by diving the number of AMs by the number of alveoli; [c] [50]; [d] [184, 188, 189]

AMs are the first line of cellular defence in the lungs. They are professional antigen-presenting cells (although poor) and fulfil multiple tasks in the regulation of host defence, inflammation, and homeostasis through secreting numerous mediators [179, 190, 191]. AMs actively contribute to clearing inhaled microorganisms, particles, toxins, drugs, and cell debris [94]. Their role has a greater importance in humans, where the mechanical clearance from the alveolar region is slow [179]. Despite their active role in lung immunity, AMs do not unnecessarily respond to antigens that do not disrupt lung structure [177]. As any other macrophages in the body, activated macrophages can be described as M1 or M2 depending on whether they have pro-inflammatory or anti-inflammatory phenotypes [192]. Macrophages with both M1 and M2 markers could be found in some diseases [192]. M1 macrophages secrete pro-inflammatory cytokines (such as TNF-α, and IL-12) and reactive nitrogen and oxygen intermediates (RNI, ROI) [60, 192]. They mediate antitumor immunity and resistance toward intracellular pathogens (bacteria, protozoa and viruses) and cause disruption of the body's normal tissue [60, 193]. M2 macrophages, on the other hand, are more involved in wound healing, tissue repair and remodelling, and pathogen clearance [60].

II.6.2. *Mechanisms of uptake by macrophages*

Macrophages are professional phagocytic cells [194, 195]. They have the ability to internalise particulate and non-particulate materials by endocytosis. Endocytosis can be grossly divided into phagocytosis (cell eating) and pinocytosis (cell drinking). Phagocytosis is the active process of engulfing particles [196]. Particles are first opsonised then bind to specific membrane receptors (Fc, complement, or receptors such as mannose/fructose-based receptor) triggering the reorganisation of the cytoskeleton and the formation of a phagosome [60]. Macrophages contain abundant lysosomes loaded with up to 50 acidic enzymes (hydrolases) active at pH ~5 [197]. Phagosomes mature and fuse with lysosomes forming phagolysosomes leading to the degradation of their content in the acidic enzyme-rich environment [198]. Pinocytosis refers to the uptake of fluids within small vesicles. Pinocytosis could be divided into macropinocytosis (0.2 -10 μm) and pinocytosis (< 0.2 μm) [60]. Macropinocytosis is dependent on actin and occurs by forming protrusions at the cell membrane. Most pinocytotic pathways are receptor-mediated and are involved in capturing specific substances. Depending on the receptors, we can distinguish clathrin-mediated, caveolin-mediated, and clathrin- and caveolin-independent endocytosis [196]. Endocytosis occurring without binding to the plasma membrane is referred to as fluid-phase pinocytosis while uptake through non-specific adsorption to the plasma membrane is called adsorptive pinocytosis (see absorption by epithelial cells).

II.6.3. *Macrophages in drug delivery*

Macromolecules and particles are subjected to AM clearance which could pose a major obstacle for either transport into the bloodstream or dwelling in the lung lumina [199]. Moderate to large-size proteins were shown to be more prone to clearance by AMs purportedly because of their lower absorption rates (hours) compared with small proteins and peptides which are absorbed rapidly (minutes) leaving little time to macrophages to eliminate them effectively [199]. Depleting AMs in rats was shown to increase the systemic absorption of IgG (150 kDa) and human chorionic gonadotropin (hCG, 39.5 kDa) several-fold but not that of insulin (5.8 kDa) and human growth hormone (22 kDa) after intratracheal instillation in rats [199]. While avoiding AM uptake is desirable in most therapeutic applications, the opposite is sought in the treatment of intracellular infections affecting macrophage (e.g., tuberculosis, pneumonia, and aspergillosis) or indirectly in the treatment of cancer and lung inflammation [60, 200].

Micron-sized or nano-sized carriers are more captured by AMs compared to free drugs [60]. The phagocytic activity is dependent on many factors such as particle size, shape, charge, hydrophobicity, softness, and surface ligands [60, 201]. Some of these are also key to the aerodynamic properties of particles and, therefore, their deposition in the lungs, as seen above [90]. Particles of sizes of 0.2-10 μm are the most accessible to AMs [60]. Chono *et al.* assessed the uptake by AMs of liposomes ranging from 0.1 to 2 μm in diameter; optimal phagocytosis was observed for particle sizes of 1-2 μm [202]. Particles such as nano-sized drug carriers (< 200 nm) are less efficiently phagocytised but could be internalised by pinocytosis [60, 186, 203, 204]. Positively charged particles are more captured by AMs than neutral or negatively charged ones [205, 206]. Several strategies have been suggested to reduce the AM clearance including (i) using inhibitors of endocytosis, (ii) using ligands competitors for macrophage membranes, (iii) incorporating drugs within large porous particles to protect them from endocytosis and/or phagocytic degradation, (iv) designing particles with high aspect ratios, and (v) coating particles with PEG [199, 207, 208].
Besides particles, proteins and other macromolecules have been shown to be captured by AMs following pulmonary delivery in different species [209]. Up to 10% of the administered doses of PEGs of 5-10 kDa were found in AMs compared to only 3% of the smaller 2-3.4 kDa PEGs and even less for PEG < 1 kDa [210]. Although AM depletion could increase the bioavailability of hCG 3-fold in rats [199], direct quantifications of proteins and their PEGylated forms in AMs following pulmonary delivery yielded amounts ranging from 0.04% to 3% of the delivered dose for rhDNase, Fab', and IFNα [83, 211, 212]. These values could be higher considering that standard procedures of BAL recover only a portion of AMs [173, 188].

Macrophage clearance of proteins could be enhanced by aggregation, which might be induced by contact with lung surfactant or defence molecules secreted by macrophages and other cells [93]. Macrophages were shown to be targeted by protein through binding to the mannose receptor, as has been demonstrated for recombinant glucocerebrosidase in the treatment of Gaucher's disease [213].

II.7. DEGRADATION IN LUNG MICROENVIRONMENT

As a portal of entry into the body, the lungs are involved in drug metabolism, albeit to a lesser extent in comparison to the liver and the gastrointestinal tract (GI tract) [55, 91]. The bioavailability of proteins by oral delivery is almost null due to the acidic conditions in the stomach, the extensive proteolytic activity and the first-pass metabolism by the oral route [9, 44, 214].

In the lungs, therapeutic proteins are also subjected to considerable threats and can be readily degraded by membrane-associated and intracellular proteases and peptidases (epithelial cells, endothelial cells, and macrophages) [10, 59, 215, 216].

Proteases in the human lungs can be classified according to their mechanism of catalysis and structure into serine, cysteinyl, aspartyl and metalloproteases [217, 218]. They can function either intracellularly or extracellularly [217]. The level of proteases is higher in macrophages than in epithelial cells [217]. Some are constituent of the apical side of the airways and alveolar epithelial cells such as endopeptidase, aminopeptidases, and various cathepsins [89, 91, 219, 220]. Cathepsin D, B, H, and L (lysosomal enzymes) are present in both AMs and alveolar epithelial cells [91]. Recenlty, Woods *et al.* have identified cathepsin D (> 90%), cathepsin H, ACE (angiotensin converting enzyme) and DPPIV (dipeptidyl peptidase IV) as the most abundant proteases in the BAL of healthy volunteers [221]. In addition to their role as proteases, they play various roles in tissue remodelling, mucin expression, regulating innate immunity and microbial killing [218].

Small proteins and peptides are more metabolised by peptidases; however, their rapid absorption could limit their degradation in some cases [55]. The bioavailability of some natural peptides such as glucagon, somatostatin, VIP (vasoactive intestinal peptide), and gastrin is minimal because of their hydrolysis by the peptidases on the apical surface of the airway and alveolar epithelium [55, 89, 222]. The bioavailability of these peptides can be significantly improved by blocking their N or C terminal ends [55]. For instance, the high availability of used calcitonin (salmon or human) is attributed to its resistance to peptidases because of the presence of a cyclic ring on one end of the molecule [55]. Likewise, the high bioavailability of leuprolide (1.2 kDa) is attributed to having both C- and N-terminals blocked [77]. Using protease inhibitors in the formulations could improve the

bioavailability of insulin and salmon calcitonin; however, protease inhibitors are toxic for the lung tissue [223, 224]. PEGylation has been shown to protect glucagon-like peptide-1, fibronectin, and calcitonin against the proteolytic breakdown in lung homogenate likely through steric hindrance [87, 225-228]. Such an effect was not observed for anti-IL13 Fab' (~ 45 kDa) upon PEGylation with 40 kDa PEG presumably due to the inherent resistance of naked Fab' to lung proteases [153].

The lining fluids of healthy lungs have low protease activity due to the secretion of abundant antiproteases eventually minimising the clearance of most proteins by this mechanism [10, 89]. Commonly found antiproteases in the lungs are serpins (inhibitors of serine proteases), TIMPs (inhibitors of metalloproteinases), cystatins (inhibitors of cysteine proteases), elafin, and SLPI (secretory leukoprotease inhibitor) [218, 229]. The enzymatic breakdown of large proteins occurs mostly inside lysosomes after being taken up by macrophages and epithelial cells [55]. They are partially spared form the action of peptidases because their poor fit in the catalytic clefts of the peptidase due to their large size or sometimes buried terminal ends [55]. However, since their absorption is slower than peptides, they are more likely to be affected by degradation and aggregation in contact with surfactant then captured by macrophages [55]. The balance protease/antiprotease could be shifted by the release of proteases into the lung fluids during infection and inflammation by immune cells. Protein contact with surface fluids (mucus, PCL, and surfactant) might cause aggregation/precipitation, which causes a loss of activity and accelerate the uptake and enzymatic degradation by macrophages [55].

III. PEGYLATED PROTEINS

PEGylation is the covalent attachment of PEG chains to proteins or other molecules [87, 230]. The term PEGylation has also been used loosely to describe noncovalent attachments [231, 232]. It was first described by Davis and Abouchowski in their seminal work on bovine serum albumin and catalase [233, 234]. The primary goal was to decrease the immunogenicity of non-human proteins intended for human therapy before recombinant proteins were widely available [235]. PEGylation had shown for the first time that such an extensive modification was not as detrimental as thought and could preserve at least some activity of the proteins [230]. Several years later (1990), this strategy culminated in the approval of the first PEGylated protein, pegademase (Adagen®), a bovine adenosine deaminase. Since then, a variety of chemical and enzymatic methods of PEGylation have been developed, and more than a dozen other products are currently marketed (Table 10) [236].

III.1. PROTEIN PEGYLATION

The traditional or "first-generation" PEGylation reactions were random as they lacked site-specificity [237]. They typically relied on amine conjugation through acylation or alkylation; other chemistries were also common [230, 231, 238]. The major drawbacks of this reaction are the massive loss in the activity due to interference with the active site and the generation of a mixture of highly heterogeneous (usually multi-PEGylated) products. This required extensive purification steps and caused difficulties in the characterisation of the final products, which was problematic from a regulatory standpoint [236]. For instance, the chromatography separation of Pegintron® (pegylated recombinant interferon α 2b) revealed up to 15 isomers and only retained 8% to 37% of the original activity of the non-conjugated protein [239]. Nevertheless, first-generation PEGylation is not entirely ineffective as most of the PEGylated drugs on the market are not produced by site-specific conjugation [231, 236]. The site-specific conjugation known as the "second generation PEGylation" has ensued in the hope to offer better-defined products but mostly to preserve more activity of the native protein [231]. It was greatly facilitated by the introduction of more specific functions of PEG molecules, allowing targeting specific moieties on the proteins [240, 241]. Site-specific conjugation is either chemical or enzymatic. N-terminal PEGylation, thiol and bridging PEGylation, and histidine tags are the most common examples of chemical methods while transglutaminase-mediated and GlycoPEGylation are examples of enzymatic PEGylation [156, 242].

Reversible conjugation of PEG to proteins through cleavable linkages has also been achieved; it presumably offers a controlled release and less inhibition of the protein [243]. Reversible PEGylation by noncovalent binding (chelation, hydrophobic, and electrostatic interactions) of modified PEG to proteins has also been demonstrated [232, 244]. The goal is to avoid the loss of protein activity while increasing the half-life classically achieved by covalent PEGylation [156]. This strategy was shown effective in suppressing or retarding the aggregation of hen egg-white lysozyme after mixing with PEGs featuring certain hydrophobic head groups such as cholesteryl, dansyl, phenylbutylamino, and tryptophan [245]. Nitrilotriacetic acid-modified PEG and polyelectrolyte functionalised PEGs have been used for ionic interactions and chelation, respectively [246, 247]. Mero *et al.* assessed the pharmacokinetics properties of PEG conjugates to G-CSF by chelation in rats; however, no significant improvement has been reported [247].

III.2. IMPACT OF PEGYLATION ON THERAPEUTIC PROTEINS

Although initially introduced to decrease the immunogenicity of proteins, PEGylation is unequivocally praised for its ability to increase the half-life of protein in the blood circulation after IV or SC injection [231, 235]. It is also the most established half-life extension strategy in clinical use [248]. Other benefits include (i) improving the solubility and stability of proteins, (ii) reducing recognition and degradation by proteolytic enzymes, and (iii) shielding receptor-mediated uptake by the reticuloendothelial system [230, 241, 249-252]. The increased blood circulation time is achieved through the expanded hydrodynamic volume of protein due to the highly solvated PEG in aqueous solution beyond the cut-off of glomerular filtration (for PEG $\geq$ 20 kDa) [253]. This effect depends on the biophysical size, whereas conferring protection against proteolysis and "stealth" properties can also be involved [231, 254]. Ameliorating the pharmacokinetic properties implies reducing the dosage and frequency of administration, thereby improving the comfort of patients [156, 231].

These advantages come at the expense of a frequent loss of biological potency of the proteins, which seldom remains unaltered upon PEGylation [87]. The loss of activity is due to the interference with the active site of the enzymes or the protein/receptor recognition process [237]. Retaining the full enzymatic activity seems to be the exception as it is the case for rhDNase [83, 255, 256].

The effectiveness of PEGylation in prolonging the residence time of several proteins in the lungs after pulmonary delivery has also been demonstrated [87]. The residence times were reportedly extended to at least 48 hours for linear 20 kDa (PEG20) a1-proteinase inhibitor [257], branched 2-

arm 40 kDa PEG (PEG40) F(ab')2 and PEG40 Fab' antibody fragments compared with less than 24 hours for their non-PEGylated counterparts [96, 153, 154]. Following pulmonary delivery in rats, PEGylation was also reported to decrease the bioavailability of proteins such as recombinant human granulocyte-colony stimulating factor (rhGCSF, 18 kDa) and IFNα2b (19 kDa) [80, 212]. Readers interested in the impact of PEGylation on the pulmonary delivery of biopharmaceuticals are directed to the review by Guichard *et al.* [87].

The long half-life of PEG in the body raises concerns of accumulation in macrophages in several tissues and epithelial cells in the kidneys, choroid plexus, pituitary gland, and choroid of the eye [258]. These toxicities were considered only adverse for PEG doses higher than 120 mg/kg/week [258]. Other drawbacks include (i) the heterogeneity of PEG and PEGylated products (ii) difficulties in purification and characterisation of the final products, (iii) low PEGylation yield, and (iv) production of antibodies against PEG and PEGylated proteins [259, 260]. Many of these drawbacks can be offset by the net gain in efficacy (lower dosage and frequency and better therapeutic coverage), resulting in an overall added value to patients *via* reduced cost, increased comfort, and better compliance [240].

Table 10. FDA approved PEGylated proteins. Adapted from [261-263]

Protein name	Trade name (s)	PEG MW in kDa (units)	Indication	Company	Route	Year	Protein origin	T ½ (h)	Ref
Adenosine deaminase	Adagen	5 (11-17)	SCID	Enzon	IM	1990	Bovine intestine	48-72	
L-asparaginase	Oncaspar	5 (69–82)	ALL	Enzon	IM, IV	1994	E. coli	357 ± 243	[264]
interferon α2b	PegIntron, Sylatron	12	Hepatitis C	Schering-Plough	SC	2000	HR (E. coli)	48–72	[239]
interferon α2a	Pegasys	40	Hepatitis C	Roche	SC	2002	HR (E. coli)	65	
Granulocyte Colony Stimulating Factor (G-CSF)	pegfilgrastim, Neulasta, Pelmeg	20	Neutropenia	Amgen	SC	2002	HR (E. coli)	42	
	Fulphila (biosimilar)	20	Neutropenia	Mylan		2018			
Growth hormone receptor antagonist	Pegvisomant, Somavert	5 (4-6)	Acromegaly	Pfizer	SC	2002	HR (E. coli)	6 days	
Continuous erythropoiesis receptor activator	Mircera	30	Anemia associated with chronic kidney diseases	Roche	SC, IV	2007	HR(CHO)	142	
Anti-TNFα Fab	Cimzia	40	Crohn's disease Rhumatoïd arthritis	UCB Pharma	SC	2007			
Mammalian urate oxidase (Uricase)	Krystexxa*	10 (10-11)	Gout	Savient	IV	2010		10–12 d	
Erythropoietin (EPO) mimetic peptide	Omontys		Anaemia	Affymax	IV, SC	2012		60	
Interferon β-1a	Plegridy		Relapsing multiple sclerosis	Biogen Idec	SC	2014			
Factor VIII	Adynovate	20 (2)	Haemophilia A	Baxalta	IV	2016	HR (CHO)		
Factor IX	Rebinyn	40	Haemophilia B	Novo Nordisk	SC	2017			

Phenylalanine ammonia lyase	Palynziq	9	PAL replacement therapy	BioMarin Pharmaceutical	SC	2018	Bacterial enzyme
Adenosine deaminase	Revcovi	5.6 (13)	SCID	Leadiant Biosciences	IM	2018	recombinant bovine (E. Coli)
L-asparaginase	Asparlas	5 (31-39)	ALL	Servier	IV	2018	E. coli enzyme
B domain-deleted FVIII	Jivi	60 (30 x 2)	Hemophilia A	Bayer	IV	2018	
Factor VIII	Esperoct		Haemophilia A	Novo Nordisk	IV	2019	14

*** Withdrawn from EMA in 2016; SCID, severe combined immunodeficiency disease; PAL, phenylalanine; HR, human recombinant; ALL, acute lymphoblastic leukaemia**

III.3. PHARMACOKINETICS OF PEGS AND PEGYLATED PROTEINS

The pharmacokinetics (PK) is the study of the fate of compounds in the living organism by describing their absorption, distribution, metabolism, and excretion [265]. PK study is important to understand and predict drugs' efficacy and safety [266]. The PK of PEGylated proteins (as any other drug) is usually well studied before obtaining the approval of the health authorities [267]. In most cases, the *in vivo* disposition of PEGylated proteins is heavily influenced by the size of the PEG and protein itself through potential receptor-mediated interactions specific to each protein [268]. Higher MW PEGs show overall slower metabolism and renal clearance, therefore, have a greater potential of increasing blood half-life, but also tissue accumulation and potential adverse effects [258, 268].

III.3.1. *Absorption*

All PEGylated proteins on the market are given by IV or SC injections, little is known about other routes of administration except the few preclinical studies after pulmonary delivery. The general assumption of the lower absorption of higher MW proteins seems to hold for PEGylated proteins, *i.e.* the higher the MW of the PEG (therefore the PEGylated protein), the less the absorption [268]. After SC administration, PEGylated proteins are usually absorbed at a slower rate than their non-PEGylated counterparts [268]. Due to the limited permeability of large macromolecules across the vascular endothelia into the blood capillaries, the absorption of large proteins form the interstitial fluid through the lymphatic capillaries becomes more important [269]. Interestingly, the SC absorption of PEGylated proteins occurs at similar rate and extent as proteins of similar MWs [10]. The oral absorption of PEGs in humans decreases with increasing MW and is almost absent at 3.4 kDa [268, 270].

- **Absorption by the pulmonary route**

After pulmonary delivery in rats, the serum concentration of PEG-FITC of 2 and 5 kDa were negligible [210]. The authors did not exclude absorption and suggested instead a potential absorption of PEGs followed by rapid clearance by the kidneys [210]. The PEGylation was found to (i) delay the time to maximal plasma concentration (Tmax), (ii) generally multiply the area under the curve (AUC), and (iii) prolong the plasma half-life of the PEGylated proteins (Table 11) [87]. These observations were correlated with the size of PEG. The increased AUC was, however, due to the prolonged half-life rather than enhanced absorption or bioavailability [87].

Table 11. PK parameters of PEGylated proteins and peptides administered by the pulmonary route.

Compound	MW (kDa)	PEG (kDa)	AUC ratio*	Species	Route	Tmax (min)	T1/2 (min)	F (%)	reference
glucagon-like peptide-1	3.3	native	1	rat	it	9	-	-	[228]
		2	3			23	-	-	
		5	8			42	-	-	
		10	11			82	-	-	
Salmon calcitonin	3.4	native	1	rat	it	15	35	-	[225]
		2	4			22	101	-	
		5	7			25	119	-	
insulin	5.8	native	1			15-24			[254, 256]
		0.75	> 1.2	rat	it	78-210	↑		
		2	5	dog	inhalation				
		5	-	rat	it			Poor	
rhGCSF	19.6	native	1	rat	it	160	-	16	[80]
		6	-			270	-	4.5	
		12	-			375	-	1.2	
IFNα2b	19	native	1	rat	it	-	-	15	[212]
		12	-			-	-	5.5	
		40	8			-	-	<0.4	

***** Relative to nonPEGylated protein; it, intratracheal instillation

III.3.2. *Distribution*

The distribution of PEGylated proteins is not entirely elucidated; however, the available literature indicates that their fate is largely governed by the PEG properties and the protein [268]. Large PEGs and PEGylated proteins are generally observed in highly perfused organs (i.e. lungs, liver, kidney, heart, and spleen) and the target organs which vary depending on the conjugated protein [268, 271]. PEGs larger than 20 kDa are retained more in the blood circulation but also distribute to peripheral organs and tissues, however much less compared with smaller PEGs [267, 271, 272]. The non-specific distribution is mostly attributed to the PEG moiety; however, uptake and accumulation of PEGylated proteins in specific tissues and organs arise from the presence of binding sites or receptors for the specific proteins. For example, the specific ependymal cell vacuolation observed with PEGylated hGH is attributed to the specific uptake of growth hormone by the ependymal cells [268].

After decoupling of the PEG moiety, its tissue distribution is overall similar to that of the unconjugated PEG [268]. Wang *et al.* have shown that 40 kDa branched 14C-PEGylated adnectin that targets both EGFR (epidermal growth factor receptor) and IGF-1R (insulin-like growth factor 1 receptor) was observed in highly perfused organs such as liver, lung, heart, and kidneys. Liver accumulation (thought to be specific because of the high expression level of EGFR in the liver) was also observed when adnectin was replaced with another protein that does not bind to the liver [273]. Authors suggested that accumulation in the liver might be simply due to phagocytosis by liver cells.

III.3.3. *Metabolism*

Phase 1 metabolism was shown to be minimal for low MW PEG (≤ 6 kDa). It involves alcohol dehydrogenase and perhaps P450 and sulphur transferases [274]. Ethylene glycol formation was suggested based on similar toxicities of PEGs to ethylene glycol and the presence of minor amounts of oxalic acid (the primary end product of ethylene glycol metabolism) in the urine after oral and IV injection [274, 275]. Nonetheless, no evidence of ethylene glycol formation has been demonstrated *in vivo* [274]. Chemical and biological chain cleavage was, however, proposed it involves CYP450-dependent oxidation and alcohol/aldehyde dehydrogenase [267].

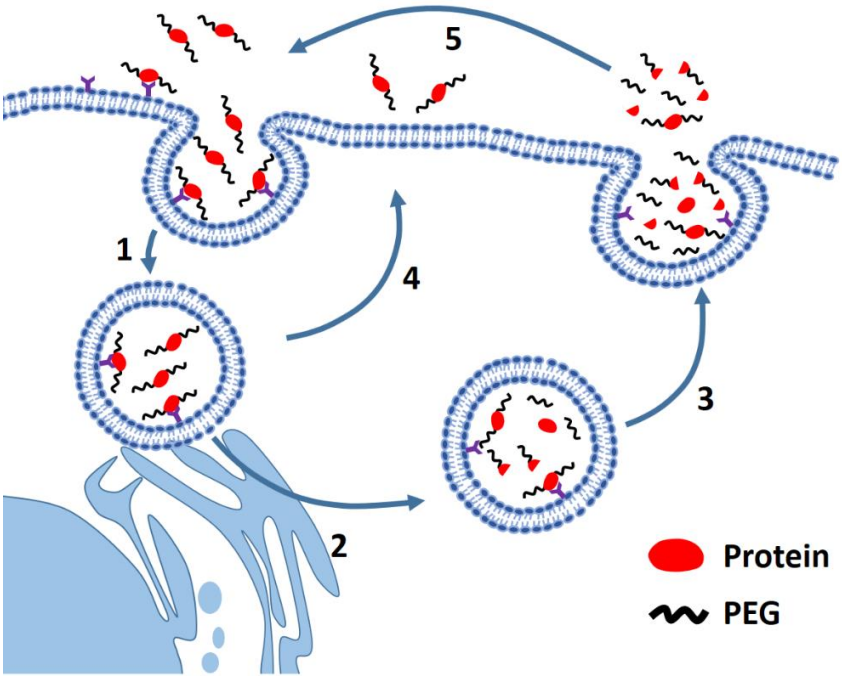

Figure 8. Proposed cellular uptake and processing pathways of PEGylated proteins. Adapted from [268]. PEGylated proteins can be internalised by pinocytosis or receptor-mediated endocytosis (1) then transported to lysosomes (2). PEGylated proteins are likely metabolised in the acidic environment of lysosomes, and their metabolites can be expelled from the cell (3). PEGylated protein can also be released from the cell without undergoing any metabolism (4). Expelled products can undergo processes 1-4 again in the same or remote tissue.

The degradation of protein could occur before and after the detachment of the PEG moiety [276, 277]. Branched PEGs could also be cleaved from the linker. PEG is thought to be internalised by cells by fluid-phase pinocytosis as there are no known receptors for PEG on the cell surface (Figure 8) [268]. Moreover, mammalian cells lack enzymes capable of degrading PEGs (etherases), which might be the reason for their accumulation in lysosomes [278]. The degradation of PEG is very slow, and it is not known whether the PEG is expelled from the cell by exocytosis or released as a result of cell turnover [268].

III.3.4. *Excretion*

PEGs are predominately excreted unchanged in the urine [279]. Generally speaking, the clearance of PEGylated moiety markedly decreases when the MW of the attached PEG is 30 kDa or higher [268]. Liver clearance of PEG increases significantly above 50 kDa [267]. However, PEGs of larger size (40 kDa), initially thought not to be filtered by renal glomeruli, were shown to be excreted unchanged in the urines of mice, rats, and humans [277, 280, 281]. Even PEG of 60 kDa (branched 2 x 30 kDa) was found nearly unchanged in the urine of rats 7 days after IV injection [271]. The elimination of 40 kDa branched PEG was very slow after the administration of insulin or erythropoiesis-stimulating agent conjugates (peginesatide), and PEG was detected in rats up to 28

and 60 days, respectively [276, 282]. Unlike proteins which are generally in a condensed state, PEG is a flexible polymer which can be extruded through small pores through changing its shape (reptation) [268]. Bauman *et al.* proposed the existence of two general pathways of PEG elimination, one rapid pathway consisting of the clearance by the kidneys and a slower pathway resulting from the slow cell release of ingested PEG by exocytosis or cell turnover [268]. Biliary excretion via hepatocyte and/or Kupffer cell uptake is also possible in the liver [283].

The life span of the cell in different tissues could be the rate-limiting factor. For instance, vacuolation tends to be observed in cells with longer life span such as macrophages and ependymal cells of the choroid plexus. However, in the case of macrophages, this is more expected due to their active role in clearance overall [268]. Bauman *et al.* argued that vacuolation is unlikely seen in neutrophils for pegfilgrastim, which is internalised into neutrophils by a receptor-mediated process because neutrophils do not survive more than one day [268]. The accumulated PEG in cells and tissues return to the lymphatics and blood to be ultimately eliminated primarily by renal filtration [268].

IV. PEGYLATED RHDNASE

IV.1. HUMAN DEOXYRIBONUCLEASE I

Deoxyribonuclease I (DNase I) belongs to the family of endonucleases which catalyse the hydrolysis of extracellular DNA by cleaving the phosphodiester bonds of double-stranded DNA [284]. Endogenous DNase I is secreted by the pancreas and parotid glands suggesting a primary role in digesting nucleic acids in the GI tract [285]. It is also present in blood and urine as well as other tissues, suggesting additional roles [284, 286]. Human DNase I is a monomeric glycoprotein of 260-amino acid chain and predicted MW of 29.3 kDa but an electrophoretic size of ca. 37 kDa on polyacrylamide gel due to the N-linked glycosylation [285]. The protein also has four cysteine residues giving rise to two disulfide bonds and has a calculated pI of 4.58, making it an acidic protein.

Recombinant human DNase I (rhDNase) was approved by the FDA in 1993 for the treatment of CF lung disease [2]. It is produced in Chinese hamster ovary cells with DNA encoding for the native human protein [4] and is commercialised under the name of Pulmozyme® (dornase alfa) (Genentech, Inc. South San Francisco, CA, USA). Tigerase® (Generium Pharmaceuticals) is a new biosimilar of dornase alfa approved in Russia in 2019.

IV.1.1. *Cystic fibrosis*

CF, first described in 1938, is the most prevalent multi-organ genetic disorder, caused by an autosomal recessive mutation in the gene coding for CF transmembrane conductance regulator (CFTR)[287]. CF occurs in every 2500 births, more common in the Caucasian ethnicity, although virtually found in all ethnic groups [288].

CFTR is present on the apical membrane of epithelial cells in several body systems, particularly in exocrine glands [288]. It functions as a chloride channel, but also regulates the activity of other ion channels such as the epithelial sodium channel (ENaC) and bicarbonate transport. Since its discovery in 1989, more than 2000 different variants of the CFTR gene have been identified, many of which have unclear clinical implications or are not associated with the development of CF [288]. Different classes (I to VI) of CFTR gene mutations affecting the structure or the function of the protein have been described; the most common is p.Phe508del. Mutations in classes I to III tend to cause more severe disease than those in classes IV to VI [289].

Defective or absent CFTR protein on the apical membrane of lung epithelial cells impairs the transport of ions and lead to uncontrolled activity of ENaC and therefore surface liquid dehydration. Dehydrated surface liquid affects the cilia beating function and the self-cleaning mechanism of the lungs, leading to recurrent cycles of airways obstruction, infection and inflammation [30]. Others hypotheses have been proposed to explain other classical features of CF such as susceptibility to chronic airway infections, impaired innate immunity and abnormally raised inflammation thought to be involved in airway remodelling from a young age [290].

Most of the morbidity and mortality of patients with CF is due to chronic airway infections leading overtime to irreversible respiratory failure. As predicted median life expectancy for CF has gone up (47.4 for newborns in 2018) [291], multisystem complications, such as diabetes, osteoporosis, liver disease, loss of fertility (in males), and depression are becoming more important [290].
The treatment of CF is ideally provided by a multidisciplinary team (pulmonologist, physiotherapist, dietician, clinical psychologist, endocrinologist, gastroenterologist, social worker, specialist nurse, pharmacist etc.). For lung disease, chest physiotherapy remains one of the treatment pillars. Treating and preventing infections by oral and/or inhaled antibiotics is crucial as well as eradication of P. aeruginosa at the first positive culture. For patients chronically colonised with P. aeruginosa, chronic suppressive antimicrobial therapy is recommended (inhaled tobramycin, colistin, aztreonam lysine, and levofloxacin) [290]. Reducing the frequency of episodes of pulmonary exacerbations is important, as exacerbations are responsible for irreversible loss in lung function in 25% of patients. Inhaled antibiotics, chronic azithromycin and mucolytic therapies (i.e. rhDNase, hypertonic saline, and mannitol) have been shown to reduce the frequency of exacerbations [290].

IV.1.2. *Clinical use of rhDNase*

Inhaled rhDNase reduces the viscoelasticity of sputum by cleaving the DNA released by neutrophils infiltrating infected airways in an attempt to combat infecting bacteria [19].
RhDNase is prescribed to patients with CF, in association with standard therapies for CF lung disease [292-294]. Several clinical trials have demonstrated the efficacy and safety of rhDNase therapy for CF in patients with mild to moderate lung disease (defined as a forced vital capacity (FVC) ≥ 40% of the predicted value) [295]. rhDNase was also shown to be safe and to improve lung function (expiratory volume in 1 second (FEV1) and FVC) and decreases the exacerbation rate in adults and children with CF [295]. A 12-week study has demonstrated that patients with advanced CF lung disease (FEV1 < 40% predicted) have also benefited from inhaled rhDNase [296].

RhDNase is approved for all ages in the US and for CF patients aged 5 years and older in Europe regardless of the severity of lung disease (although no registration studies have been performed in children younger than 6 years)[295]. Data in young children are still lacking; however, clinical indicators (e.g. pathology, pharmacokinetics, and pilot efficacy studies) suggest that rhDNase will be beneficial in CF patients under 5 year old [292, 295].

Younger patients are likely to benefit the most from long-term treatment with rhDNase and would maintain lung function at optimal levels, have lower infection risks, and a delayed progression of irreversible lung disease [295, 297, 298].

The recommended daily dose of rhDNase is 2.5 mg. Some patients might benefit from double the daily dosage and even alternative day dosing has been suggested [299]. rhDNase is administered by inhalation using jet and vibrating membrane nebulisers. This latter is considered more effective and faster (eFlow®, PARI Pharma, Munich, Germany) [255].

IV.1.3. *Limitations*

rhDNase suffers from several limitations including i) inhibition by Globular actin (G-actin) [300], ii) variation in the clinical response where around 30% of patients do not respond to rhDNase [301], and iii) short half-life in lungs, which requires administering the protein once to twice daily [285] which may lead to lower adherence of patients (mean adherence 59%) [302].

A few strategies were proposed to overcome these limitations. i) Enhancing the activity of rhDNase by increasing its binding affinity for DNA [303]; this was achieved by introducing positively charged residues (such as arginine and lysine) on rhDNase. ii) Producing actin-resistant variants of rhDNase by introducing charged, aliphatic or aromatic residues at the actin-binding interface of rhDNase [304]. Alidornase alfa (PRX-110), is an actin-resistant version of rhDNase which has successfully completed phase II clinical trials sponsored by Protalix (Karmiel, Israel) [305]. Combination of these two strategies (hyperactivity and actin-resistance) was also achieved; however, the level of hyperactivity was inversely proportional to DNA concentration and length. Therefore, the beneficial effect of hyperactive variants over non-modified rhDNase might be limited [305]. iii) Development of longer-acting versions of rhDNase by attaching PEG of 20 to 40 kDa [83, 255, 256].

IV.2. PEGYLATED RHDNASE

IV.2.1. *Production and purification*

PEGylation of rhDNase was successfully achieved with clinically available linear 20 kDa, linear 30 kDa and two-arm 40 kDa PEG (PEG20, PEG30, and PEG40 respectively) through site-specific conjugation to the N-terminal [255]. Figure 9 shows the coupling of aldehydes group of methoxy PEG propionaldehyde to the primary amines of rhDNase through a Schiff base, which is reduced to give a stable secondary amine linkage [306].

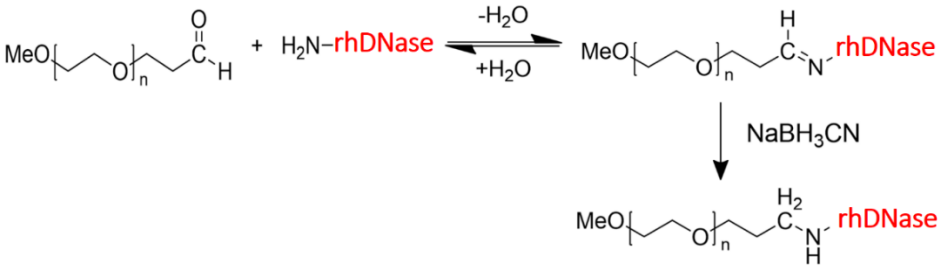

Figure 9. Scheme of the formation of a stable amino linkage between mPEG and rhDNase. Adapted from [306].

This reaction takes several hours to several days depending on the temperature, concentrations, and molar ratio of [PEG]:[rhDNase] [83, 255].

As most PEGylated proteins, PEGylated rhDNase was purified by ion-exchange chromatography (AEC) and size exclusion chromatography (SEC) [307]. PEGs do not have charge, therefore, are rapidly eluted by ion-exchange chromatography. At pH 7-8, rhDNase (pI 4.58 [285]) is negatively charged and binds to the positively charged groups of AEC column. The large size of PEG (20 to 40 kDa) significantly weakens the interaction of the protein with the column and allows the distinction of different PEGylated products [308]. PEG might also interact with some groups by hydrogen bonds of some amino acids thus changing their pKa, and perhaps shifting the pI of the protein [308]. SEC, on the other hand, allows a better separation of proteins based on their molecular size. However, the PEGs used have large hydrodynamic sizes usually close to that of the PEGylated rhDNase itself, leading to overlap in the elution peaks of PEG and PEGylated rhDNase. A common practice is to perform a first fast step of AEC with the sole purpose of getting rid of the PEG, followed by SEC to achieve the best separation between PEGylated and native rhDNase.

IV.2.2. *Activity of PEGylated rhDNase*

PEGylation was shown to preserve the secondary structure and the activity of rhDNase. Mono PEGylated rhDNase products retain their full biological activity as the PEG is attached on an opposite segment from the catalytic site of the protein [256]. This activity was shown *in vitro* on a solution of DNA and CF sputum [255, 256]. Of note, most PEGylated proteins on the market are less active than their non-PEGylated forms. For instance, only 7% and 28% of IFNα2a (Pegasys®) and adenosine deaminase (Adagen®) activity were retained after PEGylation, respectively [255]. Moreover, PEGylated rhDNase was stable (no denaturation or aggregation) to jet nebulisation currently used for the delivery of rhDNase.

IV.2.3. *Pharmacokinetics in the lungs*

The residence time of rhDNase in the lungs was extended from one day for the native rhDNase to over 20 days for the conjugated protein to PEGs of 30 and 40 kDa (PEG30-rhDNase and PEG40-rhDNase, respectively) after pulmonary delivery in mice. The length of presence time in the lungs correlated with the PEG size: the larger the PEG, the longer the presence in the lungs. Native and PEGylated rhDNase, measured by ELISA, were mainly found in the BAL and lung homogenate at early time points (< 4 h), then only in lung homogenates from day 3 onwards.
The sustained presence of active PEGylated rhDNase was verified by measuring the enzymatic activity of lung homogenates up to 20 days. PEG40-rhDNase remained as active at 15 days as at time zero; however, PEG20-rhDNase and PEG30-rhDNase progressively lost some of their activity over time.

IV.2.4. *Therapeutic efficacy in mice*

The therapeutic efficacy of PEGylated rhDNase was compared with that of rhDNase in β-ENaC mice (overexpressing β-epithelial Na+ channel), a murine model for CF [309]. β-ENaC mice suffer from chronic airway inflammation and mucus obstruction due to altered water and Na+ transport across airway epithelia similar to that observed in human CF patients. These mice have higher DNA content and inflammatory cytokines than wild type mice. A single-dose of PEG30-rhDNase or PEG40-rhDNase was as potent as 1 daily dose of rhDNase over 5 days in decreasing the concentrations of DNA in the respiratory secretions of β-ENaC mice (but not the wild type mice) compared to the control group which received only phosphate-buffered saline (Figure 10 A-C). No impact on cellular inflammation markers and cytokines in BAL was observed though. Similar results were obtained after 4 weekly doses of PEG30-rhDNase and PEG40-rhDNase (Figure 10

D-F). Moreover, both compounds exhibited a trend towards quelling inflammation by decreasing neutrophil counts in mice airways.

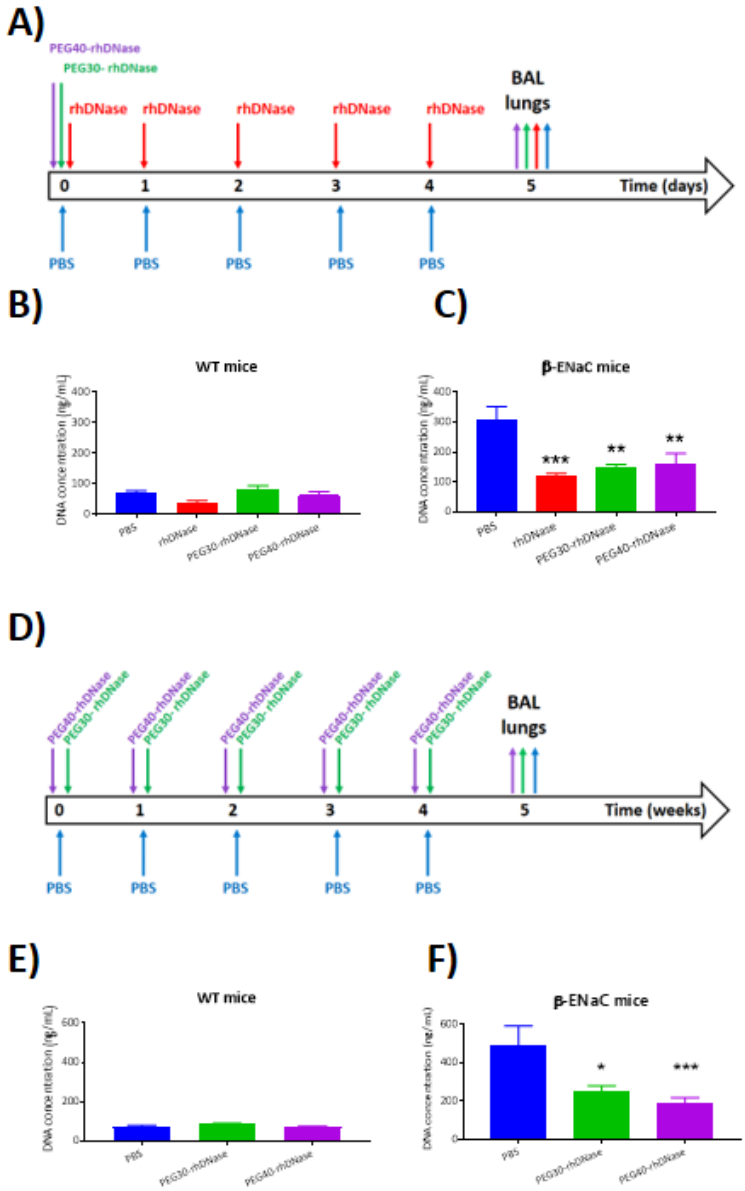

Figure 10. Short and long-term therapeutic efficacy study in β-ENaC mice (adapted form [83]). A-C, Short-term therapeutic efficacy study. One 10 µg unit dose of rhDNase, PEG30-rhDNase, or PEG40-rhDNase was intratracheally instilled in the lungs of β-ENaC mice and wild-type (WT) littermates. Timeline A), DNA content in BAL in WT (B) and β-ENaC mice (C) at day 5. D-F, Long-term therapeutic efficacy study. One 10 µg unit dose of PEG30-rhDNase or PEG40-rhDNase was intratracheally instilled in the lungs of β-ENaC mice and wild-type (WT) littermates. Timeline D), DNA content in BAL in WT (E) and β-ENaC mice (F) at week 5. The PEG was not counted in the mass of PEGylated rhDNase compounds delivered. Control mice were intratracheally instilled with phosphate buffer saline (PBS). Data are expressed as mean values (± SEM) of 4 to 7 mice per experimental group and were compared to the respective PBS group (one-way ANOVA, Dunnett's Multiple Comparison Test).

IV.2.5. *Safety*

Acute and repeated dose toxicity studies in healthy Swiss mice have demonstrated the innocuity of PEG30-rhDNase (the only PEG-rhDNase studied) to the lungs after pulmonary delivery. In the single-dose acute toxicity study, 100 μg of either rhDNase or equivalent in PEG30-rhDNase (4 mg/kg, estimated to be over 100 times the Phase III clinical high-dose) was delivered to mice *via* intratracheal instillation then mice were sacrificed on day 1 and day 14 (recovery group) after exposure. Both native and PEGylated rhDNase were well tolerated, and mice did not exhibit signs of respiratory distress, pulmonary inflammation, or clinical discomfort one and 14 days post-delivery. No significant differences were observed compared to the control group (given vehicle solution only) in terms of body weight, organ weight, or blood count [83].
The sub-chronic toxicity of PEGylated rhDNase was investigated over a period of four weeks by delivering a weekly dose of 100 μg of PEG30-rhDNase (rhDNase-equivalent) *via* intratracheal instillation. The evaluations were conducted one day and 4 weeks (recovery group) after the last dose. Only reversible higher total protein content was significant in the BAL of mice treated with PEG30-rhDNase as compared to the control. No histological evidence of significant inflammation or tissue damage in response to native or PEGylated rhDNase were found [83].
Finally, a chronic toxicity study over 12 weeks was performed only for PEG30-rhDNase (one dose per week) under two regimens, low dosage (10 μg) and high dosage (35 μg). Only an increase in basophil counts was observed for both treatment regimens compared to the control group; however, this increase was reversible after the recovery period. All other parameters were overall satisfactory [83].

IV.2.6. *Accumulation of PEGylated rhDNase in mice*

The concentrations of PEG30-rhDNase in lungs and sera of mice were measured to assess the potential lung accumulation and systemic absorption of PEG30 and rhDNase after single and repeated dose toxicity studies. As expected, higher amounts of PEG30-rhDNase were found in lung homogenates compared to BAL or alveolar macrophages [83].. The concentrations of rhDNase moieties measured 24 h after the last dose of PEG30-rhDNase in lung homogenates returned to the baseline levels 4 weeks after the end of exposure in the chronic exposure group [83]. The levels of PEG30-moiety displayed the same tendency; however, its total clearance was delayed compared to the rhDNase moiety. Low levels of rhDNase and PEG30 moieties were detected in AMs however for a longer period of time for the latter. Furthermore, rhDNase was detected in the sera of only rhDNase-treated group 24 h after single and repeated dose toxicity studies but not in PEG30-rhDNase-treated group. Only low concentrations of PEG30-moiety could be detected in the sera of PEG30-rhDNase group 24 h after single or repeated dose studies, but not after the recovery period. In conclusion, no significant accumulation of PEG in the lungs was found after repeated administrations over three months in mice [83].

V. CONCLUSIONS

Pulmonary delivery of therapeutic proteins is still a daunting challenge for the pharmaceutical industry. Despite the continuous attempts to make use of this seductive port of entry, research and development efforts have culminated in only one inhaled protein for the local treatment of CF, the mucolytic dornase alfa [310]. Proteins, by virtue of their large size, relative instability, and hydrophilic nature, have a mediocre lung penetration compared to small-molecule drugs following systemic delivery [49]. The systemic bioavailability of large proteins by inhalation is limited but still better than the oral route. Local delivery, on the other hand, present an attractive opportunity for the treatment of respiratory diseases such as asthma, COPD, alpha-1 antitrypsin deficiency, CF, and lung cancers [15]. It allows achieving higher concentrations of the protein to the target, rapid onset of the clinical response, and requires smaller doses compared to other parenteral routes; therefore, reducing systemic side effects [56, 93].

Delivery by inhalation requires preserving the structure and function of the proteins during the formulation and the aerosolisation steps. Because the lungs are exposed to continuous external assaults, they evolved to have highly efficient defence mechanisms against foreign invaders including particles and solutes. Inhaled therapeutic proteins can be eliminated by mucociliary clearance, absorbed through the respiratory epithelium, taken up and metabolised by lung cells (e.g. epithelial cells and AMs), and degraded in airspaces [12, 52, 89]. Because of these clearance mechanisms, delivered proteins to the lungs are cleared from airspaces within 24 h. This relatively short half-lives require frequent dosing regimen and might be a significant limitation for attaining the desired therapeutic efficacy.

Among the available protein conjugation strategies, PEGylation is the most promising one with tangible benefits in extending the half-life of proteins in the body following parenteral injections as well as in the lungs after pulmonary delivery. Previous works have established the extended retention of PEGylated proteins in the lungs after pulmonary administration in small animals [83, 96, 153, 154, 257]. The larger the PEG, the longer the retention [83]. Moreover, PEGylation is likely to increase the stability of the proteins and PEGs are compatible with inhalation devices. PEGylated proteins are generally stable in the same conditions as their native forms, promising thus a swift shift towards using them by inhalation without extra formulation efforts.

Several mechanisms by which PEG increases protein retention in the lungs have been proposed, including reduced systemic absorption, mucoadhesion, decreased uptake by respiratory cells, and protection against degradation in the lungs [87]. Nonetheless, most of these mechanisms remain largely unknown and therefore require further investigation.

VI. AIM

The conjugation of recombinant human deoxyribonuclease I (rhDNase) to large MW PEGs 30 and 40 kDa has been shown to prolong its local residence time in the lungs from less than 24 h to over 15 days [83].The increase in residence time was accompanied by retained activity against DNA in lung homogenates of the mice. A single dose of PEG30-rhDNase or PEG40-rhDNase over 5 days exhibited an equivalent DNA hydrolysis activity as five single doses of rhDNase (one dose per day for 5 days) in lungs of β-transepithelial Na+ channel–overexpressing mice (β-ENaC) [83]. Moreover, PEGylated rhDNase was shown to be stable to jet nebulisation, to not accumulate in the lungs after repeated administration, and to cause no lungs toxicity in acute and chronic toxicity studies.

These promising results raised questions on the mechanisms underlying the lung retention of PEGylated rhDNase. Therefore, **the present thesis aims to elucidate the mechanisms involved in the lung retention of PEGylated rhDNase.**

Objective 1: Investigate the fate of native and PEGylated rhDNase in the lungs following pulmonary delivery in mice.

Pharmacokinetics data in mice showed that PEGylated rhDNase was present in lungs for over 15 days; however, from day 3 onwards, PEGylated rhDNase was recovered only in lung homogenates and not in bronchoalveolar lavages (BALs) suggesting that PEGylated rhDNase either had penetrated the lung parenchyma or was firmly attached to respiratory epithelia. Moreover, since rhDNase cleaves extracellular DNA in the respiratory secretions of patients with CF, it is paramount to distinguish between the proportions of the enzyme in the lung parenchyma therefore unavailable from those in airspaces which are available to exert the intended mucolytic action. For this, confocal microscopy was carried out to give more information on the fate of native and PEGylated rhDNase within the lungs over time and distinguish between airway lumen and tissue parenchyma fractions.

Objective 2: Study the biodistribution of rhDNase and PEG30-rhDNase after pulmonary delivery in mice.

The elimination of PEGylated proteins from the lungs by systemic absorption would mean a risk of systemic toxicity while mucociliary clearance into the GI tract, then faeces is usually synonymous with a desirable safety profile. Organ distribution and elimination pathways were investigated by

following rhDNase and PEG30-rhDNase by near-infrared fluorescence (NIRF) imaging after intratracheal instillation and IV injection in mice.

Objective 3: Study the epithelial transport of native and PEGylated rhDNase across Calu-3 cells.

Absorption across lung epithelia is a significant pathway of clearance of low MW proteins and peptides, but less important for proteins of high MW (≥ 40 kDa). Furthermore, PEGylation was shown to decrease the bioavailability of proteins after pulmonary delivery in rats, and *in vitro* in cultures of lung epithelial Calu-3 cells [80, 154, 212]. Therefore, PEGylation of rhDNase was expected to diminish the lung absorption of rhDNase. To confirm this hypothesis, we quantified the transepithelial transport and intracellular uptake of native and PEGylated rhDNase in cultures of human broncho-epithelial cell line Calu-3 cultured at an air-liquid interface.

Objective 4: Assess the uptake of rhDNase and PEGylated rhDNase by macrophages

Alveolar macrophages contribute to the clearance of proteins in airways lumina [199, 209]. Here, we hypothesised that PEGylation decreases the macrophage uptake of rhDNase, thereby contributing to its extended retention in airways. Uptake of native and rhDNase conjugated to PEG20, PEG30, and PEG40 was assessed *in vivo* in mice as well as *in vitro* in two murine macrophage-like cell lines, interstitial J774 macrophages and alveolar MHS macrophages. Further studies were conducted to determine the endocytic pathway of rhDNase.

Objective 5: Study the interaction of native and PEGylated rhDNase with airway mucus

PEGylation has been reported to decrease protein interaction with mucus; however, long PEG chains might entangle with mucin fibres and produce the opposite effect [153]. This effect was shown for PEG 20 and 40 kDa conjugates of Fab' fragments in the mucus of healthy patients [153, 154]. To clarify this for native and PEGylated rhDNase, we investigated their diffusion and binding to porcine tracheal mucus and CF sputa by fluorescence recovery after photobleaching (FRAP). The transport across mucus layers mounted on Transwell® inserts was also assessed.

VII. REFERENCES

1. Walsh, G., *Biopharmaceutical benchmarks 2014*. Nature Biotechnology, 2014. **32**(10): p. 992-1000.
2. Walsh, G., *Biopharmaceutical benchmarks 2018*. Nat Biotechnol, 2018. **36**(12): p. 1136-1145.
3. Leader, B., Q.J. Baca, and D.E. Golan, *Protein therapeutics: A summary and pharmacological classification.* Nature Reviews Drug Discovery, 2008. **7**(1): p. 21-39.
4. Marx, V., *Watching peptide drugs grow up.* Chemical & Engineering News, 2005. **83**(11): p. 17-+.
5. Renukuntla, J., et al., *Approaches for enhancing oral bioavailability of peptides and proteins.* International Journal of Pharmaceutics, 2013. **447**(1-2): p. 75-93.
6. Agyei, D., et al., *Protein and Peptide Biopharmaceuticals: An Overview.* Protein and Peptide Letters, 2017. **24**(2): p. 94-101.
7. Morales, J.O., et al., *Challenges and Future Prospects for the Delivery of Biologics: Oral Mucosal, Pulmonary, and Transdermal Routes.* Aaps Journal, 2017. **19**(3): p. 652-668.
8. Weers, J.G., et al., *Pulmonary formulations: what remains to be done?* J Aerosol Med Pulm Drug Deliv, 2010. **23 Suppl 2**: p. S5-23.
9. van der Walle, C.F. and O. Olejnik, *Chapter 1 - An Overview of the Field of Peptide and Protein Delivery*, in *Peptide and Protein Delivery*, C. Van Der Walle, Editor. 2011, Academic Press: Boston. p. 1-22.
10. Tibbitts, J., et al., *Key factors influencing ADME properties of therapeutic proteins: A need for ADME characterization in drug discovery and development.* Mabs, 2016. **8**(2): p. 229-245.
11. Murray, J.E., N. Laurieri, and R. Delgoda, *Chapter 24 - Proteins*, in *Pharmacognosy*, S. Badal and R. Delgoda, Editors. 2017, Academic Press: Boston. p. 477-494.
12. Patton, J.S. and P.R. Byron, *Inhaling medicines: delivering drugs to the body through the lungs.* Nat Rev Drug Discov, 2007. **6**(1): p. 67-74.
13. Pfister, T., et al., *Bioavailability of Therapeutic Proteins by Inhalation-Worker Safety Aspects.* Annals of Occupational Hygiene, 2014. **58**(7): p. 899-911.
14. Gould, J.C., et al., *Bioavailability of protein therapeutics in rats following inhalation exposure: Relevance to occupational exposure limit calculations.* Regulatory Toxicology and Pharmacology, 2018. **100**: p. 35-44.
15. Hertel, S.P., G. Winter, and W. Friess, *Protein stability in pulmonary drug delivery via nebulization.* Advanced Drug Delivery Reviews, 2015. **93**: p. 79-94.
16. Depreter, F., G. Pilcer, and K. Amighi, *Inhaled proteins: Challenges and perspectives.* International Journal of Pharmaceutics, 2013. **447**(1-2): p. 251-280.
17. Rothe, C. and A. Skerra, *Anticalin(®) Proteins as Therapeutic Agents in Human Diseases.* BioDrugs : clinical immunotherapeutics, biopharmaceuticals and gene therapy, 2018. **32**(3): p. 233-243.
18. Dayan, A.D., *Pharmacological-Toxicological (Expert Report on Recombinant Human Deoxyribonuclease I (rhDNase; Pulmozyme™).* 1994. **13**(1_suppl): p. S2-S42.
19. Shak, S., *Aerosolized recombinant human DNase I for the treatment of cystic fibrosis.* Chest, 1995. **107**(2 Suppl): p. 65s-70s.
20. Janciauskiene, S.M., et al., *The discovery of alpha 1-antitrypsin and its rote in health and disease.* Respiratory Medicine, 2011. **105**(8): p. 1129-1139.
21. Edgar, R.G., et al., *Treatment of lung disease in alpha-1 antitrypsin deficiency: a systematic review.* International Journal of Chronic Obstructive Pulmonary Disease, 2017. **12**: p. 1295-1308.
22. Stolk, J., et al., *Efficacy and safety of inhaled a1-antitrypsin in patients with severe a1-antitrypsin deficiency and frequent exacerbations of COPD.* Eur Respir J, 2019. **54**(5).
23. Barrecheguren, M. and M. Miravitlles, *Treatment with inhaled a1-antitrypsin: a square peg in a round hole?* Eur Respir J, 2019. **54**(5).
24. Wenzel, S., et al., *Effect of an interleukin-4 variant on late phase asthmatic response to allergen challenge in asthmatic patients: results of two phase 2a studies.* Lancet, 2007. **370**(9596): p. 1422-31.
25. Slager, R.E., et al., *IL-4 receptor polymorphisms predict reduction in asthma exacerbations during response to an anti-IL-4 receptor alpha antagonist.* J Allergy Clin Immunol, 2012. **130**(2): p. 516-22.e4.
26. Anderson, G.P., et al., *Discovery of PRS-060, an inhalable CD123/IL4Ra/TH2 blocking anti-asthmatic anticalin protein re-engineered from endogenous lipocalin-1.* European Respiratory Journal, 2015. **46**.
27. Bruns, I., et al., *Phase 1 evaluation of the inhaled IL-4Ra antagonist, AZD1402/PRS-060, a potent and selective blocker of IL-4Ra.* European Respiratory Journal, 2019. **54**.
28. Thipphawong, J., *Inhaled cytokines and cytokine antagonists.* Advanced drug delivery reviews, 2006. **58**(9-10): p. 1089-1105.

29. Murthy, N., et al., *A macromolecular delivery vehicle for protein-based vaccines: Acid-degradable protein-loaded microgels.* Proceedings of the National Academy of Sciences of the United States of America, 2003. **100**(9): p. 4995-5000.
30. Otczyk, D.C. and A.W. Cripps, *Mucosal immunization: a realistic alternative.* Hum Vaccin, 2010. **6**(12): p. 978-1006.
31. Kunda, N.K., et al., *Pulmonary dry powder vaccine of pneumococcal antigen loaded nanoparticles.* Int J Pharm, 2015. **495**(2): p. 903-12.
32. Amorij, J.P., et al., *Needle-free influenza vaccination.* Lancet Infect Dis, 2010. **10**(10): p. 699-711.
33. Kristensen, D. and M. Zaffran, *Designing vaccines for developing-country populations: ideal attributes, delivery devices, and presentation formats.* Procedia in Vaccinology, 2010. **2**(2): p. 119-123.
34. Newman, S.P., *Drug delivery to the lungs: challenges and opportunities.* Therapeutic Delivery, 2017. **8**(8): p. 647-661.
35. Bellanti, J.A., et al., *Immunologic studies of specific mucosal and systemic immune responses in Mexican school children after booster aerosol or subcutaneous immunization with measles vaccine.* Vaccine, 2004. **22**(9-10): p. 1214-20.
36. Sabin, A.B., et al., *Successful Immunization of Children With and Without Maternal Antibody by Aerosolized Measles Vaccine: I. Different Results With Undiluted Human Diploid Cell and Chick Embryo Fibroblast Vaccines.* JAMA, 1983. **249**(19): p. 2651-2662.
37. Bennett, J.V., et al., *Aerosolized measles and measles-rubella vaccines induce better measles antibody booster responses than injected vaccines: randomized trials in Mexican schoolchildren.* Bulletin of the World Health Organization, 2002. **80**(10): p. 806-812.
38. Loira-Pastoriza, C., J. Todoroff, and R. Vanbever, *Delivery strategies for sustained drug release in the lungs.* Adv Drug Deliv Rev, 2014. **75**: p. 81-91.
39. Ugwoke, M.I., N. Verbeke, and R. Kinget, *The biopharmaceutical aspects of nasal mucoadhesive drug delivery.* J Pharm Pharmacol, 2001. **53**(1): p. 3-21.
40. Antosova, Z., et al., *Therapeutic application of peptides and proteins: parenteral forever?* Trends Biotechnol, 2009. **27**(11): p. 628-35.
41. Dumont, J.A., et al., *Delivery of an erythropoietin-Fc fusion protein by inhalation in humans through an immunoglobulin transport pathway.* J Aerosol Med, 2005. **18**(3): p. 294-303.
42. Bitonti, A.J. and J.A. Dumont, *Pulmonary administration of therapeutic proteins using an immunoglobulin transport pathway.* Advanced Drug Delivery Reviews, 2006. **58**(9-10): p. 1106-1118.
43. Bitonti, A.J., et al., *Pulmonary delivery of an erythropoietin Fc fusion protein in non-human primates through an immunoglobulin transport pathway.* Proc Natl Acad Sci U S A, 2004. **101**(26): p. 9763-8.
44. Matera, M.G., et al., *Monoclonal antibodies for severe asthma: Pharmacokinetic profiles.* Respiratory Medicine, 2019. **153**: p. 3-13.
45. Sécher, T., et al., *Therapeutic antibodies: A new era in the treatment of respiratory diseases?* Pharmacol Ther, 2018. **189**: p. 149-172.
46. Griese, M., et al., *alpha1-Antitrypsin inhalation reduces airway inflammation in cystic fibrosis patients.* Eur Respir J, 2007. **29**(2): p. 240-50.
47. Djukanović, R., et al., *The effect of inhaled IFN-β on worsening of asthma symptoms caused by viral infections. A randomized trial.* Am J Respir Crit Care Med, 2014. **190**(2): p. 145-54.
48. Respaud, R., et al., *Nebulization as a delivery method for mAbs in respiratory diseases.* Expert Opinion on Drug Delivery, 2015. **12**(6): p. 1027-1039.
49. Carter, P.J. and G.A. Lazar, *Next generation antibody drugs: pursuit of the 'high-hanging fruit'.* Nature Reviews Drug Discovery, 2018. **17**(3): p. 197-223.
50. Patton, J.S., *Mechanisms of macromolecule absorption by the lungs.* Advanced Drug Delivery Reviews, 1996. **19**(1): p. 3-36.
51. Codrons, V., et al., *Impact of formulation and methods of pulmonary delivery on absorption of parathyroid hormone (1-34) from rat lungs.* Journal of Pharmaceutical Sciences, 2004. **93**(5): p. 1241-1252.
52. Todoroff, J. and R. Vanbever, *Fate of nanomedicines in the lungs.* Current Opinion in Colloid & Interface Science, 2011. **16**(3): p. 246-254.
53. El-Sherbiny, I.M., et al., *Overcoming Lung Clearance Mechanisms for Controlled Release Drug Delivery*, in *Controlled Pulmonary Drug Delivery*, H.D.C. Smyth and A.J. Hickey, Editors. 2011. p. 101-126.
54. Ryan, G.M., et al., *Pulmonary Administration of PEGylated Polylysine Dendrimers: Absorption from the Lung versus Retention within the Lung Is Highly Size-Dependent.* Molecular Pharmaceutics, 2013. **10**(8): p. 2986-2995.

55. Patton, J.S., C.S. Fishburn, and J.G. Weers, *The lungs as a portal of entry for systemic drug delivery.* Proc Am Thorac Soc, 2004. **1**(4): p. 338-44.
56. Labiris, N.R. and M.B. Dolovich, *Pulmonary drug delivery. Part I: physiological factors affecting therapeutic effectiveness of aerosolized medications.* Br J Clin Pharmacol, 2003. **56**(6): p. 588-99.
57. Fischer, H. and J.H. Widdicombe, *Mechanisms of acid and base secretion by the airway epithelium.* The Journal of membrane biology, 2006. **211**(3): p. 139-150.
58. Siekmeier, R. and G. Scheuch, *Treatment of systemic diseases by inhalation of biomolecule aerosols.* J Physiol Pharmacol, 2009. **60 Suppl 5**: p. 15-26.
59. Agu, R.U., et al., *The lung as a route for systemic delivery of therapeutic proteins and peptides.* Respir Res, 2001. **2**(4): p. 198-209.
60. Lee, W.H., et al., *Nano- and micro-based inhaled drug delivery systems for targeting alveolar macrophages.* Expert Opin Drug Deliv, 2015. **12**(6): p. 1009-26.
61. Dolovich, M.B. and R. Dhand, *Aerosol drug delivery: developments in device design and clinical use.* Lancet, 2011. **377**(9770): p. 1032-45.
62. Zhong, Q., et al., *Effect of the Route of Administration and PEGylation of Poly(amidoamine) Dendrimers on Their Systemic and Lung Cellular Biodistribution.* Molecular Pharmaceutics, 2016. **13**(6): p. 1866-1878.
63. Wang, W., *Protein aggregation and its inhibition in biopharmaceutics.* Int J Pharm, 2005. **289**(1-2): p. 1-30.
64. Wang, W., S. Nema, and D. Teagarden, *Protein aggregation-Pathways and influencing factors.* International Journal of Pharmaceutics, 2010. **390**(2): p. 89-99.
65. Roberts, C.J., *Therapeutic protein aggregation: mechanisms, design, and control.* Trends in Biotechnology, 2014. **32**(7): p. 372-380.
66. Philo, J.S. and T. Arakawa, *Mechanisms of Protein Aggregation.* Current Pharmaceutical Biotechnology, 2009. **10**(4): p. 348-351.
67. Chang, L.L. and M.J. Pikal, *Mechanisms of protein stabilization in the solid state.* J Pharm Sci, 2009. **98**(9): p. 2886-908.
68. Manning, M.C., K. Patel, and R.T. Borchardt, *Stability of protein pharmaceuticals.* Pharm Res, 1989. **6**(11): p. 903-18.
69. Manning, M.C., et al., *Stability of Protein Pharmaceuticals: An Update.* Pharmaceutical Research, 2010. **27**(4): p. 544-575.
70. Berrill, A., J. Biddlecombe, and D. Bracewell, *Chapter 13 - Product Quality During Manufacture and Supply*, in *Peptide and Protein Delivery*, C. Van Der Walle, Editor. 2011, Academic Press: Boston. p. 313-339.
71. Frokjaer, S. and D.E. Otzen, *Protein drug stability: A formulation challenge.* Nature Reviews Drug Discovery, 2005. **4**(4): p. 298-306.
72. Lowe, D., et al., *AGGREGATION, STABILITY, AND FORMULATION OF HUMAN ANTIBODY THERAPEUTICS*, in *Advances in Protein Chemistry and Structural Biology, Vol 84*, R. Donev, Editor. 2011. p. 41-61.
73. Mahler, H.C., et al., *Protein Aggregation: Pathways, Induction Factors and Analysis.* Journal of Pharmaceutical Sciences, 2009. **98**(9): p. 2909-2934.
74. Chandel, A., et al., *Recent advances in aerosolised drug delivery.* Biomedicine & Pharmacotherapy, 2019. **112**: p. 108601.
75. Martin, A.R. and W.H. Finlay, *Nebulizers for drug delivery to the lungs.* Expert Opinion on Drug Delivery, 2015. **12**(6): p. 889-900.
76. Bodier-Montagutelli, E., et al., *PROTEIN STABILITY DURING NEBULIZATION: HOW TO MANAGE THE COLLECTION STEP?* Journal of Aerosol Medicine and Pulmonary Drug Delivery, 2019. **32**(3): p. A20-A20.
77. Clark, A.R., C.L. Stevenson, and S.J. Shire, *Formulation of Proteins for Pulmonary Delivery*, in *Protein Formulation and Delivery*, E. McNally and J. Hastedt, Editors. 2008, Boca Raton: CRC Press.
78. Scherer, T., et al., *A technical feasibility study of dornase alfa delivery with eFlow® vibrating membrane nebulizers: aerosol characteristics and physicochemical stability.* Journal of pharmaceutical sciences, 2011. **100**(1): p. 98-109.
79. Niven, R.W., et al., *SOME FACTORS ASSOCIATED WITH THE ULTRASONIC NEBULIZATION OF PROTEINS.* Pharmaceutical Research, 1995. **12**(1): p. 53-59.
80. Niven, R.W., et al., *The pulmonary absorption of aerosolized and intratracheally instilled rhG-CSF and monoPEGylated rhG-CSF.* Pharm Res, 1995. **12**(9): p. 1343-9.

81. Cipolla, D.C. and I. Gonda, *Method for Collection of Nebulized Proteins*, in *Formulation and Delivery of Proteins and Peptides*. 1994, American Chemical Society. p. 343-352.
82. Johnson, J.C., et al., *Aerosol delivery of recombinant human DNase I: in vitro comparison of a vibrating-mesh nebulizer with a jet nebulizer.* Respir Care, 2008. **53**(12): p. 1703-8.
83. Guichard, M.J., et al., *PEGylation of recombinant human deoxyribonuclease I provides a long-acting version of the mucolytic for patients with cystic fibrosis (Submitted).*
84. Niven, R.W., et al., *Protein nebulization: I. Stability of lactate dehydrogenase and recombinant granulocyte-colony stimulating factor to air-jet nebulization.* International Journal of Pharmaceutics, 1994. **109**(1): p. 17-26.
85. Hertel, S., et al., *That's cool!--Nebulization of thermolabile proteins with a cooled vibrating mesh nebulizer.* Eur J Pharm Biopharm, 2014. **87**(2): p. 357-65.
86. Respaud, R., et al., *Effect of formulation on the stability and aerosol performance of a nebulized antibody.* MAbs, 2014. **6**(5): p. 1347-55.
87. Guichard, M.J., T. Leal, and R. Vanbever, *PEGylation, an approach for improving the pulmonary delivery of biopharmaceuticals.* Current Opinion in Colloid & Interface Science, 2017. **31**: p. 43-50.
88. Villegas, M.R., A. Baeza, and M. Vallet-Regi, *Nanotechnological Strategies for Protein Delivery.* Molecules, 2018. **23**(5).
89. Hastings, R.H., H.G. Folkesson, and M.A. Matthay, *Mechanisms of alveolar protein clearance in the intact lung.* American Journal of Physiology-Lung Cellular and Molecular Physiology, 2004. **286**(4): p. L679-L689.
90. Carvalho, T.C., J.I. Peters, and R.O. Williams, 3rd, *Influence of particle size on regional lung deposition--what evidence is there?* Int J Pharm, 2011. **406**(1-2): p. 1-10.
91. Frohlich, E., *Toxicity of orally inhaled drug formulations at the alveolar barrier: parameters for initial biological screening.* Drug Delivery, 2017. **24**(1): p. 891-905.
92. Webster, M.J. and R. Tarran, *Slippery When Wet: Airway Surface Liquid Homeostasis and Mucus Hydration*, in *Cell Volume Regulation*, I. Levitane, E. Delpire, and H. RasgadoFlores, Editors. 2018. p. 293-335.
93. Osman, N., et al., *Carriers for the targeted delivery of aerosolized macromolecules for pulmonary pathologies.* Expert Opinion on Drug Delivery, 2018. **15**(8): p. 821-834.
94. Meyerholz, D.K., et al., *9 - Respiratory System*, in *Comparative Anatomy and Histology (Second Edition)*, P.M. Treuting, S.M. Dintzis, and K.S. Montine, Editors. 2018, Academic Press: San Diego. p. 147-162.
95. Fernandes, C.A. and R. Vanbever, *Preclinical models for pulmonary drug delivery.* Expert Opin Drug Deliv, 2009. **6**(11): p. 1231-45.
96. Freches, D., et al., *PEGylation prolongs the pulmonary retention of an anti-IL-17A Fab' antibody fragment after pulmonary delivery in three different species.* Int J Pharm, 2017. **521**(1-2): p. 120-129.
97. Autifi, M., A. EL-Banna, and A. El- Sayed Ebaid, *Morphological study of rabbit lung, bronchial tree and pulmonary vessels using corrosion cast technique.* AAMJ, 2015. **13**(3).
98. Harkema, J.R., S.A. Carey, and J.G. Wagner, *The Nose Revisited: A Brief Review of the Comparative Structure, Function, and Toxicologic Pathology of the Nasal Epithelium.* Toxicologic Pathology, 2006. **34**(3): p. 252-269.
99. Chamanza, R. and J.A. Wright, *A Review of the Comparative Anatomy, Histology, Physiology and Pathology of the Nasal Cavity of Rats, Mice, Dogs and Non-human Primates. Relevance to Inhalation Toxicology and Human Health Risk Assessment.* J Comp Pathol, 2015. **153**(4): p. 287-314.
100. Miller, F.J., R.R. Mercer, and J.D. Crapo, *Lower Respiratory Tract Structure of Laboratory Animals and Humans: Dosimetry Implications.* Aerosol Science and Technology, 1993. **18**(3): p. 257-271.
101. Kuempel, E.D., et al., *Evaluating the mechanistic evidence and key data gaps in assessing the potential carcinogenicity of carbon nanotubes and nanofibers in humans.* Critical reviews in toxicology, 2017. **47**(1): p. 1-58.
102. Hsia, C.C., D.M. Hyde, and E.R. Weibel, *Lung Structure and the Intrinsic Challenges of Gas Exchange.* Compr Physiol, 2016. **6**(2): p. 827-95.
103. Shapiro, S.D., *Animal models of asthma: Pro: Allergic avoidance of animal (model[s]) is not an option.* Am J Respir Crit Care Med, 2006. **174**(11): p. 1171-3.
104. Valerius, K.P., *Size-dependent morphology of the conductive bronchial tree in four species of myomorph rodents.* J Morphol, 1996. **230**(3): p. 291-7.
105. Gonda, I., *Systemic delivery of drugs to humans via inhalation.* Journal of Aerosol Medicine-Deposition Clearance and Effects in the Lung, 2006. **19**(1): p. 47-53.

106. El-Sherbiny, I.M., N.M. El-Baz, and M.H. Yacoub, *Inhaled nano- and microparticles for drug delivery.* Global cardiology science & practice, 2015. **2015**: p. 2-2.
107. Cohen, B.S., et al., *Deposition of charged particles on lung airways.* Health Phys, 1998. **74**(5): p. 554-60.
108. Miller, F.J., *Dosimetry of particles in laboratory animals and humans in relationship to issues surrounding lung overload and human health risk assessment: a critical review.* Inhal Toxicol, 2000. **12**(1-2): p. 19-57.
109. Khan, Y.S. and D.T. Lynch, *Histology, Lung.* 2019, StatPearls Publishing, Treasure Island (FL).
110. Barkauskas, C.E., et al., *Lung organoids: current uses and future promise.* Development, 2017. **144**(6): p. 986.
111. Khan, Y. and D. Lynch, *Histology, Lung*, in *StatPearls* 2020, Treasure Island (FL): StatPearls Publishing.
112. Tomashefski, J.F. and C.F. Farver, *Anatomy and Histology of the Lung*, in *Dail and Hammar's Pulmonary Pathology: Volume I: Nonneoplastic Lung Disease*, J.F. Tomashefski, et al., Editors. 2008, Springer New York: New York, NY. p. 20-48.
113. Bordon, Y., *Neuroendocrine cells regulate lung inflammation.* Nature Reviews Immunology, 2016. **16**(2): p. 77-77.
114. Ahmad, S. and A. Ahmad, *Chapter 6 - Epithelial Regeneration and Lung Stem Cells*, in *Lung Epithelial Biology in the Pathogenesis of Pulmonary Disease*, V.K. Sidhaye and M. Koval, Editors. 2017, Academic Press: Boston. p. 91-102.
115. Lankoff, A., et al., *The effect of agglomeration state of silver and titanium dioxide nanoparticles on cellular response of HepG2, A549 and THP-1 cells.* Toxicol Lett, 2012. **208**(3): p. 197-213.
116. Martin, T.R. and C.W. Frevert, *Innate immunity in the lungs.* Proceedings of the American Thoracic Society, 2005. **2**(5): p. 403-411.
117. Pabst, R. and T. Tschernig, *Bronchus-associated lymphoid tissue: an entry site for antigens for successful mucosal vaccinations?* Am J Respir Cell Mol Biol, 2010. **43**(2): p. 137-41.
118. Kirch, J., et al., *Mucociliary clearance of micro- and nanoparticles is independent of size, shape and charge--an ex vivo and in silico approach.* J Control Release, 2012. **159**(1): p. 128-34.
119. Sanders, N., et al., *Extracellular barriers in respiratory gene therapy.* Adv Drug Deliv Rev, 2009. **61**(2): p. 115-27.
120. Fahy, J.V. and B.F. Dickey, *Airway mucus function and dysfunction.* N Engl J Med, 2010. **363**(23): p. 2233-47.
121. Bansil, R. and B.S. Turner, *Mucin structure, aggregation, physiological functions and biomedical applications.* Current Opinion in Colloid & Interface Science, 2006. **11**(2): p. 164-170.
122. Rubin, B.K., *Physiology of airway mucus clearance.* Respir Care, 2002. **47**(7): p. 761-8.
123. Voynow, J.A. and B.K. Rubin, *Mucins, mucus, and sputum.* Chest, 2009. **135**(2): p. 505-512.
124. Ma, J., B.K. Rubin, and J.A. Voynow, *Mucins, Mucus, and Goblet Cells.* Chest, 2018. **154**(1): p. 169-176.
125. Ali, M.S. and J.P. Pearson, *Upper airway mucin gene expression: a review.* Laryngoscope, 2007. **117**(5): p. 932-8.
126. Garcia-Verdugo, I., et al., *Lung protease/anti-protease network and modulation of mucus production and surfactant activity.* Biochimie, 2010. **92**(11): p. 1608-1617.
127. Button, B., et al., *A periciliary brush promotes the lung health by separating the mucus layer from airway epithelia.* Science, 2012. **337**(6097): p. 937-41.
128. Randell, S.H., R.C. Boucher, and G. University of North Carolina Virtual Lung, *Effective mucus clearance is essential for respiratory health.* American journal of respiratory cell and molecular biology, 2006. **35**(1): p. 20-28.
129. Wanner, A., M. Salathé, and T.G. O'Riordan, *Mucociliary clearance in the airways.* Am J Respir Crit Care Med, 1996. **154**(6 Pt 1): p. 1868-902.
130. Hofmann, W. and B. Asgharian, *The effect of lung structure on mucociliary clearance and particle retention in human and rat lungs.* Toxicol Sci, 2003. **73**(2): p. 448-56.
131. Lai, S.K., Y.Y. Wang, and J. Hanes, *Mucus-penetrating nanoparticles for drug and gene delivery to mucosal tissues.* Adv Drug Deliv Rev, 2009. **61**(2): p. 158-71.
132. Saketkhoo, K., A. Januszkiewicz, and M.A. Sackner, *Effects of drinking hot water, cold water, and chicken soup on nasal mucus velocity and nasal airflow resistance.* Chest, 1978. **74**(4): p. 408-10.
133. Mainardes, R.M., et al., *Liposomes and micro/nanoparticles as colloidal carriers for nasal drug delivery.* Curr Drug Deliv, 2006. **3**(3): p. 275-85.

134. Mitra, A.K. and R. Krishnamoorthy, *Prodrugs for nasal drug delivery.* Adv Drug Deliv Rev, 1998. **29**(1-2): p. 135-146.
135. Wong, J.W., et al., *Effects of gravity on tracheal mucus transport rates in normal subjects and in patients with cystic fibrosis.* Pediatrics, 1977. **60**(2): p. 146-52.
136. Yeates, D.B., et al., *Coordination of mucociliary transport in human trachea and intrapulmonary airways.* Journal of applied physiology: respiratory, environmental and exercise physiology, 1981. **51**(5): p. 1057-1064.
137. Denton, R., *The rheology of human lung mucus.* Ann N Y Acad Sci, 1963. **106**: p. 746-54.
138. Yeates, D.B., T.R. Gerrity, and C.S. Garrard, *Particle deposition and clearance in the bronchial tree.* Annals of Biomedical Engineering, 1981. **9**(5): p. 577-592.
139. Foster, W.M., E. Langenback, and E.H. Bergofsky, *Measurement of tracheal and bronchial mucus velocities in man: relation to lung clearance.* J Appl Physiol Respir Environ Exerc Physiol, 1980. **48**(6): p. 965-71.
140. Donaldson, S.H., et al., *Mucociliary clearance as an outcome measure for cystic fibrosis clinical research.* Proc Am Thorac Soc, 2007. **4**(4): p. 399-405.
141. Boegh, M. and H.M. Nielsen, *Mucus as a barrier to drug delivery - understanding and mimicking the barrier properties.* Basic Clin Pharmacol Toxicol, 2015. **116**(3): p. 179-86.
142. Lillehoj, E.P. and K.C. Kim, *Airway mucus: Its components and function.* Archives of Pharmacal Research, 2002. **25**(6): p. 770-780.
143. Alqahtani, S., et al., *Development of an In Vitro System to Study the Interactions of Aerosolized Drugs with Pulmonary Mucus.* Pharmaceutics, 2020. **12**(2).
144. Sigurdsson, H.H., J. Kirch, and C.-M. Lehr, *Mucus as a barrier to lipophilic drugs.* International Journal of Pharmaceutics, 2013. **453**(1): p. 56-64.
145. Lai, S.K., et al., *Rapid transport of large polymeric nanoparticles in fresh undiluted human mucus.* 2007. **104**(5): p. 1482-1487.
146. Kirch, J., et al., *Optical tweezers reveal relationship between microstructure and nanoparticle penetration of pulmonary mucus.* 2012. **109**(45): p. 18355-18360.
147. Yudin, A.I., F.W. Hanson, and D.F. Katz, *Human cervical mucus and its interaction with sperm: a fine-structural view.* Biol Reprod, 1989. **40**(3): p. 661-71.
148. Olmsted, S.S., et al., *Diffusion of macromolecules and virus-like particles in human cervical mucus.* Biophys J, 2001. **81**(4): p. 1930-7.
149. Saltzman, W.M., et al., *Antibody diffusion in human cervical mucus.* Biophysical journal, 1994. **66**(2 Pt 1): p. 508-515.
150. Lai, S.K., et al., *Nanoparticles reveal that human cervicovaginal mucus is riddled with pores larger than viruses.* Proc Natl Acad Sci U S A, 2010. **107**(2): p. 598-603.
151. Suk, J.S., et al., *The penetration of fresh undiluted sputum expectorated by cystic fibrosis patients by non-adhesive polymer nanoparticles.* Biomaterials, 2009. **30**(13): p. 2591-7.
152. Lay, J.C., et al., *Airway retention of materials of different solubility following local intrabronchial deposition in dogs.* J Aerosol Med, 2003. **16**(2): p. 153-66.
153. Koussoroplis, S.J., et al., *PEGylation of antibody fragments greatly increases their local residence time following delivery to the respiratory tract.* Journal of Controlled Release, 2014. **187**: p. 91-100.
154. Patil, H.P., et al., *Fate of PEGylated antibody fragments following delivery to the lungs: Influence of delivery site, PEG size and lung inflammation.* Journal of Controlled Release, 2018. **272**: p. 62-71.
155. Kamiya, Y., et al., *Improved Intranasal Retentivity and Transnasal Absorption Enhancement by PEGylated Poly-L-ornithine.* Pharmaceuticals, 2018. **11**(1).
156. Pfister, D. and M. Morbidelli, *Process for protein PEGylation.* J Control Release, 2014. **180**: p. 134-49.
157. Effros, R.M. and G.R. Mason, *Measurements of pulmonary epithelial permeability in vivo.* Am Rev Respir Dis, 1983. **127**(5 Pt 2): p. S59-65.
158. Tandel, H., K. Florence, and A. Misra, *9 - Protein and Peptide Delivery through Respiratory Pathway*, in *Challenges in Delivery of Therapeutic Genomics and Proteomics*, A. Misra, Editor. 2011, Elsevier: London. p. 429-479.
159. Matsukawa, Y., et al., *Size-Dependent Dextran Transport across Rat Alveolar Epithelial Cell Monolayers.* Journal of Pharmaceutical Sciences, 1997. **86**(3): p. 305-309.
160. Mathia, N.R., et al., *Permeability characteristics of calu-3 human bronchial epithelial cells: in vitro-in vivo correlation to predict lung absorption in rats.* J Drug Target, 2002. **10**(1): p. 31-40.
161. McLaughlin, G.E., et al., *Measurement of solute fluxes in isolated rat lungs.* Respiration Physiology, 1993. **91**(2): p. 321-334.

162. Bur, M., et al., *Assessment of transport rates of proteins and peptides across primary human alveolar epithelial cell monolayers.* Eur J Pharm Sci, 2006. **28**(3): p. 196-203.
163. Stone, V., et al., *Nanomaterials Versus Ambient Ultrafine Particles: An Opportunity to Exchange Toxicology Knowledge.* Environ Health Perspect, 2017. **125**(10): p. 106002.
164. Takano, M., et al., *Receptor-mediated endocytosis of macromolecules and strategy to enhance their transport in alveolar epithelial cells.* Expert Opin Drug Deliv, 2015. **12**(5): p. 813-25.
165. Matsukawa, Y., et al., *Horseradish peroxidase transport across rat alveolar epithelial cell monolayers.* Pharm Res, 1996. **13**(9): p. 1331-5.
166. Stromhaug, P.E., et al., *Differences between fluid-phase endocytosis (pinocytosis) and receptor-mediated endocytosis in isolated rat hepatocytes.* Eur J Cell Biol, 1997. **73**(1): p. 28-39.
167. Tyteca, D., et al., *Azithromycin, a lysosomotropic antibiotic, has distinct effects on fluid-phase and receptor-mediated endocytosis, but does not impair phagocytosis in J774 macrophages.* Exp Cell Res, 2002. **281**(1): p. 86-100.
168. Lucero, D., et al., *Interleukin 10 promotes macrophage uptake of HDL and LDL by stimulating fluid-phase endocytosis.* Biochimica et Biophysica Acta (BBA) - Molecular and Cell Biology of Lipids, 2020. **1865**(2): p. 158537.
169. Kim, K.J. and A.B. Malik, *Protein transport across the lung epithelial barrier.* American Journal of Physiology-Lung Cellular and Molecular Physiology, 2003. **284**(2): p. L247-L259.
170. Mostov, K.E. and M.H. Cardone, *Regulation of protein traffic in polarized epithelial cells.* Bioessays, 1995. **17**(2): p. 129-38.
171. Apodaca, G., *Endocytic traffic in polarized epithelial cells: role of the actin and microtubule cytoskeleton.* Traffic, 2001. **2**(3): p. 149-59.
172. Oda, K., et al., *Mechanism underlying insulin uptake in alveolar epithelial cell line RLE-6TN.* Eur J Pharmacol, 2011. **672**(1-3): p. 62-9.
173. Crowell, R.E., et al., *Alveolar and interstitial macrophage populations in the murine lung.* Exp Lung Res, 1992. **18**(4): p. 435-46.
174. Lehnert, B.E., *Pulmonary and thoracic macrophage subpopulations and clearance of particles from the lung.* Environmental health perspectives, 1992. **97**: p. 17-46.
175. Wheeldon, E.B., P.L. Podolin, and R.C. Mirabile, *Alveolar Macrophage Distribution in a Mouse Model: The Importance of the Fixation Method.* Toxicol Pathol, 2015. **43**(8): p. 1162-5.
176. Geiser, M., *Update on macrophage clearance of inhaled micro- and nanoparticles.* J Aerosol Med Pulm Drug Deliv, 2010. **23**(4): p. 207-17.
177. Hussell, T. and T.J. Bell, *Alveolar macrophages: plasticity in a tissue-specific context.* Nat Rev Immunol, 2014. **14**(2): p. 81-93.
178. Brain, J.D., *Lung macrophages: how many kinds are there? What do they do?* Am Rev Respir Dis, 1988. **137**(3): p. 507-9.
179. Laskin, D.L., R. Malaviya, and J.D. Laskin, *Pulmonary Macrophages*, in *Comparative biology of the normal lung*. 2015.
180. Pinkerton, K.E., et al., *Chapter 14 - Normal Aging of the Lung*, in *The Lung (Second Edition)*, R. Harding and K.E. Pinkerton, Editors. 2014, Academic Press: Boston. p. 265-285.
181. Reddy, S.P. and D. Mehta, *Lung Interstitial Macrophages Redefined: It Is Not That Simple Anymore.* Am J Respir Cell Mol Biol, 2017. **57**(2): p. 135-136.
182. Cai, Y., et al., *In vivo characterization of alveolar and interstitial lung macrophages in rhesus macaques: implications for understanding lung disease in humans.* J Immunol, 2014. **192**(6): p. 2821-9.
183. Maus, U.A., et al., *Resident alveolar macrophages are replaced by recruited monocytes in response to endotoxin-induced lung inflammation.* Am J Respir Cell Mol Biol, 2006. **35**(2): p. 227-35.
184. Westphalen, K., et al., *Sessile alveolar macrophages communicate with alveolar epithelium to modulate immunity.* Nature, 2014. **506**(7489): p. 503-506.
185. Krombach, F., et al., *Cell size of alveolar macrophages: an interspecies comparison.* Environmental health perspectives, 1997. **105 Suppl 5**(Suppl 5): p. 1261-1263.
186. d'Angelo, I., et al., *Improving the efficacy of inhaled drugs in cystic fibrosis: challenges and emerging drug delivery strategies.* Adv Drug Deliv Rev, 2014. **75**: p. 92-111.
187. Geiser, M., et al., *Nanoparticle uptake by airway phagocytes after fungal spore challenge in murine allergic asthma and chronic bronchitis.* BMC Pulmonary Medicine, 2014. **14**(1): p. 116.
188. Li, L., G.A. Gusarova, and J. Bhattacharya, *Resident Lung Macrophages Are Sparsely Amongst Alveoli.* 2016. **30**(1_supplement): p. 1264.5-1264.5.

189. Bhattacharya, J. and K. Westphalen, *Macrophage-epithelial interactions in pulmonary alveoli.* Seminars in immunopathology, 2016. **38**(4): p. 461-469.
190. Redente, E.F., et al., *12 - Innate Immunity*, in *Murray and Nadel's Textbook of Respiratory Medicine (Sixth Edition)*, V.C. Broaddus, et al., Editors. 2016, W.B. Saunders: Philadelphia. p. 184-205.e7.
191. Vanbever, R., et al., *Cationic Nanoliposomes Are Efficiently Taken up by Alveolar Macrophages but Have Little Access to Dendritic Cells and Interstitial Macrophages in the Normal and CpG-Stimulated Lungs.* Molecular Pharmaceutics, 2019. **16**(5): p. 2048-2059.
192. He, W., et al., *Drug delivery to macrophages: A review of targeting drugs and drug carriers to macrophages for inflammatory diseases.* Advanced Drug Delivery Reviews, 2019.
193. Wang, Z.-R., Y. Cui, and Z.-Y. Qiu, *Chapter 3 - Biomimetic Mineralized Collagen Biocompatibility*, in *Mineralized Collagen Bone Graft Substitutes*, X.-M. Wang, Z.-Y. Qiu, and H. Cui, Editors. 2019, Woodhead Publishing. p. 61-98.
194. Doherty, G.J. and H.T. McMahon, *Mechanisms of endocytosis.* Annu Rev Biochem, 2009. **78**: p. 857-902.
195. Laskin, D.L., C.R. Gardner, and J.D. Laskin, *5.06 - Phagocytes*, in *Comprehensive Toxicology (Second Edition)*, C.A. McQueen, Editor. 2010, Elsevier: Oxford. p. 133-153.
196. Kuhn, D.A., et al., *Different endocytotic uptake mechanisms for nanoparticles in epithelial cells and macrophages.* Beilstein journal of nanotechnology, 2014. **5**: p. 1625-1636.
197. Takenouchi, T., et al., *Chapter 14 - Role of Autophagy in P2X7 Receptor-Mediated Maturation and Unconventional Secretion of IL-1β in Microglia*, in *Autophagy: Cancer, Other Pathologies, Inflammation, Immunity, Infection, and Aging*, M.A. Hayat, Editor. 2015, Academic Press: Amsterdam. p. 211-222.
198. Sahay, G., D.Y. Alakhova, and A.V. Kabanov, *Endocytosis of nanomedicines.* Journal of Controlled Release, 2010. **145**(3): p. 182-195.
199. Lombry, C., et al., *Alveolar macrophages are a primary barrier to pulmonary absorption of macromolecules.* Am J Physiol Lung Cell Mol Physiol, 2004. **286**(5): p. L1002-8.
200. Deol, P., G.K. Khuller, and K. Joshi, *Therapeutic efficacies of isoniazid and rifampin encapsulated in lung-specific stealth liposomes against Mycobacterium tuberculosis infection induced in mice.* Antimicrob Agents Chemother, 1997. **41**(6): p. 1211-4.
201. Makino, K., et al., *Phagocytic uptake of polystyrene microspheres by alveolar macrophages: effects of the size and surface properties of the microspheres.* Colloids and Surfaces B: Biointerfaces, 2003. **27**(1): p. 33-39.
202. Chono, S., et al., *Influence of particle size on drug delivery to rat alveolar macrophages following pulmonary administration of ciprofloxacin incorporated into liposomes.* J Drug Target, 2006. **14**(8): p. 557-66.
203. Semmler-Behnke, M., et al., *Efficient elimination of inhaled nanoparticles from the alveolar region: evidence for interstitial uptake and subsequent reentrainment onto airways epithelium.* Environ Health Perspect, 2007. **115**(5): p. 728-33.
204. Geiser, M., et al., *The role of macrophages in the clearance of inhaled ultrafine titanium dioxide particles.* Am J Respir Cell Mol Biol, 2008. **38**(3): p. 371-6.
205. Agrahari, V., V. Agrahari, and A.K. Mitra, *Nanocarrier fabrication and macromolecule drug delivery: challenges and opportunities.* Therapeutic delivery, 2016. **7**(4): p. 257-278.
206. Gallagher, J.E., G. George, and A.R. Brody, *Sialic acid mediates the initial binding of positively charged inorganic particles to alveolar macrophage membranes.* Am Rev Respir Dis, 1987. **135**(6): p. 1345-52.
207. Fontana, G., et al., *Amoxicillin-loaded polyethylcyanoacrylate nanoparticles: influence of PEG coating on the particle size, drug release rate and phagocytic uptake.* Biomaterials, 2001. **22**(21): p. 2857-65.
208. Sharma, G., et al., *Polymer particle shape independently influences binding and internalization by macrophages.* J Control Release, 2010. **147**(3): p. 408-12.
209. Vanbever, R., *Performance-driven, pulmonary delivery of systemically acting drugs.* Drug Discovery Today: Technologies, 2005. **2**(1): p. 39-46.
210. Gursahani, H., et al., *Absorption of Polyethylene Glycol (PEG) Polymers: The Effect of PEG Size on Permeability.* Journal of Pharmaceutical Sciences, 2009. **98**(8): p. 2847-2856.
211. Freches, D., et al., *Preclinical evaluation of topically-administered PEGylated Fab' lung toxicity.* Int J Pharm X, 2019. **1**: p. 100019.
212. McLeod, V.M., et al., *Optimal PEGylation can improve the exposure of interferon in the lungs following pulmonary administration.* J Pharm Sci, 2015. **104**(4): p. 1421-30.
213. Mistry, P.K., E.P. Wraight, and T.M. Cox, *Therapeutic delivery of proteins to macrophages: implications for treatment of Gaucher's disease.* Lancet, 1996. **348**(9041): p. 1555-9.

214. Calceti, P., et al., *Development and in vivo evaluation of an oral insulin-PEG delivery system.* European Journal of Pharmaceutical Sciences, 2004. **22**(4): p. 315-323.
215. Fukuda, Y., et al., *Susceptibility of insulin to proteolysis in rat lung homogenate and its protection from proteolysis by various protease inhibitors.* Biol Pharm Bull, 1995. **18**(6): p. 891-4.
216. Shen, Z., et al., *Proteolytic enzymes as a limitation for pulmonary absorption of insulin: in vitro and in vivo investigations.* Int J Pharm, 1999. **192**(2): p. 115-21.
217. Menou, A., J. Duitman, and B. Crestani, *The impaired proteases and anti-proteases balance in Idiopathic Pulmonary Fibrosis.* Matrix Biology, 2018. **68-69**: p. 382-403.
218. Greene, C.M. and N.G. McElvaney, *Proteases and antiproteases in chronic neutrophilic lung disease - relevance to drug discovery.* British journal of pharmacology, 2009. **158**(4): p. 1048-1058.
219. Cohen, A.J., et al., *Low neutral endopeptidase levels in bronchoalveolar lavage fluid of lung cancer patients.* American Journal of Respiratory and Critical Care Medicine, 1999. **159**(3): p. 907-910.
220. Juillerat-Jeanneret, L., J.D. Aubert, and P. Leuenberger, *Peptidases in human bronchoalveolar lining fluid, macrophages, and epithelial cells: dipeptidyl (amino)peptidase IV, aminopeptidase N, and dipeptidyl (carboxy)peptidase (angiotensin-converting enzyme).* J Lab Clin Med, 1997. **130**(6): p. 603-14.
221. Woods, A., et al., *Development of new in vitro models of lung protease activity for investigating stability of inhaled biological therapies and drug delivery systems.* Eur J Pharm Biopharm, 2020. **146**: p. 64-72.
222. Folkesson, H.G., et al., *Alveolar epithelial clearance of protein.* Journal of Applied Physiology, 1996. **80**(5): p. 1431-1445.
223. Okamoto, H., et al., *Dry Powders for Pulmonary Delivery of Peptides and Proteins.* KONA, 2002. **20**: p. 71–83.
224. Amancha, K.P. and A. Hussain, *Effect of protease inhibitors on pulmonary bioavailability of therapeutic proteins and peptides in the rat.* Eur J Pharm Sci, 2015. **68**: p. 1-10.
225. Youn, Y.S., et al., *Improved intrapulmonary delivery of site-specific PEGylated salmon calcitonin: Optimization by PEG size selection.* Journal of Controlled Release, 2008. **125**(1): p. 68-75.
226. Youn, Y.S., et al., *Evaluation of therapeutic potentials of site-specific PEGylated glucagon-like peptide-1 isomers as a type 2 anti-diabetic treatment: Insulinotropic activity, glucose-stabilizing capability, and proteolytic stability.* Biochem Pharmacol, 2007. **73**(1): p. 84-93.
227. Zhang, C., et al., *PEGylation of lysine residues improves the proteolytic stability of fibronectin while retaining biological activity.* Biotechnol J, 2014. **9**(8): p. 1033-43.
228. Lee, K.C., et al., *Intrapulmonary potential of polyethylene glycol-modified glucagon-like peptide-1s as a type 2 anti-diabetic agent.* Regulatory Peptides, 2009. **152**(1-3): p. 101-107.
229. Shapiro, S.D. and E.J. Campbell, *Chapter 29 - Matrix Degrading Proteinases*, in *Asthma and COPD*, P.J. Barnes, et al., Editors. 2002, Academic Press: London. p. 273-282.
230. Veronese, F.M. and G. Pasut, *PEGylation, successful approach to drug delivery.* Drug Discov Today, 2005. **10**(21): p. 1451-8.
231. Gupta, V., et al., *Protein PEGylation for cancer therapy: bench to bedside.* J Cell Commun Signal, 2019. **13**(3): p. 319-330.
232. Reichert, C. and G. Borchard, *Noncovalent PEGylation, An Innovative Subchapter in the Field of Protein Modification.* Journal of Pharmaceutical Sciences, 2016. **105**(2): p. 386-390.
233. Abuchowski, A., et al., *ALTERATION OF IMMUNOLOGICAL PROPERTIES OF BOVINE SERUM-ALBUMIN BY COVALENT ATTACHMENT OF POLYETHYLENE-GLYCOL.* Journal of Biological Chemistry, 1977. **252**(11): p. 3578-3581.
234. Abuchowski, A., et al., *EFFECT OF COVALENT ATTACHMENT OF POLYETHYLENE-GLYCOL ON IMMUNOGENICITY AND CIRCULATING LIFE OF BOVINE LIVER CATALASE.* Journal of Biological Chemistry, 1977. **252**(11): p. 3582-3586.
235. Davis, F.F., *The origin of pegnology.* Adv Drug Deliv Rev, 2002. **54**(4): p. 457-8.
236. Hou, Y.Q. and H. Lu, *Protein PEPylation: A New Paradigm of Protein-Polymer Conjugation.* Bioconjugate Chemistry, 2019. **30**(6): p. 1604-1616.
237. Pasut, G. and F.M. Veronese, *State of the art in PEGylation: the great versatility achieved after forty years of research.* J Control Release, 2012. **161**(2): p. 461-72.
238. Roberts, M.J., M.D. Bentley, and J.M. Harris, *Chemistry for peptide and protein PEGylation.* Adv Drug Deliv Rev, 2002. **54**(4): p. 459-76.
239. Wang, Y.S., et al., *Structural and biological characterization of pegylated recombinant interferon alpha-2b and its therapeutic implications.* Adv Drug Deliv Rev, 2002. **54**(4): p. 547-70.

240. Bailon, P. and C.Y. Won, *PEG-modified biopharmaceuticals.* Expert Opinion on Drug Delivery, 2009. **6**(1): p. 1-16.
241. Jevsevar, S., M. Kunstelj, and V.G. Porekar, *PEGylation of therapeutic proteins.* Biotechnol J, 2010. **5**(1): p. 113-28.
242. Sato, H., *Enzymatic procedure for site-specific pegylation of proteins.* Adv Drug Deliv Rev, 2002. **54**(4): p. 487-504.
243. Dhiman, S., N. Mishra, and S. Sharma, *Development of PEGylated solid lipid nanoparticles of pentoxifylline for their beneficial pharmacological potential in pathological cardiac hypertrophy.* Artif Cells Nanomed Biotechnol, 2016. **44**(8): p. 1901-1908.
244. Mummidivarapu, V.V.S., et al., *Noncovalent PEGylation via Sulfonatocalix 4 arene-A Crystallographic Proof.* Bioconjugate Chemistry, 2018. **29**(12): p. 3999-4003.
245. Mueller, C., et al., *Noncovalent PEGylation: different effects of dansyl-, L-tryptophan-, phenylbutylamino-, benzyl- and cholesteryl-PEGs on the aggregation of salmon calcitonin and lysozyme.* J Pharm Sci, 2012. **101**(6): p. 1995-2008.
246. Khondee, S., et al., *Noncovalent PEGylation by polyanion complexation as a means to stabilize keratinocyte growth factor-2 (KGF-2).* Biomacromolecules, 2011. **12**(11): p. 3880-94.
247. Mero, A., et al., *Multivalent and flexible PEG-nitrilotriacetic acid derivatives for non-covalent protein pegylation.* Pharm Res, 2011. **28**(10): p. 2412-21.
248. Swierczewska, M., K.C. Lee, and S. Lee, *What is the future of PEGylated therapies?* Expert opinion on emerging drugs, 2015. **20**(4): p. 531-536.
249. Dozier, J.K. and M.D. Distefano, *Site-Specific PEGylation of Therapeutic Proteins.* International Journal of Molecular Sciences, 2015. **16**(10): p. 25831-25864.
250. Veronese, F.M., *Peptide and protein PEGylation: a review of problems and solutions.* Biomaterials, 2001. **22**(5): p. 405-17.
251. Harris, J.M. and R.B. Chess, *Effect of pegylation on pharmaceuticals.* Nat Rev Drug Discov, 2003. **2**(3): p. 214-21.
252. Wu, C., et al., *Preparation of monoPEGylated Cyanovirin-N's derivative and its anti-influenza A virus bioactivity in vitro and in vivo.* J Biochem, 2015. **157**(6): p. 539-48.
253. Pasut, G. and F.M. Veronese, *Polymer-drug conjugation, recent achievements and general strategies.* Progress in Polymer Science, 2007. **32**(8-9): p. 933-961.
254. Sheth, P. and P.B. Myrdal, *Excipients Utilized for Modifying Pulmonary Drug Release*, in *Controlled Pulmonary Drug Delivery*, H.D.C. Smyth and A.J. Hickey, Editors. 2011, Springer New York: New York, NY. p. 237-263.
255. Guichard, M.J., et al., *Production and characterization of a PEGylated derivative of recombinant human deoxyribonuclease I for cystic fibrosis therapy.* International Journal of Pharmaceutics, 2017. **524**(1-2): p. 159-167.
256. Guichard, M.J., et al., *Impact of PEGylation on the mucolytic activity of recombinant human deoxyribonuclease I in cystic fibrosis sputum.* Clin Sci (Lond), 2018. **132**(13): p. 1439-1452.
257. Cantin, A.M., et al., *Polyethylene glycol conjugation at Cys232 prolongs the half-life of alpha1 proteinase inhibitor.* Am J Respir Cell Mol Biol, 2002. **27**(6): p. 659-65.
258. Fletcher, A.M., et al., *Adverse vacuolation in multiple tissues in cynomolgus monkeys following repeat-dose administration of a PEGylated protein.* Toxicology Letters, 2019. **317**: p. 120-129.
259. Gebauer, M. and A. Skerra, *Prospects of PASylation (R) for the design of protein and peptide therapeutics with extended half-life and enhanced action.* Bioorganic & Medicinal Chemistry, 2018. **26**(10): p. 2882-2887.
260. Schlapschy, M., et al., *PASylation: a biological alternative to PEGylation for extending the plasma half-life of pharmaceutically active proteins.* Protein Engineering Design & Selection, 2013. **26**(8): p. 489-501.
261. Ramos-de-la-Peña, A.M. and O. Aguilar, *Progress and Challenges in PEGylated Proteins Downstream Processing: A Review of the Last 8 Years.* International Journal of Peptide Research and Therapeutics, 2020. **26**(1): p. 333-348.
262. Bossard, M.J. and M.J. Vicent, *2 - PEGylated proteins: A rational design for mitigating clearance mechanisms and altering biodistribution*, in *Polymer-Protein Conjugates*, G. Pasut and S. Zalipsky, Editors. 2020, Elsevier. p. 23-40.
263. Alconcel, S.N.S., A.S. Baas, and H.D. Maynard, *FDA-approved poly(ethylene glycol)–protein conjugate drugs.* Polymer Chemistry, 2011. **2**(7): p. 1442-1448.
264. Fu, C.H. and K.M. Sakamoto, *PEG-asparaginase.* Expert Opin Pharmacother, 2007. **8**(12): p. 1977-84.

265. Turfus, S.C., et al., *Chapter 25 - Pharmacokinetics*, in *Pharmacognosy*, S. Badal and R. Delgoda, Editors. 2017, Academic Press: Boston. p. 495-512.
266. Hvidberg, E.F., *Why do we need pharmacokinetic studies?* American Journal of Obstetrics and Gynecology, 1990. **163**(1, Part 2): p. 316-318.
267. Ivens, I.A., et al., *PEGylated therapeutic proteins for haemophilia treatment: a review for haemophilia caregivers.* Haemophilia, 2013. **19**(1): p. 11-20.
268. Baumann, A., et al., *Pharmacokinetics, metabolism and distribution of PEGs and PEGylated proteins: quo vadis?* Drug Discovery Today, 2014. **19**(10): p. 1623-1631.
269. McLennan, D.N., C.J. Porter, and S.A. Charman, *Subcutaneous drug delivery and the role of the lymphatics.* Drug Discov Today Technol, 2005. **2**(1): p. 89-96.
270. Pelham, R.W., et al., *Clinical trial: single- and multiple-dose pharmacokinetics of polyethylene glycol (PEG-3350) in healthy young and elderly subjects.* Aliment Pharmacol Ther, 2008. **28**(2): p. 256-65.
271. Baumann, A., et al., *Pharmacokinetics, excretion, distribution, and metabolism of 60-kDa polyethylene glycol used in BAY 94-9027 in rats and its value for human prediction.* European Journal of Pharmaceutical Sciences, 2019. **130**: p. 11-20.
272. Yamaoka, T., Y. Tabata, and Y. Ikada, *Distribution and tissue uptake of poly(ethylene glycol) with different molecular weights after intravenous administration to mice.* J Pharm Sci, 1994. **83**(4): p. 601-6.
273. Wang, H., et al., *Development of a carbon-14 labeling approach to support disposition studies with a pegylated biologic.* Drug Metab Dispos, 2012. **40**(9): p. 1677-85.
274. Webster, R., et al., *PEG and PEG conjugates toxicity: towards an understanding of the toxicity of PEG and its relevance to PEGylated biologicals*, in *PEGylated Protein Drugs: Basic Science and Clinical Applications*, F.M. Veronese, Editor. 2009, Birkhäuser Basel: Basel. p. 127-146.
275. Fruijtier-Polloth, C., *Safety assessment on polyethylene glycols (PEGs) and their derivatives as used in cosmetic products.* Toxicology, 2005. **214**(1-2): p. 1-38.
276. Elliott, V.L., et al., *Evidence for Metabolic Cleavage of a PEGylated Protein in Vivo Using Multiple Analytical Methodologies.* Molecular Pharmaceutics, 2012. **9**(5): p. 1291-1301.
277. Parton, T., et al., *P-0167: The PEG Moiety of Certolizumab Pegol is Rapidly Cleared From the Blood of Humans by the Kidneys Once it is Cleaved From the Fab'.* Inflammatory Bowel Diseases, 2009. **15**(suppl_2): p. S56-S56.
278. Stidl, R., et al., *Safety of PEGylated recombinant human full-length coagulation factor VIII (BAX 855) in the overall context of PEG and PEG conjugates.* Haemophilia, 2016. **22**(1): p. 54-64.
279. Webster, R., et al., *PEGylated proteins: evaluation of their safety in the absence of definitive metabolism studies.* Drug Metab Dispos, 2007. **35**(1): p. 9-16.
280. Longley, C.B., et al., *Biodistribution and excretion of radiolabeled 40 kDa polyethylene glycol following intravenous administration in mice.* Journal of Pharmaceutical Sciences, 2013. **102**(7): p. 2362-2370.
281. Parton, T., et al., *P068 Investigation of the Distribution and Elimination of the PEG Component of Certolizumab Pegol in Rats.* Journal of Crohn's and Colitis Supplements, 2008. **2**(1): p. 26-26.
282. Woodburn, K.W., et al., *Absorption, distribution, metabolism and excretion of peginesatide, a novel erythropoiesis-stimulating agent, in rats.* Xenobiotica, 2012. **42**(7): p. 660-70.
283. Bjørnsdottir, I., et al., *Pharmacokinetics, tissue distribution and excretion of 40kDa PEG and PEGylated rFVIII (N8-GP) in rats.* Eur J Pharm Sci, 2016. **87**: p. 58-68.
284. Yang, W., *Nucleases: diversity of structure, function and mechanism.* Q Rev Biophys, 2011. **44**(1): p. 1-93.
285. Lazarus, R.A. and J.S. Wagener†, *Recombinant Human Deoxyribonuclease I*, in *Pharmaceutical Biotechnology: Fundamentals and Applications*, D.J.A. Crommelin, R.D. Sindelar, and B. Meibohm, Editors. 2019, Springer International Publishing: Cham. p. 471-488.
286. Keyel, P.A., *Dnases in health and disease.* Developmental Biology, 2017. **429**(1): p. 1-11.
287. Davis, P.B., *Cystic fibrosis since 1938.* Am J Respir Crit Care Med, 2006. **173**(5): p. 475-82.
288. Yang, C. and M. Montgomery, *Dornase alfa for cystic fibrosis.* The Cochrane database of systematic reviews, 2018. **9**(9): p. CD001127-CD001127.
289. Bell, S.C., et al., *The future of cystic fibrosis care: a global perspective.* Lancet Respir Med, 2020. **8**(1): p. 65-124.
290. Di Paolo, M., et al., *Cystic fibrosis*, in *ERS Handbook of Respiratory Medicine*. 2019.
291. Marshall, B., et al. *2018 Patient Registry Annual Data Report* 2018 [cited 2020; Available from: https://www.cff.org/Research/Researcher-Resources/Patient-Registry/2018-Patient-Registry-Annual-Data-Report.pdf.

292. Hurt, K. and D. Bilton, *Inhaled Interventions in Cystic Fibrosis: Mucoactive and Antibiotic Therapies.* Respiration, 2014. **88**(6): p. 441-448.
293. DeSimone, E., et al., *Cystic Fibrosis Update on Treatment Guidelines and New Recommendations.* Us Pharmacist, 2018. **43**(5): p. 16-21.
294. Elborn, J.S., *Cystic fibrosis.* Lancet, 2016. **388**(10059): p. 2519-2531.
295. Pressler, T., *Review of recombinant human deoxyribonuclease (rhDNase) in the management of patients with cystic fibrosis.* Biologics : targets & therapy, 2008. **2**(4): p. 611-617.
296. McCoy, K., S. Hamilton, and C. Johnson, *Effects of 12-week administration of dornase alfa in patients with advanced cystic fibrosis lung disease. Pulmozyme Study Group.* Chest, 1996. **110**(4): p. 889-95.
297. Konstan, M.W., et al., *Clinical use of dornase alpha is associated with a slower rate of FEV1 decline in cystic fibrosis.* Pediatr Pulmonol, 2011. **46**(6): p. 545-53.
298. Konstan, M.W., *Dornase alfa and progression of lung disease in cystic fibrosis.* 2008. **43**(S9): p. S24-S28.
299. Suri, R., et al., *Effects of recombinant human DNase and hypertonic saline on airway inflammation in children with cystic fibrosis.* Am J Respir Crit Care Med, 2002. **166**(3): p. 352-5.
300. Lazarides, E. and U. Lindberg, *Actin Is the Naturally Occurring Inhibitor of Deoxyribonuclease I.* 1974. **71**(12): p. 4742-4746.
301. Sanders, N.N., et al., *Role of magnesium in the failure of rhDNase therapy in patients with cystic fibrosis.* 2006. **61**(11): p. 962-966.
302. Nasr, S.Z., et al., *Adherence to dornase alfa treatment among commercially insured patients with cystic fibrosis.* J Med Econ, 2013. **16**(6): p. 801-8.
303. Pan, C.Q. and R.A. Lazarus, *Engineering hyperactive variants of human deoxyribonuclease I by altering its functional mechanism.* Biochemistry, 1997. **36**(22): p. 6624-32.
304. Ulmer, J.S., et al., *Engineering actin-resistant human DNase I for treatment of cystic fibrosis.* Proceedings of the National Academy of Sciences of the United States of America, 1996. **93**(16): p. 8225-8229.
305. Guichard, M.J., *Development of a long-acting version of recombinant human deoxyribonuclease i for the treatment of cystic fibrosis lung disease*, in *Biomedical and Pharmaceutical Sciences*. 2018, Université catholique de Louvain.
306. Bonora, G.M. and S. Drioli, *Reactive PEGs for protein conjugation*, in *PEGylated Protein Drugs: Basic Science and Clinical Applications*, F.M. Veronese, Editor. 2009, Birkhäuser Basel: Basel. p. 33-45.
307. Mayolo-Deloisa, K., et al., *Current advances in the non-chromatographic fractionation and characterization of PEGylated proteins.* 2011. **86**(1): p. 18-25.
308. Fee, C.J., *Protein conjugates purification and characterization*, in *PEGylated Protein Drugs: Basic Science and Clinical Applications*, F.M. Veronese, Editor. 2009, Birkhäuser Basel: Basel. p. 113-125.
309. Zhou, Z., et al., *The ENaC-overexpressing mouse as a model of cystic fibrosis lung disease.* J Cyst Fibros, 2011. **10 Suppl 2**: p. S172-82.
310. Oleck, J., S. Kassam, and J.D. Goldman, *Commentary: Why Was Inhaled Insulin a Failure in the Market?* 2016. **29**(3): p. 180-184.

CHAPTER II

BIODISTRIBUTION AND ELIMINATION PATHWAYS OF PEGYLATED RECOMBINANT HUMAN DEOXYRIBONUCLEASE I AFTER PULMONARY DELIVERY IN MICE

Adapted from

Mahri, S., Rondon, A., Bosquillon, C., Vanbever, R. Biodistribution and elimination pathways of PEGylated recombinant human deoxyribonuclease I after pulmonary delivery in mice. Submitted to Journal of Controlled Release on May 20, 2020 (under revision).

ABSTRACT

Conjugation of recombinant human deoxyribonuclease I (rhDNase) to polyethylene glycol (PEG) of 20 to 40 kDa was previously shown to prolong the residence time of rhDNase in the lungs of mice after pulmonary delivery while preserving its full enzymatic activity. This work aimed to study the fate of native and PEGylated rhDNase in the lungs and to elucidate their biodistribution and elimination pathways after intratracheal instillation in mice. *In vivo* fluorescence imaging revealed that PEG30 kDa-conjugated rhDNase (PEG30-rhDNase) was retained in mouse lungs for a significantly longer period of time than native rhDNase (12 days *vs* 5 days). Confocal microscopy confirmed the presence of PEGylated rhDNase in lung airspaces for at least 7 days. In contrast, the unconjugated rhDNase was cleared from the lung lumina within 24 hours and was only found in the lung parenchyma and alveolar macrophages thereafter. Systemic absorption of intact rhDNase and PEG30-rhDNase was observed. However, this was significantly lower for the latter. Catabolism, primarily in the lungs and secondarily in the blood and/or liver, followed by renal excretion were the predominant elimination pathways for both native and PEGylated rhDNase. Catabolism was nevertheless more extensive for the native protein. On the other hand, mucociliary clearance appeared to play a less prominent role in the clearance of those proteins after pulmonary delivery. The prolonged presence of PEGylated rhDNase in lung airspaces would be ideal for its mucolytic action in cystic fibrosis patients.

KEYWORDS

Recombinant human deoxyribonuclease I, protein, PEGylation, pulmonary delivery, biodistribution, cystic fibrosis.

GRAPHICAL ABSTRACT

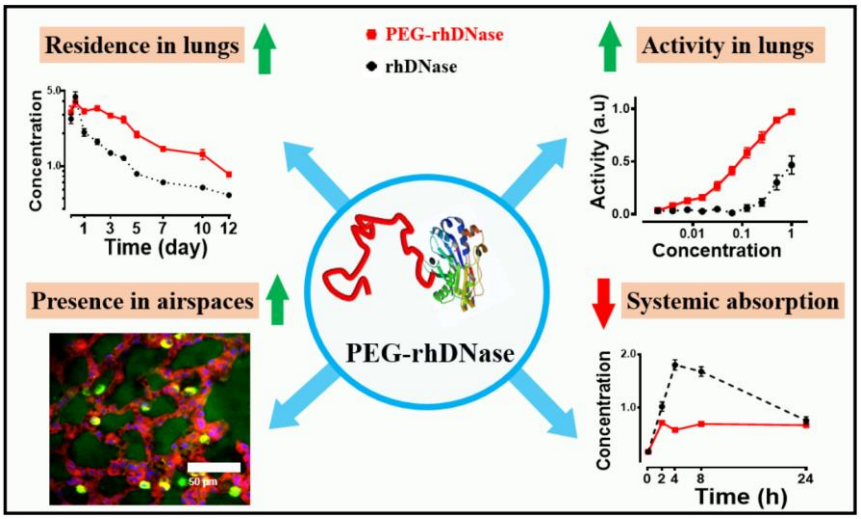

TABLE OF CONTENTS

I. INTRODUCTION

Therapeutic proteins currently account for more than half of the approved biopharmaceuticals and considering their steady growth, their market share is likely to expand further in future years [1, 2]. As compared to traditional low molecular weight drugs, therapeutic proteins are endowed with higher potency and specificity, reduced toxicity and organ accumulation, and lower interaction with other drugs [3-7]. Despite obvious benefits for the topical treatment of respiratory diseases and active research in the area, pulmonary delivery of therapeutic proteins is still in its infancy. Inhaled dornase alfa, a mucolytic agent for the management of patients with cystic fibrosis (CF) was approved in 1993 and so far, remains the only therapeutic protein for inhalation on the market. Several other therapeutic proteins are under development for the local treatment of lung diseases such as asthma, lung infections, CF or alpha-1 antitrypsin deficiency, with some in advanced stages of clinical trials [8, 9]. However, proteins for inhalation face two major obstacles to successful clinical use in lung topical treatment: first, a likely physicochemical degradation during production, formulation, storage, and nebulization and, secondly, a short residence time in the airways [10]. Most proteins are indeed cleared from the lungs within 24 hours [11] due to the combination of effective clearance mechanisms, i.e., mucociliary transport toward the upper airways then elimination through the mouth and stomach, absorption across lung epithelia into the systemic circulation, both enzymatic and non-enzymatic degradation processes, and uptake by lung cells, particularly alveolar macrophages [12-14].

Using the available protein modification toolbox, most efforts are tailored towards increasing the half-life of short-acting proteins after intravenous (IV) injection. Polyethylene glycol (PEG) backed by a long history of clinical use, safety, and a mastery of its chemistry, is by far the most explored protein modifier and it is likely to remain so for the foreseeable future. PEGylation, especially with high MW PEGs, was demonstrated effective in increasing the blood circulation time of proteins following injection by reducing their rapid glomerular filtration in the kidneys [15-17]. Preventing the enzymatic degradation and decreasing the immunogenicity of proteins are other suggested mechanisms for their increased half-life in the blood circulation [15-17].

Furthermore, a few studies have demonstrated a long local residence time of PEGylated proteins in the lungs following their pulmonary delivery, especially when PEG ≥ 20kDa [10]. The residence times were reportedly extended to at least 48 hours for linear 20 kDa (PEG20) a1-proteinase inhibitor [18], branched 2-arm 40 kDa PEG (PEG40) F(ab')2 and PEG40 Fab' antibody fragments compared with less than 24 hours for their non-PEGylated counterparts [13, 19, 20]. The longer lung retention was accompanied by improved efficacy in small animal models [18, 19].

Recombinant human deoxyribonuclease I (rhDNase) plays an essential role in the management of CF symptoms along with the current standard medications [21]. rhDNase decreases the viscoelasticity of respiratory secretions by cleaving the extracellular DNA primarily released by neutrophils into the airspaces [22]. However, the short residence time (< 24 hours) of rhDNase in the lungs is a considerable drawback to its full clinical benefit [23]. Therefore, prolonging its residence time in the lungs would alleviate the burden of frequent and cumbersome administrations of the drug while maintaining or even enhancing its therapeutic efficacy, thereby improving patient's life quality [10]. PEGylation of rhDNase was successfully performed with PEG20, PEG30, and PEG40 through site-specific conjugation to the N-terminal which allowed preserving the conformation and the full enzymatic activity of the protein [23, 24].

In a recent publication, pharmacokinetic studies in healthy mice following intratracheal instillation showed that 30 and 40 kDa PEG conjugates of rhDNase were present in the lungs for more than 15 days. Unconjugated rhDNase, on the other hand, had a retention of less than 24 hours. Furthermore, a single dose of PEG30-rhDNase or PEG40-rhDNase exhibited an equivalent DNA hydrolysis activity after 5 days as one daily dose of rhDNase during 5 days in β-transepithelial Na+ channel–overexpressing mice (β-ENaC) [25].

Following pulmonary administration of proteins, their pathways of clearance from the lungs might involve the mucociliary escalator towards the mouth then gastrointestinal tract (GI tract), transport across respiratory epithelia towards the bloodstream, uptake by lung cells and alveolar macrophages, and catabolism [10]. The elimination of PEGylated proteins from the lungs by systemic absorption would mean a risk of systemic toxicity, while clearance into faeces is usually synonymous with a desirable safety profile. Since rhDNase cleaves extracellular DNA in the respiratory secretions of patients with CF, it is paramount to distinguish between the ratios of the enzyme in lung parenchyma (unavailable) from those in airspaces, available to exert the intended mucolytic action.

The purpose of the present work was to investigate the elimination pathways and fate of native and PEGylated rhDNase in the lungs following pulmonary delivery in mice. First, PEG20, PEG30, and PEG40 were site-specifically conjugated to rhDNase and then labelled with different fluorochromes to be administered *via* intratracheal instillation. The fate of the native and PEGylated rhDNase compounds and PEG30 was then examined in the lungs using confocal microscopy. Finally, near-infrared fluorescence imaging (NIRF) was performed after administration of rhDNase and PEG30-rhDNase, either intratracheally or intravenously, to assess their *in vivo* biodistribution and elimination pathways.

II. MATERIAL AND METHODS

II.1. MATERIALS

Commercial recombinant human deoxyribonuclease I (rhDNase, Pulmozyme®) was obtained from Genentech, Inc. (South San Francisco, CA, USA). Linear methoxy PEG propionaldehyde of 20 kDa and 30 kDa and two-arm methoxy PEG propionaldehyde of 40 kDa (PEG20, PEG30, and PEG40, respectively) were obtained from NOF Corporation (Tokyo, Japan). Alexa Fluor™ 488 TFP ester and Rhodamine B were purchased from Life Technologies (B.V., Gent, Belgium). MitoTracker® Red CMXRos, MitoTracker® Deep Red FM, and Draq5™ were purchased from Invitrogen™ (B.V., Gent, Belgium). Rhodamine-PEG30 was purchased from Creative PEGWorks (Winston Salem, NC, USA). NHS-VivoTag-S ® 750 (VT750) was purchased from Perkin Elmer (Waltham, MA, USA). Unless otherwise mentioned, all other chemicals and reagents were purchased from Sigma-Aldrich (St. Louis, MO, USA).

II.2. PEGYLATION OF RHDNASE

The PEGylation of rhDNase was adapted from the method described by Guichard *et al.* [23, 25]. PEG20-rhDNase, PEG30-rhDNase, and PEG40-rhDNase were produced by conjugation of rhDNase to PEG20, PEG30, and PEG40 respectively. Reductive amination in 0.1 M sodium acetate buffer (CH_3CO_2Na, pH 5) was performed using rhDNase at 10 mg/ml and a molar ratio PEG: rhDNase of 4:1 in the presence of sodium cyanoborohydride ($NaBH_3CN$) as a reducing agent (100 molar excess). The reaction mixtures were stirred overnight at room temperature. The mono-PEGylated products were purified by anion exchange chromatography on a Resource Q, 1mL column with ÄKTA™ purifier 10 system then by size exclusion chromatography (SEC) on a HiLoad 16/60 superdex 200 column (GE Healthcare Bio-Sciences AB, Uppsala, Sweden) (Figure S1). Native and PEGylated rhDNase products were stored at 4 °C in 150 mM NaCl, 1 mM $CaCl_2$ as the marketed dornase alfa product, Pulmozyme®.

II.3. FLUORESCENT LABELLING OF RHDNASE AND PEGYLATED RHDNASE

Alexa Fluor™ 488 TFP ester was used for labelling rhDNase and PEGylated rhDNase products for confocal imaging experiments while NIR dye NHS-VivoTag-S ® 750 (VT750) was used for labelling rhDNase and PEG30-rhDNase for the biodistribution study by NIRF imaging. To this end, all solutions of rhDNase or PEG-rhDNases were exchanged against 1 mM $CaCl_2$ in phosphate buffer saline (PBS) by ultrafiltration using vivaspin® Turbo 4, 3 kDa (Sartorius; Stonehouse,

Gloucestershire, UK). The appropriate volume of dye at 10 mg/ml in DMSO was then added to the protein solution at a molar ratio dye: protein of 10:1 and the reaction mixtures were kept at room temperature in dark under mild agitation for 1 h. The bulk of free dye was removed by ultrafiltration using vivaspin® Turbo 15, 10 kDa MWCO (Sartorius; Stonehouse, Gloucestershire, UK). Labelled rhDNase and PEGylated rhDNase were then further purified by SEC (HiLoad Superdex 200 pg, GE, Belgium), concentrated, filtered through 0.22 μm PVDF filters, and stored at 4 °C in a solution of 150 mM NaCl and 1 mM $CaCl_2$ (Figure S2 and S3). The same degree of labelling (DOL) was achieved for all products (Table S1). The fluorescence signal of near-infrared labelled compounds was further verified by NIRF imaging (Figure S4).

II.4. CONFOCAL IMAGING OF MOUSE LUNGS FOLLOWING INTRATRACHEAL INSTILLATION OF PEG30 AND NATIVE AND PEGYLATED RHDNASES

II.4.1. *Animals*

All experimental protocols were approved by the Institutional Animal Care and Use Committee of the Université Catholique de Louvain (Permit number 2016/UCL/MD/019 and 2019/UCL/MD/044). 6-week old Female RjOrl SWISS mice (Elevage Janvier, Le Genest-St-Isle, France) were kept under conventional housing conditions and were allowed 1 week of acclimation before starting the experiments. Mice were fed a normal chow diet and had access to water *ad libitum*.

For intratracheal instillation, mice were anaesthetized with ketamine/xylazine (90/10 mg/kg), while for *in vivo* imaging mice were anaesthetized by 1.5–2% isoflurane (Isoflutek™, Karizoo SA, Barcelona, Spain) in oxygen.

II.4.2. *Intratracheal instillation*

Mice were anaesthetised by intraperitoneal injection of ketamine/xylazine (90/10 mg/kg) then fixed on an inclined board (~45°) in a supine position using surgical tape. With the aid of a small laryngoscope (Penn-CenturyTM– Model LS-2, Philadelphia, USA), mice were intubated with a 20 G catheter (VWR International BVBA, Leuven, Belgium), then 30 ± 2 μl of samples or controls were administered intratracheally into the lungs using a precision syringe (100 μl, Model 710, Hamilton, Bonaduz, Switzerland) followed by an air bolus of 200 μl using 1ml syringe (HSW SOFT-JECT®, VWR International BVBA, Leuven, Belgium). Immediately after intratracheal instillation, mice were placed in an upright position for 20-30 seconds before further studies.

II.4.3. *Confocal imaging*

Mice were intratracheally instilled with 1 nmol of labelled compounds (A488-rhDNase, A488-PEG20-rhDNase, A488-PEG30-rhDNase, A488-PEG40-rhDNase, or rhodamine-PEG30). Rhodamine B was used as a control to study the fate of the free dye. 15 min (0.25 h), 4 h, 24 h, 48 h, 4 days, 7 days, or 15 days following administration, the mice were euthanized by cervical dislocation, and the lungs and tracheas were removed, roughly cut into ca. 2 mm slices by a razor blade then stained for confocal laser microscopy. Tissue was stained with MitoTracker® at 2 μM (MitoTracker® Red CMXRos or MitoTracker® Deep Red FM) and nuclei with either Draq5™ at 30 μM or Hoechst 33342 at 90 μM final concentration. All stains were prepared in 400 μl of 4% formaldehyde PBS solution then lung slices from the same mouse were dipped in the staining mixture for 15 min then transferred to 4% formaldehyde PBS solution until imaged. Slices were imaged within an hour using Cell Observer Spinning Disk (COSD, Zeiss, Germany) and were recorded in blue (405 nm), green (488 nm), red (561 nm), and far-red (635 nm) channels. All images were acquired at 25 magnification and stored in 16-bit format. A laser exposure time of 200 ms was used throughout the experiments.

Images were processed using ImageJ software (1.47v, NIH, USA). The detection threshold for compounds was set by choosing a cut-off so that to remove unspecific autofluorescence background (Figure S6A).

II.5. BIODISTRIBUTION OF RHDNASE AND PEG30-RHDNASE IN MICE AFTER INTRATRACHEAL INSTILLATION

II.5.1. *Longitudinal near-infrared fluorescence imaging study*

Mice (6-7 per group) were intratracheally instilled with 2 nmol of VT750-rhDNase, VT750-PEG30-rhDNase, or VT750 (dye). Blank consisted of mice with no instillation. Three mice of each group were spared for the *ex vivo* study and the rest (3 to 4 mice) were imaged separately in dorsal and ventral positions at times 2-3 min, 15 min, 4 h, 8 h, and 24 h post-delivery, then every 1-3 days thereafter up to two weeks.

For the intravenous study, three mice per group were injected *via* the tail with 2 nmol of either VT750-rhDNase or VT750-PEG30-rhDNase (100 μl). Imaging was proceeded as above.

All images were acquired by an IVIS Spectrum in vivo imaging system (PerkinElmer, France) using 2D epifluorescence mode at 745/800 nm (excitation /emission) with automated exposure time and binning. Living Image® software (PerkinElmer, France) was used for image acquisition and

processing. The same regions of interest (ROIs) were consistently applied to all animals (Figure 2I). The same threshold and scale (minimum to maximum) were used for comparisons among groups. The baseline fluorescence values (autofluorescence) were estimated from a group of untreated mice ($n \geq 6$) and were used to set the minimum threshold.

II.5.2. *Detection of rhDNase and PEG30-rhDNase in blood, urine and faeces*

Blood was collected from the tail using heparinised capillary tubes (60 µl haematocrit capillary, Hirschmann, Germany) at 2, 4, 8, and 24 h. Blood samples were imaged and ROIs were drawn around blood in microtubes. Blood samples were then centrifuged at 2500 rpm for 15 min to collect the plasma. Mice from different groups were housed in separate cages and the bedding was changed before instillation, 12 h, and 24 h post-delivery and faecal pellets were collected and imaged by IVIS Spectrum. Urines were collected at 2 h and when possible at 24 h by scuffing the mice against a metallic grid until urination then urines were collected by pipetting from a Petri dish placed underneath. Plasma and urines were frozen at -20 °C until further assayed.

II.5.3. *Ex vivo near-infrared fluorescence imaging*

Three mice of each group were sacrificed by cervical dislocation 24 h post-delivery. The blood was collected first v*ia* opened intracardiac puncture and the following organs were harvested and imaged *ex vivo*: lungs, liver, kidneys, heart, spleen, bladder, stomach, small and large intestines, and caecum. ROIs were drawn around organs placed in multiwall plates. Organs were frozen at -20 °C until further assayed.

II.5.4. *SDS-PAGE gel electrophoresis of samples*

Small pieces of lungs, liver, and kidneys were weighed and homogenised in 500 µl RIPA lysis buffer (Abcam, Cambridge, UK) using a tissue grinder (Polytron; Kinematica, Luzern, Switzerland). Tissue homogenates were then centrifuged at 4000 g at 4 °C for 10 min and the supernatants were stored at −20 °C. An amount of 15 µl of tissue homogenate was mixed with 5 µl of loading buffer (4x Laemmli Sample Buffer, BioRad, Belgium) then the mixture was directly loaded onto SDS-PAGE gel (4–20% Mini-PROTEAN® TGX™ Precast Protein Gels, BioRad, Belgium). Plasma (5 µl) and urine (≤ 30 µl) samples were first diluted in PBS if needed then loaded on the gel with loading buffer (3:1 sample: loading buffer). The gels were run at 120 V for 60 min then imaged immediately by IVIS Spectrum. Known amounts of VT750-rhDNase, VT750-PEG30-rhDNase, and VT750 were loaded on each gel as controls.

II.5.5. *Activity of rhDNase and PEG30-rhDNase in lung and liver homogenates*

The activity of rhDNase and PEG30-rhDNase in lung and liver homogenates was assessed using the methyl green (MG) assay described earlier [23, 26]. Briefly, the hydrolysis of the DNA-Methyl Green substrate (DNA-MG) by deoxyribonuclease releases free MG in solution, the colour of this latter fades out to colourless with time leading to a decreasing optical density (OD) at 620 nm.

DNA-MG solution was prepared the day before by mixing 77% v/v of DNA from salmon testes at 2 mg/ml in buffer A (25 mM HEPES, 1 mM EDTA, pH 7.5), 4.6% of 0.4% w/v MG in buffer B (20 mM sodium acetate, pH4.2), and 18.4% of buffer C (25mM HEPES, 4 mM $CaCl_2$, 4 mM $MgCl_2$, 0.1% BSA, 0.01% thimerosal, 0.05% Tween20, pH 7.5).

Lung and liver homogenates were first diluted in buffer C (40-fold and 80-fold respectively) then further serial 2-fold dilutions of samples and controls (100 µl) were prepared in buffer C in 96-well plates. 100 µl of DNA-MG solution was added to each well and the plates were sealed and incubated in a humid chamber at 37 °C for 24 h. At the end of incubation time, the absorbance was measured at 620 nm by SpectraMax i3 (Molecular Devices, US).

II.6. STATISTICS

All data are presented as mean ± SEM. All statistical inferences are based on a two-sided significance level of * $p < 0.05$, ** $p < 0.01$, and *** $p < 0.001$ and were carried out using GraphPad Prism version 8.00 (GraphPad Software, La Jolla California USA). ANOVA was used for multiple group comparisons ($n \geq 3$), while t-test was used for two group comparisons.

III. RESULTS AND DISCUSSION

Previously published works have shown that conjugation of proteins to PEGs of MWs ≥ 20 kDa has a high potential for increasing their residence time in the lungs [13, 18-20, 27]. More recently, 30 and 40 kDa PEG conjugates of rhDNase were shown to be retained in the lungs of mice for more than 15 days compared to merely 24 h for the unconjugated rhDNase [25]. In the current study, we investigated the influence of PEGylation on the biodistribution and elimination pathways of rhDNase in mice following intratracheal instillation using confocal microscopy and NIRF imaging.

III.1. LUNG LOCAL DISTRIBUTION OF NATIVE AND PEGYLATED RHDNASE

The local presence of rhDNase in airspaces is paramount for the mucolytic action of the enzyme and therefore its therapeutic efficacy. To assess the impact of PEGylation and PEG size on the local distribution of rhDNase in the lungs after pulmonary delivery, the fate of rhDNase, PEG20-rhDNase, PEG30-rhDNase, PEG40-rhDNase, PEG30, and rhodamine was followed over time in mice by confocal microscopy.

Shortly after intratracheal instillation (15 min), all compounds were distributed to most lobes and covered many regions of the lungs. In these regions, the signal distribution in airspaces was relatively homogenous evenly filling the airspaces with no particular accumulation pattern (Figure 1 at 0.25 h, Figure S5). The fluorescence signal from the trachea was hardly detectable even at early time points; probably due to the presence of negligible amounts or the washout of compounds during the staining step. The free dye was cleared very fast on account of its low MW (~ 480 Da) and hydrophobic nature as no signal was detected at 4 h in either alveolar spaces or lung cells (Figure S6B).

The signal intensity in airspaces decreased faster for rhDNase where the signal was barely detectable beyond 24 h except in alveolar macrophages and faintly in lung parenchyma. The PEGylated forms of rhDNase continued to be present in the airspaces for at least 4 days for PEG20-rhDNase and 7 days for PEG30-rhDNase and PEG40-rhDNase as well as PEG30 alone (Figure 1, S5 and S7). The fluorescent signal in alveolar macrophages was detected 4 h post instillation and persisted even after the disappearance of fluorescence from the airspaces. It lasted 4 days for rhDNase and 15 days for PEG30-rhDNase, PEG40-rhDNase, and PEG30 alone.

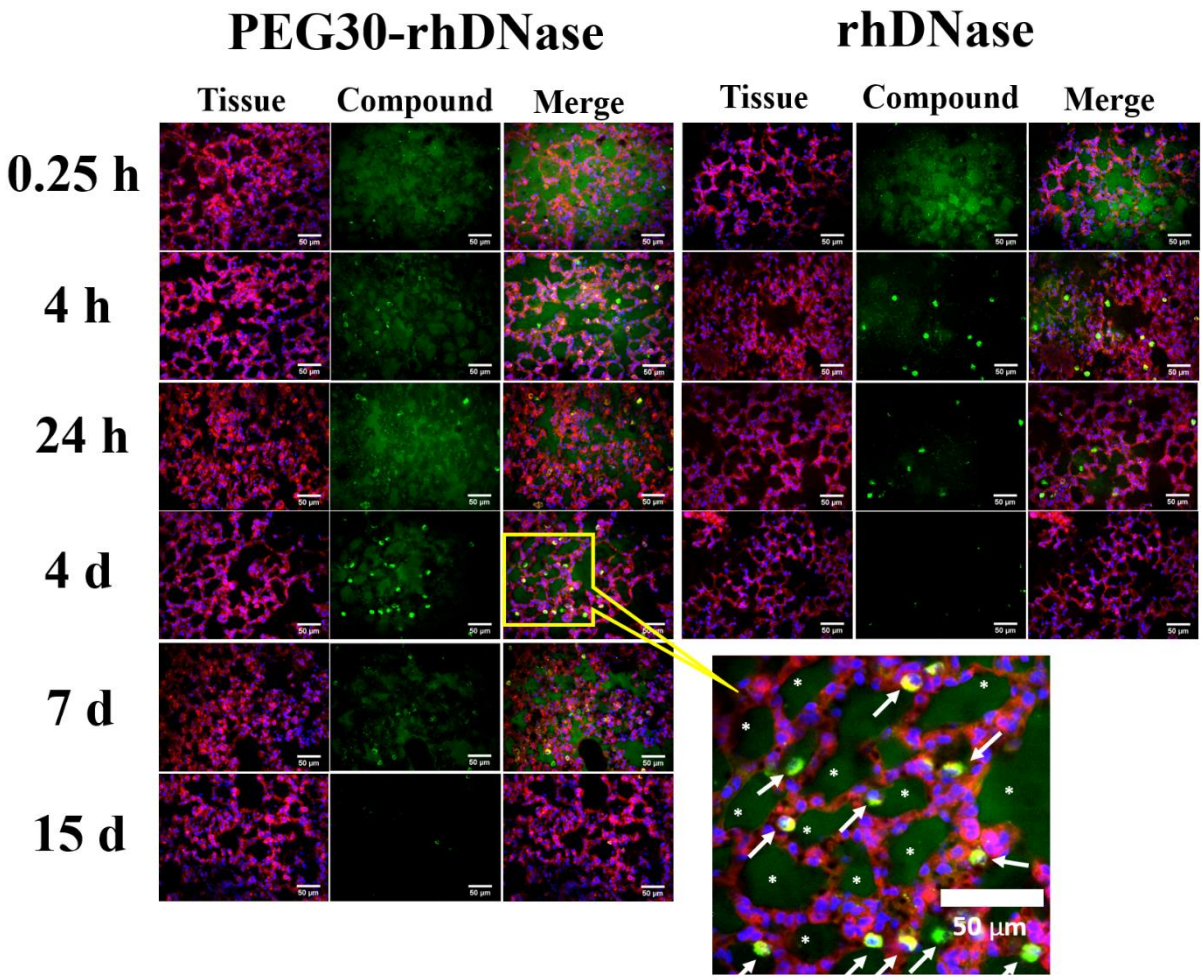

Figure 1. Representative confocal imaging of rhDNase and PEG30-rhDNase in mouse lungs. One nmol of Alexa488-rhDNase or Alexa488-PEG30-rhDNase was administered by intratracheal instillation. Mice were sacrificed at specific time points and the lungs were sliced and stained with MitoTracker® for tissue and Draq5™ for nuclei. Sections were imaged with Cell Observer Spinning Disk (COSD, Zeiss, Germany). Compounds were pseudocoloured in green, tissue in red, and nuclei in blue. Each experimental condition was repeated at least twice. Lower right image shows the presence of PEG30-rhDNase in alveolar macrophages (arrows →), and alveolar spaces (stars *) at day 4 post-instillation. Images were processed by ImageJ software (1.47v, NIH, USA). Scale bars, 50 µm.

The longer persistence of PEGylated rhDNase and PEG30 in alveolar macrophages compared with non-PEGylated rhDNase could be ascribed to the longer availability of the formers in the airspaces. They could also be taken up more slowly or be more resistant to degradation by alveolar macrophages [19, 27].

Numerous alveolar macrophages are actively patrolling the alveolar spaces and engulfing therapeutic particles and proteins in the epithelial lining fluid, thus considerably limiting the efficacy of pulmonary drug delivery, unless they are themselves targeted [28-30]. Overcoming the barrier of macrophage uptake through surface coating of particles with PEG was indeed shown to increase their residence time in the lungs [31]. Along this line, depleting alveolar macrophages led to a

significant increase in the systemic absorption of human chorionic gonadotropin (hCG, 39.5 kDa) and IgG (150 kDa) after pulmonary administration in mice [32].

Macrophage uptake was also reported for PEG40-Fab', PEG30-rhDNase, and PEGs of up to 40 kDa after pulmonary delivery [19, 25, 27, 33]. While no quantitative data were collected in the present work, another study from our laboratory demonstrated that the uptake of PEGylated anti-IL13 Fab' by alveolar macrophages was slightly less efficient than its non-PEGylated counterpart in mice [19].

Protection against aggregation is another likely explanation for the lower uptake of PEGylated rhDNase. Indeed, because large proteins are poorly absorbed through the lungs, they are prone to aggregation and precipitation in lung lining fluid thus accelerating their uptake by alveolar macrophages [34]. However, stability studies in contact with BAL revealed that PEGylation only confers slight protection to rhDNase against aggregation and loss of activity in the absence, but not the presence, of calcium ions (Figure S8 and S9). Therefore, a potential decrease in the uptake of PEGylated rhDNase by alveolar macrophages through preventing aggregation in lung lining fluid might not be significant. In alignment with our observations, previous work published by Freches et al. concluded that PEGylation delayed the clearance of Fab' fragment by alveolar macrophages and that the PEG40 moiety persisted longer than the Fab' moiety inside the cells [27].

Furthermore, our data are consistent with previous work by Guichard *et al.* in which the increase in residence time of rhDNase was in accordance with the increased length of the PEG [25]. Bulkier PEGs could better protect proteins from aggregation and enzymatic degradation and reduce cell uptake and systemic absorption more efficiently [10, 25]. Patil *et al.* compared the lung retention of conjugated anti-IL-17A to PEG20 and PEG40 and nevertheless concluded that the PEG size did not affect the lung retention of anti-IL-17A to a large extent [13]. Finally, the fate of the PEG30 in mouse lungs was similar to that of the PEG30-rhDNase in terms of local distribution and retention time indicating that the fate of the PEG30-rhDNase in the lungs is highly influenced by the presence of the PEG moiety.

III.2. LUNG CLEARANCE OF RHDNASE AND PEG30-RHDNASE AFTER PULMONARY DELIVERY

Based on the confocal images and the previously published pharmacokinetic data of Guichard et al. demonstrating the effectiveness of PEG30-rhDNase in extending the presence of rhDNase in the lungs [25], we selected PEG30-rhDNase to carry out further biodistribution studies.

For this purpose, the NIRF signal was followed overtime after the intratracheal instillation of 2 nmol of VT750-rhDNase, VT750-PEG30-rhDNase or VT750 dye alone, in mice. As expected, a fluorescent signal was observed in the thorax immediately after instillation. The signal intensity from the ventral view was consistently higher than that from the dorsal view due to the shallower depth of the lungs from the former (Figure 2A-B). Despite being less intense, the signal from the dorsal view was less prone to interference with the signal from other organs especially at early time points (< 24 h). For instance, the fluorescent signals present in lungs, stomach and liver overlapped at 8 h post-instillation in the VT750-rhDNase group leading to an overestimation of the signal at this time point from a ventral view (Figure 2B). The contribution of other adjacent organs (i.e. the heart) to the *in vivo* apparent fluorescent signal in the thorax was negligible as was confirmed by *ex vivo* NIRF imaging at 24 h post-instillation (Figure 3A-B). It is worth mentioning that the apparent fluorescence signal detected from the lungs is underestimated compared with the signal from other relatively superficial or unprotected organs such as the liver, the stomach, and the bladder because the lungs are buried deep in the chest cavity. The fluorescence signal was present in the lungs up to 5-7 days for VT750-rhDNase and 12-14 days for VT750-PEG30-rhDNase (Figure 2A-B), in clear contrast to the VT750 dye which was cleared within 24 h (Figure S10).

Immediately after intratracheal instillation, the signal was observed in the lungs, trachea, mouth, and nose then rapidly spread throughout the whole body within 15 min indicating a systemic absorption of VT750-rhDNase, VT750-PEG30-rhDNase, and free VT750 dye (Figure 2B and Figure S10). The signal in the thorax ROI increased between time 2 min and 8 h. This artefact is ascribed to the increased signal in the blood over time, which gives rise to a higher apparent epifluorescence signal in the thorax ROI by NIRF imaging as blood vessels are located superficially beneath the surface of the skin, therefore, closer to the camera (Figure 2D). The signal in the thoracic region increased to an even higher extent in the case of the VT750 dye that is absorbed more quickly due to its hydrophobic nature and low MW (i.e. 1.18 kDa *vs* 37 or 67 kDa for rhDNase or PEG30-rhDNase, respectively). Geyer *et al.* reported similar findings after pulmonary delivery of 2.5 or 10 μg of Alexa-750-siRNA to mice [35]. In that study, the fluorescence signals in the thorax increased compared to the initial measurements for the same mice 6 and 24 h post-delivery.

In our case, at 24 h post-delivery and beyond, the signals were less than those initially and that of VT750-PEG30-rhDNase in the lungs was 1.5 to 2-fold higher than that of VT750-rhDNase until total clearance from the lungs.

III.3. BIODISTRIBUTION OF RHDNASE AND PEG30-RHDNASE AFTER INTRAVENOUS DELIVERY

The biodistribution of rhDNase and PEG30-rhDNase after intravenous injection was also examined. Immediately after delivery, the signal was spread throughout the whole body and the images were similar to those collected 15 min to 24 h following intratracheal instillation, confirming that a systemic absorption occurred after pulmonary delivery. In addition, as soon as 15 min after IV injection, a strong signal appeared in the bladder and the liver indicating a liver clearance and renal excretion of rhDNase and PEG30-rhDNase as degradation products, free dye, and intact proteins (Figure 2C), although the renal excretion of intact PEG30-rhDNase is unlikely (*cf.* section III.6). VT750-rhDNase did not persist in the liver for as long as VT750-PEG30-rhDNase (5 days *vs* 22 days) (Figure 2G). Moreover, *in vivo* data did not reveal any significant distribution for both compounds in other organs including the lungs. The longer half-life and liver retention of PEGylated rhDNase were expected and are likely the result of the increased protein hydrodynamic size and thereby the reduced glomerular filtration. A delayed proteolytic degradation of PEGylated rhDNase is also possible [36-39].

III.4. ORGAN DISTRIBUTION OF RHDNASE AND PEG30-RHDNASE AFTER PULMONARY DELIVERY

Ex vivo imaging of organs at 24 h post-instillation clearly showed a dominant signal in the lungs for both VT750-rhDNase and VT750-PEG30-rhDNase groups compared to the other organs (Figure 3A and B, Figure S11, and S12). The percentage of lung signal accounted for 91 ± 4% (mean ± SEM) of the total signal of harvested organs for VT750-PEG30-rhDNase, compared with 66 ± 6% for VT750-rhDNase (Figure 3A and B). In addition, the total lung signal was 1.75 times higher for VT750-PEG30-rhDNase compared with that of VT750-rhDNase, consistent with the *in vivo* imaging at 24 h post-instillation (Figures 2D, 3C and 3D).

The signal in the liver peaked around 8 h and was 8-fold higher in VT750-rhDNase group compared with VT750-PEG30-rhDNase at 24 h *ex vivo* (27 ± 3% *vs* 3 ± 1%) (Figure 2E and Figure 3E). This is mainly attributed to the lower systemic absorption of VT750-PEG30-rhDNase preventing its significant accumulation in the liver and other distant organs. Higher signals were

also detected in the heart for VT750-rhDNase compared with VT750-PEG-rhDNase ($p < 0.05$), but not in the kidneys, the spleen or the GI tract (Figure 3E).

Clearance via the urine seemed to be predominant for all compounds as indicated by the presence of fluorescence signal in the bladder from early time points until the total clearance of compounds from the body (Figure 2B). Nevertheless, analysis of urines showed that most of the fluorescent signal stems from the free dye and degradation products rather than the intact proteins (*cf.* section III.6). Due to the irregularity of urination, the signal from the bladder was not used for comparison between groups and the *ex vivo* signal in the kidneys was used instead (Figure 3E and S11B). In contrast, no distinct signal from the kidneys could be obtained in live animals in Figure 2 due to the weak fluorescent signal.

On the other hand, mucociliary clearance followed by digestive elimination appeared to contribute to the clearance of rhDNase and PEG30-rhDNase after pulmonary delivery but to a lower extent and indifferently to the compound. The fluorescence signal in the stomach was not detectable at early time points (< 15 min), in contradiction with an expected rapid accumulation of compounds initially deposited in the mouth during instillation (Figure 2F). It then built up to reach a maximum at 8 h suggesting mucociliary clearance followed by swallowing occurred. It is nevertheless noteworthy that fluorescence in the stomach was easier to spot in the VT750-PEG30-rhDNase group at 4 and 8 h as the signal from the liver did not interfere at these time point (Figure 2B 8 h). The signal in the faecal pellets collected up to 24 h post instillation represented only a tiny fraction of the total signal (Figure S13) and that in the GI tract represented no more than 3% at 24 h with no difference between the VT750-rhDNase and PEG30-rhDNase groups (Figure 3E and Figure S14).

These observations support the suggestion of Hastings *et al.* [14] who argued that the mucociliary clearance is not a significant mechanism of protein clearance from the lungs, particularly after delivery to distal airways [13]. Its contribution could be even less effective in respiratory diseases such as chronic obstructive pulmonary disease (COPD), CF, and asthma where the mucociliary clearance is impaired [40, 41].

The longer residence time of PEGylated rhDNase compared with rhDNase in the lungs is expected to be observed if compounds were administered by nebulisation or as dry powders. In the case of nebulisation, lung deposition is more homogeneous and peripheral compared to intratracheal instillation; therefore, the systemic absorption and cell uptake of both proteins is expected to be higher by nebulisation but the involvement of mucociliary clearance would be undermined. In the case of dry powder inhalers (DPI), the clearance of solid particles is driven by their physico-

chemical properties; once proteins are released from their carriers in contact with lung lining fluids, the longer residence time of PEGylated rhDNase compared to rhDNase would hold due to the lower absorption and cell uptake of the former.

The pharmacokinetic advantages of PEGylated rhDNase are also expected to be observed in diseased CF lungs. Guichard et al. have shown that PEGylation increased the stability of rhDNase in CF respiratory secretions [24]. Moreover, the efficacy studies in β-ENaC mice showed that a single dose of PEG30-rhDNase or PEG40-rhDNase exhibited an equivalent DNA hydrolysis activity after 5 days as one daily dose of rhDNase during 5 days. These results suggest that PEGylated rhDNase was also retained longer in murine inflamed lungs [25].

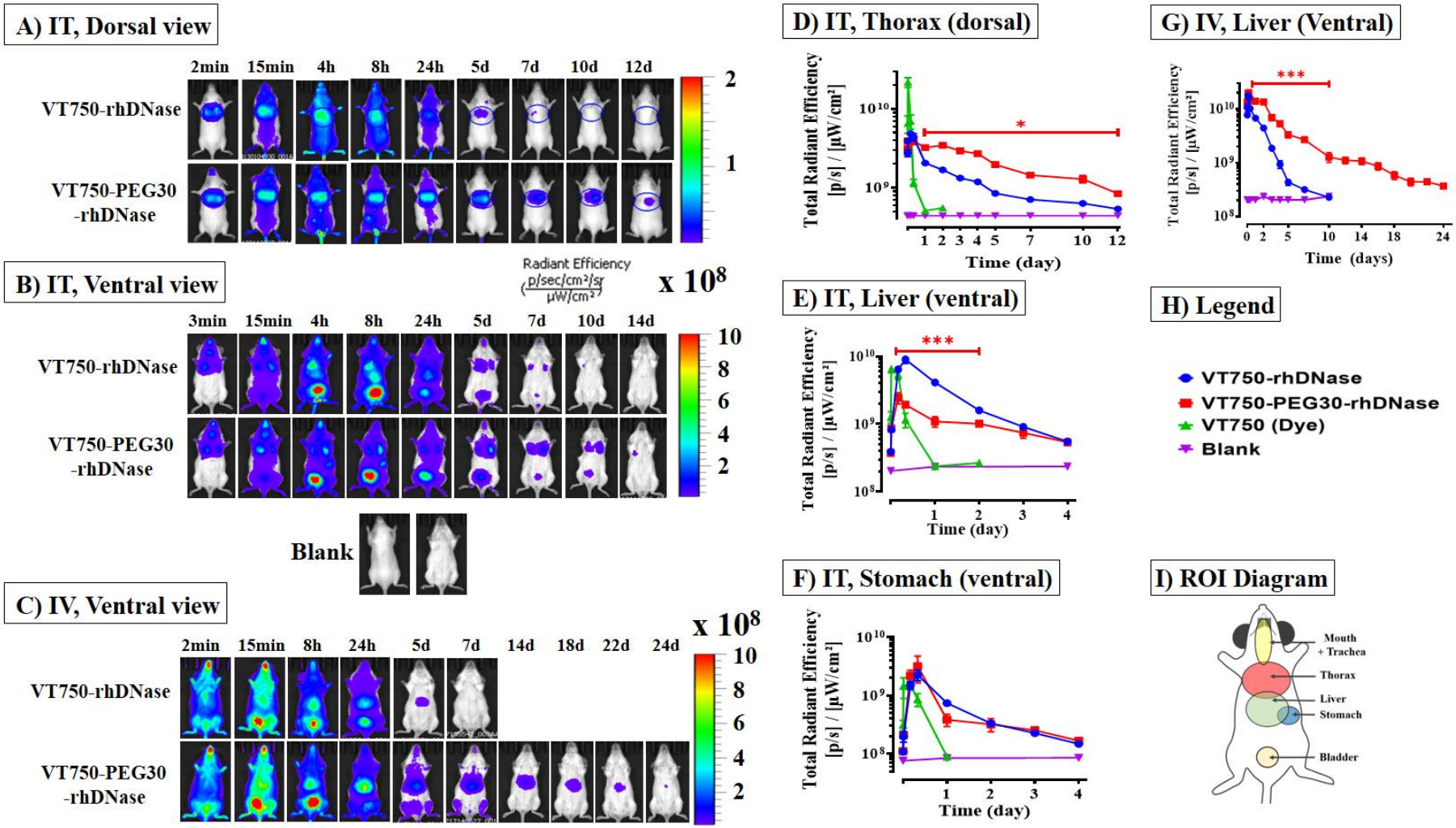

Figure 2. *In vivo* NIRF imaging in mice after intratracheal and intravenous administration. Swiss mice received 2 nmol of VT750-rhDNase, VT750-PEG30-rhDNase, or VT750 by intratracheal instillation (IT, A, B, and D-F). C and G, mice were injected intravenously (IV) *via* the tail with 2 nmol of VT750-rhDNase or VT750-PEG30-rhDNase. Blank mice did not receive any compound. Mice were imaged by IVIS Spectrum in 2D epifluorescence mode at 745/800 nm (ex/em). A and B, representative images from dorsal and ventral views, respectively after IT; D-F, quantification of ROIs in the thorax, liver, and stomach. C, representative images from ventral views after IV injection; G, quantification of ROIs in the liver. H, legend of figures D-G. I, ROI diagram. Data points represent the mean ± SEM of the total fluorescence signal (n = 3). Significant differences between VT750-rhDNase and VT750-PEG30-rhDNase are indicated by * for $p < 0.05$, ** for $p < 0.01$, and *** for $p < 0.001$ (repeated measures two-way ANOVA followed by Tukey's post hoc test).

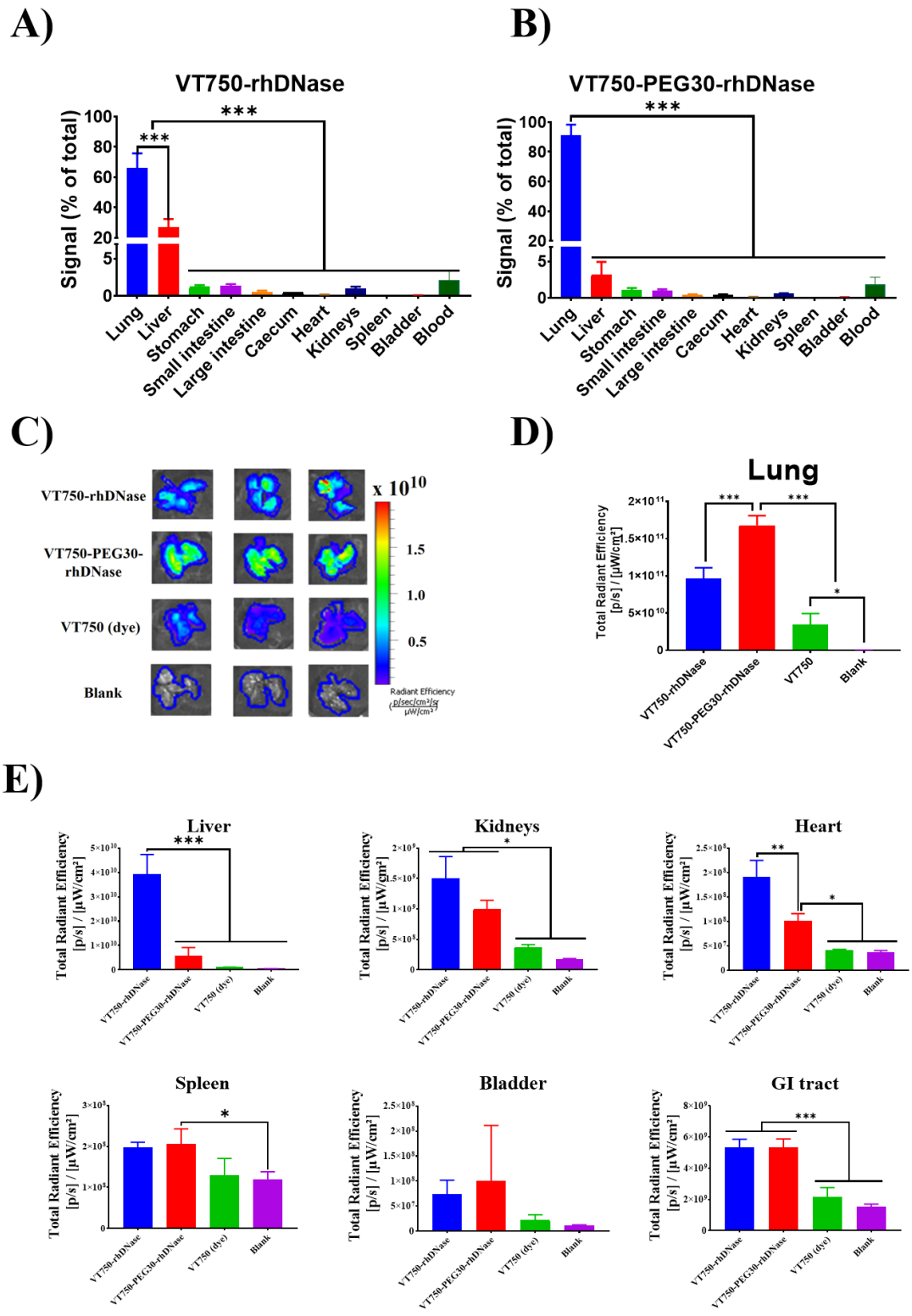

Figure 3. Ex vivo organ imaging in mice at 24 h post intratracheal instillation of 2 nmol of VT750-rhDNase, VT750-PEG30-rhDNase, or VT750 free dye. Mice were sacrificed, blood and organs were collected for epifluorescence quantification by IVIS Spectrum at 745/800 nm (ex/em). A and B represent the percentage of signal from each organ to the total signal from all organs for VT750-rhDNase and VT750-PEG30-rhDNase, respectively. C, NIRF images of lungs ex vivo and D, signal quantification ROIs in C. E, signal quantification in other organs, the GI tract signal is the sum signal from the stomach, small intestine, large intestine and caecum. Bar charts represent the mean ± SEM (n = 3). Significant differences are indicated by * $p < 0.05$, ** $p < 0.01$, or *** $p < 0.001$ (one-way ANOVA followed with Tukey's post hoc test).

III.5. INTEGRITY OF RHDNASE AND PEG30-RHDNASE IN LUNG HOMOGENATES

In a previous work [25], sustained retention of PEG30-rhDNase over 15 days in mouse lungs was reported, which agrees with the present data (Figure 2A-B). Nonetheless, the total clearance of unconjugated rhDNase from the lungs occurred within 24 h compared with 5 to 7 days in our experiments. To reconcile both findings, we suggest that the fluorescent signal detected for VT750-rhDNase in mouse lungs beyond 24 h might arise from degraded rhDNase in alveolar macrophages and lung parenchyma. Indeed, the signal followed by NIRF imaging originates not only from intact compounds but also from their degradation products and the released dye. It is well-established that the lungs are involved in protein metabolism, albeit to a lesser extent than the liver for example [34]. Moreover, for PEGylation to be effective as a method of improving the therapeutic efficacy of rhDNase, the enzymatic activity of PEGylated rhDNase should be preserved *in vivo*. Altogether, it was therefore important to investigate the integrity and enzymatic activity of rhDNase and PEG30-rhDNase in the lungs.

Gel electrophoresis of lung homogenates revealed the presence of distinct bands corresponding to the intact proteins as well as byproducts of VT750-rhDNase and VT750-PEG30-rhDNase at 24 h (Figure 4A and B). The intensity of the bands corresponding to intact VT750-PE30-rhDNase was 18.9 ± 1.0% of the total signal, 10-fold higher than that of VT750-rhDNase (1.8 ± 0.4%) (Figure 4A-C). This is in correlation with the 10-fold higher enzymatic activity on DNA of VT750-PEG30-rhDNase in lung homogenates compared with VT750-rhDNase (Figure 4D).

Bands corresponding to the released VT750 dye and rhDNase fragments of roughly estimated MWs between 10 and 20 kDa were detected in lung homogenates for both VT750-rhDNase and VT750-PEG30-rhDNase groups (arrows in Figure 4A). Interestingly, no bands corresponding to the MW of rhDNase (~37 kDa) were visible for the VT750-PEG30-rhDNase group. The most plausible explanation is that the degradation of the protein moiety in PEG30-rhDNase occurs first, while still attached to the PEG, which is then followed by the cleavage of the PEG moiety [42]. The band observed just below that of VT750-PEG30-rhDNase likely corresponds to the same fragments of rhDNase (10-20 kDa) still attached to the PEG30 moiety (Figure 4A and B).

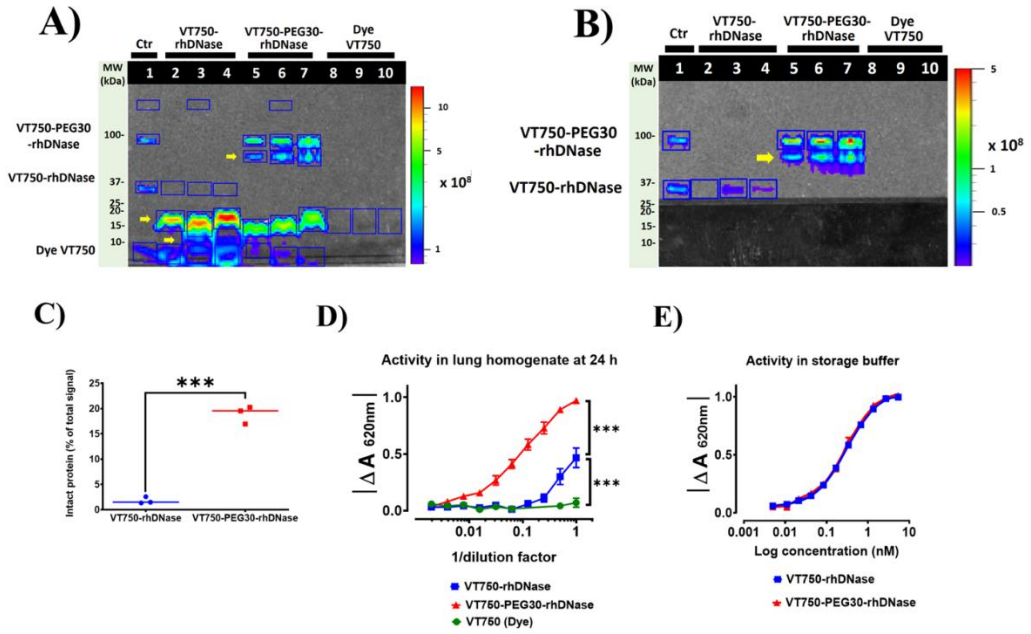

Figure 4. Ex vivo analysis of lung homogenates 24 h post instillation of 2 nmol of VT750- rhDNase, VT750-PEG30-rhDNase, or VT750 (dye). A) SDS-PAGE of lung homogenates, arrows point to degradation fragments. B) Same image as A after concealing the bottom part of the gel and amplifying the signal to visualise VT750-rhDNase bands. Lane 1, Control loaded with VT750-rhDNase (~10 ng), VT750-PEG30-rhDNase, and VT750; Lanes 2-10, samples from different mice. Gel was imaged by IVIS Spectrum (745/800 nm ex/em). Scale in radiant efficiency ([p/s/cm²/sr] / [µW/cm²]). C) Percentage of signal intensities of intact bands to the total signal intensity of all bands in the same lane. D) Enzymatic activity of lung homogenates on DNA-MG substrate. E) Enzymatic activity of stock solutions of VT750-rhDNase and VT750-PEG30-rhDNase, showing their similar enzymatic activity. DNA hydrolysis releases MG in solution leading to a decrease in the absorbance at 620 nm after 24 h of incubation at 37 °C. Data represent mean ± SEM (n = 3, t-test (C) and ANOVA two ways followed with Tukey's post hoc test (D-E), ** $p < 0.01$, and *** $p < 0.001$). MW, molecular weight.

The degradation of the protein moiety of PEGylated proteins was demonstrated by Elliot *et al.* who followed the fate of PEG40-insulin in the plasma of rats after intravenous administration [43]. Using antibodies directed against PEG (anti-PEG) and insulin (anti-insulin), they detected the PEG moiety over a much longer period of time than insulin by Western blot but could not detect the native unmodified insulin, therefore, concluded that insulin was most likely degraded while still coupled to the PEG moiety, losing, thus, its antigenic epitopes.

Our data suggest that PEG30-rhDNase suffered less degradation in the lungs and, therefore, retained more activity compared with rhDNase, which was extensively degraded at 24 h.

Taken together with the confocal images (Figure 1) and the pharmacokinetic data of Guichard *et al.*[25] in which rhDNase was cleared from lungs within 24 h, it is likely that the intact fractions of rhDNase and PEG30-rhDNase in lung homogenates at 24 h are localised extracellularly whereas the intracellular signal observed in alveolar macrophages and epithelial cells by confocal imaging corresponds mostly to degraded fragments.

III.6. SYSTEMIC ABSORPTION OF RHDNASE AND PEG30-RHDNASE AFTER PULMONARY DELIVERY

Systemic absorption to the bloodstream is another clearance mechanism of proteins from the lungs besides mucociliary clearance and local degradation. The systemic absorption of rhDNase after a single inhalation has been shown to range from less than 2% in monkeys up to 15% in rats [44]. Proteins of similar or larger MWs such as human chorionic gonadotropin (hCG, 39.5 kDa), human albumin (68 kDa), and IgG (150 kDa) have also been reported to be absorbed into the blood after pulmonary delivery, albeit poorly [32, 34]. However, a few studies have reported a decrease in lung absorption of proteins upon their PEGylation. Following pulmonary delivery in rats, the bioavailability of recombinant human granulocyte-colony stimulating factor (rhGCSF, 18 kDa) dropped threefold after conjugation to 6 kDa PEG (11.9% to 4.5%) and even lower after conjugation to 12 kDa PEG (1.6%) [45]. A similar decrease was observed for IFNα2b (19 kDa), with its bioavailability reduced from 15% to 5.5% and < 0.4% when conjugated to PEGs of 12 kDa and 40 kDa, respectively [7]. Patil *et al.* showed that PEGylation of anti-IL-13 and anti-IL-17A (47 kDa) with PEG40 reduced both their uptake and transport across Calu-3 human lung epithelial cells [13]. Based on these studies and the general assumption that larger proteins are less absorbed from the lungs [7, 46], PEGylation is expected to diminish the absorption of rhDNase across the lung epithelial barrier.

Systemic absorption of both VT750-rhDNase and VT750-PEG30-rhDNase was suspected from observations in live animals and isolated organs (Figure 2 and Figure 3). This was confirmed by monitoring the presence of the proteins in the blood. The maximum blood signals of VT750-rhDNase were higher than those of VT750-PEG30-rhDNase (Figure 5A and C and Figure S15). The signal of VT750-rhDNase in the blood peaked at around 4 h post-delivery then decreased slowly thereafter, whereas that of VT750-PEG30-rhDNase increased initially then remained relatively steady from 2 h to 24 h. The absorption of intact compounds was confirmed by the presence of bands corresponding to MWs of both intact VT750-rhDNase and VT750-PEG30-rhDNase in plasma by gel electrophoresis (Figure 5C). The signal intensity patterns of VT750-rhDNase and VT750 PEG30-rhDNase bands in plasma were overall in agreement with the signals from the whole blood. Besides the free dye detected in all groups, faint bands corresponding to degraded fragments of VT750-rhDNase and VT750-PEG30-rhDNase similar to those detected in lung homogenates at 24 h were detected in plasma at 4 h and 24 h (Figure 5B). These degradation fragments likely diffused from the lungs into the systemic circulation, however, degradation of

VT750-rhDNase and VT750 PEG30-rhDNase could also have occurred in plasma or liver after systemic absorption.

Gel electrophoresis of urine samples collected 2 h after intratracheal instillation showed the presence of intact VT750-rhDNase (Figure 5C). Renal excretion is expected to be relatively rapid due to the low MW of rhDNase compared with the threshold of renal filtration (60-70 kDa) [39, 47-50]. On the other hand, no traces of intact VT750-PEG30-rhDNase could be detected in the urine at 2 h and 24 h, likely due to its large molecular volume (Figure 5C and Figure S16). Our measurements of the hydrodynamic size of rhDNase and PEG30-rhDNase by dynamic light scattering indicate a size of ~ 4.8 nm for rhDNase and ~10 nm for PEG30-rhDNase (Table S2). The hydrodynamic size of the latter is larger than that of serum albumin (68 kDa, ~6 nm), a protein of similar MW [51]. It is known that the molecular size of PEGylated proteins is much larger than proteins of similar MWs [39, 45]. In fact, the hydrodynamic volume of PEG 18 kDa alone is greater than that of serum albumin [52]. Therefore, the renal filtration of intact PEG30-rhDNase should in principle be negligible. It is worthwhile to mention that PEGs as big as 40 kDa were shown to be excreted in the urines of mice, rats, and humans [53-55].

No bands of either VT750-rhDNase or VT750-PEG30-rhDNase could be detected in the kidneys which could be also explained by the weak signal obtained in the kidneys *ex vivo* at 24 h (Figure S17). Only degraded fragments of VT750-rhDNase were detected in the liver for VT750-rhDNase group at 24 h, suggesting the potential implication of the liver in the catabolism of the protein after absorption from the lung. On the other hand, the signal intensity in the liver was too low to detect any bands for the VT750-PEG30-rhDNase group (Figure S17).

III.7. ELIMINATION OF RHDNASE AND PEG30-RHDNASE AFTER INTRAVENOUS DELIVERY

After IV injection, VT750-rhDNase was cleared from the blood faster than VT750-PEG30-rhDNase (Figure 5D). Plasma concentrations of VT750-rhDNase were already lower than those of VT750-PEG30-rhDNase at 2 h and were barely detectable at 24 h (Figure 5D-E). Gel electrophoresis of plasma collected 4 h and 24 h post-injection showed similar degradation products for both VT750-rhDNase and VT750-PEG30-rhDNase (Figure 5E). These degradation products are also similar to those found in the plasma 24 h post-instillation (Figure 5B). This confirms our earlier suggestion that further degradation in the liver or plasma could occur following systemic absorption of both intact and degraded rhDNase and PEG30-rhDNase from the lungs.

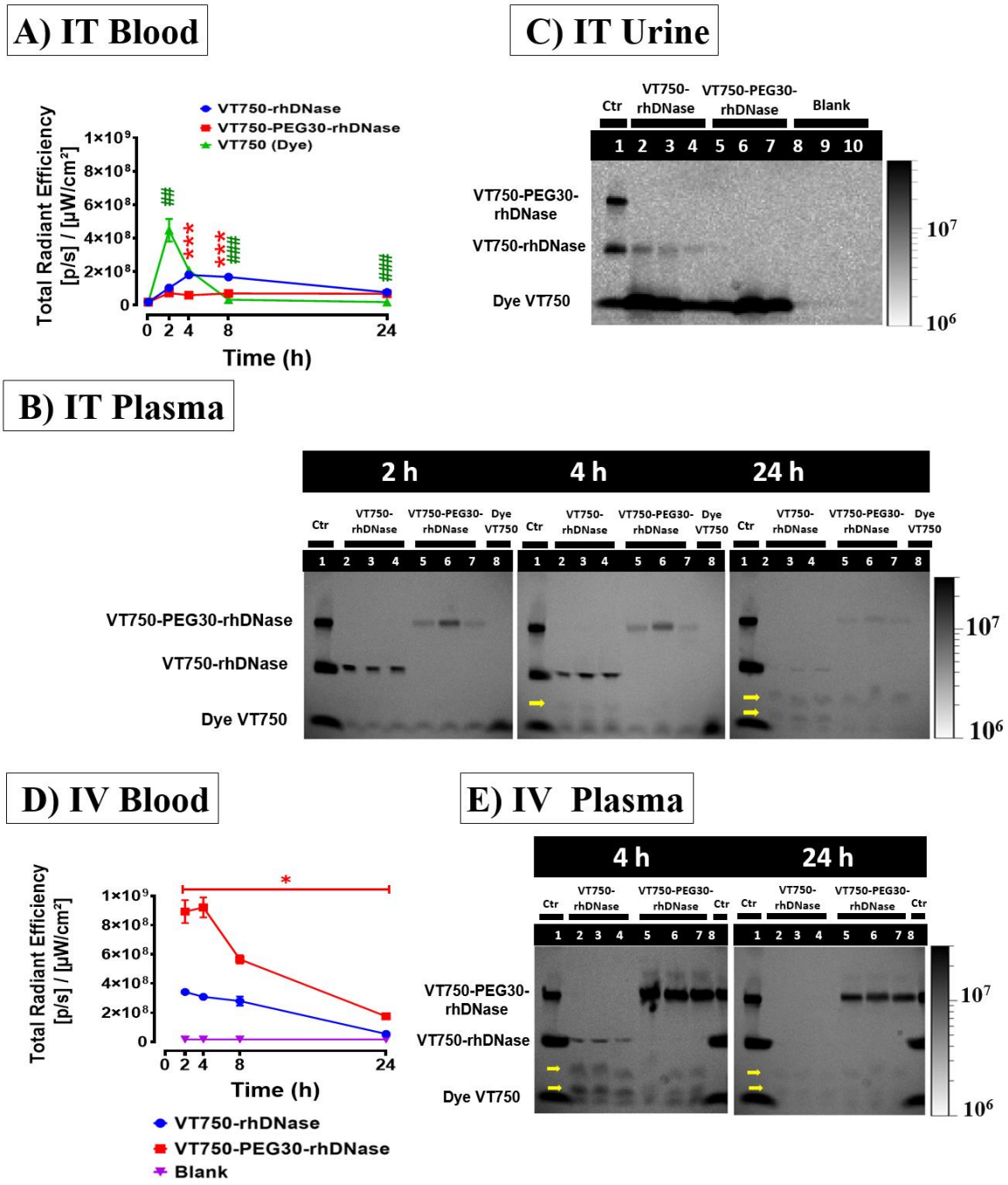

Figure 5. Analysis of blood, plasma, and urine by NIRF imaging. Mice received 2 nmol of VT750-rhDNase, VT750-PEG30-rhDNase, or VT750 by intratracheal instillation (IT, A-C) or intravenous injection (IV, D and E). **A, D)** Quantification of signal in blood samples collected at 2, 4, 8, and 24 h post-delivery by IVIS Spectrum at 745/800 nm (ex/em). **B)** SDS-PAGE of plasma (5 µl) at 2, 4, and 24 h post-instillation. **C**) SDS-PAGE of urines (30 µl) collected at 2 h post-instillation. **E**) SDS-PAGE of plasma (5 µl) at 2 and 24 h post-injection. Arrows point to degradation fragments. Samples were mixed with loading buffer (3:1 sample: 4x Laemmli) then loaded on the gel (4–20%) and run at 120 V for 60 min. Lane 1, Control loaded with VT750-rhDNase (~10 ng), VT750-PEG30-rhDNase, and VT750; Lanes 2-10, samples from different mice. Gels were imaged by IVIS Spectrum (745/800 nm ex/em). Scale in radiant efficiency ([p/s/cm²/sr] / [µW/cm²]). Data points represent the mean ± SEM (n = 3). Significant differences from VT750-rhDNase are indicated by *** $p < 0.001$ for VT750-PEG30-rhDNase and ### $p < 0.001$ for VT750 (two-way ANOVA followed with Tukey's post hoc test).

IV. CONCLUSIONS

In this work, the fate in the lungs and elimination pathways of native and PEGylated rhDNase were investigated following intratracheal delivery to healthy mice. Native rhDNase was cleared from the lungs within 24 h whereas conjugation to PEGs of 20 to 40 kDa sustained the presence of the enzyme in lung airspaces for more than 4 days (PEG20-rhDNase) or 7 days (PEG30-rhDNase and PEG40-rhDNase) after a single dose. Reduced degradation within the lungs and lower systemic absorption were identified as major mechanisms driving the longer retention of PEGylated rhDNase in the lungs. Both rhDNase and PEG30-rhDNase were primarily degraded in the lungs and secondarily in the blood and/or liver, followed by renal excretion. Interestingly, the degradation of PEG30-rhDNase likely involves an initial fragmentation of the protein followed by a detachment of the PEG moiety. Following intratracheal instillation, no accumulation of the proteins was seen in other organs at the exception of rhDNase in the liver. However, liver accumulation was prominent after IV injection and was more marked for PEG30-rhDNase. Alveolar macrophages were shown to actively take up both PEGylated and native rhDNase as well as PEG alone. Deeper mechanistic studies are being conducted to determine the influence of PEGylation on the stability of rhDNase in contact with lung media, the uptake by macrophages, and the transport across lung epithelial cells. Overall, the prolonged presence of PEGylated rhDNase in lung airspaces would be ideal for its mucolytic action in patients with CF.

V. REFERENCES

1. Walsh, G., *Biopharmaceutical benchmarks 2014.* Nature Biotechnology, 2014. **32**(10): p. 992-1000.
2. Walsh, G., *Biopharmaceutical benchmarks 2018.* Nat Biotechnol, 2018. **36**(12): p. 1136-1145.
3. Marx, V., *Watching peptide drugs grow up.* Chemical & Engineering News, 2005. **83**(11): p. 17-+.
4. Renukuntla, J., et al., *Approaches for enhancing oral bioavailability of peptides and proteins.* International Journal of Pharmaceutics, 2013. **447**(1-2): p. 75-93.
5. Agyei, D., et al., *Protein and Peptide Biopharmaceuticals: An Overview.* Protein and Peptide Letters, 2017. **24**(2): p. 94-101.
6. Leader, B., Q.J. Baca, and D.E. Golan, *Protein therapeutics: A summary and pharmacological classification.* Nature Reviews Drug Discovery, 2008. **7**(1): p. 21-39.
7. McLeod, V.M., et al., *Optimal PEGylation can improve the exposure of interferon in the lungs following pulmonary administration.* J Pharm Sci, 2015. **104**(4): p. 1421-30.
8. de Kruijf, W. and C. Ehrhardt, *Inhalation delivery of complex drugs - the next steps.* Current Opinion in Pharmacology, 2017. **36**: p. 52-57.
9. Bodier-Montagutelli, E., et al., *Designing inhaled protein therapeutics for topical lung delivery: what are the next steps?* Expert Opinion on Drug Delivery, 2018. **15**(8): p. 729-736.
10. Guichard, M.J., T. Leal, and R. Vanbever, *PEGylation, an approach for improving the pulmonary delivery of biopharmaceuticals.* Current Opinion in Colloid & Interface Science, 2017. **31**: p. 43-50.
11. Todoroff, J. and R. Vanbever, *Fate of nanomedicines in the lungs.* Current Opinion in Colloid & Interface Science, 2011. **16**(3): p. 246-254.
12. Villegas, M.R., A. Baeza, and M. Vallet-Regi, *Nanotechnological Strategies for Protein Delivery.* Molecules, 2018. **23**(5).
13. Patil, H.P., et al., *Fate of PEGylated antibody fragments following delivery to the lungs: Influence of delivery site, PEG size and lung inflammation.* Journal of Controlled Release, 2018. **272**: p. 62-71.
14. Hastings, R.H., H.G. Folkesson, and M.A. Matthay, *Mechanisms of alveolar protein clearance in the intact lung.* American Journal of Physiology-Lung Cellular and Molecular Physiology, 2004. **286**(4): p. L679-L689.
15. Werle, M. and A. Bernkop-Schnurch, *Strategies to improve plasma half life time of peptide and protein drugs.* Amino Acids, 2006. **30**(4): p. 351-67.
16. Veronese, F.M. and A. Mero, *The impact of PEGylation on biological therapies.* BioDrugs, 2008. **22**(5): p. 315-29.
17. Pasut, G. and F.M. Veronese, *State of the art in PEGylation: the great versatility achieved after forty years of research.* J Control Release, 2012. **161**(2): p. 461-72.
18. Cantin, A.M., et al., *Polyethylene glycol conjugation at Cys232 prolongs the half-life of alpha1 proteinase inhibitor.* Am J Respir Cell Mol Biol, 2002. **27**(6): p. 659-65.
19. Koussoroplis, S.J., et al., *PEGylation of antibody fragments greatly increases their local residence time following delivery to the respiratory tract.* Journal of Controlled Release, 2014. **187**: p. 91-100.
20. Freches, D., et al., *PEGylation prolongs the pulmonary retention of an anti-IL-17A Fab' antibody fragment after pulmonary delivery in three different species.* Int J Pharm, 2017. **521**(1-2): p. 120-129.
21. DeSimone, E., et al., *Cystic Fibrosis Update on Treatment Guidelines and New Recommendations.* Us Pharmacist, 2018. **43**(5): p. 16-21.
22. Shak, S., et al., *Recombinant human DNase I reduces the viscosity of cystic fibrosis sputum.* Proc Natl Acad Sci U S A, 1990. **87**(23): p. 9188-92.
23. Guichard, M.J., et al., *Production and characterization of a PEGylated derivative of recombinant human deoxyribonuclease I for cystic fibrosis therapy.* International Journal of Pharmaceutics, 2017. **524**(1-2): p. 159-167.
24. Guichard, M.J., et al., *Impact of PEGylation on the mucolytic activity of recombinant human deoxyribonuclease I in cystic fibrosis sputum.* Clin Sci (Lond), 2018. **132**(13): p. 1439-1452.
25. Guichard, M.J., et al., *PEGylation of recombinant human deoxyribonuclease I provides a long-acting version of the mucolytic for patients with cystic fibrosis (Submitted).*
26. Sinicropi, D., et al., *Colorimetric determination of DNase I activity with a DNA-methyl green substrate.* Anal Biochem, 1994. **222**(2): p. 351-8.
27. Freches, D., et al., *Preclinical evaluation of topically-administered PEGylated Fab' lung toxicity.* Int J Pharm X, 2019. **1**: p. 100019.

28. Lombry, C., et al., *Confocal imaging of rat lungs following intratracheal delivery of dry powders or solutions of fluorescent probes.* J Control Release, 2002. **83**(3): p. 331-41.
29. Hastings, R.H., et al., *Cellular uptake of albumin from lungs of anesthetized rabbits.* Am J Physiol, 1995. **269**(4 Pt 1): p. L453-62.
30. Lehnert, B.E., *Pulmonary and thoracic macrophage subpopulations and clearance of particles from the lung.* Environmental health perspectives, 1992. **97**: p. 17-46.
31. Shen, T.W., et al., *Distribution and Cellular Uptake of PEGylated Polymeric Particles in the Lung Towards Cell-Specific Targeted Delivery.* Pharm Res, 2015. **32**(10): p. 3248-60.
32. Lombry, C., et al., *Alveolar macrophages are a primary barrier to pulmonary absorption of macromolecules.* Am J Physiol Lung Cell Mol Physiol, 2004. **286**(5): p. L1002-8.
33. Gursahani, H., et al., *Absorption of Polyethylene Glycol (PEG) Polymers: The Effect of PEG Size on Permeability.* Journal of Pharmaceutical Sciences, 2009. **98**(8): p. 2847-2856.
34. Patton, J.S., C.S. Fishburn, and J.G. Weers, *The lungs as a portal of entry for systemic drug delivery.* Proc Am Thorac Soc, 2004. **1**(4): p. 338-44.
35. Geyer, A., et al., *Fluorescence- and computed tomography for assessing the biodistribution of siRNA after intratracheal application in mice.* Int J Pharm, 2017. **525**(2): p. 359-366.
36. Kozlowski, A., S.A. Charles, and J.M. Harris, *Development of pegylated interferons for the treatment of chronic hepatitis C.* BioDrugs, 2001. **15**(7): p. 419-29.
37. Fletcher, A.M., et al., *Adverse vacuolation in multiple tissues in cynomolgus monkeys following repeat-dose administration of a PEGylated protein.* Toxicology Letters, 2019. **317**: p. 120-129.
38. Zbyszynski, P., et al., *Probing the subcutaneous absorption of a PEGylated FUD peptide nanomedicine via in vivo fluorescence imaging.* Nano Convergence, 2019. **6**.
39. Caliceti, P. and F.M. Veronese, *Pharmacokinetic and biodistribution properties of poly(ethylene glycol)-protein conjugates.* Advanced Drug Delivery Reviews, 2003. **55**(10): p. 1261-1277.
40. Rogers, D.F., *Physiology of airway mucus secretion and pathophysiology of hypersecretion.* Respiratory Care, 2007. **52**(9): p. 1134-1149.
41. Whitsett, J.A., *Airway Epithelial Differentiation and Mucociliary Clearance.* Annals of the American Thoracic Society, 2018. **15**(Suppl 3): p. S143-S148.
42. Tibbitts, J., et al., *Key factors influencing ADME properties of therapeutic proteins: A need for ADME characterization in drug discovery and development.* Mabs, 2016. **8**(2): p. 229-245.
43. Elliott, V.L., et al., *Evidence for Metabolic Cleavage of a PEGylated Protein in Vivo Using Multiple Analytical Methodologies.* Molecular Pharmaceutics, 2012. **9**(5): p. 1291-1301.
44. Tandel, H., K. Florence, and A. Misra, *9 - Protein and Peptide Delivery through Respiratory Pathway*, in *Challenges in Delivery of Therapeutic Genomics and Proteomics*, A. Misra, Editor. 2011, Elsevier: London. p. 429-479.
45. Niven, R.W., et al., *PULMONARY ABSORPTION OF POLYETHYLENE GLYCOLATED RECOMBINANT HUMAN GRANULOCYTE-COLONY-STIMULATING FACTOR (PEG RHG-CSF).* Journal of Controlled Release, 1994. **32**(2): p. 177-189.
46. Patton, J.S., *Mechanisms of macromolecule absorption by the lungs.* Advanced Drug Delivery Reviews, 1996. **19**(1): p. 3-36.
47. Buchanan, A. and J.D. Revell, *Chapter 8 - Novel Therapeutic Proteins and Peptides*, in *Novel Approaches and Strategies for Biologics, Vaccines and Cancer Therapies*, M. Singh and M. Salnikova, Editors. 2015, Academic Press: San Diego. p. 171-197.
48. Turecek, P.L., et al., *PEGylation of Biopharmaceuticals: A Review of Chemistry and Nonclinical Safety Information of Approved Drugs.* Journal of Pharmaceutical Sciences, 2016. **105**(2): p. 460-475.
49. Veronese, F.M. and G. Pasut, *PEGylation, successful approach to drug delivery.* Drug Discov Today, 2005. **10**(21): p. 1451-8.
50. Mitragotri, S., P.A. Burke, and R. Langer, *Overcoming the challenges in administering biopharmaceuticals: formulation and delivery strategies.* Nature Reviews Drug Discovery, 2014. **13**(9): p. 655-672.
51. Hushcha, T.O., A.I. Luik, and Y.N. Naboka, *Conformation changes of albumin in its interaction with physiologically active compounds as studied by quasi-elastic light scattering spectroscopy and ultrasonic method.* Talanta, 2000. **53**(1): p. 29-34.
52. Sherman, M.R., et al., *Conjugation of high-molecular weight poly(ethylene glycol) to cytokines: Granulocyte-macrophage colony-stimulating factors as model substrates*, in *Poly(Ethylene Glycol): Chemistry and Biological Applications*, J.M. Harris and S. Zalipsky, Editors. 1997. p. 155-169.

53. Parton, T., et al., *P-0167: The PEG Moiety of Certolizumab Pegol is Rapidly Cleared From the Blood of Humans by the Kidneys Once it is Cleaved From the Fab'*. Inflammatory Bowel Diseases, 2009. **15**(suppl_2): p. S56-S56.
54. Longley, C.B., et al., *Biodistribution and excretion of radiolabeled 40 kDa polyethylene glycol following intravenous administration in mice*. Journal of Pharmaceutical Sciences, 2013. **102**(7): p. 2362-2370.
55. Parton, T., et al., *P068 Investigation of the Distribution and Elimination of the PEG Component of Certolizumab Pegol in Rats*. Journal of Crohn's and Colitis Supplements, 2008. **2**(1): p. 26-26.

SUPPLEMENTARY MATERIAL

List of contents

Table S1. Calculating the degree of labelling (DOL) of rhDNase and PEG30-rhDNase with VivoTag-S ® 750.

	rhDNase	**PEG30-rhDNase**	**Comment**
Molecular weight	37,000	67,000	
Molar extinction coefficient (L. mol^{-1}.cm^{-1}) at 280 nm	55,000	55,000*	*The same as rhDNase as the PEG moiety does not contribute to the absorption at 280 nm.
A280* (cm)	1.15	0.78	Measured by nanodrop 2000
A750* (cm)	4.12	2.76	
Corrected A280 (cm)	0.90	0.61	Corrected A280 = A280- (0.06 x A750)
Protein (mol/L)	1.63 10^{-5}	1.10 10^{-5}	The final products were concentrated to **6.49 10^{-5} M (2.4 mg/ml for rhDNase)**
Dye (mol/L)	1.71 10^{-5}	1.15 10-5	Molar extinction coefficient of VivoTag-S ® 750 = 240,000 L. mol^{-1}.cm^{-1}
DOL = Dye: Protein ratio	**1.05**	**1.05**	
*A280 and A750 are absorbance at 280 nm and 750 nm, respectively			

Table S2. Hydrodynamic size of native and PEGylated rhDNase by dynamic light scattering (DLS). Samples were prepared at concentrations of 1.0 mg/ml in 150 mM NaCl and 1 mM CaCl2 then filtered through two PVDF 0.22 µm pore size filters. Measurements were performed at a temperature of 25 °C on a Zetasizer Ultra (Malvern Instruments, UK). Disposable glass capillaries were from Malvern Instruments (Part No.ZSU0003) with a 1.0 mm x 1.0 mm square internal bore and a wall thickness of 200 µm. Polydispersity index (PDI) was < 0.1 for all samples. Bars represent means ± SD (n = 3).

Values in nm	**Volume mean (SD)**	**PDI (SD)**
rhDNase	4.79 (0.20)	0.092 (0.011)
PEG30- rhDNase	9.95 (0.43)	0.099 (0.019)

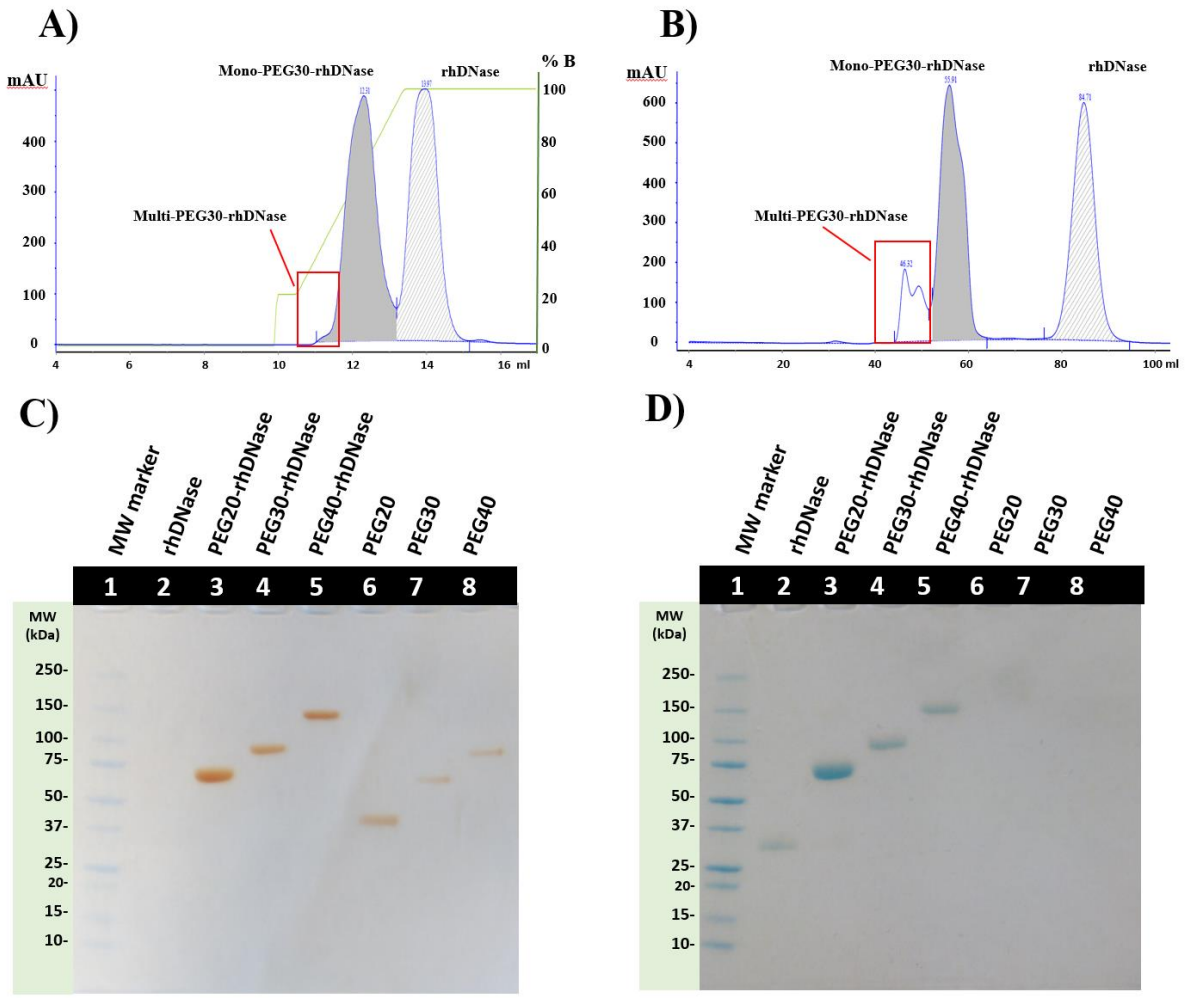

Figure S1. Purification and characterisation of PEGylated rhDNase with PEGs of 20, 30, and 40 kDa. A and B, purification of the PEGylation reaction of rhDNase with PEG30 propionaldehyde. A) Elimination of unreacted PEG30 by anion-exchange chromatography (elution buffer 500 mM NaCl, 1 mM CaCl2). The chromatogram shows from left to right: PEG30-rhDNase (plain peak, multi and mono PEGylated) and rhDNase (hatched peak). B) Size exclusion chromatography of all peaks collected from A. Chromatogram shows from left to right, multi-PEG30-rhDNase (empty peak), mono-PEG30-rhDNase (plain peak), and rhDNase (hatched peak). C and D, SDS-PAGE of rhDNase, PEGylated rhDNase, and free PEGs. 0.5 to 2 μg of proteins or PEGs were loaded on 4–20% Mini-PROTEAN®TGXTM precast gel and run for 60 min at 120 V. The same gel was stained for PEGs (C, brown bands), then for proteins (D, blue bands). PEGs were stained with a barium iodide solution according to Guichard *et al.* [23]). Proteins were visualised using GelCode™ Blue Stain Reagent (Thermo Fisher Scientific, Rockford, IL, USA). Note that only PEGylated rhDNase products were stained for both PEG and protein.

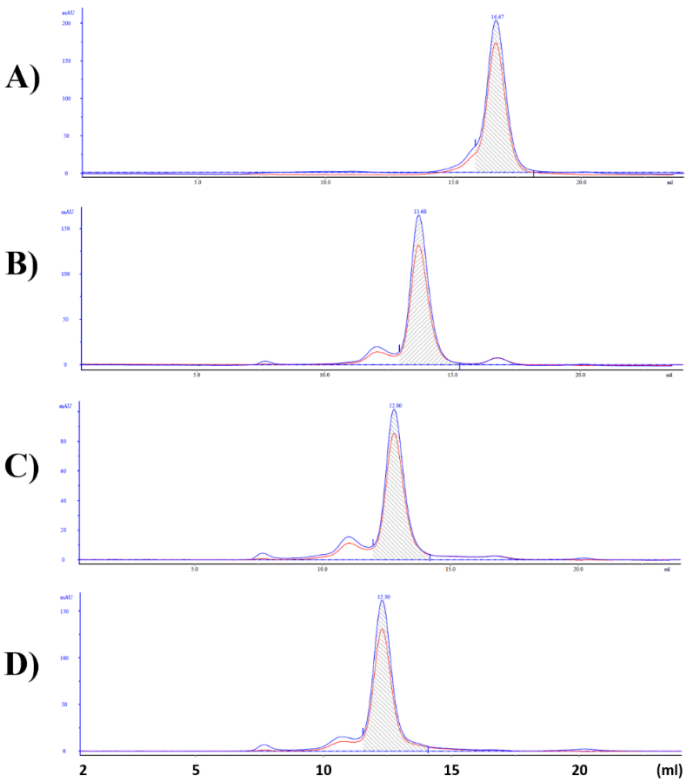

Figure S2. Size exclusion chromatography (SEC) of Alexa488-labelled native and PEGylated rhDNase with PEG20, PEG30, and PEG40 kDa (A to D respectively). Labelled proteins were extensively dialysed against 150 mM NaCl, 1 mM $CaCl_2$ solution then injected in Superose 6 Increase 10/300 GL (column (GE Healthcare Bio-Sciences AB, Uppsala, Sweden). Labelled proteins were eluted with 150 mM NaCl, 1 mM $CaCl_2$ (1 ml/min). Elution was monitored by measuring the absorbance at 280 nm (blue, protein) and 490 nm (magenta, dye). Elution volumes are inversely proportional to the MW of the protein-PEG conjugate. Shaded areas represent the collected fractions corresponding to labelled rhDNase (A) and labelled mono-PEGylated proteins (B-D).

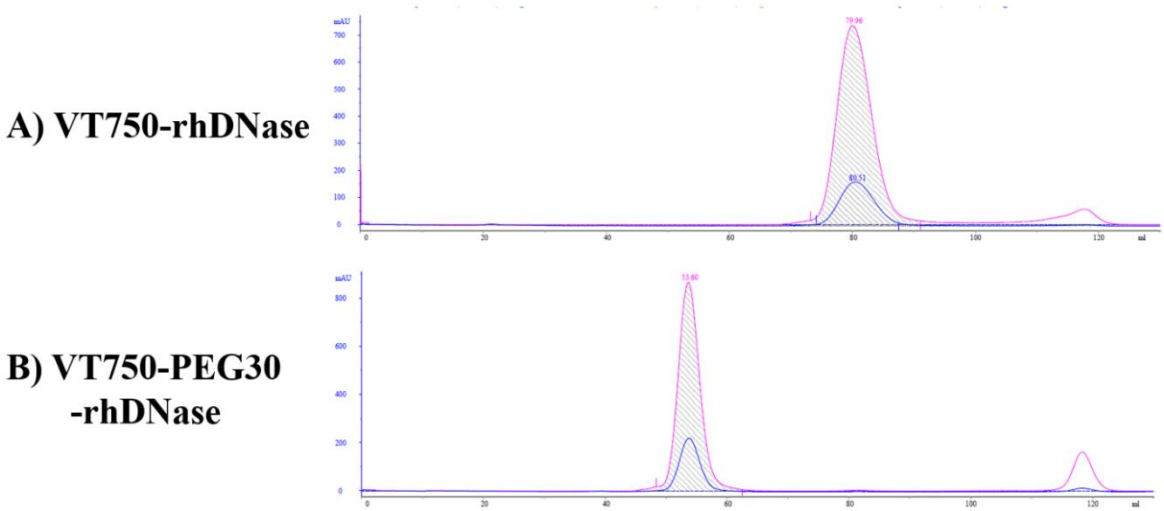

Figure S3. Size exclusion chromatography of VT750-rhDNase (a) and VT750-PEG30-rhDNase (b) using HiLoad Superdex 200 pg column. Labelled proteins were eluted with 150 mM NaCl and 1 mM CaCl2 at 1 mL/min. Elution was monitored by measuring the absorbance at 280 nm (blue) and 700 nm (magenta). The retention times are 80.0 ml for VT750-rhDNase, 53.6 ml for VT750-PEG30-rhDNase, and around 118 ml for the unreacted dye (VT750).

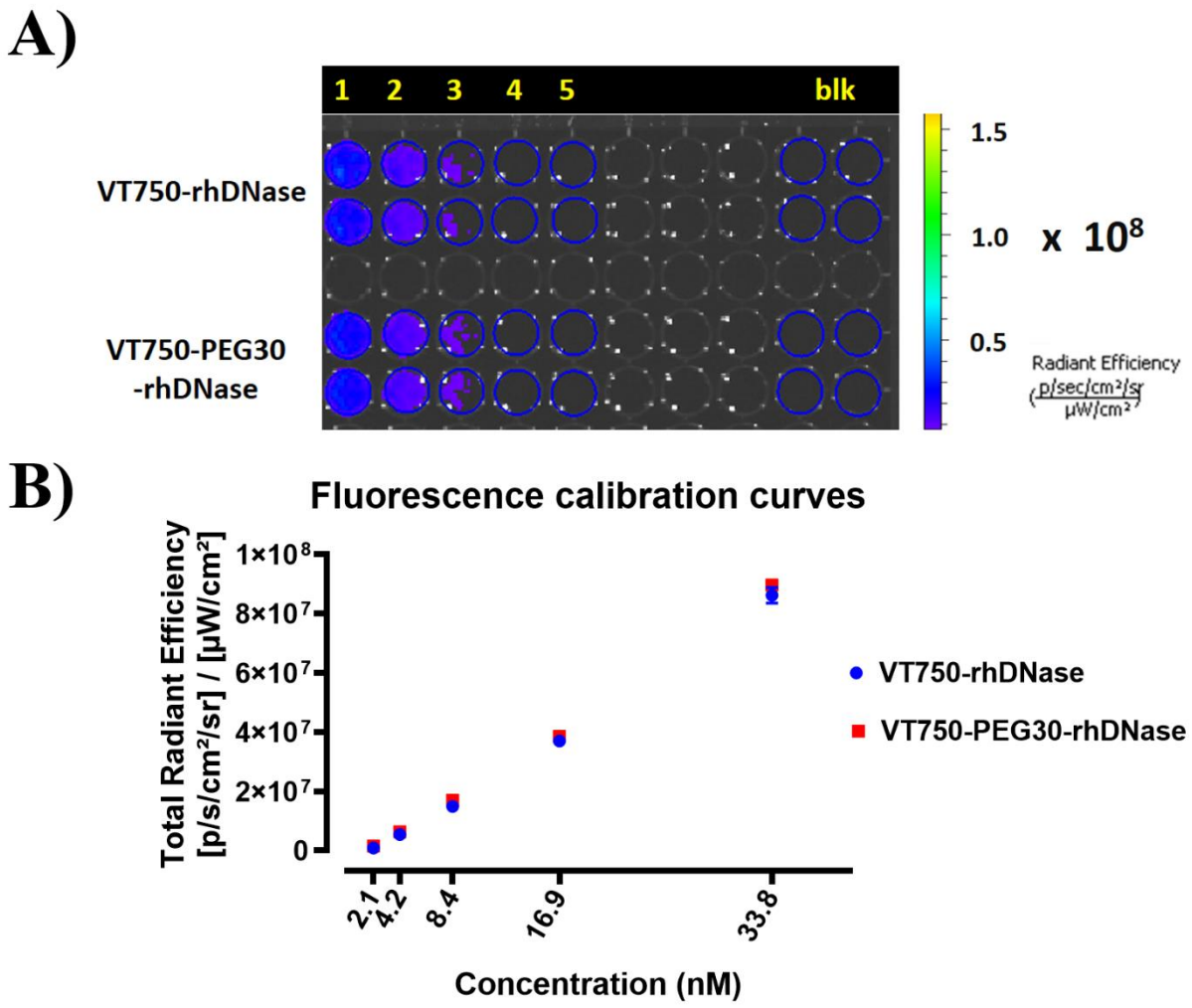

Figure S4. Calibration curves of VT750-rhDNase and VT750-PEG30-rhDNase in phosphate buffered saline (PBS). A) Calibration curves on a 96-well dark plate were imaged by IVIS (745/800 nm); Five serial 2-fold dilutions (in duplicates) of VT750-rhDNase and VT750-PEG30-rhDNase in PBS (100 µl). blk, blank. B) Calibration curves based on the quantification of the ROIs in A after subtraction of the blank. Data indicate identical fluorescence signals for VT750-rhDNase and VT750-PEG30-rhDNase across the tested concentration.

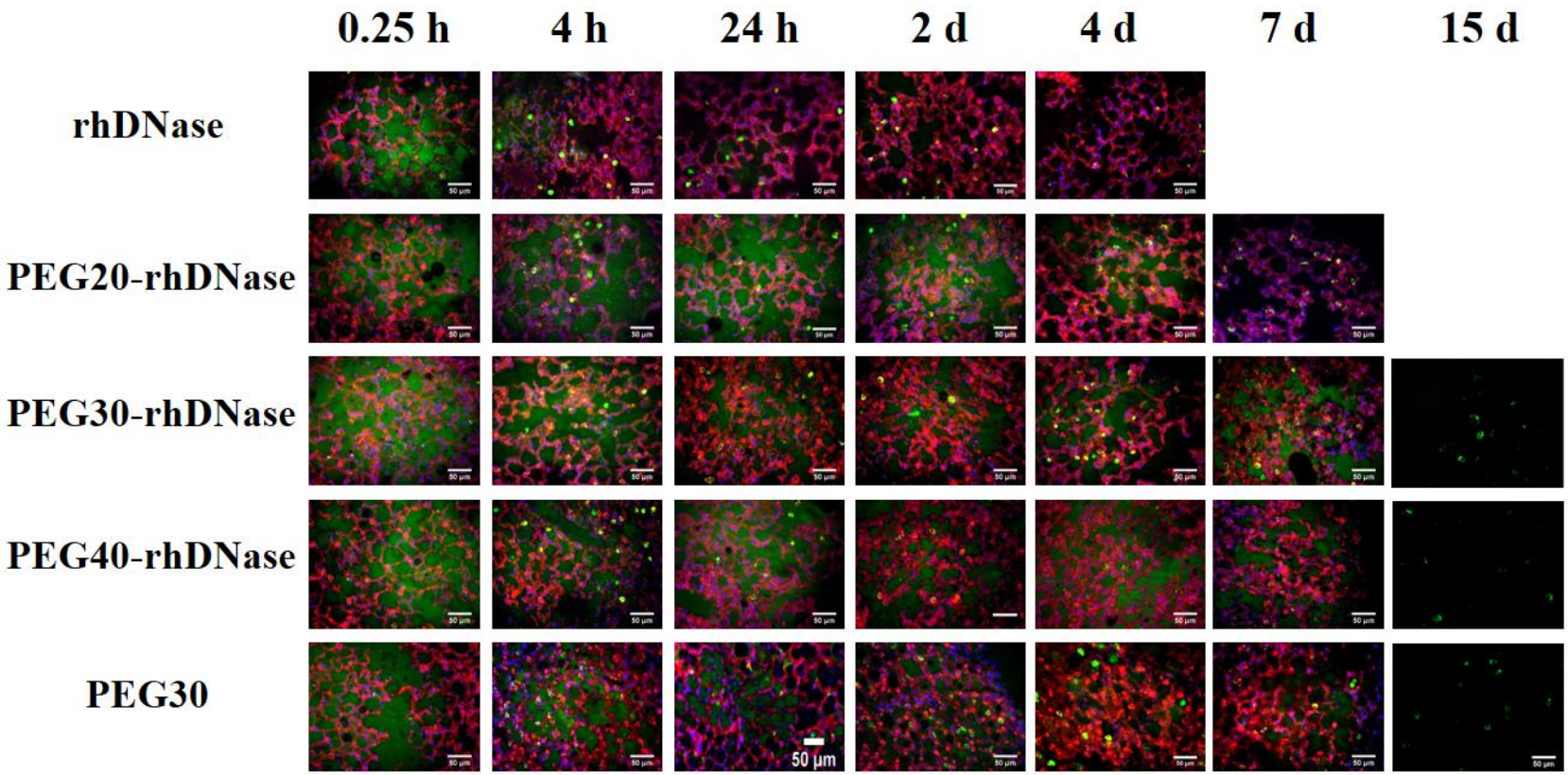

Figure S5. Fate of rhDNase, PEGylated rhDNase, and PEG30 in mouse lungs after intratracheal instillation by confocal imaging. One nmol of A488-rhDNase, A488-PEG20-rhDNase, A488-PEG30-rhDNase, A488-PEG40-rhDNase, or rhodamine-PEG30 were administered by intratracheal instillation. Lung slices were stained with MitoTracker® (Red CMXRos or MitoTracker® Deep Red FM) for tissue and either Draq5™ or Hoechst 33342 for nuclei. Sections were imaged within an hour of staining with Cell Observer Spinning Disk (COSD, Zeiss, Germany) and recorded in all channels. For ease of visualisation, all compounds were coloured in green, tissue in red, and nuclei in blue. Due to the weak signal, images at day 15 show only the compounds. Each experimental condition was repeated at least twice. Images were processed in ImageJ (1.47v, NIH, USA). Scale bars, 50 µm.

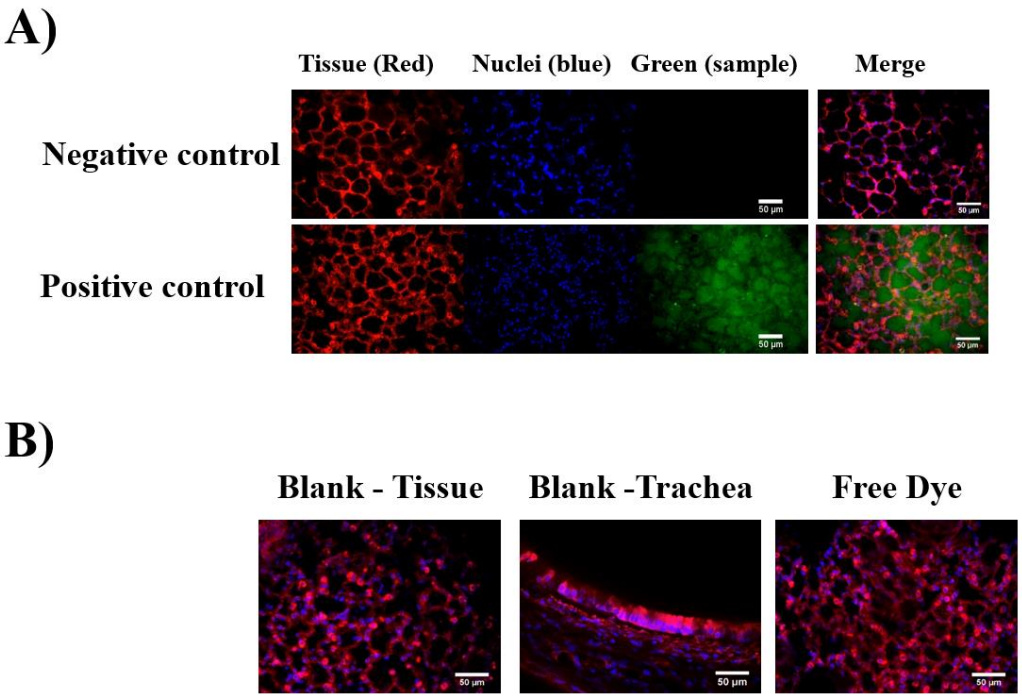

Figure S6. Confocal images of lung and trachea sections. Sections were stained with MitoTracker® (Red CMXRos or MitoTracker® Deep Red FM) for the tissue and either Draq5™ or Hoechst 33342 for the nuclei. A) Image mounting of negative and positive control of lung sections; Negative control consisted of a lung section with no instillation; Positive control represents a lung section on which Alexa488-rhDNase was added after cutting. B) Images of trachea and lung sections 4 h after instillation of 2 nmol of rhodamine B (presented in green pseudocolour). No signal could be detected in trachea or lung slices after 4 h of instillation. Images were acquired with Cell Observer Spinning Disk (COSD, Zeiss, Germany) and processed in ImageJ (1.47v, NIH, USA).

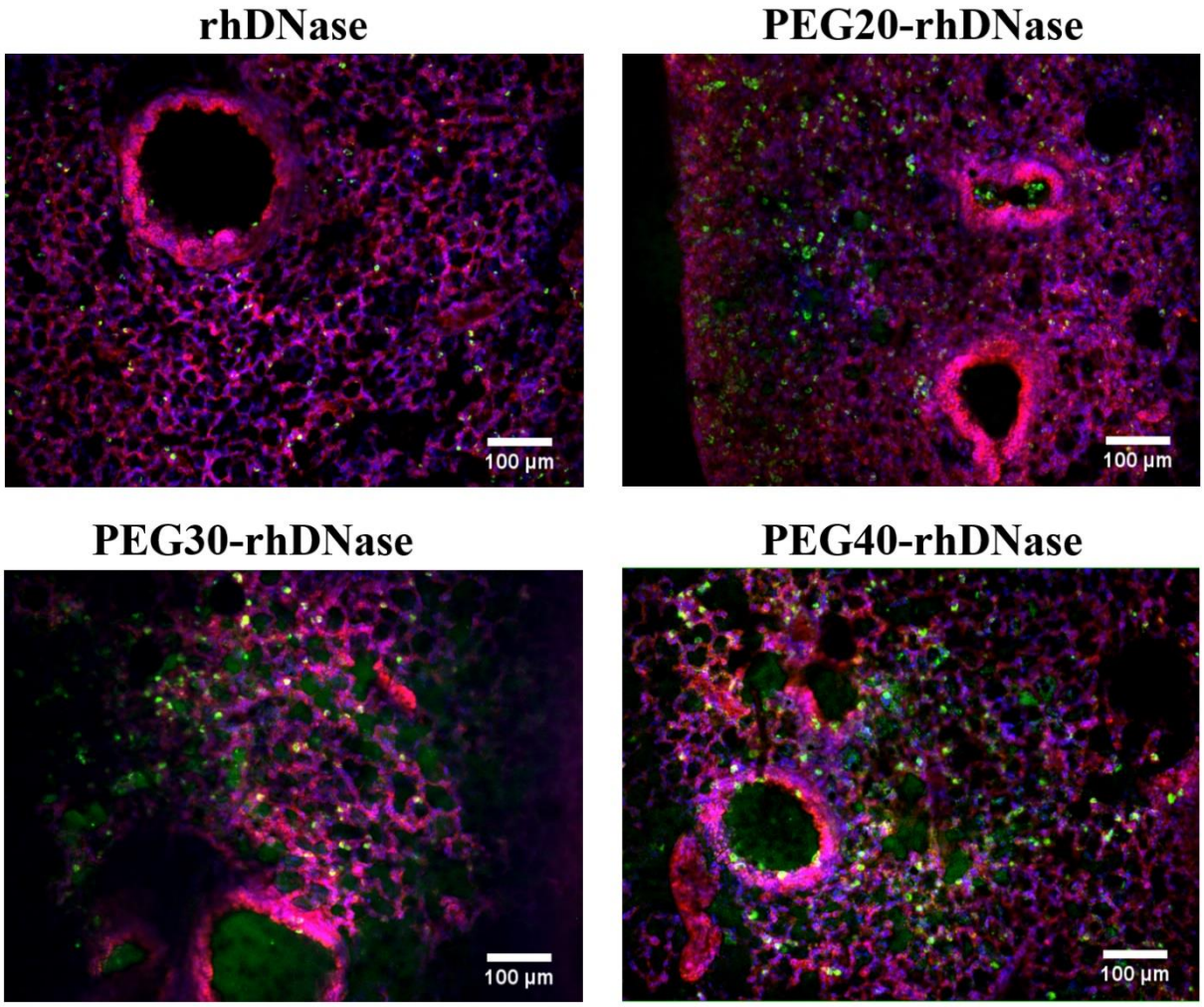

Figure S7. Confocal imaging of rhDNase, PEG20-rhDNase, PEG30-rhDNase, and PEG40-rhDNase in mouse lungs at 96 h. One nmol of Alexa488-rhDNase, Alexa488-PEG20-rhDNase, Alexa488-PEG30-rhDNase or Alexa488-PEG40-rhDNase was administered by intratracheal instillation. Mice were sacrificed at 96 h post-instillation and the lungs were sliced and stained with MitoTracker® for tissue and Draq5™ for nuclei. Sections were imaged with Cell Observer Spinning Disk (COSD, Zeiss, Germany). Compounds were pseudocoloured in green, tissue in red, and nuclei in blue. Images were processed by ImageJ software (1.47v, NIH, USA). Scale bars, 100 µm.

STABILITY OF RHDNASE AND PEG30-RHDNASE IN CONTACT WITH BAL

To see whether PEGylation protects rhDNase form degradation and aggregation within the lungs, the stability of the enzyme was assessed in bronchoalveolar lavage fluids (BALs) of mice. Calcium is crucial for the activity and stability of the rhDNase; therefore, the stability tests were performed in the presence and absence of calcium [1]. Of note, commercial rhDNase formulation (Pulmozyme ®) contains 1 mM of Ca^{+2}.Reported concentrations of Ca^{+2} in CF sputa ranges from 1.1 to 3 mM [2-4].

BALs (with and without calcium), were then spiked with NHS-rhodamine labelled rhDNase or PEG30-rhDNase at a final concentration of 2.7 μM (corresponding to 100 μg/ml of rhDNase) in sealed 1.5 ml Eppendorf® microtubes and incubated in a humid chamber at 37 °C for 0 h, 8 h, 24 h, 48 h, 4 days, and 7days. BALs were then stored at -20 °C. The enzymatic activity of BALs was assessed by methyl green assay. For this, BALs were diluted to a nominal concentration of 5.4 nM of rhDNase or PEG30-rhDNase (equivalent to 200 ng/ml of rhDNase) on 96 well plate followed by serial 2-fold dilutions. 100 μl of DNA-MG substrate were added to all wells, and the assay proceeded as described above.

Assessment of soluble aggregates. BALs without added calcium were analysed by SEC. For this, BALs were centrifuged at 10,000 g for 10 min then the supernatants were injected into a superpose ™ 6 increase 10/300 GL column (GE Healthcare Bio-Sciences AB, Uppsala, Sweden). Elution was monitored at 280 nm for proteins and 555 nm for free rhodamine or rhodamine-labelled fragments.

Results

No loss of activity was noticed for both rhDNase and PEG30-rhDNase in the presence of 1 mM calcium ions (**Erreur ! Source du renvoi introuvable.** A and D). However, in the absence of calcium, there was a progressive loss of activity. The loss of activity was slightly faster for rhDNase compared with PEG30-rhDNase (Figure S8 B, E, and G). The same trends were registered in HBSS in the absence of calcium (Figure S8 B, C, F and G). This could be attributed to the presence of small amounts of calcium in the normal BAL (was not measured).

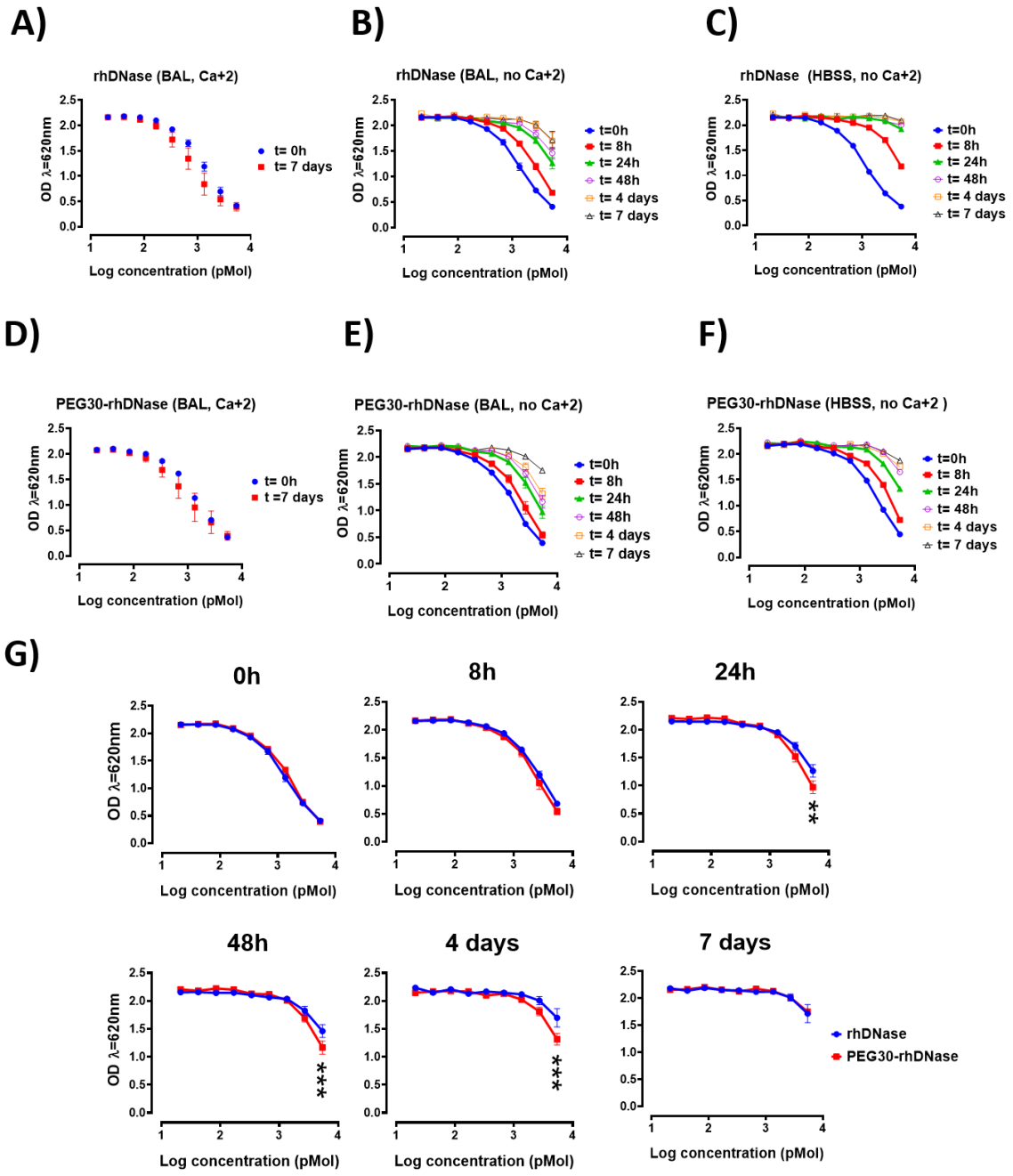

Figure S8. Stability of rhDNase and PEG30-rhDNase in bronchoalveolar lavage (BAL). BALs (250 µg/ml of proteins) were spiked with either rhDNase (A-C) or PEG30-rhDNase (D-F) at a final concentration of 2.7 µM (corresponding to 100 µg/ml of rhDNase) in the presence (A, D) or absence of 1 mM of CaCl2 (B, C, and E-G). BALs were incubated at 37 °C in humid conditions up to 7days. G) Detailed comparison of the enzymatic activity of rhDNase and PEG30-rhDNase in the absence of added calcium at each time point by methyl green assay (reproduced from B and E). For the methyl green assay, BALs were diluted to a nominal concentration of 5.4 nM of rhDNase or PEG30-rhDNase then serial 2-fold dilutions of each sample were incubated for 6 h at 37 °C with DNA-methyl green substrate. The absorbance was read at 620 nm. Data are expressed as mean ± SEM (n = 3). Significant differences in (G) are indicated by ** $p < 0.01$, or *** $p < 0.001$ (two-way ANOVA followed by Sidak posttest).

Assessment of soluble aggregates in contact with BAL without added calcium ions.

Only BALs without added calcium showed a loss of activity over time; therefore, they were analysed by SEC to assess the degradation and aggregation of rhDNase and PEG30-rhDNase. Figure S9 shows the presence of soluble aggregates at 24 h. At 96 h, no soluble aggregates were detected in the case of rhDNase, but not PEG30-rhDNase. The presence of small amounts of intact PEG30-rhDNase at 96 h is no clear.

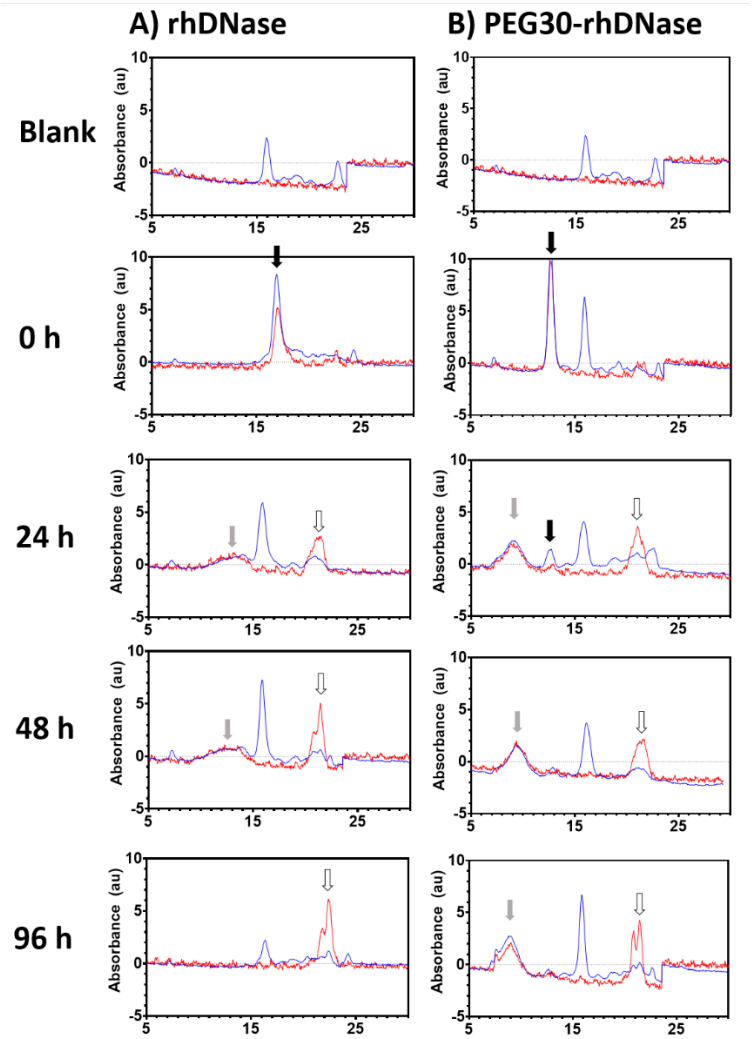

Figure S9. Assessment of soluble aggregates of rhDNase (A) and PEG30-rhDNase (B) in bronchoalveolar lavage (BAL) without Ca^{+2}. BAL fluid (250 µg/ml of protein content) were spiked with rhodamine-labelled rhDNase or PEG30-rhDNase at a final concentration of 1.35 µM (50 µg/ml of rhDNase). BALs were then incubated at 37 °C in a humid chamber up to 96 h. BALs were sampled at 0, 24, 48, and 96 h, centrifuged at 10,000 g for 10 min to eliminate insoluble aggregates then analysed by size exclusion chromatography (SEC) using superpose TM 6 increase 10/300 GL column (GE Healthcare Bio-Sciences AB, Uppsala, Sweden). Elution was monitored at 280 nm (blue) and 555 nm (red). Chromatograms show the presence of soluble aggregates (grey arrows, eluted before the protein) and free dye (empty arrows, eluted after the protein) along with the labelled proteins (black arrows).

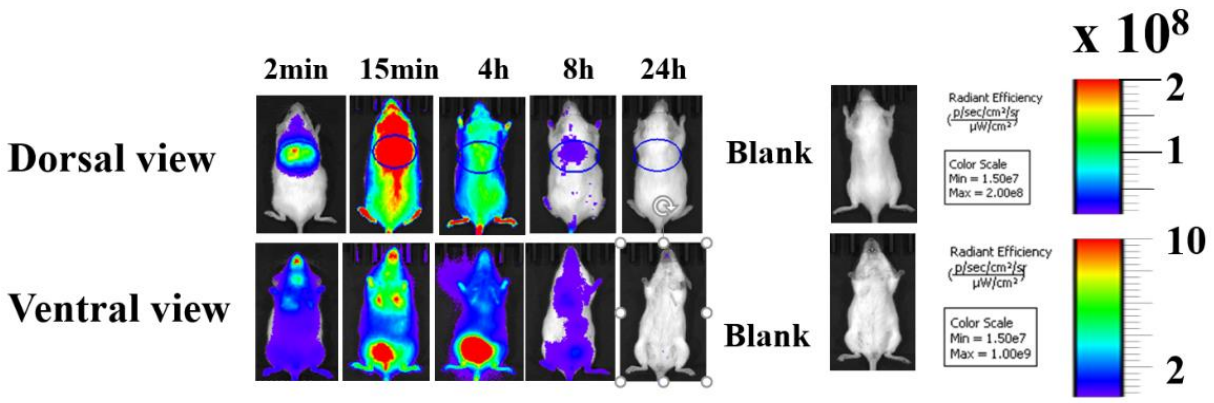

Figure S10. Representative images for *in vivo* NIRF imaging in mice after intratracheal instillation of 2 nmol of VT750. Blank mice did not receive any compound. Mice (n = 3) were imaged by IVIS spectrum in 2D epifluorescence mode at 745/800 nm (ex/em).

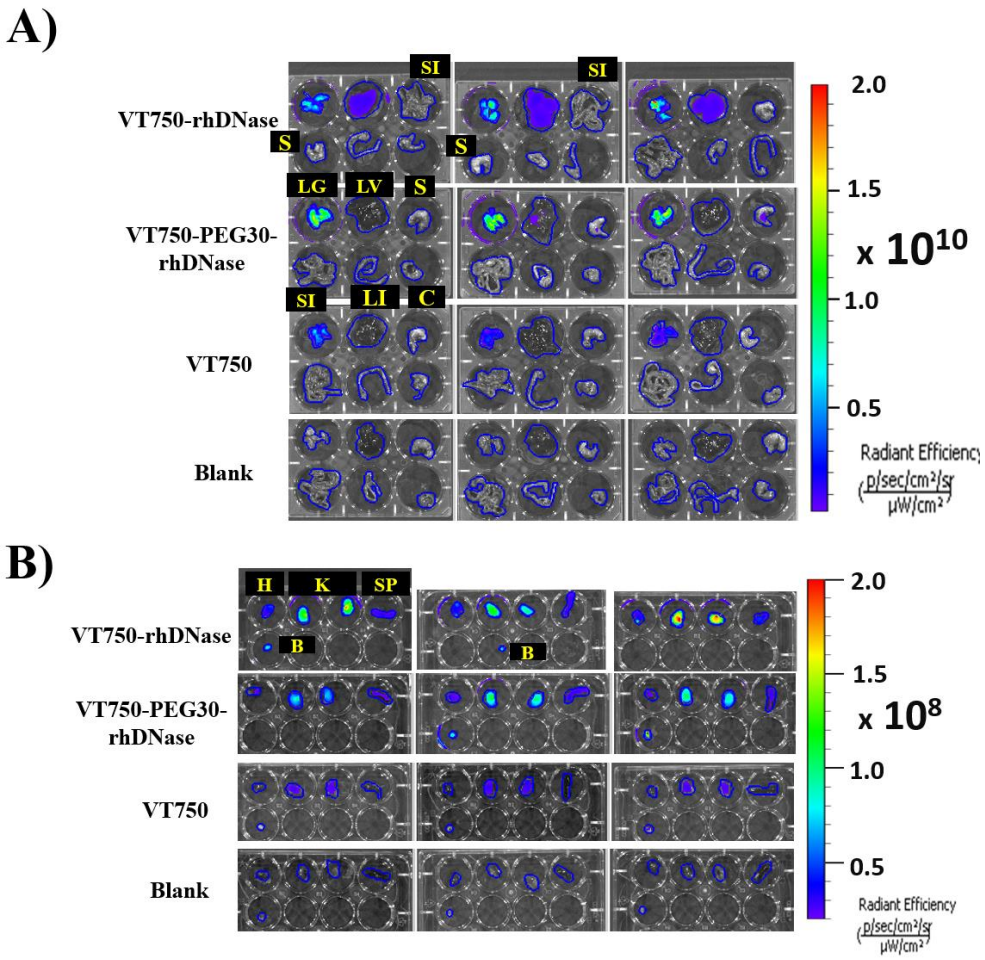

Figure S11. *Ex vivo* organ imaging 24 h post pulmonary delivery. 24 h after intratracheal instillation of VT750-rhDNase, VT750-PEG30-rhDNase, or VT750, mice were sacrificed, and organs were collected for quantification by IVIS at 745/800 nm (ex/em). A) Lung (LG), liver (LV), stomach (S), small intestine (SI), large intestine (LI), and caecum (C). B) Heart (H), kidneys (K), spleen (SP), and bladder (B). Each rectangular groups organs from the same mouse. Note that organ position varies slightly in panel A for VT750-rhDNase in the left and middle rectangle (SI and S are inverted).

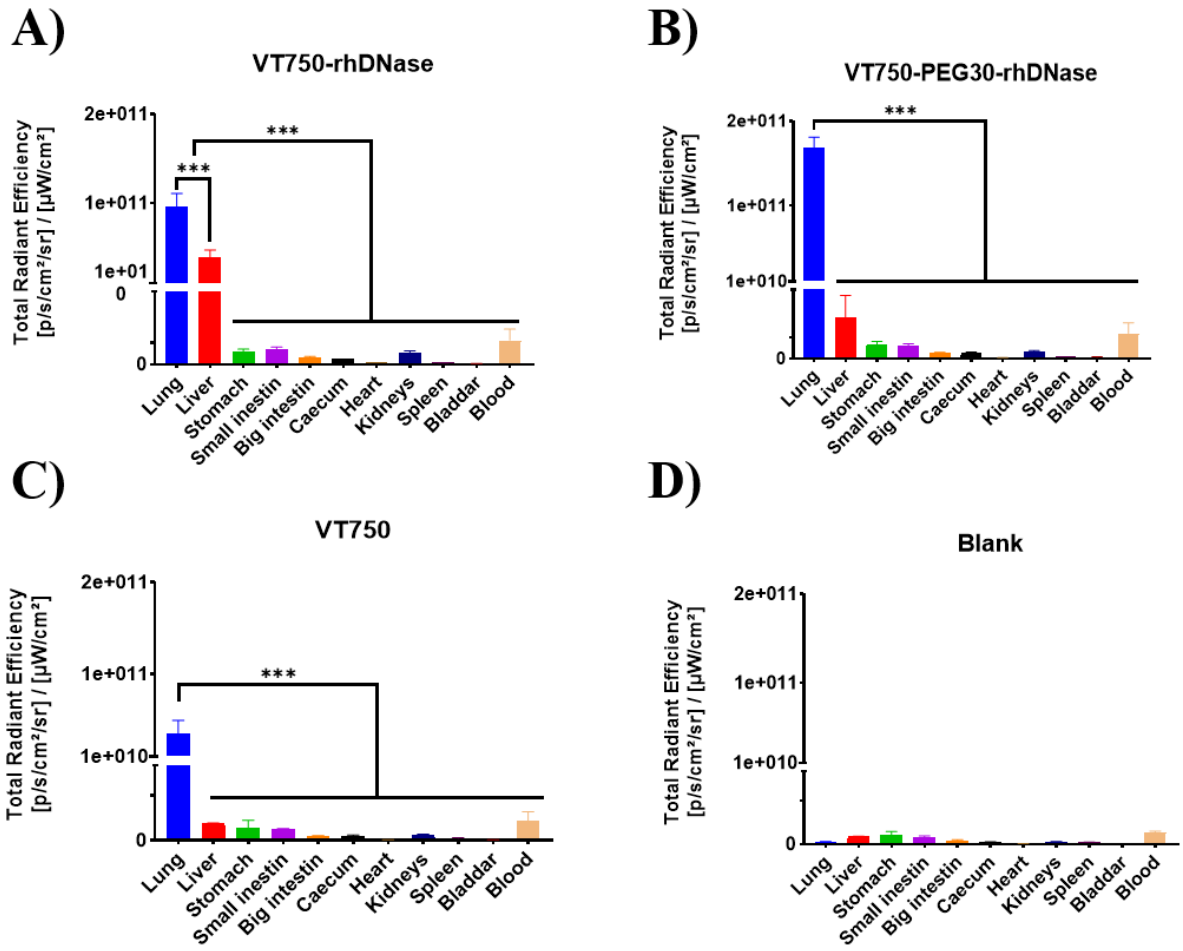

Figure S12. *Ex vivo* organ distribution 24 h after intratracheal instillation of 2 nmol of VT750-rhDNase (A) VT750-PEG30-rhDNase (B), VT750 (C) or no instillation (D) mice were sacrificed and blood and organs were collected for quantification by IVIS at 745/800 nm (ex/em). Bars represent the total fluorescent signal of each organ by IVIS Spectrum (n = 3). Significant differences are indicated by *** $p < 0.001$ (one-way ANOVA followed with Tukey's post hoc test).

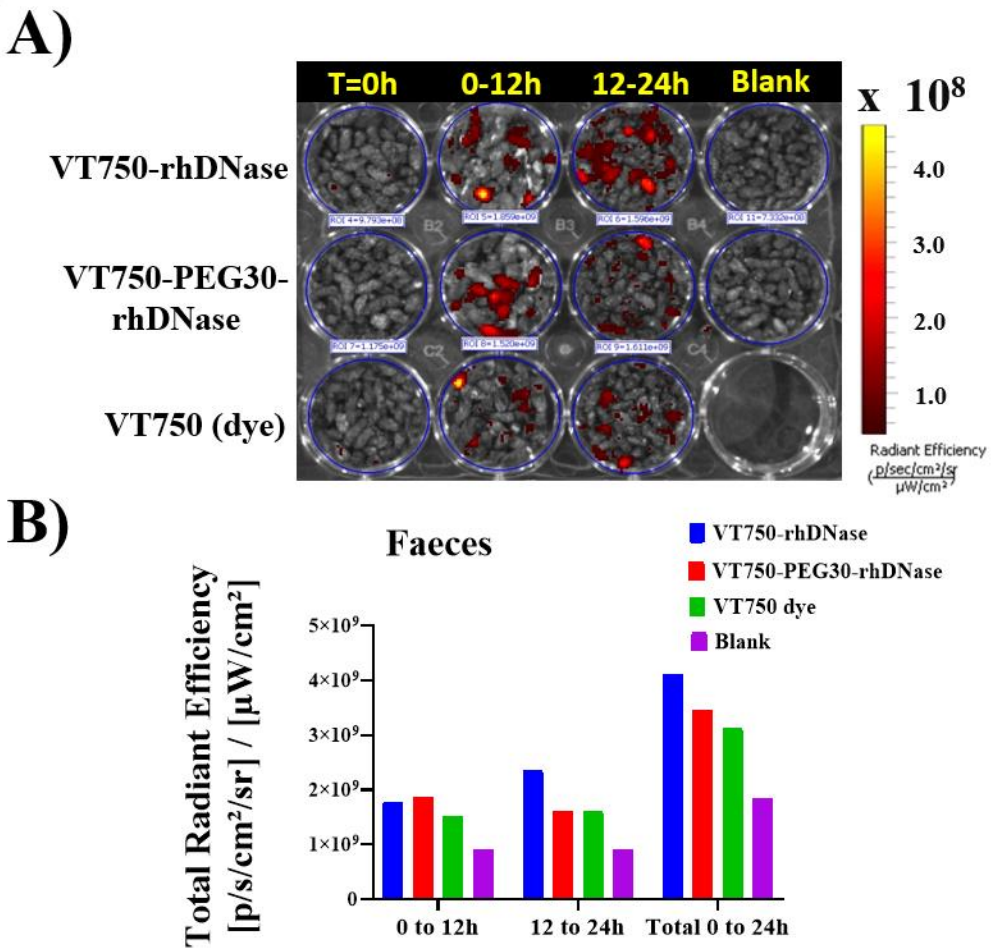

Figure S13. Fluorescence signal in the stool material of mice after intratracheal instillation of VT750-rhDNase, VT750-PEG30-rhDNase or VT750. Mice of each group were housed separately. The bedding of each group was collected and replaced with a new one before instillation (t = 0), at 12 h (0-12 h) and 24 h (12-24 h) after instillation. Faecal pellets were separated, weighed, and imaged by IVIS Spectrum (745/800 nm) (A) Quantification results are presented in (B).

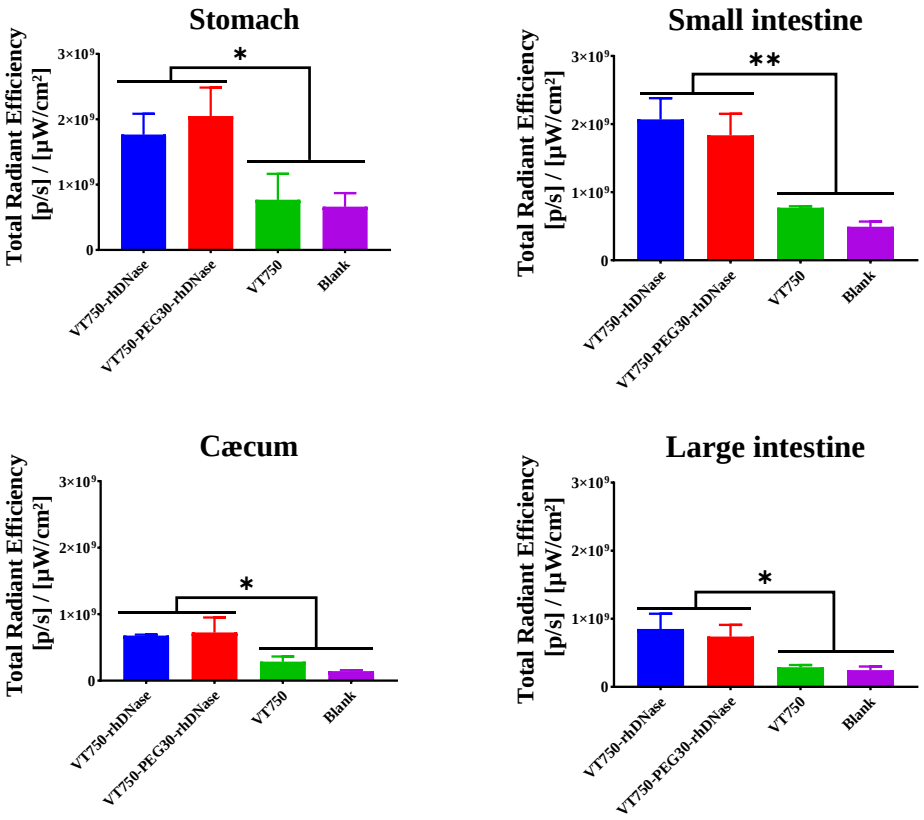

Figure S14. Biodistribution in the gastrointestinal tract (GI tract) after pulmonary delivery. 24 h after intratracheal instillation of 2 nmol of VT750-rhDNase, VT750-PEG30-rhDNase, or VT750 mice were sacrificed and stomach, small intestine, caecum, and large intestine were collected for quantification by IVIS (745/800 nm). Bars represent the fluorescent signal in each organ (n = 3). Significant differences are indicated by * $p < 0.05$ or ** $p < 0.01$ (one-way ANOVA followed with Tukey's post hoc test).

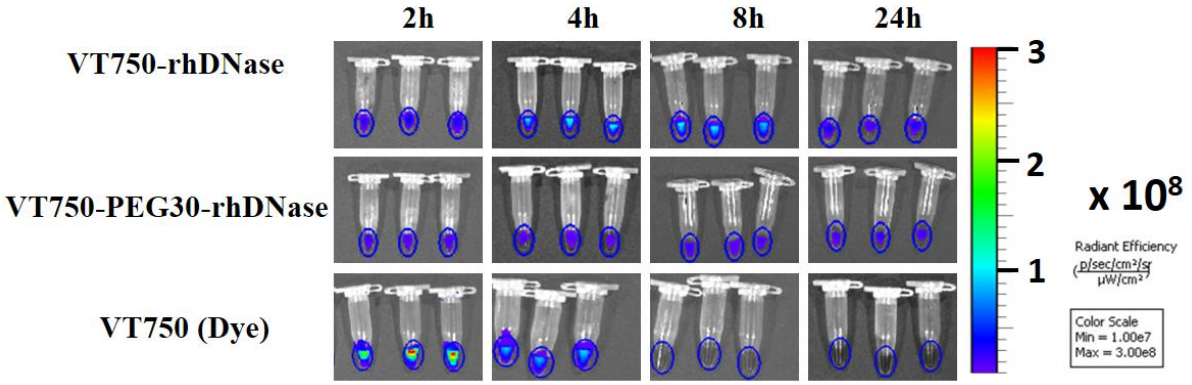

Figure S15. Blood samples image by IVIS (745/800 nm) after intratracheal instillation of 2 nmol of VT750-rhDNase, VT750-PEG30-rhDNase, or VT750 (dye).

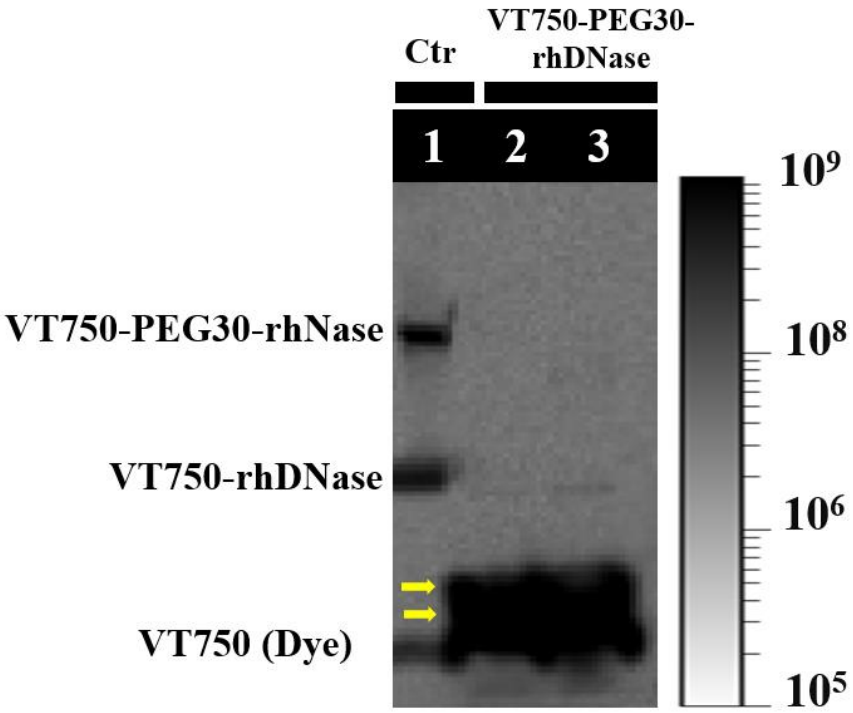

Figure S16. SDS-PAGE of urines from VT750-PEG30-rhDNase mice group. Mice received 2 nmol of VT750-PEG30-rhDNase by intratracheal instillation then the urine was collected 24 h. 15 µl of urine was mixed with at 5 µl loading buffer (4x Laemmli Sample Buffer, BioRad, Belgium) then loaded on the gel (4–20% Mini-PROTEAN® TGX™ Precast Protein Gels, BioRad, Belgium). The gel was run for 60 min at 120 V then imaged by IVIS Spectrum (745/800 nm ex/em). Lane 1, Control loaded with VT750-rhDNase (~10 ng), VT750-PEG30-rhDNase, and VT750; Lanes 2 and 3 urine from two different mice; arrows point to degradation fragments. Scale in radiant efficiency ([p/s/cm²/sr] / [µW/cm²]).

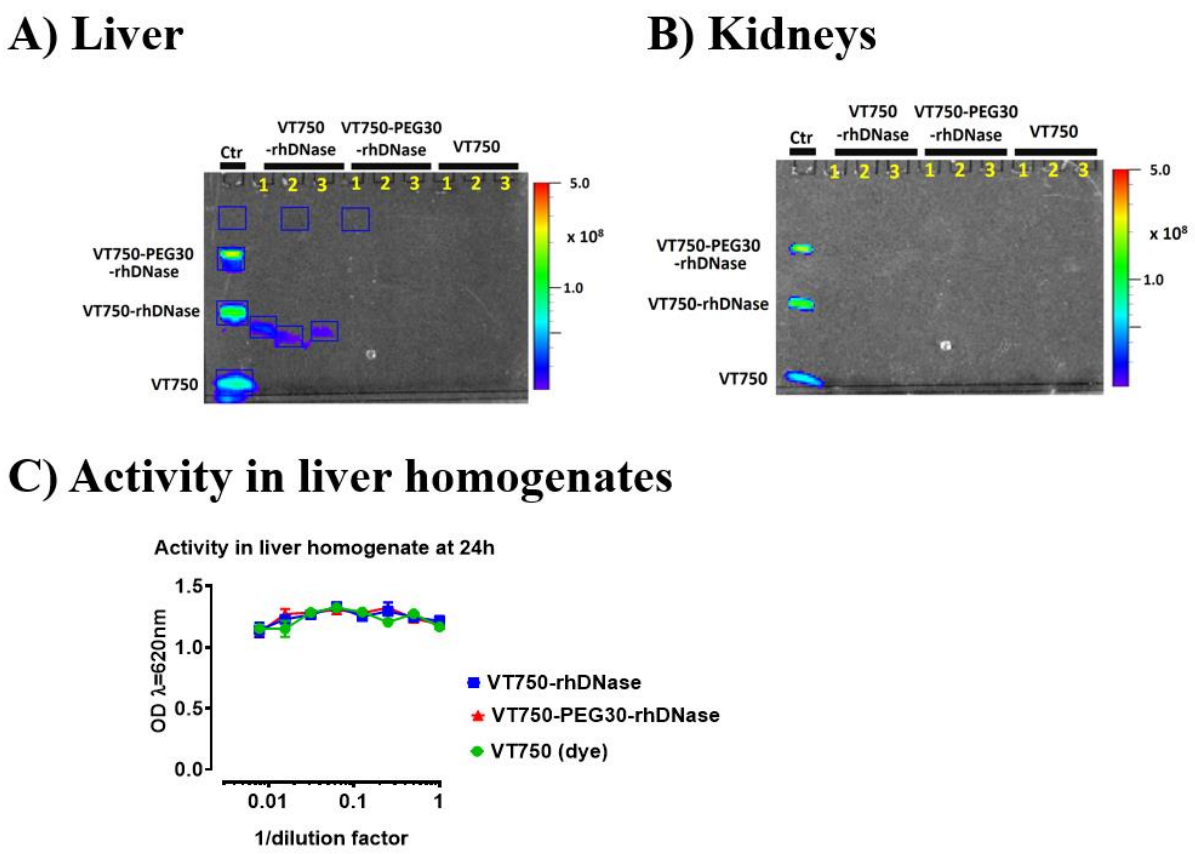

Figure S17. Ex vivo analysis of liver and kidneys homogenates. SDS-PAGE (sodium dodecyl sulfate-polyacrylamide gel electrophoresis) for liver (A) and kidneys (B) homogenates 24 h post instillation of 2 nmol VT750-rhDNase, VT750-PEG30-rhDNase or VT750. A) 15 µl of tissue homogenates from different mice (n = 3) were mixed with 5 µl of loading buffer (4x Laemmli Sample Buffer, BioRad, Belgium) then the mixture was loaded on the gel (4–20% Mini-PROTEAN® TGX™ Precast Protein Gels, BioRad, Belgium). The gel was run at 120 V for 60 min then imaged by IVIS Spectrum (745/800 nm). Ctr. Control lane loaded with VT750-rhDNase (~40ng), VT750-PEG30-rhDNase and VT750. Scale in radiant efficiency ([p/s/cm²/sr] / [µW/cm²]). C) Enzymatic activity of liver homogenates on DNA-MG substrate. Data represent mean ± SEM (n = 3).

REFERENCES

1. Chen, B., et al., *Influence of calcium ions on the structure and stability of recombinant human deoxyribonuclease I in the aqueous and lyophilized states.* J Pharm Sci, 1999. **88**(4): p. 477-82.
2. Guichard, M.J., et al., *Impact of PEGylation on the mucolytic activity of recombinant human deoxyribonuclease I in cystic fibrosis sputum.* Clin Sci (Lond), 2018. **132**(13): p. 1439-1452.
3. Kilbourn, J.P., *Composition of sputum from patients with cystic fibrosis.* Current Microbiology, 1984. **11**(1): p. 19-22.
4. Sanders, N.N., et al., *Role of magnesium in the failure of rhDNase therapy in patients with cystic fibrosis.* 2006. **61**(11): p. 962-966.

CHAPTER III

IMPACT OF THE PEGYLATION OF RHDNASE ON ITS TRANSPORT ACROSS LUNG EPITHELIAL CELLS, UPTAKE BY MACROPHAGES, AND INTERACTION WITH THE RESPIRATORY MUCUS

Adapted from

Mahri, S., Hardy, E., Wilms, T., De Keersmaecker, H., Braeckmans, K., De Smedt, S., Bosquillon, C., Vanbever, R. PEGylation of recombinant human deoxyribonuclease I deceases its uptake by macrophages and transport across lung epithelial cells (submitted).

ABSTRACT

Conjugation to high molecular weight (MW) polyethylene glycol (PEG) was previously shown to largely prolong the lung residence time of recombinant human deoxyribonuclease I (rhDNase) and improve its therapeutic efficacy following pulmonary delivery in mice. In this paper, we investigated the mechanisms promoting the extended lung retention of PEG-rhDNase conjugates cell culture models and lung biological media. Uptake by alveolar macrophages was also assessed *in vivo*. Transport experiments showed that PEGylation reduced the uptake and transport of rhDNase across monolayers of Calu-3 cells cultured at an air-liquid interface. PEGylation also decreased the uptake of rhDNase by macrophages *in vitro* whatever the PEG size as well as *in vivo* 4 h following intratracheal instillation in mice. However, the reverse was observed at 24 h. The uptake of rhDNase by macrophages was dependent on energy, time, and concentration and occurred at rates indicative of adsorptive endocytosis. The diffusion of PEGylated rhDNase in porcine tracheal mucus and cystic fibrosis sputa was slower compared with that of rhDNase. Nevertheless, no significant binding of PEGylated rhDNase to both media was observed. In conclusion, decreased transport across lung epithelial cells and uptake by macrophages appear to contribute to the longer retention of PEGylated rhDNase in the lungs.

KEYWORDS

Recombinant human deoxyribonuclease I, PEGylation, pulmonary delivery, alveolar macrophages, transport across Calu-3, diffusion in mucus.

GRAPHICAL ABSTRACT

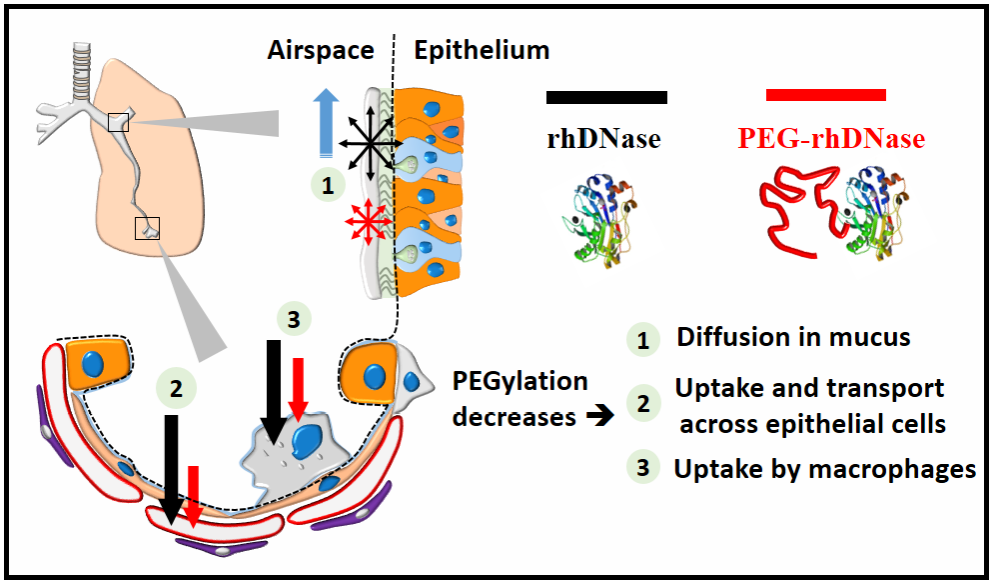

TABLE OF CONTENTS

I. INTRODUCTION

Since the emergence of recombinant human insulin in the early 1980s, the number of therapeutic proteins never ceased to grow to our days to become a therapeutic class on their own [1, 2]. Currently, the number of approved products with distinct active protein ingredients exceeds a couple of hundred products, and many more are in clinical trials [3].

Despite this success, therapeutic proteins face several challenges, including instability, short half-life, immunogenicity, and low penetration through biological barriers [4, 5]. Several of these drawbacks could be overcome by conjugation to natural or synthetic polymers [4]. PEGylation, defined as the covalent coupling to polyethylene glycol (PEG) chain, is the prevailing protein modification strategy with the most clinical success so far. As per early 2020, over 15 PEGylated proteins have been approved by the FDA [6, 7]. All of them are administered by injection and none by other routes of drug administration.

Therapeutic proteins present an attractive opportunity for the treatment of respiratory diseases such as asthma, cystic fibrosis (CF), chronic obstructive pulmonary disease (COPD), alpha-1 antitrypsin deficiency, and lung cancers [8]. Local delivery to the lungs allows i) achieving higher concentrations of the protein to the target, ii) promoting a rapid clinical response, and iii) administering only fractions of the doses otherwise given by parenteral routes; therefore, iv) mitigating the risk of systemic side effects [9, 10].

The lack of marketed PEGylated proteins for pulmonary delivery reflects the paucity of approved proteins for the inhalation route in the first place. The only approved inhaled protein for local lung delivery is the mucolytic recombinant human DNase I (rhDNase, Pulmozyme®) for the symptomatic management of CF [7]. Because of its rapid clearance from the lungs, rhDNase is administered once or twice a day by nebulisation [11]. The nebulisation time of 3 to 10 min and the daily burden of multiple drugs taken by inhalation often limit adherence of patients with CF to their treatment. Therefore, extending the residence time of rhDNase in the lungs would be beneficial to those patients [11]. To our knowledge, PEGylation is the only protein conjugation strategy in the literature with tangible benefits in extending the half-life of proteins in the lungs after pulmonary delivery. Previous works have established the extended retention of PEGylated proteins in the lungs after pulmonary administration in small animals [7, 12-16]. The larger the PEG, the longer the retention [7]. Most markedly, the residence time of PEGylated rhDNase in murine lungs after intratracheal instillation was extended to over 15 days with PEGs of 30 kDa and 40 kDa compared with less than 24 h for native rhDNase [7]. Reduced systemic absorption,

mucoadhesion, decreased uptake by respiratory cells, and protection against degradation in the lungs are the main mechanisms evoked to explain the longer retention of PEGylated proteins [17].

The absorption of proteins by the lungs is influenced, to a great extent, by their molecular size and nature, and the bioavailability does not exceed, in general, 5% for large proteins (molecular weight, MW ≥ 40 kDa) [18-20]. PEGylation has been shown to reduce the systemic absorption of recombinant human granulocyte-colony stimulating factor (rhGCSF, 18 kDa), IFNα2b (19 kDa), and recently rhDNase following pulmonary delivery in small animals [16, 21, 22]. The same trend has also been shown *in vitro* in Calu-3 human lung epithelial cells for PEGylated anti-IL-13 and anti-IL-17A (~ 47 kDa) [14].

A wide range of proteins has also been shown to be captured by alveolar macrophages following pulmonary delivery in different species [23]. This uptake was shown to affect large proteins more efficiently than small proteins and peptides purportedly due to the longer presence of the formers within the airspaces [24]. Uptake of PEG and PEGylated proteins by alveolar macrophages *in vivo* has also been demonstrated previously [7, 12, 16, 25, 26].

PEGylation with large MW has been reported to confer mucoadhesion properties to antibody fragments (Fab') [12, 14]. Strong adhesion to mucus hinders the diffusion and penetration of proteins through the mucus which could lead to a fast elimination in the upper airways where the mucociliary clearance is fast [12, 27, 28]. On the other hand, adhesion to mucus could be advantageous for extending the local retention of proteins in the distal airways and alveolar region where the mucociliary escalator is less efficient [12].

The purpose of this work was to investigate the impact of PEGylation of rhDNase on its transport across lung epithelial cells, uptake by macrophages, and interaction with respiratory mucus. We hypothesised that PEGylation of rhDNase would i) decrease its transport across epithelial cells, ii) reduce its uptake by macrophages, and iii) hinder its diffusion in respiratory mucus, thus, contributing to the longer retention of rhDNase in lung airspaces. Calu-3 cells, cultured at the air-liquid interface (ALI), were used as a model to study the uptake and transport of rhDNase and PEG30-rhDNase across lung epithelia. The uptake by macrophages was assessed for rhDNase and its conjugates with PEGs of 20 kDa, 30 kDa, and 40 kDa in mice and in vitro on two murine macrophage-like cell lines, interstitial J774 macrophages and alveolar MHS macrophages. Mechanistic studies were further conducted to elucidate the pathway of endocytosis. Finally, the interaction of native and PEGylated rhDNase with tracheal mucus and CF sputa was assessed by fluorescence recovery after photobleaching (FRAP).

II. MATERIALS AND METHODS

II.1. MATERIALS

Commercial recombinant human deoxyribonuclease I (rhDNase, Pulmozyme®) was obtained from Genentech, Inc. (South San Francisco, CA, USA). Linear methoxy PEG propionaldehyde of 20 kDa and 30 kDa and two-arm methoxy PEG propionaldehyde of 40 kDa (PEG20, PEG30, and PEG40 respectively) were obtained from NOF Corporation (Tokyo, Japan). NHS-Rhodamine was purchased from Thermo Fisher Scientific (Gent, Belgium). Rhodamine-PEG30 was purchased form Creative PEGWorks (Winston Salem, NC, USA). L-lactate dehydrogenase (LDH) from rabbit muscle, rhodamine B isothiocyanate–Dextran of average MW 70 kDa (D70), albumin from human serum (96-99%), and Fluorescein isothiocyanate–dextran of average MW 40 kDa and 70 kDa (FD40 and FD70 respectively) were purchased from Sigma-Aldrich (St. Louis, MO, USA). 4-(2hydroxyethyl)-1-piperazineethanesulfonic acid (HEPES), Trypan Blue Solution (0.4%), RPMI-1640 medium, Dulbecco's Modified Eagle's Medium/Nutrient Mixture F-12 Ham (DMEM- F12), and cell culture supplements were obtained from Gibco (Life Technologies, Gent, Belgium). FITC (5/6-fluorescein isothiocyanate) mixed isomer was obtained from Thermofisher (Gent, Belgium). RIPA lysis buffer was purchased from Abcam (Cambridge, UK). Resource Q 1 mL and HiLoad 16/60 superdex 200 columns were obtained from GE Healthcare (Bio-Sciences AB, Uppsala, Sweden). Unless otherwise mentioned, other chemicals were purchased from Sigma-Aldrich (St. Louis, MO, USA).

II.2. PEGYLATION OF RHDNASE

rhDNase was conjugated with PEG20 kDa, PEG30 kDa, and PEG40 kDa to obtain PEG20-rhDNase, PEG30-rhDNase, and PEG40-rhDNase, respectively. The PEGylation was performed by reductive amination, as previously reported [7, 11]. Briefly, commercial rhDNase (Pulmozyme®, Genentech, Inc. CA, USA) was concentrated to 5-10 mg/ml in 1 mM $CaCl_2$, 100 mM CH_3CO_2Na (sodium acetate buffer, pH 5) then added to PEG propionaldehyde at a molar ratio PEG: rhDNase of 4:1 in the presence of 34 mM $NaBH_3CN$ (cyanoborohydride, reducing agent). The reaction mixtures were stirred at room temperature overnight. The mono-PEGylated products were purified by anion exchange chromatography on a Resource Q, 1 mL column with ÄKTA™ purifier 10 system then by size exclusion chromatography (SC) on HiLoad 16/60 superdex 200 column (GE Healthcare Bio-Sciences AB, Uppsala, Sweden). rhDNase and PEGylated rhDNase products were filtered through 0.22 µm PVDF membranes and stored at 4 °C in 150 mM NaCl, 1 mM $CaCl_2$ as the marketed rhDNase.

II.3. FLUORESCENT LABELLING OF PROTEINS

NHS-Rhodamine was used for labelling rhDNase, PEGylated rhDNases, albumin, and LDH. To this end, rhDNase or PEG-rhDNase products were exchanged against phosphate buffer saline (PBS, pH 7.4), 1 mM $CaCl_2$, by ultrafiltration using Vivaspin® Turbo 4, 3 kDa (Sartorius; Stonehouse, Gloucestershire, UK). NHS-Rhodamine dye at 10 mg/ml in DMSO was added to protein solutions at a molar ratio dye: protein of 10:1 and the reaction mixtures were kept at room temperature in the dark under constant stirring for 1 hour. The mixtures were ridded of the excess unreacted dye by dialysis against 1 mM $CaCl_2$, 150 mM NaCl (Spectra/Por molecular porous membrane tubing MWCO 6–8 kD, Spectrum). Labelled proteins were further purified by SEC on HiLoad Superdex 200 pg column using 1 mM $CaCl_2$, 150 mM NaCl as eluent, concentrated by ultrafiltration (Vivaspin® Turbo 15, 5 kDa MWCO), filtered through 0.22 µm PVDF membranes, and stored at 4 °C in 1 mM $CaCl_2$, 150 mM NaCl (

Figure **S1** and Figure S2). The same degree of labelling (DOL) of one dye molecule per protein molecule was achieved for rhDNase and PEG-rhDNase products. No detectable levels of lipopolysaccharide (LPS) were found in stock solutions of native and PEGylated rhDNase used for the *in vivo* experiment (Figure S3). The same labelling procedure was used for albumin and LDH using PBS instead of $CaCl_2$, NaCl in all steps.

II.4. TRANSPORT ACROSS EPITHELIAL CELLS

II.4.1. *Culture of Calu-3*

Calu-3, lung adenocarcinoma epithelial cells, were purchased from the American Type Culture Collection (Rockville, MD, USA) and used between passage 32 and 37. Cells were maintained in Dulbecco's Modified Eagle's Medium/Nutrient Mixture F-12 Ham (DMEM- F12) supplemented with 10% v/v of FBS and 1% v/v of Penicillin-Streptomycin. The cell cultures were maintained at 37 °C in a humidified atmosphere of 5% CO_2 with medium changes every other day and passaging at ~ 80% confluency.

II.4.2. *Culture of Calu-3 on Air-Liquid Interface (ALI)*

Calu-3 cells were seeded at a density of 1 x 10^5 cell/cm^2 on Transwell® inserts (PET, 1.12 cm^2, 0.4 µm pore size; Corning Life Sciences, MA, USA). Two to four days later, cells were raised to ALI by removing the medium from both apical and basolateral sides of the Transwell® inserts and only replacing the latter with fresh medium (500 µl). The medium on the basolateral side was changed

every other day thereafter until the day of the experiment. Mucus was removed once a week by gentle washing by Hank's Balanced Salt Solution (HBSS). Transepithelial electrical resistance (TEER) measurements were performed using EVOM meter with chopstick electrodes (World Precision Instruments, Stevenage, UK). For this, cells were equilibrated in HBSS by adding 500 µl in the apical side and 1500 µl in the basolateral side. The monolayer integrity was confirmed by TEER values ≥ 450 $\Omega.cm^2$.

II.4.3. *Transport across Calu-3 cell monolayer*

On the experiment day, TEER measurements were taken, and the basolateral side was changed with 500 µl of fresh medium. 5 µl containing 270 picomols of rhDNase (10 µg), PEG30-rhDNase, D70, or PEG30 in 1 mM $CaCl_2$, 150 mM NaCl was applied directly on the apical side of Calu-3 cells. Transwell® inserts were then incubated at 37 °C and 5% CO_2 without shaking. Zero, 2, 4, 8, 12, and 24 h post-exposure, 100 µl of the medium was sampled from the basolateral side of each Transwell® insert and replaced by 100 µl of fresh medium. At 24 h, the basolateral medium was recovered, and the apical side was gently washed with HBSS (2 x 500 µl). TEER was measured again as described above. All cell layers maintained a TEER ≥ 450 $\Omega.cm^2$. Finally, cells were detached with trypsin, washed, and each cell sample was divided into two parts. One half was analysed by flow cytometry (LSR Fortessa, BD Biosciences, San Jose, USA) using 561 nm (yellow-green laser) with at least 10,000 events recorded for each sample. The other half was lysed by adding 100 µl RIPA lysis buffer, centrifuged for 10 min at 14,000 g at 4 °C and the supernatants were stored at -20 °C.

The concentrations of compounds in the apical side, basolateral side, or cell layers were measured by fluorescence spectrometry at 555/580 nm (ex/em) in black 384 well plates (Greiner Bio-One GmbH, Frickenhausen, Germany) against the corresponding calibration curves in the appropriate media (HBSS, medium, or RIPA for apical side, basolateral side, and cell layer, respectively). The cumulative quantities for compounds in the basolateral side were reported as a percentage of the initial dose (270 picomols), taking into account the amounts removed from the system during sampling. Quantities in the cell layer were expressed in picomol per mg of cell protein content. Protein content was determined by Pierce™ BCA Protein Assay Kit (Thermo Scientific™ Pierce™, Gent, Belgium).

II.4.4. *Activity of rhDNase and PEG30-rhDNase in apical and basolateral side by methyl green assay*

The activity of rhDNase and PEG30-rhDNase in the apical and basolateral sides of the Transwell® inserts was assessed using methyl green (MG) assay described elsewhere [11, 29]. Briefly, the hydrolysis of the DNA-methyl green substrate (DNA-MG) by deoxyribonuclease releases free MG in solution, the colour of this latter fades out to colourless with time leading to a decreased optical density (OD) at 620 nm. Samples from the basolateral side at 4 h and 24 h were initially diluted threefold then 50 µl was placed on the first column of a 96-well plate with controls of rhDNase and PEG30-rhDNase of known concentrations (16.2 nM, equivalent to 600 ng/ml of rhDNase). Samples and controls underwent further 2-fold serial dilutions on the 96-well plate then 50 µl of DNA-MG solution was added to all wells. Plates were sealed and incubated in a humid chamber at 37 °C for 24 h. At the end of the incubation time, the OD was measured at 620 nm by SpectraMax i3 (Molecular Devices, CA, USA).

Samples from the apical side were diluted to a nominal concentration of 5.4 nM (equivalent to 200 ng/ml of rhDNase) then analysed by MG assay. For this, 100 µl of diluted samples were incubated with 100 µl of DNA-MG solution for 6 h along with controls of rhDNase and PEG30-rhDNase of known concentrations.

II.4.5. *Uptake by Calu-3 cells in immersion*

Calu-3 cells were seeded in 24-well plates at a cell density of 2 x 10^5 cell/well and incubated at 37 °C and 5% CO_2 until near-confluence. Cells were then exposed to 162 nM of rhDNase (6 µg/ml), PEG30-rhDnase, D70, or PEG30 for 24 h. After 24 h exposure, the cells were washed by DPBS (6 x 1 ml), detached, and analysed by flow cytometry as described above.

II.5. *IN VIVO* UPTAKE BY ALVEOLAR MACROPHAGES

II.5.1. *Animals*

All experimental protocols were approved by the Institutional Animal Care and Use Committee of the Université Catholique de Louvain (Permit number 2016/UCL/MD/019). 6-week Female RjOrl SWISS mice (Elevage Janvier, Le Genest-St-Isle, France) were kept under conventional housing conditions and were allowed at least one week of acclimation before being used for experimentation between 7 and 8 weeks of age.

II.5.2. *Intratracheal instillation*

One nmol of rhodamine-labelled LPS-free rhDNase (37 μg), PEG20-rhDNase (57 μg), PEG30-rhDNase (67 μg), or PEG40-rhDNase (77 μg) were administered to mice by intratracheal instillation. Control mice received the vehicle solution (1 mM $CaCl_2$, 150 mM NaCl). For instillation, mice were anaesthetised by intraperitoneal injection of ketamine/xylazine (90/10 mg/kg) then held in a supine position by surgical tape on an inclined board (~ 45°). Mice were then intubated with 20G catheter (VWR International BVBA, Leuven, Belgium) using a small laryngoscope (Penn-Century™– Model LS-2, Philadelphia, USA). 25 ± 2 μl of compounds (containing 1 nmol of protein) or control were administered intratracheally into the lungs using a precision syringe (100 μl, Model 710, Hamilton, Bonaduz, Switzerland) followed by an air bolus of 200 μl (1 ml syringe, HSW SOFT-JECT®, VWR International BVBA, Leuven, Belgium). Immediately after instillation, mice were placed in an upright position for 20-30 seconds before being transferred back to their cage.

II.5.3. *BAL collection and flow cytometry*

4 or 24 h post-delivery, mice were euthanised by cervical dislocation, and bronchoalveolar lavage fluid (BAL) was collected (4 x 1 ml) using 0.1 mM EDTA-DPBS (Dulbecco's phosphate-buffered saline, no Ca^{+2} or Mg^{+2}). BALs were centrifuged at 300 g for 5 min; then, 500 μl of Ammonium-Chloride-Potassium lysing buffer (ACK Lysing Buffer, Gibco™, Life Technologies, Gent, Belgium) was added to cell pellets to lyse red blood cells. BALs were then centrifuged again (300 g for 5 min). Finally, the cellular fractions were resuspended in 500 μl PBA (DPBS supplemented with 1% bovine serum albumin, BSA). Cell viability was assessed on a small subset and cells were counted using the trypan blue exclusion test on TC20™ Automated Cell Counter (Bio-Rad, Hercules, CA, USA). The remaining cells were incubated at 4 °C for 30 min with Allophycocyanin (APC) anti-mouse F4/80 antibody (1 μg per 2 million cells/ml; Biolegend, Germany) to mark alveolar macrophages. After incubation, cells were analysed by the flow cytometer LSR Fortessa (BD Biosciences, San Jose, USA) using 561 nm (yellow-green laser) and 639 nm (red laser). 10,000 events (cells positive to F4/80) per sample were recorded. Data were analysed with FlowJo software (TreeStar, Ashland, OR, USA).

II.6. *IN VITRO* UPTAKE BY MACROPHAGES

II.6.1. *Cell culture of J774 and MHS*

Murine macrophage-like J774A.1 (ATCC® TIB67™) and murine alveolar macrophages MHS (ATCC® CRL-2019™) were maintained at 37 °C and 5% CO_2 in RPMI-1640 medium [L-Glutamine]. For J774 cells, the medium was supplemented with 10% heat-inactivated Foetal Bovine Serum (FBS) and 100 U/ml Penicillin/Streptomycin. For MHS, the medium was supplemented with 10% FBS and 2-mercaptoethanol at a final concentration of 0.05 mM. Cells were subcultured every 2-3 days and used at passage numbers between 12 and 20. Unless otherwise mentioned, MHS and J774 cells were seeded in 24-well plates at a cell density of 10^5 cells/well and incubated overnight at 37 °C and 5% CO_2 before exposure to test compounds or controls.

II.6.2. *Effect of PEGylation and PEG size on uptake by macrophages*

MHS and J774 cells were exposed to 500 µl of 162 nM of rhDNase (6 µg/ml), PEG20-rhDNase, PEG30-rhDNase, or PEG40-rhDNase for 4 h. The negative control consisted of untreated cells. After incubation, the supernatants were discarded, and cells were washed (6 x 1 ml) with DPBS, detached by adding 150 µl of 0.25% trypsin-EDTA solution, centrifuged at 300 g for 5 min. Cell pellets were resuspended in PBA (DPBS, 1% BSA) for flow cytometry analysis. 5,000 to 10,000 events were recorded for each condition on LSR Fortessa using 561 nm (yellow-green laser). Data were analysed with FlowJo software (TreeStar, Ashland, OR, USA).

II.6.3. *Characterisation of endocytosis pathway*

Effect of temperature. MHS and J774 were exposed to 162 nM (500 µl) of rhDNase or PEG30-rhDNase for 30 min either at 4 °C or 37 °C and 5% CO_2. Time was kept short (30 min) to avoid potential cell damage due to long time exposure to low temperatures. For plates incubated at 4 °C, test compounds were prepared in pre-cooled media and cells were washed with chilled DPBS (3 x 1 ml) immediately before exposure. After incubation cells were then detached for flow cytometry analysis as described above.

Time-dependent uptake. J774 were exposed to 162 nM (500 µl) of rhDNase or PEG30-rhDNase then incubated at 37 °C and 5% CO_2 for 30 min,1 ,2 ,4 , or 6 h. After the incubation time, cells were harvested and analysed by flow cytometry as described above.

Concentration-dependent uptake. MHS were seeded at 2 x 10^5 cell/well in 24 well-plate; next day, cells were exposed for 2 h to increasing concentrations (0.46-30 µM) of rhDNase, human

albumin, or D70 prepared in FBS-free cell culture medium. The incubation time was kept relatively short (2 h) to limit potential cell damage incurred by the lack of FBS in the medium. Cells were then washed with DPBS (6 x 1 ml) then lysed by adding 200 µl of chilled RIPA lysis buffer. Plates were shaken for 10 minutes. The lysates were collected in 1.5 mL Eppendorf® tubes and centrifuged for 10 min at 14,000 g at 4 °C and supernatants were stored at -20 °C. The concentrations of compounds in the supernatants were determined by measuring the fluorescence at 555/580 nm (ex/em) (SpectraMax i3, Molecular Devices, CA, USA) against the corresponding calibration curve in RIPA lysis buffer. The uptake was reported in picomol of compound per mg of total protein content. Total protein content in the supernatants was measured by Pierce™ BCA Protein Assay Kit. Of note, the normal culture medium is spiked with 10% FBS and therefore abound in albumin; the estimated concentration of albumin in the culture medium is around 1.4 mg/ml, which does not differ a lot from the highest concentration of albumin in our experiments of 2 mg/ml (30 µM, albumin MW 65 kDa).

Rate of uptake is expressed in µl/mg/h. It was calculated as the slope of *uptake vs concentration* / exposure time (2h). Only the linear range of the slope of *uptake vs concentration* (0-15 µM) was considered

Markers of endocytosis. The uptake of rhDNase, PEG30-rhDNase, and PEG30 was compared with controls of fluid phase and adsorptive endocytosis, D70 and LDH, respectively [30, 31]. MHS and J774 cells were exposed to 162 nM (500 µl) of rhDNase, PEG30-rhDNase, or controls for 4 h at 37 °C and 5% CO_2 then cells were harvested and analysed by flow cytometry as described above.

Possible artefacts due to the adsorption of rhDNase and PEG30-rhDNases on cells were avoided by washing the cells with 1 ml of DPBS 3, 6, or 9 times. The washing did not have a significant impact on the uptake of rhDNase and PEG30-rhDNase by macrophages (Figure S4).

II.7. DIFFUSION OF PROTEINS AND DEXTRAN IN PORCINE MUCUS AND CF SPUTA

II.7.1. *Collection of mucus and CF sputa*

Mucus was collected from the tracheas of healthy pigs obtained from a local abattoir according to the procedure previously described [32, 33]. Briefly, tracheas pieces (10 - 15 cm) were cut longitudinally, and the inner walls were cleaned from contaminating blood and dirt then scraped gently by a spatula to collect mucus. Mucus from several tracheas was pooled in Eppendorf tubes then diluted 1:3 in 150 mM NaCl, stirred at 4 °C for 30 minutes and centrifuged at 14, 000 g at

4 °C for 15 minutes. The supernatant was then discarded, and the clean mucus was stored at -80 °C until needed. Sputa from CF patients were collected by expectoration during physiotherapy and stored at -80 °C (approved by the Ethics Committee of the Université Catholique de Louvain [UCL]; registration number: B403201422928).

II.7.2. *Protein labelling*

FITC (5/6-fluorescein isothiocyanate) was used for labelling rhDNase, PEG20-rhDNase, PEG30-rhDNase, and PEG40-rhDNase. The labelling reaction was performed in a solution of 1 mM $CaCl_2$ in PBS (pH adjusted to 8.5). All other steps were carried out as described for NHS-rhodamine labelling.

II.7.3. *Fluorescence recovery after photobleaching (FRAP)*

FRAP was used to measure the diffusion of FITC-labelled proteins (rhDNase, PEG20-rhDNase, PEG30-rhDNase, and PEG40-rhDNase) or dextrans (FD40 and FD70) in porcine mucus. FITC-labelled proteins or dextrans with stock concentrations of 2-4 mg/ml were diluted 1:10 to 1:30 in the different media. A volume of 5 µl of the diluted sample was sandwiched between a microscopy glass slide and a cover glass (# 1.5) sealed with an adhesive spacer of a 120 µm thickness (S24737, Secure-Seal™ Spacer, Thermofisher, Gent, Belgium) to create a 3D environment for diffusing without flow in the sample. All FRAP measurements were carried out at room temperature.

The experiments were performed on a C2 confocal laser scanning microscope (Nikon, Japan) equipped with an Apo 10x NA 0.45 objective lens (Nikon, Japan). The 488 nm Argon ion laser (40 mW, CVI Melles Griot, CA) was used for photobleaching and imaging. A disk with a radius of 30 µm was photobleached using an intense laser beam. The laser power was adjusted to obtain a bleaching parameter K_0 between 0.5 and 2 to limit the influence of the bleaching depth. A pre bleach image was taken, and fluorescence recovery due to diffusion in and out of the bleached region was imaged by a time-lapse of 30 frames with a time interval of 1 s or 1.6 s for buffer or mucus/sputa, respectively. The time interval was chosen to match the recovery speed depending on the diffusion coefficient and the bleached area. The pinhole size was set to 30 µm. Between 9 and 15 technical replicates were measured of each sample, and three biological replicates were used for the mucus solution.

The diffusion coefficient (D) and the mobile fraction were calculated by fitting the fluorescence recovery data to the theoretical model developed by Braeckmans *et al.* [34] using in-house code in

Matlab (The Matworks, Natick, MA, USA). In this model, the average fluorescence recovery inside a bleached disc with radius w is described by:

$$\frac{F(t)}{F_0} = 1 + (e^{-K_0} - 1)\left[1 - e^{\frac{-w^2}{2Dt}}\left(I_0\left(\frac{w^2}{2Dt}\right) + I_1\left(\frac{w^2}{2Dt}\right)\right)\right] \dots (1)$$

where $F_0$is the fluorescence in the disc before bleaching, D is the diffusion coefficient and K_0 is the bleaching parameter. I_0 and I_1 are modified Bessel functions of the first kind of zeroth and first order, respectively. To take a mobile k (and immobile) fraction into account, the formula 1 is substituted into the right part of:

$$\frac{F(t)}{F_0} = 1 + k\left(\frac{F(t)}{F_0} - 1\right) \dots (2)$$

II.8. STATISTICS

All statistical inferences are based on a two-sided significant level of * $p < 0.05$, ** $p < 0.01$, *** $p < 0.001$ and were carried out using GraphPad Prism version 8.00 (GraphPad Software, La Jolla California, USA).

III. RESULTS

III.1. TRANSPORT ACROSS EPITHELIAL CELLS

In our previous work, we have shown that PEG30-rhDNase was absorbed systemically to a lower extent than rhDNase after intratracheal instillation in mice [16]. Here we quantified the uptake and transport of rhDNase and PEG30-rhDNase through Calu-3 cells cultured at ALI (Figure 1A) and in immersion and compared it to that of PEG 30 kDa and dextran 70 kDa (D70). D70 is a natural polymer with an average MW of 70 kDa, close to that of PEG30-rhDNase (67 kDa).

The transport data across Calu-3 cells showed a significant decrease in the transport of PEG30-rhDNase compared with rhDNase ($p < 0.001$) (Figure 1B). At 24 h, 28% of the apically applied amount of rhDNase was found on the basolateral side, 1.75 times higher than that of PEG30-rhDNase (16%). Both proteins were transported to a higher extent than D70 (< 2%) and PEG30 (< 1%) ($p < 0.001$).

To clarify whether rhDNase and PEG30-rhDNase remain active after transport across Calu-3 cells, we assessed the activity of both proteins in the basolateral chamber at 4 h and 24 h, and on the apical side of the layers at the end of the experiment (24 h) (Figures 1 C-F). After 24 h, only 2.1% of the applied dose of rhDNase was found active in the basolateral side compared to 0.2% for PEG30-rhDNase (Figure 1C), i.e., respectively 13 to 75 times less than the protein quantities measured by spectrofluorimetry (Figure 1B). However, consistent with the data obtained by spectrofluorimetry, the concentrations of PEG30-rhDNase on the basolateral side were significantly lower compared with those of rhDNase both at 4 h and 24 h (Figure 1C). These data also indicate a lower degradation for rhDNase. Of note, the quantities estimated in the basolateral side at 4 h and 24 h using the enzymatic activity assay are underestimated as they do not take into account the proteins sampled at previous time points. In contrast, the activity of rhDNase and PEG30-rhDNase in the apical side was preserved after 24 h of cell exposure (Figure 1F).

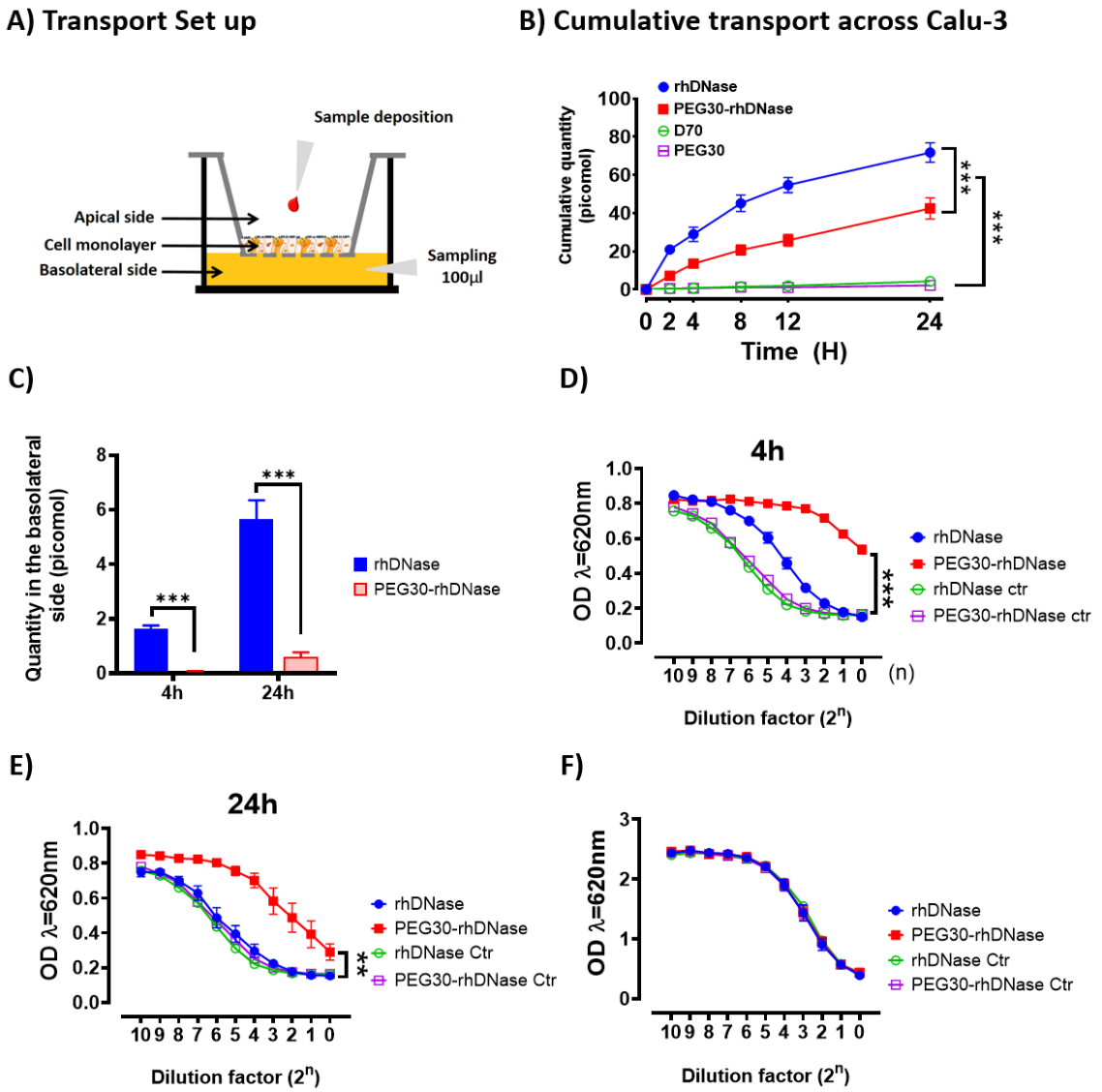

Figure 1. Transport across Calu-3 cells at the air-liquid interface (ALI). A) Culture set-up. B) Cumulative quantities in the basolateral side over time. C) Estimated quantities of rhDNase and PEG30-rhDNase in the basolateral side at 4 h and 24 h from D and E. D and E, enzymatic activity of rhDNase and PEG30-rhDNase in the basolateral side at 4 h (D) and 24 h (E) post-exposure by methyl green assay. F) Enzymatic activity of rhDNase and PEG30-rhDNase in the apical side at the end of 24 h exposure time. Data represent mean ± SEM (n = 6-8 inserts). Significant differences among groups are presented by * for $p < 0.05$, ** for $p < 0.01$, and *** for $p < 0.001$ (Student (C) and two-way ANOVA, Tukey's posthoc test (B, D-F).

The uptake of compounds was quantified in Calu-3 cells by flow cytometry and spectrofluorimetry at the end of the exposure time (24 h). The amounts detected in cells were very low and presented less than 0.12% of the applied dose for rhDNase, roughly 4 times higher than that PEG30-rhDNase, D70, and PEG30 ($p < 0.01$) (Figure 2A and B). The amounts of active proteins in the basolateral side (Figure 1C) were 5 to 16 times those in the cell layer for PEG30-rhDNase and rhDNase, respectively.

Exposing Calu-3 to low concentrations of compounds in immersion only showed a significant difference between rhDNase and PEG30-rhDNase ($p < 0.05$), the uptake of this latter was threefold lower than the former ($p < 0.05$) (Figure 2C). The uptake of D70 and PEG30 was not statistically significant from that of PEG30-rhDNase or rhDNase.

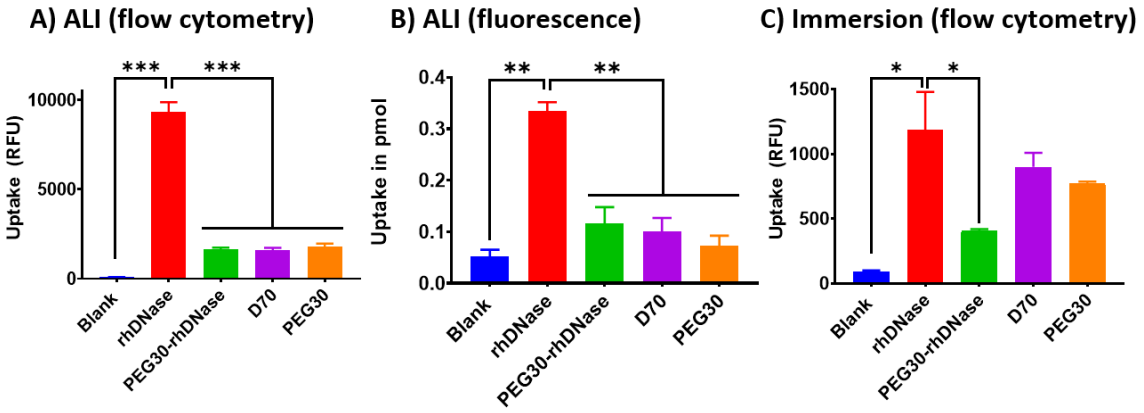

Figure 2. Uptake by Calu-3 cells at the air-liquid interface (ALI) and in immersion. Calu-3 were cultured at ALI for 22 ± 2 days then exposed to 270 picomols of rhodamine-labelled rhDNase (10 µg), PEG30-rhDNase, dextran, or PEG30. 24 h later cells were detached by trypsin then half of the cells were analysed by flow cytometry (A), and the other half were lysed by RIPA lysis buffer (B), and compounds were quantified in the supernatant by spectrofluorimetry (555/580 nm). C) Calu-3 were cultured in immersion to confluency; cells were exposed to 270 nM of rhDNase, PEG30-rhDNase, D70, and PEG30; 24 h post-exposure, cells were detached by trypsin and analysed by flow cytometry. Bars represent mean ± SEM (n = 3-8). Significant differences among groups were checked by one-way ANOVA, Tukey's posthoc test, * for $p < 0.05$ and *** for $p < 0.001$. RFU, relative fluorescence units.

III.2. INFLUENCE OF PEGYLATION AND PEG SIZE ON THE UPTAKE OF RHDNASE BY MACROPHAGES

Preceding reports have highlighted the role of alveolar macrophages in the sequestration and clearance of proteins, PEGylated or not, after pulmonary delivery [12, 22, 26]. The contribution of alveolar macrophages in the uptake of native and PEGylated rhDNase was also suggested *in vivo* in our laboratory [7, 16]. Here we further investigated the impact of PEGylation and PEG size on the uptake of native and PEGylated rhDNase by alveolar macrophages *in vivo* and *in vitro* on two macrophage cell lines (J774 and MHS). The mechanism of uptake was then studied and compared with markers of fluid-phase and adsorptive endocytosis.

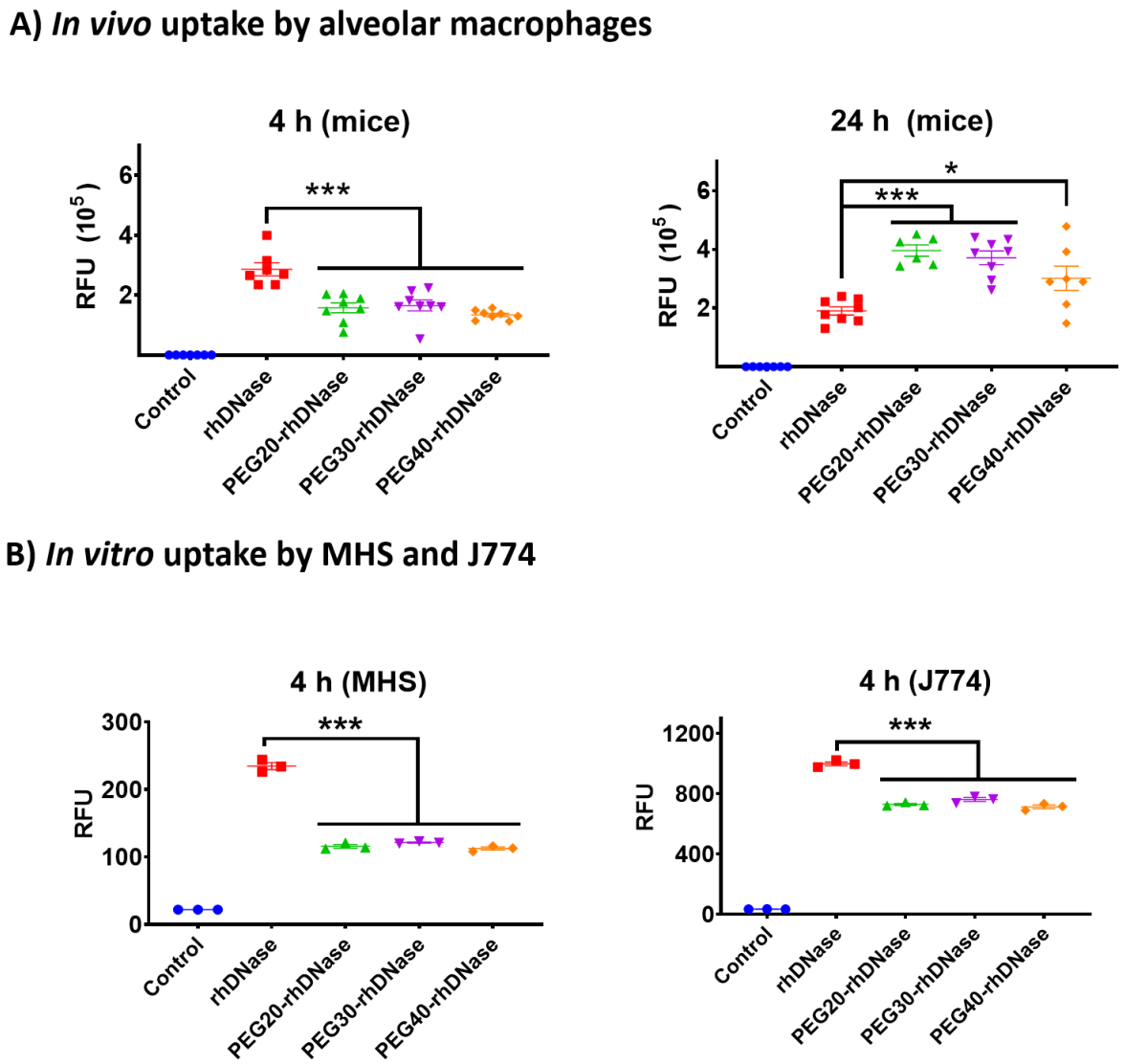

Figure 3. *In vivo* and *in vitro* uptake of rhDNase and PEGylated rhDNase by macrophages. A) *In vivo* uptake by alveolar macrophages. B) *In vitro* uptake by J774 and MHS macrophages; cells were exposed to 162 nM of compounds (equivalent to 6 µg/ml of rhDNase) for 4 h at 37 °C and 5% CO_2 then cells were washed, detached, and analysed by flow cytometry (n = 3); control represents cells in the culture medium. Data represent individual values of median fluorescence intensities, and horizontal lines represent mean ± SEM. Significant differences among groups were checked by one-way ANOVA, * for $p < 0.05$ and *** for $p < 0.001$. RFU, relative fluorescence units.

Regardless of the PEG size, the uptake of PEGylated rhDNase by alveolar macrophages was lower compared with rhDNase at 4 h post-intratracheal instillation in mice ($p < 0.001$)(Figure 3A). The uptake of rhDNase was roughly double that of PEG20-rhDNase, PEG30-rhDNase, and PEG40-rhDNase. The opposite was observed 24 h post-delivery where the content of rhDNase within the macrophages was almost half that of PEGylated rhDNase ($p < 0.05$). Interestingly the amounts of rhDNase associated with the alveolar macrophages at 24 h were even less than those at 4 h ($p < 0.001$). No significant difference among the three PEGylated products of rhDNase could be

inferred neither at 4 h nor at 24 h ($p > 0.05$). Cell viability in BAL, assessed by trypan blue exclusion assay, was above 90% and was similar for all groups and time points (Figure S5).

The uptake of rhDNase and PEG-rhDNases were also assessed *in vitro* in two murine macrophage cell lines, MHS (alveolar) and J774 (ascites' derived). Consistent with *in vivo* observations, the uptake of PEG-rhDNases was less than that of rhDNase at 4 h in both cell lines ($p < 0.001$), with no significant difference according to the PEG size ($p > 0.05$). The decrease was more marked in MHS compared with J774 (2-fold vs 1.4-fold), albeit the uptake was overall higher in J744.

III.3. CHARACTERISATION OF ENDOCYTOSIS BY MACROPHAGES FOR NATIVE AND PEGYLATED RHDNASE

Since no significant difference in the uptake of the PEGylated forms of rhDNase was observed, only PEG30-rhDNase was selected to further investigate the mechanisms of uptake by macrophages *in vitro*.

The effect of temperature was tested by comparing the uptake of rhDNase and PEG30-rhDNase by J774 and MHS at 4 °C and 37 °C. After a short incubation time of 30 min at low temperature, the uptake of both rhDNase and PEG30-rhDNase dropped by 4-5 fold compared with that at 37 °C in both cell lines ($p < 0.01$) (Figure 4A).

We also quantified the protein uptake in J774 cells at 37°C up to 6 h. This was time-dependent for both proteins and significantly lower for PEG30-rhDNase in comparison with rhDNase (Figure 4B). The uptake of rhDNase, albumin, and D70 was additionally studied over a range of concentrations at 37 °C up to 30 μM in FBS-free medium to avoid the potential competition of FBS with the studied serum albumin. Albumin is present in the alveolar surface fluid of healthy lungs [35]. It has been used as a marker for both adsorptive and fluid phase endocytosis [36-40] while D70 is a well-established marker of fluid phase endocytosis [41, 42].

The uptake of rhDNase, albumin, and D70 was concentration-dependent and significantly higher for albumin and rhDNase compared with D70 ($p < 0.05$) (Figure 4C). The uptake of D70 was linear with concentration ($R^2=0.99$); however, that of rhDNase and albumin showed a saturation trend at the highest concentrations (30 μM). All compounds exhibited low rates of uptake: 5.91 μl/mg/h (95% CI, 5.22-6.60) for albumin, 4.18 μl/mg/h (2.92-5.44) for rhDNase, and 1.36 μl/mg/h (1.13-1.59) for D70.

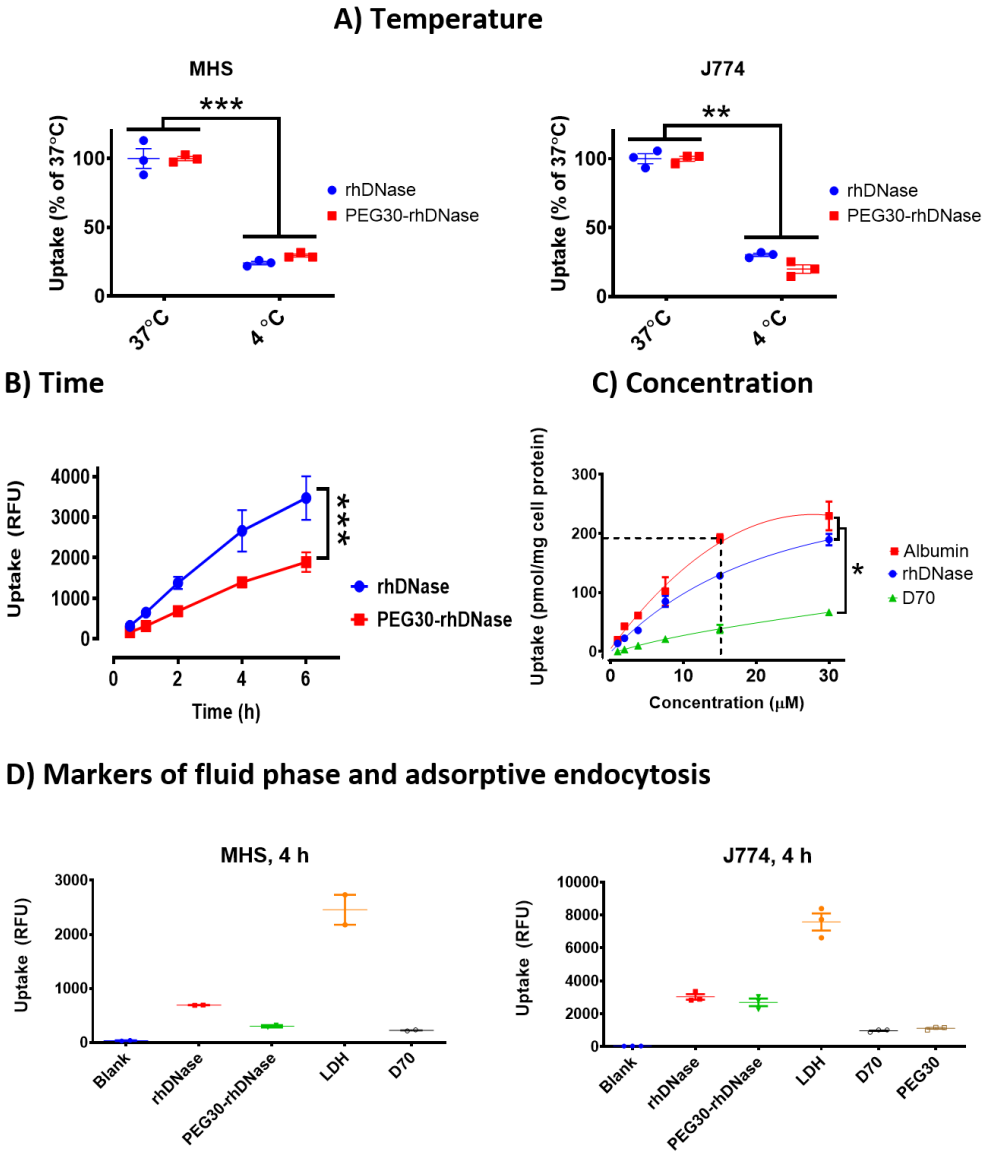

Figure 4. Endocytosis mode involved in rhDNase uptake by macrophages. A) Effect of temperature on the uptake of rhodamine-labelled rhDNase and PEG30-rhDNase in J774 and MHS macrophages; cells were exposed to 162 nM of either compound at 37 °C or 4 °C for 30 min; Data were normalised to median fluorescence signal at 37 °C. B) Time-dependent uptake of 162 nM of rhDNase and PEG30-rhDNase (162 nM) by J774 at 37 °C. C) Concentration-dependent uptake by MHS; cells were exposed to increasing concentrations (0.46-30 µM) of rhodamine-labelled rhDNase, albumin, or D70 in the absence of FBS in the medium for 2 h; Cells were then washed, lysed by RIPA and concentrations of compounds were measured in the supernatants by spectrofluorimetry (555/580 nm). D) Controls of fluid phase and adsorptive endocytosis; J774 and MHS macrophages were exposed to 162 nM of rhodamine-labelled rhDNase, PEG30-rhDNase, LDH, D70, or PEG30 at 37 °C and 5% CO_2 for 4 h. In A, B, and D, cells were washed by DPBS, detached, and analysed by flow cytometry (561 nm laser). Data represent individual values, and horizontal lines represent mean ± SEM. Significant differences among groups were checked by t-test (A) one-way ANOVA (D) or two-way ANOVA (B, C) followed by Tukey's posthoc test, * for $p < 0.05$ and *** for $p < 0.001$. RFU, relative fluorescence units.

To have more insights into the mechanisms of uptake of rhDNase, D70 and LDH (a known marker of adsorptive endocytosis which, at the pH of the cell culture medium, is positively charged due to its isoelectric point, pI 7.7) were tested in J774 and MHS [30, 31] (Figure 4D). Fluid phase endocytosis is a process by which macrophages probe fluids from the surrounding microenvironment [43]. It is a slow non-specific process that does not require binding to the cell membrane compared with adsorptive endocytosis which is also a non-specific process, however, occurs at higher rates than fluid-phase endocytosis and involves adsorption to the cell surface [31, 44, 45]. The uptake of rhDNase was twice that of PEG30-rhDNase, 3 times higher than D70 and only a third that of LDH in MHS. A similar trend was found in J774 except that the uptake of PEG30-rhDNase was only 0.9 that of rhDNase, and LDH was 2.5-fold higher than rhDNase.

III.4. DIFFUSION IN MUCUS AND CF SPUTA

To determine if PEGylation affected the diffusion and binding of rhDNase to the respiratory mucus, we assessed the diffusion of native and PEGylated rhDNase by fluorescence recovery after photobleaching (FRAP) in porcine tracheal mucus and CF sputa. Dextran of 40 kDa (FD40) and 70 kDa (FD70) were used as controls to assess the impact of MW and macromolecule nature on the diffusion.

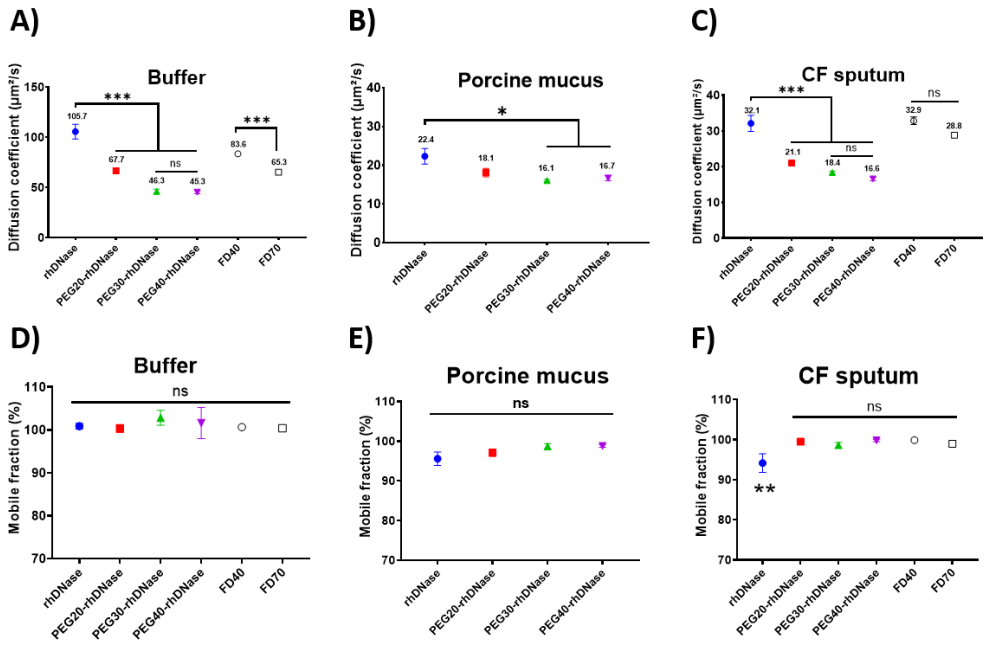

Figure 5. Diffusion of FITC-labelled native and PEGylated rhDNase and dextrans through porcine tracheal mucus, CF sputum and buffer by fluorescence recovery after photobleaching (FRAP). Diffusion coefficient (µm²/s) and mobility (%) respectively in buffer (A, D), porcine mucus (B, E), or CF sputa (C, F). Data represent mean ± SEM different mucus samples (n = 3). Significant differences among groups are presented by * for $p < 0.05$, ** for $p < 0.01$, and *** for $p < 0.001$ (one-way ANOVA, Tukey's posthoc test).

The diffusion of native rhDNase was faster than that of PEGylated rhDNase in all media (buffer, porcine mucus, and CF sputa) with no difference in diffusion rate observed between PEG30-rhDNase and PEG40-rhDNase (Figure 5 A-C). The diffusion of all compounds was slowed down in the porcine mucus and CF sputum compared to the buffer (Figure 5B and C). The diffusion of rhDNase in porcine mucus was 4.8-fold slower compared with the buffer, whereas it was 3.7, 2.9, and 2.7 fold slower for PEG20-rhDNase, PEG30-rhDNase, and PEG40-rhDNase respectively (Table S1). All compounds diffused freely with no binding to the media (100% mobile fraction) at the exception of rhDNase, whose mobile fraction was lower (94%) in CF sputum ($p < 0.01$) (Figure 5D-F).

Transport experiments across a thin layer of porcine tracheal mucus spread at the surface of Transwell® inserts (Figure S6) showed that the half-lives (the time needed for 50% of the initial dose to cross the mucus layers mounted on inserts) or crossing the mucus layer were qualitatively in line with the FRAP experiments. The half-lives were 24 (95% CI, 23-26), 47 (44-51), 56 (52-61), and 60 (55-65) minutes for rhDNase, PEG20-rhDNase, PEG30-rhDNase, and PEG40-rhDNase, respectively.

IV. DISCUSSION

Recently, a long-acting version of rhDNase was proposed for the treatment of CF consisting of conjugated rhDNase to PEGs of 30 kDa or 40 kDa [7]. Here, we investigated potential mechanisms for the longer retention of PEGylated rhDNase in the lungs, namely, lower transport across epithelial cells, decreased uptake by alveolar macrophages, and adhesion to the respiratory mucus.

Transport across Calu-3 monolayers to the basolateral side was lower for PEG30-rhDNase compared with that of rhDNase. The activity of rhDNase and PEG30-rhDNase was preserved on the apical side but largely lost on the basolateral side indicating a significant degradation of both proteins during transport. Both rhDNase and PEG30-rhDNase were transported to a higher extent than D70 and PEG30. These findings point towards a rather significant contribution of transcellular transport; however, paracellular transport cannot be dismissed.

Proteins could be absorbed through epithelial cells transcellularly in endocytic vesicles, paracellularly through tight junctions or both [18, 35]. We propose that PEGylation with large PEGs could reduce transport by both pathways. PEGylated proteins are more hydrophilic than their corresponding unconjugated proteins, therefore, likely to interact less with the cell membrane or membrane receptors and thus not be as effectively taken up by cells. On the other hand, the relatively small size of rhDNase (37 kDa, ~ 4.8 nm) suggests that it could be transported by the paracellular route more efficiently than the larger PEG30-rhDNase (67 kDa, ~ 10 nm) [16]. This suggestion is based on the general assumption that proteins smaller than 40 kDa or 5-6 nm in size can diffuse through small pores in lung epithelia [20, 35]; however, the presence of pores of 5-12 nm in diameter and even larger was suggested in intact alveolar epithelium and lung epithelial cell monolayers [35, 42, 46].

These findings are in line with our previously published work where both intact rhDNase and PEG30-rhDNase were absorbed into the blood after intratracheal instillation in mice, however, to a lower extent for the latter [16]. Patil *et al.* have also demonstrated that PEGylation of anti-IL-13 and anti-IL-17A with PEG40 kDa reduced their uptake and transport across Calu-3 cells cultured at ALI [14]. Furthermore, the bioavailability of PEG 12 kDa conjugates of IFNα2b (19 kDa) and rhGCSF (18 kDa) were respectively 3 and 10-fold lower compared with their unconjugated counterparts after pulmonary delivery in rats [21, 22].

While PEGylation has been shown to promote particle evasion from macrophages [47-49], such an effect has not been shown conclusively for PEGylated proteins, although a reduced macrophage uptake of PEGylated Fab' fragments has been suggested [12]. Direct quantification of proteins

(PEGylated or not) in alveolar macrophages recovered by BAL following pulmonary delivery did not exceed 3% of the administered doses [7, 22, 26]. However, this percentage is probably largely underestimated because BAL only recovers a small fraction of alveolar macrophages [26]. On the other hand, a more significant contribution of alveolar macrophages was suggested by Lombry *et al.* who reported a 3-fold increase in the bioavailability of human chorionic gonadotropin hCG (from 17.6% to 59.7%) after depleting alveolar macrophages from rat lungs [24].

Regardless of the PEG size, the uptake of PEGylated rhDNase was half that of rhDNase by macrophages *in vitro* and 4 h post-delivery *in vivo*. However, a higher concentration of PEGylated rhDNase associated with the macrophages was measured 24 h post-delivery. This observation could be attributed to (i) the prolonged presence of PEG30-rhDNase in lungs airspaces and, therefore, more availability for macrophage uptake, and (ii) potentially, the higher resistance of PEGylated rhDNase to degradation within macrophages [17, 26]. Similarly, higher amounts of PEGylated rhDNase and Fab' fragments were detected in alveolar macrophages 24 h post-delivery compared to their corresponding non-PEGylated counterparts [7, 26].

The uptake of rhDNase in vitro was energy, time, and concentration-dependent. Unlike that of dextran, the uptake of both rhDNase and albumin reached saturation at the highest concentration (30 μM), which is more in favour of adsorptive endocytosis. Nevertheless, because both albumin (pI 4.7) and rhDNase (pI 4.58) are negatively charged at a neutral pH, they are unlikely to interact strongly with either negatively charged or hydrophobic sites on the cell surface [50]. Both rhDNase and albumin could be adsorbed to the cell surface, albeit weakly compared with more positively charged (e.g. LDH) or hydrophobic proteins. According to this assumption, the hydrophilic nature of PEG could decrease the adsorption of rhDNase onto the cell membrane and, therefore, decreases its uptake by macrophages. In fact, Yamamoto *et al.* have shown that the PEGylation of lipid membranes prevented the adsorption of bovine serum albumin [51]. Likewise, we expect the PEGylated proteins to be less adsorbed onto lipid cell membranes.

Because macrophages are more efficient in scavenging protein aggregates [18], the lower uptake of PEG30-rhDNase by alveolar macrophages at 4 h *in vivo* could be partly ascribed to the protective effect of PEG against the aggregation of rhDNase in contact with lung lining fluids. However, preservation of the full enzymatic activity *in vitro* on the apical side of Calu-3 layers also suggests no aggregate formation. Moreover, in a recent work, we have shown that the PEGylation only confers slight protection to rhDNase against aggregation and loss of activity in contact with BAL in the absence, but not the presence, of calcium ions [16]. Therefore, we conclude that the

decreased uptake of PEGylated rhDNase by alveolar macrophages might not be related to protection against aggregation.

The diffusion of PEGylated rhDNase through porcine mucus and CF sputa was, as expected, slower than that of native rhDNase due to the increased hydrodynamic diameter of PEG conjugates. Mechanical trapping of proteins and dextrans in the mesh-like network of mucus is unlikely due to the large pore size of tracheal mucus (20 nm to several micrometres [52, 53]) relative to the size of our tested compounds (≤ 10 nm). It is, however, possible that this hindrance is partially caused by the high crosslinking and tortuous pathways of concentrated mucus and purulent CF sputa [34, 54].

FRAP measurements of the mobility of PEGylated rhDNase and dextrans in porcine mucus indicate no strong chemical interaction of these compounds with the mucus. rhDNase, on the other hand, exhibited a slight decrease in the mobile fraction in porcine mucus and CF sputa (4% and 6%, respectively) likely due to binding to mucus components, although we cannot speculate on the nature of these interactions. Moreover, the diffusion rates of proteins in porcine mucus and CF sputa were 2.7 to 4.8 times slower than that in the buffer. The larger the PEG the least this diffusion was slowed in mucus compared to buffer. These data indicate that longer PEG chains might be more efficient in preventing interactions with mucus constituents.

Contrary to our finding, the conjugation to 20 kDa and 40 kDa PEGs was shown to cause binding of Fab' fragments to the mucus; this adhesion was attributed to the entanglement of PEG with the mucin fibres [12, 14].

Finally, the mucus layer covering the airway epithelium is 2-55 μm thick [49, 55]. It is thin to absent in the lung periphery and thicker in the upper airways. Thus, the rapid diffusion rate of native and PEGylated rhDNase in mucus (16 – 32 μm2/s, Figure 5B and C) means that they can penetrate the mucus almost instantly and that PEGylation would not significantly impact the mucociliary clearance of rhDNase based solely on this criterion.

V. CONCLUSIONS

In this work, we have shown that the prolonged presence of PEGylated rhDNase in the lungs is likely promoted by lower absorption through epithelial cells and decreased uptake by alveolar macrophages as compared to the native protein. On the other hand, protection against aggregation and altered binding to airway mucus do not appear to be notable factors affecting its fate in the lungs.

VI. REFERENCES

1. Carter, P.J., *Introduction to current and future protein therapeutics: A protein engineering perspective.* Experimental Cell Research, 2011. **317**(9): p. 1261-1269.
2. Walsh, G., *Biopharmaceutical benchmarks 2014.* Nature Biotechnology, 2014. **32**(10): p. 992-1000.
3. Walsh, G., *Biopharmaceutical benchmarks 2018.* Nat Biotechnol, 2018. **36**(12): p. 1136-1145.
4. Zaman, R., et al., *Current strategies in extending half-lives of therapeutic proteins.* Journal of Controlled Release, 2019. **301**: p. 176-189.
5. Kintzing, J.R., M.V. Filsinger Interrante, and J.R. Cochran, *Emerging Strategies for Developing Next-Generation Protein Therapeutics for Cancer Treatment.* Trends Pharmacol Sci, 2016. **37**(12): p. 993-1008.
6. Moncalvo, F., M.I.M. Espinoza, and F. Cellesi, *Nanosized Delivery Systems for Therapeutic Proteins: Clinically Validated Technologies and Advanced Development Strategies.* Frontiers in Bioengineering and Biotechnology, 2020. **8**: p. 22.
7. Guichard, M.J., et al., *PEGylation of recombinant human deoxyribonuclease I provides a long-acting version of the mucolytic for patients with cystic fibrosis (Submitted).*
8. Hertel, S.P., G. Winter, and W. Friess, *Protein stability in pulmonary drug delivery via nebulization.* Advanced Drug Delivery Reviews, 2015. **93**: p. 79-94.
9. Labiris, N.R. and M.B. Dolovich, *Pulmonary drug delivery. Part I: physiological factors affecting therapeutic effectiveness of aerosolized medications.* Br J Clin Pharmacol, 2003. **56**(6): p. 588-99.
10. Osman, N., et al., *Carriers for the targeted delivery of aerosolized macromolecules for pulmonary pathologies.* Expert Opinion on Drug Delivery, 2018. **15**(8): p. 821-834.
11. Guichard, M.J., et al., *Production and characterization of a PEGylated derivative of recombinant human deoxyribonuclease I for cystic fibrosis therapy.* International Journal of Pharmaceutics, 2017. **524**(1-2): p. 159-167.
12. Koussoroplis, S.J., et al., *PEGylation of antibody fragments greatly increases their local residence time following delivery to the respiratory tract.* Journal of Controlled Release, 2014. **187**: p. 91-100.
13. Freches, D., et al., *PEGylation prolongs the pulmonary retention of an anti-IL-17A Fab' antibody fragment after pulmonary delivery in three different species.* Int J Pharm, 2017. **521**(1-2): p. 120-129.
14. Patil, H.P., et al., *Fate of PEGylated antibody fragments following delivery to the lungs: Influence of delivery site, PEG size and lung inflammation.* Journal of Controlled Release, 2018. **272**: p. 62-71.
15. Cantin, A.M., et al., *Polyethylene glycol conjugation at Cys232 prolongs the half-life of alpha1 proteinase inhibitor.* Am J Respir Cell Mol Biol, 2002. **27**(6): p. 659-65.
16. Mahri, S., et al., *Biodistribution and elimination pathways of PEGylated recombinant human deoxyribonuclease I after pulmonary delivery in mice (Submitted).*
17. Guichard, M.J., T. Leal, and R. Vanbever, *PEGylation, an approach for improving the pulmonary delivery of biopharmaceuticals.* Current Opinion in Colloid & Interface Science, 2017. **31**: p. 43-50.
18. Patton, J.S., C.S. Fishburn, and J.G. Weers, *The lungs as a portal of entry for systemic drug delivery.* Proc Am Thorac Soc, 2004. **1**(4): p. 338-44.
19. Gould, J.C., et al., *Bioavailability of protein therapeutics in rats following inhalation exposure: Relevance to occupational exposure limit calculations.* Regulatory Toxicology and Pharmacology, 2018. **100**: p. 35-44.
20. Pfister, T., et al., *Bioavailability of Therapeutic Proteins by Inhalation-Worker Safety Aspects.* Annals of Occupational Hygiene, 2014. **58**(7): p. 899-911.
21. Niven, R.W., et al., *PULMONARY ABSORPTION OF POLYETHYLENE GLYCOLATED RECOMBINANT HUMAN GRANULOCYTE-COLONY-STIMULATING FACTOR (PEG RHG-CSF).* Journal of Controlled Release, 1994. **32**(2): p. 177-189.
22. McLeod, V.M., et al., *Optimal PEGylation can improve the exposure of interferon in the lungs following pulmonary administration.* J Pharm Sci, 2015. **104**(4): p. 1421-30.
23. Vanbever, R., *Performance-driven, pulmonary delivery of systemically acting drugs.* Drug Discovery Today: Technologies, 2005. **2**(1): p. 39-46.
24. Lombry, C., et al., *Alveolar macrophages are a primary barrier to pulmonary absorption of macromolecules.* Am J Physiol Lung Cell Mol Physiol, 2004. **286**(5): p. L1002-8.
25. Gursahani, H., et al., *Absorption of Polyethylene Glycol (PEG) Polymers: The Effect of PEG Size on Permeability.* Journal of Pharmaceutical Sciences, 2009. **98**(8): p. 2847-2856.
26. Freches, D., et al., *Preclinical evaluation of topically-administered PEGylated Fab' lung toxicity.* Int J Pharm X, 2019. **1**: p. 100019.

27. Wanner, A., M. Salathé, and T.G. O'Riordan, *Mucociliary clearance in the airways.* Am J Respir Crit Care Med, 1996. **154**(6 Pt 1): p. 1868-902.
28. Kirch, J., et al., *Mucociliary clearance of micro- and nanoparticles is independent of size, shape and charge--an ex vivo and in silico approach.* J Control Release, 2012. **159**(1): p. 128-34.
29. Sinicropi, D., et al., *Colorimetric determination of DNase I activity with a DNA-methyl green substrate.* Anal Biochem, 1994. **222**(2): p. 351-8.
30. Li, L., et al., *The effect of the size of fluorescent dextran on its endocytic pathway.* Cell Biol Int, 2015. **39**(5): p. 531-9.
31. Kooistra, T., M.K. Pratten, and K.E. Williams, *Endocytosis of simple proteins by rat yolk sacs and by rat peritoneal macrophages incubated in vitro.* Acta Biol Med Ger, 1981. **40**(10-11): p. 1637-46.
32. Cingolani, E., et al., *In vitro investigation on the impact of airway mucus on drug dissolution and absorption at the air-epithelium interface in the lungs.* Eur J Pharm Biopharm, 2019. **141**: p. 210-220.
33. Alqahtani, S., et al., *Development of an In Vitro System to Study the Interactions of Aerosolized Drugs with Pulmonary Mucus.* Pharmaceutics, 2020. **12**(2).
34. Braeckmans, K., et al., *Three-Dimensional Fluorescence Recovery after Photobleaching with the Confocal Scanning Laser Microscope.* Biophysical Journal, 2003. **85**(4): p. 2240-2252.
35. Patton, J.S., *Mechanisms of macromolecule absorption by the lungs.* Advanced Drug Delivery Reviews, 1996. **19**(1): p. 3-36.
36. Ducreux, J., et al., *PEGylation of anti-sialoadhesin monoclonal antibodies enhances their inhibitory potencies without impairing endocytosis in mouse peritoneal macrophages.* Bioconjug Chem, 2009. **20**(2): p. 295-303.
37. Williams, K.E., et al., *Quantitative studies of pinocytosis. II. Kinetics of protein uptake and digestion by rat yolk sac cultured in vitro.* J Cell Biol, 1975. **64**(1): p. 123-34.
38. Lucero, D., et al., *Interleukin 10 promotes macrophage uptake of HDL and LDL by stimulating fluid-phase endocytosis.* Biochimica Et Biophysica Acta-Molecular and Cell Biology of Lipids, 2020. **1865**(2): p. 15.
39. Hastings, R.H., et al., *Cellular uptake of albumin from lungs of anesthetized rabbits.* Am J Physiol, 1995. **269**(4 Pt 1): p. L453-62.
40. Longoni, D., et al., *Interleukin-10 increases mannose receptor expression and endocytic activity in monocyte-derived dendritic cells.* Int J Clin Lab Res, 1998. **28**(3): p. 162-9.
41. Elbert, K.J., et al., *Monolayers of human alveolar epithelial cells in primary culture for pulmonary absorption and transport studies.* Pharm Res, 1999. **16**(5): p. 601-8.
42. Matsukawa, Y., et al., *Size-Dependent Dextran Transport across Rat Alveolar Epithelial Cell Monolayers.* Journal of Pharmaceutical Sciences, 1997. **86**(3): p. 305-309.
43. Buckley, C.M. and J.S. King, *Drinking problems: mechanisms of macropinosome formation and maturation.* Febs j, 2017. **284**(22): p. 3778-3790.
44. Pratten, M.K. and J.B. Lloyd, *Effects of temperature, metabolic inhibitors and some other factors on fluid-phase and adsorptive pinocytosis by rat peritoneal macrophages.* Biochem J, 1979. **180**(3): p. 567-71.
45. Lloyd, J.B. and K.E. Williams, *NON-SPECIFIC ADSORPTIVE PINOCYTOSIS.* Biochemical Society Transactions, 1984. **12**(3): p. 527-528.
46. Mathia, N.R., et al., *Permeability characteristics of calu-3 human bronchial epithelial cells: in vitro-in vivo correlation to predict lung absorption in rats.* J Drug Target, 2002. **10**(1): p. 31-40.
47. Verhoef, J.J. and T.J. Anchordoquy, *Questioning the Use of PEGylation for Drug Delivery.* Drug Deliv Transl Res, 2013. **3**(6): p. 499-503.
48. Patel, B., V. Gupta, and F. Ahsan, *PEG-PLGA based large porous particles for pulmonary delivery of a highly soluble drug, low molecular weight heparin.* J Control Release, 2012. **162**(2): p. 310-20.
49. Sanders, N., et al., *Extracellular barriers in respiratory gene therapy.* Adv Drug Deliv Rev, 2009. **61**(2): p. 115-27.
50. Livesey, G. and K.E. Williams, *Rates of pinocytic capture of simple proteins by rat yolk sacs incubated in vitro.* Biochem J, 1981. **198**(3): p. 581-6.
51. Yamamoto, T., et al., *Interaction of poly(ethylene glycol)-conjugated phospholipids with supported lipid membranes and their influence on protein adsorption.* Science and Technology of Advanced Materials, 2016. **17**(1): p. 677-684.
52. Button, B., et al., *A periciliary brush promotes the lung health by separating the mucus layer from airway epithelia.* Science, 2012. **337**(6097): p. 937-41.
53. Kirch, J., et al., *Optical tweezers reveal relationship between microstructure and nanoparticle penetration of pulmonary mucus.* 2012. **109**(45): p. 18355-18360.

54. Rubin, B.K., *Mucus structure and properties in cystic fibrosis.* Paediatr Respir Rev, 2007. **8**(1): p. 4-7.
55. Todoroff, J. and R. Vanbever, *Fate of nanomedicines in the lungs.* Current Opinion in Colloid & Interface Science, 2011. **16**(3): p. 246-254.
56. Martin, C.A. and M.E. Dorf, *Interleukin-6 production by murine macrophage cell lines P388D1 and J774A.1: stimulation requirements and kinetics.* Cell Immunol, 1990. **128**(2): p. 555-68.

SUPPLEMENTARY MATERIALS

List of contents

Table S1. Coefficient of diffusion ratios between buffer and mucus/sputa.

	FD40	**FD70**	**rhDNase**	**PEG20-rhDNase**	**PEG30-rhDNase**	**PEG40-rhDNase**
$D_{Buffer/Porcine\ mucus}$ (SD)	-	-	4.80 (0.70)	3.71 (0.37)	2.88 (0.09)	2.72 (0.19)
$D_{Buffer/CF\ sputum}$ (SD)	2.55 (0.14)	2.27 (0.05)	3.32 (0.38)	3.17 (0.06)	2.52 (0.08)	2.74 (0.014)

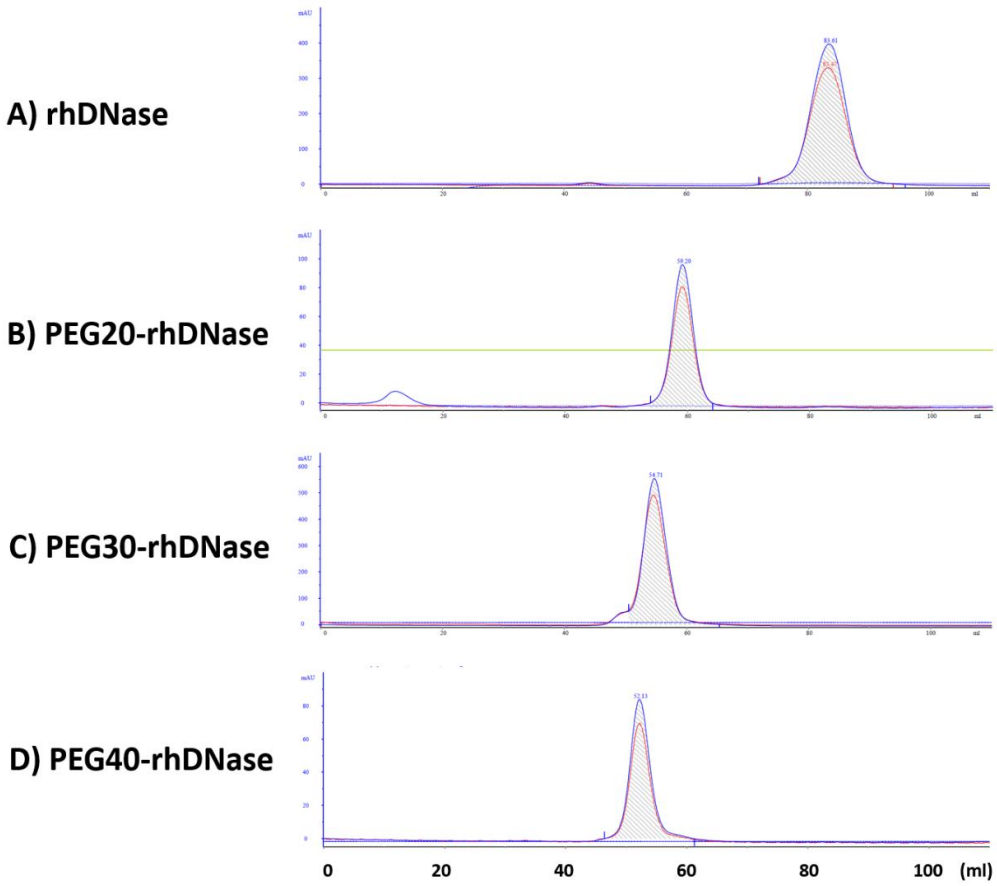

Figure S1. Size exclusion chromatography (SEC) of rhodamine-labelled native and PEGylated rhDNase with PEG20, PEG30, and PEG40 kDa (A to D, respectively). Labelled proteins eluted with 1 mM $CaCl_2$ 150 mM NaCl (1 mL/min) on HiLoad Superdex 200 pg column. Elution was monitored by measuring the absorbance at 280 nm (blue, protein) and 555 nm (magenta, dye). Elution volumes are inversely proportional to the MW of the protein-PEG conjugate. Chromatograms shows no degradation or aggregated products. Shaded areas correspond to the collected fractions.

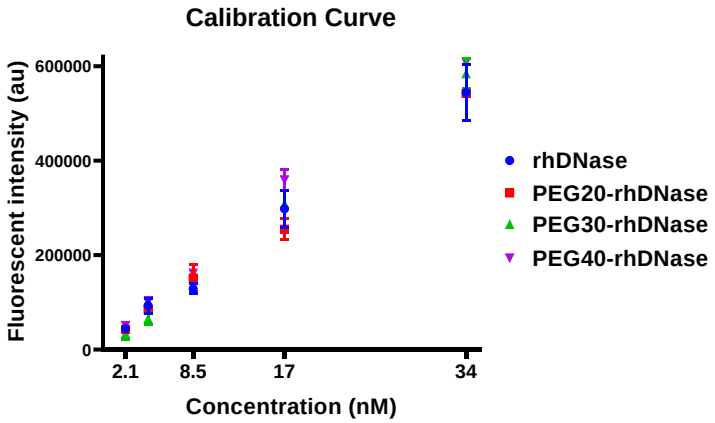

Figure S2. Calibration curves of rhodamine labelled rhDNase and PEGylated rhDNase in 1 mM CaCl2 150 mM NaCl buffer. Fluorescence was measured in dark 96 well plate at wavelength 555/580 nm for excitation and emission.

Quantification of lipopolysaccharide (LPS) levels for protein stock solutions

LPS content in protein stock solutions was tested on murine macrophage tumour lines P388D1 (ATCC®). This cell line is known to secrete interleukin 6 (IL-6) after stimulation by lipopolysaccharide [56]. Non-adherent P388D1 macrophages were maintained in RPMI 1640 medium supplemented with 15% FBS at 37 °C and 5% CO_2. Cells were seeded in 96 well plates at a density of 8x 10^4 cell/well for 48 h at 37 °C and 5% CO_2 with serial concentrations of LPS standard or protein solutions prepared in cell culture media. The LPS used was from Escherichia coli O111: B4, #L4391, lot 088M4067V, potency 500000 EU/mg, Sigma-Aldrich, MO, USA). After 48 h plates were centrifuged at 300 g for 5 min to precipitate cells and the supernatant was collected for IL-6 quantification. IL-6 levels in the supernatant were measured by ELISA (Mouse IL-6 DuoSet ELISA, Bio-Techne, Minneapolis, USA). LPS levels in samples were then calculated from the levels of IL-6 induced for known standards of LPS.

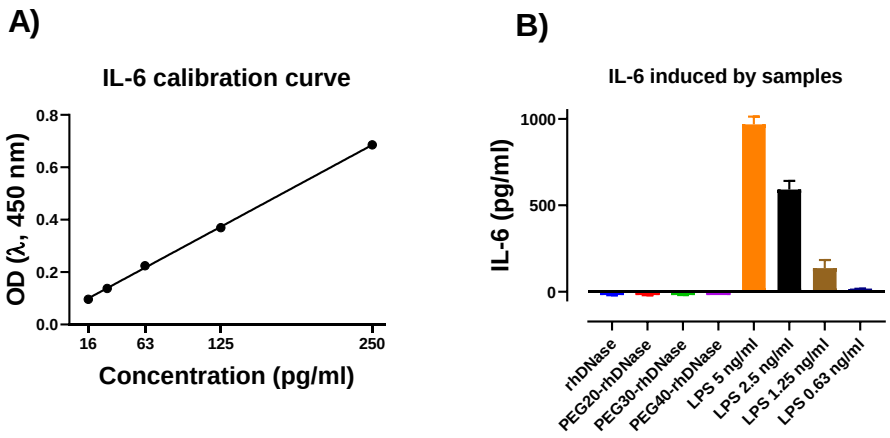

Figure S3. Determination of concentrations of lipopolysaccharide (LPS) in protein stock solutions. A) Calibration curve of IL-6. B) Levels of IL-6 produced by P388D1 macrophages after exposure to different concentrations of LPS or proteins stock solutions.

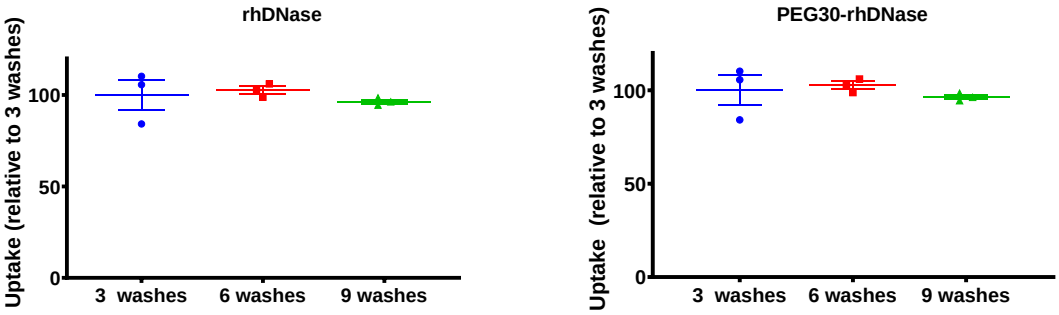

Figure S4. Impact of the number of washes on the uptake of rhDNase and PEG30-rhDNase in J774. Cells were exposed to 1.62 nM of rhDNase or PEG30-rhDNase for 4 h 37 °C and 5% CO_2. Cells were then washed 3, 6, or 9 times with PBS (1ml each) then detached and analysed by flow cytometry at 561 nm laser. Data represent individual values of median fluorescence intensities, and horizontal lines represent mean ± SEM (n = 3). No statistical difference was found (one-way ANOVA, Tukey's posthoc test).

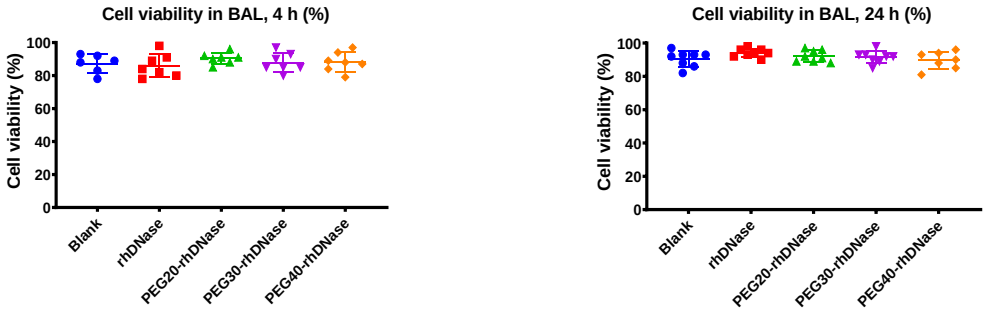

Figure S5. Cell viability in BAL by trypan blue exclusion test. BALs was collected 4 h and 24 h after instillation of compounds or controls. Data represent individual values for each BAL, and horizontal lines are mean ± SEM. No statistical differences among groups could be inferred (one-way ANOVA, Tukey's posthoc test).

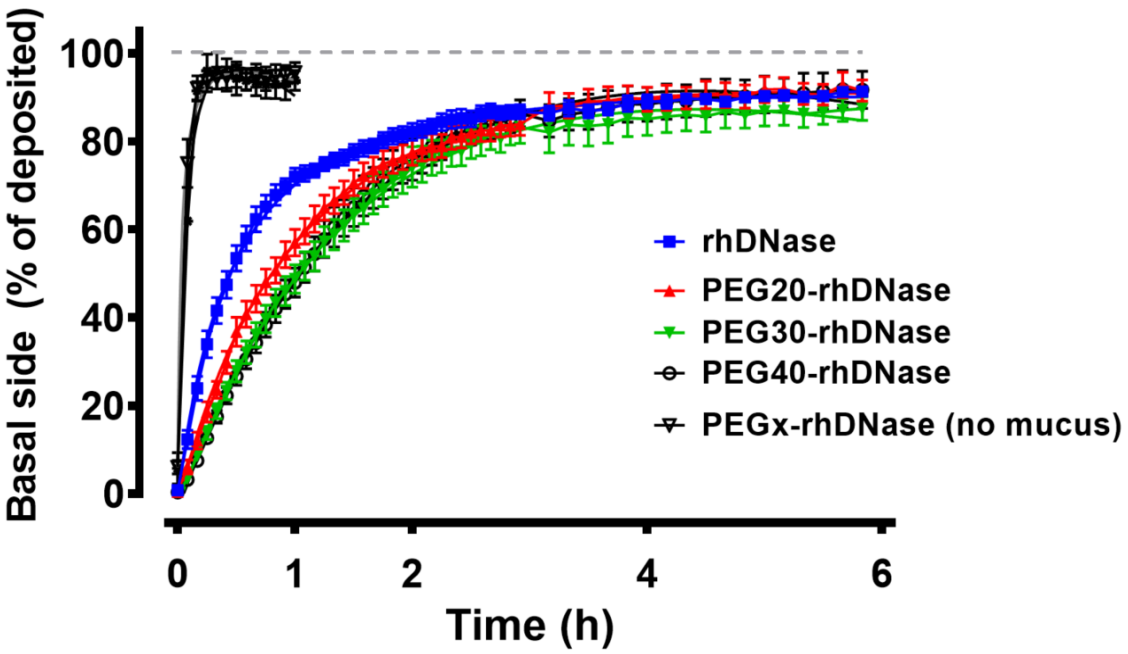

Figure S6. Transport of native and PEGylated rhDNase across porcine tracheal mucus in Transwell® inserts. Mucus was prepared on Transwell® inserts as previously described [32, 33]. Twelve mg of porcine mucus was diluted in 300 µl of 100 mM NaCl and laid on the Transwell® membrane. Inserts placed in 12 well plates were then centrifuged for 15 min at 1500 rpm followed by a careful aspiration of the excess NaCl solution. 500 µl of Hank's Balanced Salt Solution (HBSS) was added to the basolateral chamber. The calculated thickness of the mucus is ~ 100 µm. C) Transport kinetics of proteins across the mucus in Transwell® inserts. Rhodamine labelled-rhDNase, PEG20-rhDNase, PEG30- rhDNase or PEG40-rhDNase. 135 nM of each compound (5 µg of rhDNase in 5 µl of HBSS) was pipetted on the top of the mucus then the plate was kept at 35.5 ± 0.5 °C under constant orbital shaking in the plate reader (Tecan Spark 10M, Männedorf, Switzerland). Fluorescence was recorded every 5 min from the bottom (555/600 nm, ex/em). Bars represent mean ± SEM (n = 3) of the percentage of the dose deposited on mucus detected in the lower chamber.

The data in Figure S6 show that the PEGylation delays the transport of rhDNase across the mucus. The complete transport across the mucus takes hours because of the (i) higher thickness of the mucus layer, (ii) the presence of an additional barrier represented by the insert membrane. Complete transport across empty Transwell® inserts occurs in 5-10 min for all proteins.

CHAPTER IV

DISCUSSION AND PERSPECTIVES

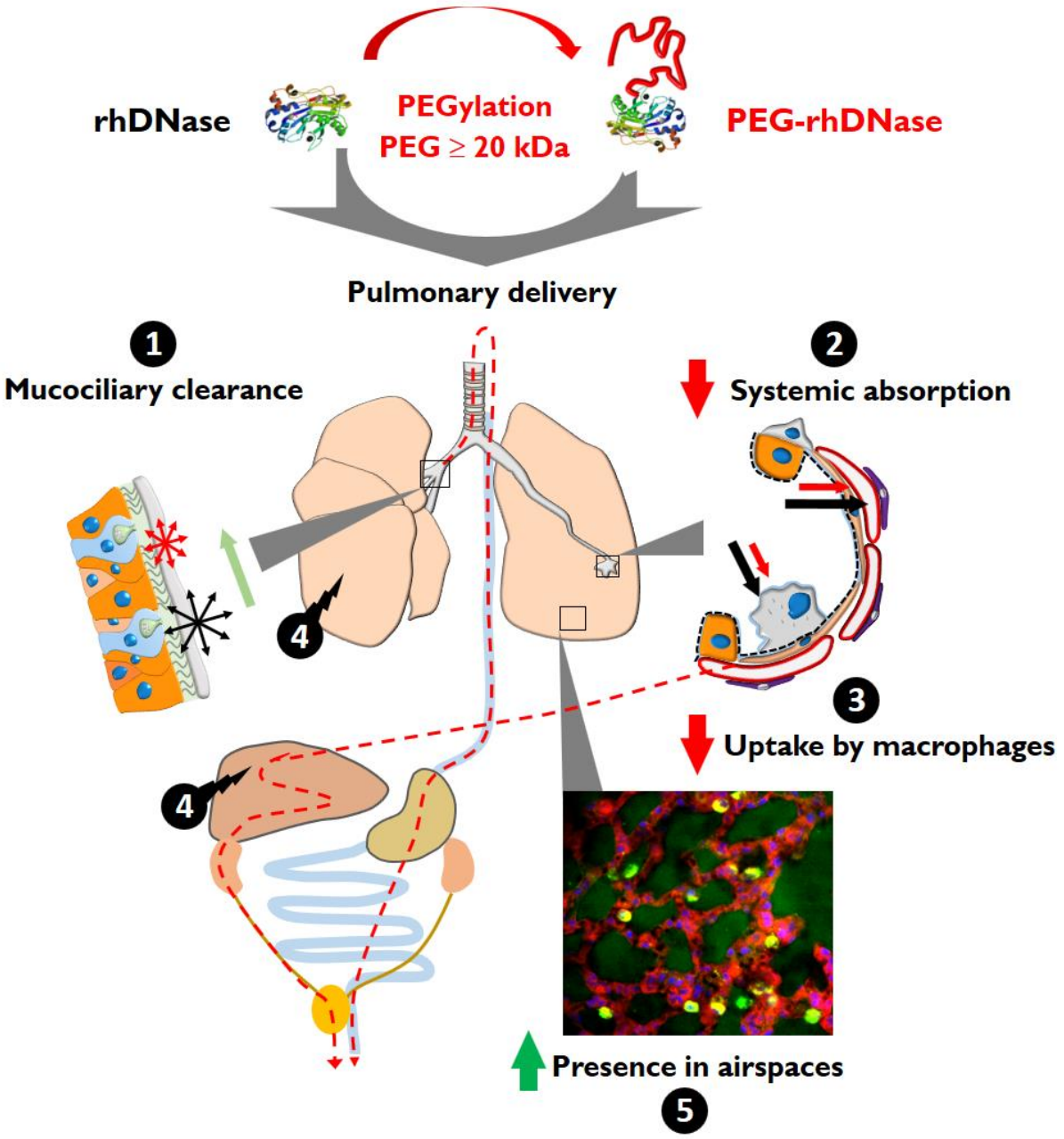

Graphical abstract. Mechanisms of the longer retention of PEGylated rhDNase in the lungs. PEGylation of rhDNase with PEG of MW ≥ 20 kDa decreases the diffusion of rhDNase in the mucus but does not affect its mucociliary clearance significantly (1). PEGylation of rhDNase decreases its absorption from the lungs (2), uptake by alveolar macrophages (3), and degradation, primarily in the lungs (4), leading to a longer retention of PEGylated rhDNase in lung airspaces (5).

TABLE OF CONTENTS

I. MAIN ACHIEVEMENTS

Delivery of therapeutic proteins to the lungs holds plenty of promise for local and systemic therapies. Despite the market gradual shift towards developing therapeutic proteins in recent years, the exploitation of the pulmonary route is failing to catch up [1, 2]. The market release of inhaled dornase alfa has given this field the impetus to pursue further developments. However, almost three decades later, the success of dornase alfa remains singular. Despite this, the pulmonary delivery of proteins seems to keep its attractiveness, especially for the local delivery of large proteins, otherwise, poorly available to the lungs by other routes of administration [3].

Guichard *et al.* have developed a PEGylated version of rhDNase that could sustain the presence of the enzyme in the lungs and thereby improve its therapeutic efficacy. In this project, we investigated the mechanisms of the lung longer retention of conjugated rhDNase with linear 20 kDa, linear 30 kDa, and two-arm 40 kDa PEG following pulmonary delivery.

In vivo fluorescence imaging showed that the presence of PEGylated rhDNase in lungs was sustained for 10-12 days compared with 5-7 days for the unconjugated rhDNase following pulmonary delivery in mice. Confocal imaging of mouse lungs has shown that the extended retention of PEGylated rhDNase was associated with its presence in airspaces as well as in AMs, contrary to rhDNase, where its presence beyond the first 24 h was only associated with lung parenchyma and AMs. The presence of PEGylated rhDNase in airspaces is ideal for exerting the mucolytic activity of the enzyme.

PEGylated rhDNase was less absorbed to the blood *in vivo* and across Calu-3 lung epithelial cells *in vitro*. The larger size of PEGylated rhDNase and the hydrophilic nature of the PEG were suggested to reduce both transcellular and paracellular transport across epithelial cells.

Native and PEGylated rhDNase were shown to be taken up significantly by macrophages *in vitro and in vivo* after intratracheal instillation. The uptake of PEGylated rhDNase was half that of rhDNase at 4 h *in vivo* and *in vitro* showing that PEGylation decreased the uptake of rhDNase regardless of the PEG size. The opposite was seen *in vivo* at 24 h post-instillation where the amounts associated with AMs were twice higher for PEGylated rhDNase. The uptake of rhDNase by macrophages was energy and time-dependent and saturable at high concentrations, which is indicative of adsorptive endocytosis. Decreasing the interactions with the cell membrane due to the hydrophilic nature of PEG might explain this reduction; however, more experiments need to be conducted to confirm this hypothesis.

The mucociliary clearance of both proteins was demonstrated *in vivo*; however, with no significant difference between rhDNase and PEG30-rhDNase, suggesting that a decrease in mucociliary clearance might not be the main cause for the longer retention of PEGylated rhDNase. PEGylation was shown to decrease the diffusion rate of rhDNase in porcine tracheal mucus and CF sputa. No strong binding to the mucus and CF sputa was found except for rhDNase which showed 4 to 6% of its quantity immobilised. These differences might not be significant *in vivo* as the diffusion rates of both proteins was relatively fast (16-32 $\mu m^2/s$) relative to the thickness of the mucus in the respiratory tract ($\leq$ 55 μm).

PEGylated rhDNase was significantly less degraded than rhDNase in lung homogenates at 24 h post-instillation. This protection against degradation might be the results of decreased uptake by AMs and epithelial cells rather than increased stability of rhDNase in airspaces. Further catabolism in the liver and eventually the blood occurred after absorption. PEGylated rhDNases suffered slightly more aggregation and loss of activity in contact with the bronchoalveolar lavage fluid but only in the absence of calcium ions. This slightly increased stability of PEGylated rhDNase in lung fluid might not be relevant to the *in vivo* scenario were calcium concentrations in lung lining fluids and mucus are high enough [4-7].

In vivo NIFR imaging showed a similar distribution of native and PEGylated rhDNase in the whole body, particularly in highly irrigated organs. Transient accumulation of native but not PEGylated rhDNase in the liver was attributed to the higher absorption of rhDNase and its degradation products from the lungs compared with PEGylated rhDNase rather than a higher affinity or retention of rhDNase in the liver. This suggestion was supported by the more prolonged accumulation of PEG30-rhDNase in the liver following IV injection. Renal excretion was observed following pulmonary absorption however it was only for intact rhDNase but not PEG30-rhDNase.

In summary, reduction in systemic absorption as well as macrophage and epithelial cell uptake seemed to play a significant role in the extended retention of PEGylated rhDNase in the lungs. Mucociliary clearance, as well as aggregation in the lungs, were involved in the clearance of both forms of rhDNase but are unlikely to play a very significant role in their differential retention in the lungs.

II. DISCUSSION

Conjugation to MW PEGs ≥ 20 kDa has been demonstrated to increase the residence time of proteins in the lungs [8-11]. More recently, remarkable results have been achieved for rhDNase following conjugation to PEGs of 30 kDa and 40 kDa [5, 12, 13]. PEGylation did not alter the enzymatic activity of rhDNase on DNA solution and CF sputa. The lung residence time was prolonged to over 15 days instead of 24 h for the unconjugated rhDNase. The extended residence time translated into an improved efficacy of the PEGylated form: one single dose of PEGylated rhDNase over 5 days was as effective as one daily dose of rhDNase during 5 days in decreasing the DNA content in lung airspaces of β-ENaC mice [13]. Moreover, the safety profile was satisfactory in the short and long term toxicities studies in mice [13].

Here, we investigated the mechanisms for the longer retention of PEGylated rhDNase, namely, i) mucociliary clearance and interaction with the mucus, ii) the transport across epithelial cells, iii) uptake by alveolar macrophages and iv) degradation within the lungs. We also investigated the biodistribution and elimination pathways of native and PEGylated rhDNase after intratracheal instillation and intravenous injection.

II.1. MUCOCILIARY CLEARANCE AND INTERACTION WITH THE MUCUS

Mucus is the first surface encountered by aerosols in the respiratory tract. Entrapment in the mucus could be beneficial for the retention of drugs delivered to the deep lungs but detrimental in the upper airways where the mucociliary clearance is more effective [9, 14, 15]. In this work, mucociliary clearance followed by elimination by the GI tract contributed to the clearance of rhDNase and PEG30-rhDNase after pulmonary delivery. However, the signal in the GI tract and the faecal pellets at 24 h post-instillation represented only 5% of the total signal suggesting a less significant contribution than the systemic absorption and retention in the lung parenchyma. Moreover, PEGylated and non-PEGylated rhDNase did not seem to be affected differently by the mucociliary clearance. In contrast, Patil *et al.* reported higher mucociliary clearance of Fab' fragments by measuring up to 29% of the administered dose in the stomach of mice 4 h after deep lung delivery [3]. The amounts in the stomach were significantly lower for anti-IL-17A-PEG20 (22%) and anti-IL-17A-PEG40 (15%) [10]. Hastings *et al.* argued that the mucociliary clearance is not a significant mechanism of protein clearance from the lungs, particularly after delivery to distal airways [10, 16]. The elimination by this pathway would be even less significant in patients with CF where the mucociliary clearance is impaired [17, 18].

The diffusion of PEGylated rhDNase in the porcine mucus and CF sputa was slower than that of rhDNase due to the increased hydrodynamic size of the PEG conjugates. It is known that because of to the highly solvated PEG, the hydrodynamic size of PEGylated proteins is higher than expected based on their MW in comparison with proteins of the same size [19, 20].

The diffusion of native and PEGylated rhDNase was up to 5 times slower in mucus and CF sputa compared with buffer probably because of the lower viscosity of the latter [21, 22] and possibly the longer distances macromolecules have to travel because of the tortuous pathways created by mucin fibres. Braeckmans *et al.* reported a ~ 3-fold decrease in the diffusion rates of dextran of 167 to 2000 kDa in CF mucus compared to the buffer [23]. Mechanical trapping of proteins and dextran in the mesh-like network of mucus is unlikely due to the large pore size of tracheal mucus (20 nm to several micrometres [22, 24, 25]) relative to the size of our tested compounds (< 10 nm). Unlike PEGylated rhDNase, rhDNase exhibited a slight decrease in mobility in porcine tracheal mucus and CF sputa where 4% and 6% of rhDNase were immobile, respectively. The immobile fractions of rhDNase are likely due to binding to the mucus components; however, we cannot speculate on the nature of these interactions. We are also unable to relate our findings to the previous work of Patil *et al.* who found the that conjugated Fab with PEGs of 20 kDa and 40 kDa caused binding of the Fab' fragments to healthy respiratory mucus [9, 10].

The mucus layer covering the airway epithelium is 2-55 μm thick [26, 27]. It is thin to absent in the lung periphery and thicker in the upper airways. Thus, the rapid diffusion rate of native and PEGylated rhDNase in mucus (16 – 32 $\mu m^2/s$) means that they can penetrate the mucus almost instantly and that the PEGylation would not significantly affect the mucociliary clearance of rhDNase based solely on this criterion.

II.2. ABSORPTION THROUGH THE LUNG EPITHELIA TO THE BLOODSTREAM

Systemic absorption to the bloodstream is an important clearance mechanism of proteins from the lungs; therefore, its decrease could significantly extend the retention of proteins in airspaces.

The systemic absorption of rhDNase after a single inhalation has been shown to range from less than 2% in monkeys up to 15% in rats [28]. Based on the general assumption that larger proteins are less absorbed from the lungs [29-32], PEGylation was expected to diminish the absorption of rhDNase across the lung epithelial barrier. The few studies in the literature about the absorption of PEGylated proteins have also shown a decrease in lung absorption following pulmonary delivery in rats. The bioavailability of rhGCSF (18 kDa) dropped threefold after conjugation to 6 kDa PEG (11.9% to 4.5%) and even lower after conjugation to 12 kDa PEG (1.6%) [33]. A similar decrease

was observed for IFNα2b (19 kDa), with its bioavailability reduced from 15% to 5.5% and < 0.4% when conjugated to PEGs of 12 kDa and 40 kDa, respectively [34]. Patil *et al.* showed that PEGylation of anti-IL-13 and anti-IL-17A (47 kDa) with PEG40 reduced both their uptake and transport across Calu-3 human lung epithelial cells [10].

NIRF imaging showed an early signal diffusion (<15min) throughout the whole body for rhDNase and PEG30-rhDNase following intratracheal instillation. Intact proteins were detected *in vivo* in sera and *in vitro* in the basolateral side of Calu-3 monolayers. In both cases, the absorption was lower for PEG30-rhDNase. The signal of rhDNase in the blood peaked at around 4 h post-delivery then decreased slowly thereafter, whereas that of PEG30-rhDNase increased initially then remained relatively steady from 2 h to 24 h. The signal in the blood originates from intact and degraded proteins as shown by gel electrophoresis of sera. Likewise, the *in vitro* amounts of proteins in the basolateral side estimated by activity were much lower than those measured by spectrofluorimetry. Moreover, the presence of degraded proteins in the basolateral side but not the apical side and the higher uptake of rhDNase by Calu-3 cells *in vitro* suggest that degradation occurred during transport, which is indicative of transcytosis. Nevertheless, the possibility of paracellular transport is not dismissed.

The presence of degradation products in sera from 4 h onward but not at 2 h suggests that absorption might have occurred initially for intact proteins by paracellular transport at high concentrations in the airspaces. This relatively fast absorption could have been followed by a longer absorption phase by transcellular transport. The presence of intact rhDNase but not its degradation fragments nor those of PEG30-rhDNase in the urines collected 2 h post-instillation supports this suggestion. The presence of other fragments in sera, lungs, and urines at 24 h after intratracheal instillation and in sera after IV injection suggest that degradation occurred before and after absorption.

Conjugation to large PEGs is likely to reduce the transport of proteins through epithelial cells by both transcellular and paracellular pathways [29]. PEGylated proteins are more hydrophilic than the corresponding unconjugated proteins, therefore, likely to interact less with the cell membrane and thus to be less taken up by cells. Moreover, the relatively small size of rhDNase (37 kDa, ~ 4.8 nm) suggests that it could be transported by paracellular pathway as well unlike the larger PEG30-rhDNase (67 kDa, ~ 10 nm) [35]. This suggestion is based on the general assumption that proteins smaller than 40 kDa or 5-6 nm in size can diffuse through small pores in lung epithelia [31]; however, pores of 5-12 nm in diameter and even larger were also suggested in intact alveolar epithelium and lung epithelial cell monolayers [29, 36, 37].

II.3. UPTAKE BY MACROPHAGES

Macrophages are the primary phagocytic cells in the lungs and the second line of defence after mucociliary clearance [38]. They are responsible for clearing microbes, particles, and foreign substances including proteins, especially in the lower airways and the alveolar region in compensation of the lower mucociliary clearance [38, 39]. Uptake by alveolar macrophages is more important for large proteins because of their low absorption and therefore longer dwelling in airspaces [40]. Here we have shown that PEGylation decreases the uptake of rhDNase by macrophages *in vitro* and *in vivo* at 4 h post-delivery. Contrary to this, the *in vivo* uptake of PEGylated rhDNase was higher at 24 h likely due to their higher concentrations in airspaces compared with rhDNase. The higher availability of PEGylated rhDNase in the airspaces was shown by confocal images as well as by ELISA in BALs [13]. The unexpectedly lower signal of rhDNase in AMs at 24 h compared with 4 h suggests that the rate of protein degradation and release by macrophages is higher than that of the uptake. This occurs when there is a lack of rhDNase in the airspaces, which is in line with the pharmacokinetic data in BAL obtained by Guichard *et al.* [13].

Several authors reported the contribution of alveolar macrophages to protein clearance from the lungs after pulmonary delivery. Lombry *et al.* reported an increase in the bioavailability of hCG (from 17.6% to 59.7%) and IgG (4.5% to 10.5 %) in AM-depleted rats [40]. However, such an increase was not reported for insulin by the same authors because of the rapid absorption of insulin by the lungs. Other authors reported a minor role of AMs in proteins clearance from the lungs. For example, direct quantifications of proteins in AMs were less than 1% for ^{125}I-albumin and IFNα2b (PEGylated or not) after intratracheal instillation in sheep and rats, respectively [34, 41]. Values up to 3% were reported for PEGylated Fab' in AMs in mice [42], and recently less than 1% for rhDNase and PEG30-rhDNase in mice [13]. These values could be higher, considering that standard procedures of BAL recover only a portion of alveolar macrophages [43]. Compared with mice, human alveoli are more numerous, larger, and host more AMs [44]. Surprisingly, the number of AMs per alveolar surface area is constant across species [38], but their volume in humans is at least 2-3 times bigger than that of mice [44, 45]. Therefore, the uptake capacity of AMs per unit of alveolar surface area is higher in humans, assuming a correlation between the volume of and the endocytotic activity of AMs.

The endocytic capacity of AMs is also higher than that of type II cells [16], which is in turn higher than that of type I cells [46]. In fact, confocal images revealed brighter signals in AMs compared with alveolar septa. Because of the higher number of epithelial cells compared to AMs in mice and human lungs (10 to 1 ratio) [44], their contribution of the latter would be less significant. Takano

et al. have estimated that type II cells cultured in vitro contributed to more than 70% of the uptake of albumin while the remaining (< 30%) is taken up by type I cells. Based on these estimations and cell distribution of type II: type I: AM of 67:40:12 per alveolus in humans [44], the contribution of AMs in the uptake of albumin would be higher than 10% of the overall uptake in the alveolar region. This role in the clearance would be even less for rapidly absorbed proteins [40].

The uptake of rhDNase by macrophages was energy, time, and concentration-dependent, and reached saturation at the highest concentration (30 μM). It occurred at a rate comparable with that of albumin at high concentrations, but significantly higher than that of dextran of 70 kDa. Because both albumin (pI 4.7) and rhDNase (pI 4.58) are negatively charged at a neutral pH, they are unlikely to interact strongly with neither negatively charged nor hydrophobic sites on the cell surface [47]. However, both rhDNase and albumin could be adsorbed to the cell surface, albeit weakly compared with more positively charged (LDH) or hydrophobic proteins. This potential adsorption could explain the higher uptake rates of albumin and rhDNase relative to D70, adding thus to their basal rate of uptake by fluid-phase endocytosis. According to this assumption, the hydrophilic nature of PEG could decrease the adsorption rhDNase to the cell membrane and, therefore, reduces its uptake by macrophages. This effect would not have been observed for pure fluid-phase endocytosis which is size-independent and binding to the cell surface is not required for internalisation. Limiting the interaction with cell membrane upon PEGylation was shown by Yamamoto *et al.,* who found that the PEGylation of lipid membranes prevented the adsorption of bovine serum albumin [42]. We expect the opposite to be accurate, i.e., PEGylated proteins are likely less adsorbed on lipid membranes such as those of cells [48].

Confocal images have shown the more extended presence of PEGylated rhDNase and PEG30 alone in AMs compared with rhDNase. The size of PEG did not appear to influence the uptake of PEGylated rhDNase by macrophages significantly. If our hypothesis about decreasing the interactions with cell membranes is correct, transcytosis across epithelial cells would not differ among the studied conjugated forms of rhDNase. In this case, the shorter residence time of PEG20-rhDNase in the lungs could be due to difference in paracellular transport, even though the size of PEG20-rhDNase does not differ much from that of PEG30-rhDNase (9.4 nm *vs* 10 nm respectively).

II.4. DISTRIBUTION AND STABILITY WITHIN THE LUNGS

The local presence of intact rhDNase in airspaces is paramount for the mucolytic action of the enzyme and, therefore, its therapeutic efficacy. Confocal imaging showed that proteins clearance from lung airspaces occurred within 24 h for unconjugated rhDNase, 4 days for PEG20-rhDNase and 7 days for PEG40-rhDNase and PEG30-rhDNase. Beyond that, the signal was significantly present only in alveolar macrophages as shown by confocal images. Higher amounts of PEGylated rhDNase in the lungs at 24 h by NIRF imaging were associated with higher amounts of intact protein by gel electrophoresis, which in turn correlated with the enzymatic activity. Moreover, *in vitro* transport across Calu-3 cells has shown that rhDNase and PEG30-rhDNase were intact in contact with the apical side of the cell monolayers but not on the basolateral side. Therefore, we expect that most of the *in vivo* signal in airspaces observed by confocal imaging corresponds to intact proteins.

It is well-established that the lungs are involved in protein metabolism, albeit to a lesser extent than the liver and the GI tract [29]. The degradation of rhDNase and PEG30-rhDNase occurred most likely in lung cells (i.e. epithelial cells and alveolar macrophages). The degradation of PEG30-rhDNase did not produce rhDNase moieties suggesting that the detachment of the PEG moiety occurs after degradation of the protein moiety. Degraded products are then cleared to the bloodstream (or the lymph) where further degradation occurred for intact and degraded proteins. Degraded proteins within macrophages or airspaces could also be transported through epithelial cells or undergo other cycles of uptake and release by AMs and epithelial cells. The fate of PEG30 in mouse lungs was reasonably similar to that of PEG30-rhDNase regarding local distribution and retention time, indicating that the PEG moiety influenced the fate of PEG30-rhDNase in the lungs.

Protection against aggregation is another likely explanation for the lower uptake of PEGylated rhDNase. Indeed, because large proteins are poorly absorbed through the lungs, they are prone to aggregation and precipitation in lung lining fluid thus accelerating their uptake by alveolar macrophages [39]. Stability studies in BAL revealed that PEGylation only conferred slight protection to rhDNase against aggregation and loss of activity in the absence of calcium ions but not in its presence. This slight protection might be explained by the inherent high stability of rhDNase [49] and resistance to proteases present in lung airspaces. Calcium ions are primordial to the stability and function of rhDNase [49, 50]. Its concentration in the commercial product, Pulmozyme® is 1mM. Higher concentrations were reported in animal epithelial lining fluid (double those in plasma) [4]and CF sputa (1.1 to 3 mM) [5-7]. Therefore, instability due to the lack of calcium ions in lung airspaces is unlikely.

II.5. BIODISTRIBUTION AND ELIMINATION

Both native and PEGylated rhDNase were dominantly retained in the lungs until their total clearance from the body. The organ distribution did not differ between native and PEGylated rhDNase and was recorded in highly irrigated organs. The signal in the liver by NIRF imaging peaked around 8 h *in vivo* for rhDNase and was 8-fold higher compared with PEG30-rhDNase at 24 h *ex vivo*. We attributed this higher transient liver accumulation for rhDNase to its higher systemic absorption compared with PEG30-rhDNase, where the low absorption prevented its significant accumulation in the liver and other distant organs. Higher signals were also detected in the heart for rhDNase compared with PEG-rhDNase but not in the kidneys, the spleen or the GI tract. Clearance via the urine seemed to be predominant for all compounds as indicated by the presence of fluorescence signal in the bladder from early time points until the total clearance of compounds from the body; nevertheless, analysis of urines showed that most of the signal originated from the free dye and degradation products rather than the intact proteins.

Contrary to rhDNase, no intact PEG30-rhDNase was detected in urine, indicating an unlikely passage of intact PEG30-rhDNase into the urine although this event is not entirely excluded. Bauman *et al.* suggested that this possibility could occur due to the flexibility of the PEG polymer, which can extend and follow the protein head through the pores by reputation [51]. It is worthwhile to mention that PEGs as large as 40 kDa were detected in the urines of mice, rats, and humans [52-54]. It would have been interesting to have stained urine gels for PEG.

The biodistribution of rhDNase and PEG30-rhDNase after intravenous injection was also examined. Data confirmed liver accumulation followed by renal excretion for degraded proteins (and intact rhDNase). RhDNase did not persist in the liver for as long as PEG30-rhDNase (5 days vs 22 days). Moreover, *in vivo* data did not reveal a significant distribution of both compounds in the lungs. As no *ex vivo* data are available after IV injection, a typical distribution to other highly irrigated organs is expected. The longer half-life and liver retention of PEGylated rhDNase were expected and are likely the result of the increased protein size and thereby the reduced glomerular filtration and possible protection against proteolytic degradation of PEGylated rhDNase [55-58].

In summary, the presented work showed that the lower uptake and transport across epithelial cells contributed to the longer retention of PEGylated rhDNase in the lungs. The mucociliary clearance contributed to the clearance of both forms of rhDNase at early time points; however, indifferently. AMs intervened early after instillation and their role became more apparent over time, especially for PEGylated proteins as they resided longer in airspaces. The contribution of uptake and transport by epithelial cells in the clearance process is likely more significant as they outnumber

AMs in a ratio of ca. 10 to 1 [44]. Degradation of native and PEGylated rhDNase occurred within the lungs but also after absorption in the liver and perhaps the serum. Although PEGylation could slightly prevent the aggregation and activity loss of rhDNase in BAL in the absence of calcium ions, its contribution might not be that significant in normal or even diseased lungs where calcium concentrations are sufficiently high. Finally, the more proteolytic environment and a higher number of macrophages and other immune cells associated with inflammation in the lungs of patients with CF would not change the trend of longer retention of PEGylated rhDNase compared with rhDNase in the lungs.

III. LIMITATIONS AND PERSPECTIVES

III.1. FLUORESCENT LABELLING

A limitation in our studies is the fluorescence labelling. All proteins were labelled using NHS chemistry (N-hydroxysuccinimide) in which the NHS-dye reacts with the primary amines (lysine residues) of the protein at pH 7.0–9.0. This reaction is fast, have a high yield, and is random, especially at pH values close to 9.0 [59]. In addition to the N-terminal amine, rhDNase has 6 lysine residues, making the maximal number of dye attachment sites 7 in theory (some are not accessible) [60]. Since the N-terminal is an easier target for dye coupling, the labelling pattern could slightly differ between PEGylated and non-PEGylated rhDNase as the N-terminal is occupied by the PEG molecule in the latter. Our practice resulted in a degree of labelling of 1 to 1.5 (molecule of dye per molecule of protein). Labelled native and PEGylated rhDNase were less active than the corresponding unlabelled proteins. However, the decrease affected both proteins similarly and was more pronounced for VivoTag dye (1.18 kDa) compared with rhodamine (0.53 kDa). Careful purification steps were performed to ascertain the purity of the compounds and the absence of aggregates.

The fate of free dyes controls *in vivo* were significantly different from the tested proteins and PEG. This means that the fluorescence signal reflects somehow the fate of proteins and PEGs and not simply the detached dye as this latter is likely to be cleared rapidly once detached. Moreover, the dye was coupled to the protein moiety for native and PEGylated rhDNase. Therefore, the fate of PEG-rhDNase might not necessarily reflect that of the PEG moiety in case this latter is detached from the protein. Despite these possible artefacts, apparent differences could be observed among tested compounds showing the usefulness of the fluorescence labelling strategy in our experiments.

III.2. RHDNASE AS A PROTEIN MODEL

The scope of this work is limited to only one protein, rhDNase. RhDNase is an extracellular glycoprotein with a MW of 37 kDa and pI around 4.58 [60] making it negatively charged at the slightly acidic pH of the respiratory tract [32]. Moreover, there is not known receptors of rhDNase on lung cells, which might limit its uptake and transport across the lungs by receptor-mediated transport.

In view of our findings, the PEGylation of other proteins would also decrease their absorption by increasing their size and decreasing the interaction with cell membranes or receptors on the cell surface. The fate of proteins that tend aggregate in lungs and interact with the mucus might be

more likely impacted upon PEGylation. In fact, all PEGylated proteins in the literature were retained longer in the lungs. These proteins are: Fab/F(ab')$_2$ fragments (~ 50 kDa, pI > 6.5) [9-11], rhGCSF (18 kDa, pI = 6.1) [33], and IFNα2b (19 kDa, pI ≥ 5.7) [34].

Other proteins with different sizes and properties (hydrophobicity, pI, cell receptors) should be assessed to have a broader view on the fate of proteins and their PEGylated forms in the lungs. Most therapeutic proteins have a pI of 4.5 to 9, with most antibodies in the range of 7 to 9 [61]. Proteins such as antibodies (150 kDa, pI 7-9), lactoferrin (80 kDa, pI 8.6), albumin (68 kDa, pI 4.7), AAT (52 kDa, pI ~ 4.5), nanobodies (~ 15 kDa), as well as classic peptides such as insulin (5.8 kDa, pI 5.3) could be used as examples.

III.3. TWEAKED PEGS

Mechanistic studies have shown that the more extended retention of PEGylated rhDNase was greatly influenced by the lower absorption across epithelia and the decreased uptake by lung cells (*i.e.* AMs and epithelial cells). We hypothesised that these effects are ascribed to the hydrophilic nature and the larger hydrodynamic size of PEG, the larger the PEG the better. However, large PEGs are also more likely to accumulate in cells and tissues. Therefore, synthesising polymers that could induce similar effects *i.e.* less absorption and cell uptake, without the tendency of accumulation in tissue would beneficial. Such polymers would have ideally a large hydrodynamic size, neutral or negative charge, do not have receptors on pulmonary cells, and are more readily cleavable or degradable inside cells. This could be achieved by using repetitive units (*n*) of PEGs of low MW (*a* kDa) separated by cleavable linkers, where $n \times \alpha \geq 20$. Several degradable PEGs have been developed by introducing disulphide bridges, acid-labile acetals, amide bonds and others between oligomeric PEG units [62-67]. However these PEG derivatives suffer from several problems: a) they change properties upon adding cleavable linkers, b) they are ill-defined products, c) could not achieve large polymer size, d) are not very stable at physiological pH, e) not applicable to proteins, or f) did not demonstrate beneficial pharmacokinetics *in vivo* [62-67]. More details about PEG alternatives could be found in Pelegri-O'Day *et al.* [68].

III.4. DOSE

The doses used for *in vivo* experiments were in the range of 1-2 nmol. Despite being much higher than those used in the efficacy studies (≤ 0.14 nmol); even higher doses were shown to be safe in the signal dose toxicity studies (2.7 nmol) [40]. In fact, high doses may change the clearance pattern of proteins compared to low doses. Lombry *et al.* found that increasing doses of IgG by intratracheal instillation to rats led to a decrease in the relative bioavailability [40].

The long residence times observed at high doses by imaging were surprisingly not different from those gleaned from the pharmacokinetic studies at low doses. One possible explanation is that the ELISA method used in pharmacokinetic studies is more sensitive than fluorescence. High doses were selected based on a pilot study and were deemed necessary to obtain signals above the background autofluorescence. The lungs are notoriously autofluorescent in the green channel; these properties have even been exploited for label-free imaging of the lungs in mice [69-72]. In hindsight, fluorophores of higher excitation/emission wavelengths (in red or near infra-red region) would have been preferred for the labelling proteins in the confocal studies. In fact, the autofluorescence of lung tissue (data not shown) was lower when excited with 551nm and 633 nm laser compared with 488 nm (green channel).

III.5. OF MICE AND HUMANS

The respiratory system is one of the systems where mice and humans differ to some extent. There are many anatomical and physiological differences, such as the branching pattern, relative airways diameters, breathing frequency, cell types, and cell distribution. Many of these differences are compensatory for the differences in size and metabolic rate [73]. Among rodents, rats are better models for predicting the pharmacokinetic data of inhaled drugs in humans. Due to the small number of comparative studies in the literature between humans and pre-clinical animal models for inhaled drugs, accurate projections from mice to humans are difficult to make. Phillips *et al.* demonstrated that allometric scaling based on body mass is useful in predicting the efficacious dose of small drugs from rodents to humans [74]. The mucociliary clearance is faster in rodents than in larger mammals (2-3 fold); however, AMs are 2-3 fold larger in humans [42, 75]. Despite the significant differences between species, the optimal size of aerosol particles for alveolar deposition is not significantly influenced [75]. Freches *et al.* compared the residence time of PEGylated anti-IL-17A Fab' in mice, rats, and rabbits and noted no significant differences among species, however, a tendency to longer residence times in larger species was seen [42]. We assume that other factors

affecting the differential retention of PEGylated and native rhDNase such as absorption across epithelial cells and uptake by AMs macrophage to be relatively conserved across species. Therefore, the longer retention of PEGylated rhDNase in the lungs would also be somehow preserved.

III.6. HEALTHY VS CF LUNGS

The results of the efficacy studies in β-ENaC mice suggest that PEGylated rhDNase was retained longer in mouse lungs [13]. β-ENaC mice (a murine model for CF) suffer from chronic airway inflammation and mucus obstruction due to altered water and Na+ transport across airway epithelia similar to that observed in human CF patients. These mice have higher DNA content and inflammatory cytokines than wild type mice [76]. Studying the fate of proteins in β-ENaC mice would have been useful; however, due to the breeding difficulties, these mice were prioritised for the efficacy studies. In the following paragraph, we discuss the impact of altered parameters in CF lungs that could impact the fate of rhDNase and PEGylated rhDNase, namely, the mucociliary clearance, inflammation, proteases, and rhDNase inhibitors in airspaces.

We have suggested that the lower diffusion rate of PEGylated rhDNase compared with rhDNase in healthy mucus and CF sputa would have no impact on the mucociliary clearance of both proteins *in vivo*. This impact would be even less in patients with CF where the mucociliary clearance is compromised and might not be improved by rhDNase [77, 78]. Moderate to severe obstructions of the airways would limit the penetration of aerosol to the distal airways and alveolar region and therefore undermine the role of absorption and AMs in the clearance of both proteins. This could eventually lessen the advantages of PEGylated rhDNase over rhDNase.

The inflammation process in CF lungs is associated with an influx of immune cells and neutrophils in particular, and the activation of AMs. Neutrophils represent up to 70% of the inflammatory cell population [79]. This could be in favour of the longer retention of PEGylated rhDNase assuming a lower uptake of PEGylated rhDNase by neutrophils and other immune cells. Neutrophils are also the origin of most proteases in lung airspaces such as neutrophil elastase (NE), Proteinase 3, and matrix metalloproteinases (MMPs) [79-81]. Studies conducted in our lab have shown that rhDNase is quite resistant to NE and Proteinase 3 in the presence of calcium ions (unpublished data). Moreover, Guichard *et al.* have shown that PEGylation increased the stability of rhDNase in CF respiratory secretions, but did not prevent its inhibition by globular actin (G-actin), a potent inhibitor present in CF sputa [5].

III.7. OTHER EXPERIMENTAL LIMITATIONS (TABLE 1)

Intratracheal instillation was used for the delivery of all compounds throughout the study. Solutions tend to be deposited in the central airways and give a regional heterogeneity compared with inhalation where the compounds are distributed more homogenously and reach the distal airways and alveolar regions and therefore result usually in higher availability. Although confocal imaging showed the presence of compounds in distal and alveolar regions, the distribution throughout the whole lungs was not homogenous. Depositing samples centrally would lessen the uptake by macrophages and epithelial cells and accelerate the mucociliary clearance; however, it might not affect the longer retention of PEG30-rhDNase in the lungs compared with rhDNase. Studying the fate of proteins by inhalation would be interesting. Considering the very low deposition rate by inhalation in small animals (< 3 %), conducting a study of the kind would be expensive. Using bovine DNase I or more affordable proteins could alleviate the costs.

AMs are less numerous than epithelial cells; however, they have more active endocytosis which might affect the fate of large proteins. The rate of uptake and transport across epithelial cells could be far more important for small proteins and peptides as well as for proteins transported rapidly through receptors. A way to assess the relative contribution of macrophages vs epithelial cells *in vitro* is to compare the uptake rate of native and PEGylated proteins in both cell lines in immersion to have quick answers, or ideally set up co-cultures of epithelial cells and macrophages at ALI. Proteins could also be administered *in vivo*, then the uptake by different cell types will be assessed *ex vivo* after digestion of lungs and analysis of the uptake in different cell populations by flow cytometry.

FRAP gives useful information on the diffusion and binding properties of proteins to the mucus, however, it does not take into consideration the deposition step where aerosol particles come into contact with the mucus surface first. FRAP does not assess the partition of the drug between mucus and other media such as surfactant and periciliary liquid found in *in vivo* situation. Transport studies through inserts have the advantage to add an aqueous layer underneath the mucus, however, the thickness of the mucus is high (100 μm vs < 55 μm) and the Transwell® membrane adds an extra barrier causing further transport delay and might adsorb proteins differently; however, this last artefact was not significant between native and PEGylated rhDNase.

Lung surfactant is the outermost layer in the alveolar region; therefore, it might alter the fate of inhaled therapies in the air lumen or constitute a considerable hurdle to the efficient absorption. Preliminary data (Figure S1) showed that lung surfactant (Curosurf™) caused a loss of activity of rhDNase and PEG30-rhDNase. The loss of activity was proportional to the concentration of the

surfactant in the solution. The *in vivo* relevance of the concentrations used, the role of different constituents (lipids and proteins) and the nature of interactions between the surfactant and PEG(rhDNase) have not been yet explored and deserve further investigation

Finally, typical BAL uses 1 ml of solution in mice; this large volume dilutes the lung lining fluid for mice (≤ 15 µl) and therefore might not reflect accurately the *in vivo* conditions [75]. More relevant information could be obtained by instilling fluorescently labelled proteins then collecting the BALs to assess aggregates and potential degradation products in airspaces by SEC or SDS-PAGE/followed by imaging.

.

Table 1. Experimental limitations and possible improvements

Experiment	Advantages	Limitations	Improvements / Alternatives	Cons
Instillation	- Controlled dose - Needs small doses - Bypass nose and mouth	- Unnatural and invasive - High volume relative to ELF - Non-uniform distribution - Underestimate absorption	- Use aerosolisation, which is more physiologically relevant.	- Poor control of dose - Significant losses due to low deposition
Confocal imaging	- Easy, fast, and economical - Show the main features of the lung - Minimal processing - Trace up to 2 proteins using different dye for each.	- Possible sample washout - Interference - Poorly quantitative	- Use vibratome/ microtome - IHC - Multiphoton microscopy and other 3D fluorescence	- Spongy texture; OCT might change the local distribution of proteins and wash out compounds. - Time-consuming - Scan limited areas of the lungs
NIRF imaging (epifluorescence)	- Easy and informative - Longitudinal study - Good sensitivity	- Underestimated amounts in deep organs - Follow the tracer instead of the protein - Interference	-Transillumination mode (less interference) - Couple with CT - PET/SPECT	- Time consuming and less sensitive - Low resolution - Slow image acquisition - Radiolabelling/ionising radiations
Uptake by macrophages	- *In vivo* relevance - Mechanistic studies *in vitro*	- Only murine model used - Immersed cells - No ELF or mucus	- Use human macrophages - Use macrophages at ALI - Co-culture with epithelial cells	- More difficult to set up and validate
Transport across Calu-3 cells	- ALI mimics *in vivo* epithelium	- Static model - Extra barrier (membrane) - Deposition of a solution	- Use dynamic model - Use aerosols for exposure	- Difficult to set up - More expensive - Requires special device
FRAP	Advantages: - Tracheal mucus easy to obtain - Measures diffusion rates and mobile/immobile fractions - No extra barriers (i.e. insert membrane, filters)		Limitations: - Proteins are pre-mixed in the mucus before measurement - Does not assess the partition and transport across different media - In-house set-up	
Transport across mucus layer	- Easy set-up - Can be exposed using aerosols - Assess the transport from the mucus to the aqueous solution		- Mucus preparation might change its properties - Presence of extra barrier represented (insert membrane) - Thick mucus layer	

CT, computerised tomography; ELF, Epithelium lining fluid; FMT, fluorescence molecular tomography; IHC, Immunohistochemistry; OCT, Optimal cutting temperature compound; PET, positron emission tomography; SPECT, Single photon emission computed tomography

III.8. TOWARDS THE CLINIC

In recent years, remarkable progress has been made towards treating the underlying cause of CF. Small molecules known as CFTR modulators can target specific mutations in patients with CF [82, 83]. They can be classified into five main groups: potentiators, correctors, stabilisers, read-through agents, and amplifiers [82, 83]. Only four drugs from the first two categories have reached the market [28, 29]. Potentiators improve the activity of the channel while correctors ensure the proper protein trafficking to the cell surface [83]. Kalydeco® (ivacaftor, a potentiator) was approved in 2012 for patients with G551D-CFTR mutation affecting 5% of patients with CF [82]. In 2015, Orkambi® (ivacaftor and lumacaftor, a corrector) was approved in F508del-homozygous patients aged ≥ 12 years [82]. In 2018, Symdeko ® (ivacaftor and tezacaftor, a corrector) was approved in F508del-homozygous patients or those with at least a single copy of one of the 26 CFTR mutations that respond to ivacaftor and tezacaftor [84]. More recently, Trikafta® (ivacaftor and two correctors, elexacaftor and tezacaftor) was approved in patients 12 years and older with at least one copy of the F508del mutation present in about 90% of patients [85].

Physiotherapy, antibiotics and inhaled mucolytics are the pillars of the current symptomatic treatment of CF lung disease [86]. CFTR modulators are not intended to substitute the current standard therapy of CF in which rhDNase plays an essential role and is expected to be used for the coming years [87]. Moreover, CFTR modulators are prohibitively expensive, their clinical response is variable, and their long-term efficacy and safety are not known [13].

Even though PEGylated rhDNase might appear as an improvement of rhDNase, from a regulatory point of view, it is considered as a new drug entity and, therefore, requires going through the traditional phases of clinical trials as any other drug. Moreover, PEGs of large MW have not been approved for lung delivery yet, meaning that extensive pre-clinical toxicology studies will have to be undertaken before clinical trials are authorised. Small PEGs (*e.g.* 600 Da) are currently included in inhalation products such as cromoglycate (Lomudal®) as excipients, showing the safely of the nature of PEG to the lungs [88]. PEG of 3.35 kDa MW was shown to have a low to mild toxicity in rats, manifested as alveolar histiocytosis and vacuolated macrophages at doses equal or higher than 567 mg/m^3 after 6 h daily exposure for 2 weeks (5 days a week) [89, 90]. Recent work of Guichard *et al.* has demonstrated the tolerability of PEGylated rhDNase in short and long term toxicity studies in mice [13]. These results are promising; however, further in-depth studies in bigger rodents and non-rodent species such as rats and dogs, respectively, are warranted [91, 92].

One considerable advantage for PEGylated rhDNase is the availability of data from the development of dornase alfa (Pulmozyme®) which would save lots of efforts in designing the trials. It is also more straightforward to keep the same formulation and target the same population of patients with CF, those with a forced vital capacity (FVC) ≥ 40% of predicted.

CF is a rare disease with a prevalence of 7.97/100 000 in the USA and 7.37/100 000 in Europe and the United States [93]. The total number of patients based on the current population is around 55,000 and 26,000 in Europe and USA respectively. The low number of patients, presence of underlying comorbidities, and competing clinical trials limit the access to patients and makes conducting multicentric clinical trials across several countries (*e.g.* Europe) almost inevitable. Other difficulties of clinical trials also apply, such as patients' selection and recruitment, randomisation, dropouts, and high costs.

Selecting the right dosage for PEGylated rhDNase might be the most strategic decision. Currently, rhDNase is given once or twice a day using jet or vibrating mesh nebulisers [13]. The longer residence time of PEGylated rhDNase in the lungs could translate into using lower doses or less frequent inhalations. Using less frequent inhalations such as once weekly, would be more beneficial to patients provided the same efficacy is demonstrated in humans. Opting for reduced daily doses of PEGylated rhDNase might not be the best option as patients might stick to current dornase alfa therapy.

The efficacy study of PEG30-rhDNase in mice showed that the frequency of administration could be reduced to once per week [13]. Pursuing this avenue, it would be more straightforward to keep the same formulation and delivery method as the current rhDNase.

Depending on the devices, the administration process takes from 3-10 min for the delivery of a dose of 2.5 mg at 1 mg/ml [94]. Because of the good solubility of rhDNase and PEG30-rhDNase (at least 15-20 mg/ml), formulating more concentrated solutions would reduce the solution volumes and therefore the nebulisation time. However, because of the dead volume in most nebulisers (up to 100 µl), using very low volumes is to be avoided. Decreasing the delivery volume to less than 100 µl will open doors to using multidose devices [95]. Respimat®, for instance, has a capacity of 15 µl [96]; therefore, a single inhalation could deliver the daily dose of PEG30-rhDNase, considering using 20% of the current rhDNase dose and a PEG30-rhDNase solution of 30 mg/ml instead of 1 mg/ml. Using less concentrated solutions and several puffs in a single session or multiple daily doses will not be a problem because of the ease of administration by such a device. The problem with multidose systems is that they require using preservatives that are safe for the

lungs and compatible with the proteins [95] as well as assuring the protein stability at high concentrations.

Dry powder inhalers (DPI) are more convenient and portable, and the formulations are more stable in general [35]. However, these latter are device-specific and more challenging to formulate, which may add more barriers to fast clinical development [95]. DPI are not recommended for frail patients, not desired by some patients, and not adapted to emergencies. Moreover, dry powders formulation has been tested for rhDNase by spray-drying with and without lactose [97]. However, in the presence of lactose, the powder tends to crystallise affecting its dispersibility [97].

IV.REFERENCE

1. Walsh, G., *Biopharmaceutical benchmarks 2014*. Nature Biotechnology, 2014. **32**(10): p. 992-1000.
2. Walsh, G., *Biopharmaceutical benchmarks 2018*. Nat Biotechnol, 2018. **36**(12): p. 1136-1145.
3. Carter, P.J. and G.A. Lazar, *Next generation antibody drugs: pursuit of the 'high-hanging fruit'*. Nature Reviews Drug Discovery, 2018. **17**(3): p. 197-223.
4. Haslam, P.L. and R.P. Baughman, *Report of ERS Task Force: guidelines for measurement of acellular components and standardization of BAL*. Eur Respir J, 1999. **14**(2): p. 245-8.
5. Guichard, M.J., et al., *Impact of PEGylation on the mucolytic activity of recombinant human deoxyribonuclease I in cystic fibrosis sputum*. Clin Sci (Lond), 2018. **132**(13): p. 1439-1452.
6. Kilbourn, J.P., *Composition of sputum from patients with cystic fibrosis*. Current Microbiology, 1984. **11**(1): p. 19-22.
7. Sanders, N.N., et al., *Role of magnesium in the failure of rhDNase therapy in patients with cystic fibrosis*. 2006. **61**(11): p. 962-966.
8. Cantin, A.M., et al., *Polyethylene glycol conjugation at Cys232 prolongs the half-life of alpha1 proteinase inhibitor*. Am J Respir Cell Mol Biol, 2002. **27**(6): p. 659-65.
9. Koussoroplis, S.J., et al., *PEGylation of antibody fragments greatly increases their local residence time following delivery to the respiratory tract*. Journal of Controlled Release, 2014. **187**: p. 91-100.
10. Patil, H.P., et al., *Fate of PEGylated antibody fragments following delivery to the lungs: Influence of delivery site, PEG size and lung inflammation*. Journal of Controlled Release, 2018. **272**: p. 62-71.
11. Freches, D., et al., *PEGylation prolongs the pulmonary retention of an anti-IL-17A Fab' antibody fragment after pulmonary delivery in three different species*. Int J Pharm, 2017. **521**(1-2): p. 120-129.
12. Guichard, M.J., et al., *Production and characterization of a PEGylated derivative of recombinant human deoxyribonuclease I for cystic fibrosis therapy*. International Journal of Pharmaceutics, 2017. **524**(1-2): p. 159-167.
13. Guichard, M.J., et al., *PEGylation of recombinant human deoxyribonuclease I provides a long-acting version of the mucolytic for patients with cystic fibrosis (Submitted)*.
14. Wanner, A., M. Salathé, and T.G. O'Riordan, *Mucociliary clearance in the airways*. Am J Respir Crit Care Med, 1996. **154**(6 Pt 1): p. 1868-902.
15. Kirch, J., et al., *Mucociliary clearance of micro- and nanoparticles is independent of size, shape and charge--an ex vivo and in silico approach*. J Control Release, 2012. **159**(1): p. 128-34.
16. Hastings, R.H., H.G. Folkesson, and M.A. Matthay, *Mechanisms of alveolar protein clearance in the intact lung*. American Journal of Physiology-Lung Cellular and Molecular Physiology, 2004. **286**(4): p. L679-L689.
17. Rogers, D.F., *Physiology of airway mucus secretion and pathophysiology of hypersecretion*. Respiratory Care, 2007. **52**(9): p. 1134-1149.
18. Whitsett, J.A., *Airway Epithelial Differentiation and Mucociliary Clearance*. Annals of the American Thoracic Society, 2018. **15**(Suppl 3): p. S143-S148.
19. Fee, C.J., *Protein conjugates purification and characterization*, in *PEGylated Protein Drugs: Basic Science and Clinical Applications*, F.M. Veronese, Editor. 2009, Birkhäuser Basel: Basel. p. 113-125.
20. Pasut, G. and F.M. Veronese, *Polymer-drug conjugation, recent achievements and general strategies*. Progress in Polymer Science, 2007. **32**(8-9): p. 933-961.
21. Rubin, B.K., *Mucus structure and properties in cystic fibrosis*. Paediatr Respir Rev, 2007. **8**(1): p. 4-7.
22. Cingolani, E., et al., *In vitro investigation on the impact of airway mucus on drug dissolution and absorption at the air-epithelium interface in the lungs*. Eur J Pharm Biopharm, 2019. **141**: p. 210-220.
23. Braeckmans, K., et al., *Three-Dimensional Fluorescence Recovery after Photobleaching with the Confocal Scanning Laser Microscope*. Biophysical Journal, 2003. **85**(4): p. 2240-2252.
24. Button, B., et al., *A periciliary brush promotes the lung health by separating the mucus layer from airway epithelia*. Science, 2012. **337**(6097): p. 937-41.
25. Kirch, J., et al., *Optical tweezers reveal relationship between microstructure and nanoparticle penetration of pulmonary mucus*. 2012. **109**(45): p. 18355-18360.
26. Todoroff, J. and R. Vanbever, *Fate of nanomedicines in the lungs*. Current Opinion in Colloid & Interface Science, 2011. **16**(3): p. 246-254.
27. Sanders, N., et al., *Extracellular barriers in respiratory gene therapy*. Adv Drug Deliv Rev, 2009. **61**(2): p. 115-27.

28. Tandel, H., K. Florence, and A. Misra, *9 - Protein and Peptide Delivery through Respiratory Pathway*, in *Challenges in Delivery of Therapeutic Genomics and Proteomics*, A. Misra, Editor. 2011, Elsevier: London. p. 429-479.
29. Patton, J.S., C.S. Fishburn, and J.G. Weers, *The lungs as a portal of entry for systemic drug delivery.* Proc Am Thorac Soc, 2004. **1**(4): p. 338-44.
30. Gould, J.C., et al., *Bioavailability of protein therapeutics in rats following inhalation exposure: Relevance to occupational exposure limit calculations.* Regulatory Toxicology and Pharmacology, 2018. **100**: p. 35-44.
31. Pfister, T., et al., *Bioavailability of Therapeutic Proteins by Inhalation-Worker Safety Aspects.* Annals of Occupational Hygiene, 2014. **58**(7): p. 899-911.
32. Patton, J.S., *Mechanisms of macromolecule absorption by the lungs.* Advanced Drug Delivery Reviews, 1996. **19**(1): p. 3-36.
33. Niven, R.W., et al., *The pulmonary absorption of aerosolized and intratracheally instilled rhG-CSF and monoPEGylated rhG-CSF.* Pharm Res, 1995. **12**(9): p. 1343-9.
34. McLeod, V.M., et al., *Optimal PEGylation can improve the exposure of interferon in the lungs following pulmonary administration.* J Pharm Sci, 2015. **104**(4): p. 1421-30.
35. Mahri, S., et al., *Biodistribution and elimination pathways of PEGylated recombinant human deoxyribonuclease I after pulmonary delivery in mice (Submitted).*
36. Mathia, N.R., et al., *Permeability characteristics of calu-3 human bronchial epithelial cells: in vitro-in vivo correlation to predict lung absorption in rats.* J Drug Target, 2002. **10**(1): p. 31-40.
37. Matsukawa, Y., et al., *Size-Dependent Dextran Transport across Rat Alveolar Epithelial Cell Monolayers.* Journal of Pharmaceutical Sciences, 1997. **86**(3): p. 305-309.
38. Konstan, M.W. and F. Ratjen, *Effect of dornase alfa on inflammation and lung function: potential role in the early treatment of cystic fibrosis.* J Cyst Fibros, 2012. **11**(2): p. 78-83.
39. Laskin, D.L., R. Malaviya, and J.D. Laskin, *Pulmonary Macrophages*, in *Comparative biology of the normal lung*. 2015.
40. Lombry, C., et al., *Alveolar macrophages are a primary barrier to pulmonary absorption of macromolecules.* Am J Physiol Lung Cell Mol Physiol, 2004. **286**(5): p. L1002-8.
41. Berthiaume, Y., et al., *Protein clearance from the air spaces and lungs of unanesthetized sheep over 144 h.* 1989. **67**(5): p. 1887-1897.
42. Freches, D., et al., *Preclinical evaluation of topically-administered PEGylated Fab' lung toxicity.* Int J Pharm X, 2019. **1**: p. 100019.
43. Crowell, R.E., et al., *Alveolar and interstitial macrophage populations in the murine lung.* Exp Lung Res, 1992. **18**(4): p. 435-46.
44. Stone, K.C., et al., *Allometric relationships of cell numbers and size in the mammalian lung.* Am J Respir Cell Mol Biol, 1992. **6**(2): p. 235-43.
45. Haley, P.J., et al., *Comparative morphology and morphometry of alveolar macrophages from six species.* 1991. **191**(4): p. 401-407.
46. Takano, M., et al., *Receptor-mediated endocytosis of macromolecules and strategy to enhance their transport in alveolar epithelial cells.* Expert Opin Drug Deliv, 2015. **12**(5): p. 813-25.
47. Livesey, G. and K.E. Williams, *Rates of pinocytic capture of simple proteins by rat yolk sacs incubated in vitro.* Biochem J, 1981. **198**(3): p. 581-6.
48. Yamamoto, T., et al., *Interaction of poly(ethylene glycol)-conjugated phospholipids with supported lipid membranes and their influence on protein adsorption.* Science and Technology of Advanced Materials, 2016. **17**(1): p. 677-684.
49. Shire, S.J., *Stability characterization and formulation development of recombinant human deoxyribonuclease I [Pulmozyme, (dornase alpha)].* Pharm Biotechnol, 1996. **9**: p. 393-426.
50. Chen, B., et al., *Influence of calcium ions on the structure and stability of recombinant human deoxyribonuclease I in the aqueous and lyophilized states.* J Pharm Sci, 1999. **88**(4): p. 477-82.
51. Baumann, A., et al., *Pharmacokinetics, metabolism and distribution of PEGs and PEGylated proteins: quo vadis?* Drug Discovery Today, 2014. **19**(10): p. 1623-1631.
52. Parton, T., et al., *P-0167: The PEG Moiety of Certolizumab Pegol is Rapidly Cleared From the Blood of Humans by the Kidneys Once it is Cleaved From the Fab'.* Inflammatory Bowel Diseases, 2009. **15**(suppl_2): p. S56-S56.
53. Longley, C.B., et al., *Biodistribution and excretion of radiolabeled 40 kDa polyethylene glycol following intravenous administration in mice.* Journal of Pharmaceutical Sciences, 2013. **102**(7): p. 2362-2370.

54. Parton, T., et al., *P068 Investigation of the Distribution and Elimination of the PEG Component of Certolizumab Pegol in Rats.* Journal of Crohn's and Colitis Supplements, 2008. **2**(1): p. 26-26.
55. Kozlowski, A., S.A. Charles, and J.M. Harris, *Development of pegylated interferons for the treatment of chronic hepatitis C.* BioDrugs, 2001. **15**(7): p. 419-29.
56. Fletcher, A.M., et al., *Adverse vacuolation in multiple tissues in cynomolgus monkeys following repeat-dose administration of a PEGylated protein.* Toxicology Letters, 2019. **317**: p. 120-129.
57. Caliceti, P. and F.M. Veronese, *Pharmacokinetic and biodistribution properties of poly(ethylene glycol)-protein conjugates.* Advanced Drug Delivery Reviews, 2003. **55**(10): p. 1261-1277.
58. Zbyszynski, P., et al., *Probing the subcutaneous absorption of a PEGylated FUD peptide nanomedicine via in vivo fluorescence imaging.* Nano Convergence, 2019. **6**.
59. Nanda, J.S. and J.R. Lorsch, *Chapter Eight - Labeling a Protein with Fluorophores Using NHS Ester Derivitization*, in *Methods in Enzymology*, J. Lorsch, Editor. 2014, Academic Press. p. 87-94.
60. Lazarus, R.A. and J.S. Wagener†, *Recombinant Human Deoxyribonuclease I*, in *Pharmaceutical Biotechnology: Fundamentals and Applications*, D.J.A. Crommelin, R.D. Sindelar, and B. Meibohm, Editors. 2019, Springer International Publishing: Cham. p. 471-488.
61. Tibbitts, J., et al., *Key factors influencing ADME properties of therapeutic proteins: A need for ADME characterization in drug discovery and development.* Mabs, 2016. **8**(2): p. 229-245.
62. Lee, Y., et al., *Poly(ethylene oxide sulfide): New Poly(ethylene glycol) Derivatives Degradable in Reductive Conditions.* Biomacromolecules, 2005. **6**(1): p. 24-26.
63. Lundberg, P., et al., *Poly[(ethylene oxide)-co-(methylene ethylene oxide)]: A hydrolytically degradable poly(ethylene oxide) platform.* ACS Macro Letters, 2012. **1**(11): p. 1240-1243.
64. Dingels, C., et al., *Universal Concept for the Implementation of a Single Cleavable Unit at Tunable Position in Functional Poly(ethylene glycol)s.* Biomacromolecules, 2013. **14**(2): p. 448-459.
65. Wang, J., et al., *Monodisperse and Polydisperse PEGylation of Peptides and Proteins: A Comparative Study.* Biomacromolecules, 2020.
66. Knorr, V., et al., *An Acetal-Based PEGylation Reagent for pH-Sensitive Shielding of DNA Polyplexes.* Bioconjugate Chemistry, 2007. **18**(4): p. 1218-1225.
67. Sun, K.H., Y.S. Sohn, and B. Jeong, *Thermogelling Poly(ethylene oxide-b-propylene oxide-b-ethylene oxide) Disulfide Multiblock Copolymer as a Thiol-Sensitive Degradable Polymer.* Biomacromolecules, 2006. **7**(10): p. 2871-2877.
68. Pelegri-O'Day, E.M., E.-W. Lin, and H.D. Maynard, *Therapeutic Protein–Polymer Conjugates: Advancing Beyond PEGylation.* Journal of the American Chemical Society, 2014. **136**(41): p. 14323-14332.
69. Yang, L., et al., *Three-dimensional quantitative co-mapping of pulmonary morphology and nanoparticle distribution with cellular resolution in non-dissected murine lungs.* ACS Nano, 2019. **13**(2): p. 1029-1041.
70. Xu, X., et al., *Multimodal non-linear optical imaging for label-free differentiation of lung cancerous lesions from normal and desmoplastic tissues.* Biomed Opt Express, 2013. **4**(12): p. 2855-68.
71. Detampel, P., et al., *In vivo clearance of nanoparticles by transcytosis across alveolar epithelial cells.* PloS one, 2019. **14**(9): p. e0223339-e0223339.
72. Thiberville, L., et al., *Human in vivo fluorescence microimaging of the alveolar ducts and sacs during bronchoscopy.* 2009. **33**(5): p. 974-985.
73. Meyerholz, D.K., et al., *9 - Respiratory System*, in *Comparative Anatomy and Histology (Second Edition)*, P.M. Treuting, S.M. Dintzis, and K.S. Montine, Editors. 2018, Academic Press: San Diego. p. 147-162.
74. Phillips, J.E., *Inhaled efficacious dose translation from rodent to human: A retrospective analysis of clinical standards for respiratory diseases.* Pharmacology & Therapeutics, 2017. **178**: p. 141-147.
75. Fernandes, C.A. and R. Vanbever, *Preclinical models for pulmonary drug delivery.* Expert Opin Drug Deliv, 2009. **6**(11): p. 1231-45.
76. Zhou, Z., et al., *The ENaC-overexpressing mouse as a model of cystic fibrosis lung disease.* J Cyst Fibros, 2011. **10 Suppl 2**: p. S172-82.
77. Laube, B.L., et al., *Effect of rhDNase on airflow obstruction and mucociliary clearance in cystic fibrosis.* Am J Respir Crit Care Med, 1996. **153**(2): p. 752-60.
78. Robinson, M., et al., *Effect of a short course of rhDNase on cough and mucociliary clearance in patients with cystic fibrosis.* Pediatr Pulmonol, 2000. **30**(1): p. 16-24.
79. Kelly, E., C.M. Greene, and N.G. McElvaney, *Targeting neutrophil elastase in cystic fibrosis.* Expert Opin Ther Targets, 2008. **12**(2): p. 145-57.

80. Julie, L., R. Anjali, and H. Dominik, *Neutrophils in cystic fibrosis.* Biological Chemistry, 2016. **397**(6): p. 485-496.
81. Quinn, D.J., S. Weldon, and C.C. Taggart, *Antiproteases as therapeutics to target inflammation in cystic fibrosis.* The open respiratory medicine journal, 2010. **4**: p. 20-31.
82. Lopes-Pacheco, M., *CFTR Modulators: The Changing Face of Cystic Fibrosis in the Era of Precision Medicine.* Front Pharmacol, 2019. **10**: p. 1662.
83. Guimbellot, J., J. Sharma, and S.M. Rowe, *Toward inclusive therapy with CFTR modulators: Progress and challenges.* Pediatr Pulmonol, 2017. **52**(S48): p. S4-S14.
84. Mospan, C., et al., *Drug updates and approvals: 2018 in review.* Nurse Practitioner, 2018. **43**(12): p. 23-32.
85. Voelker, R., *Patients With Cystic Fibrosis Have New Triple-Drug Combination.* JAMA, 2019. **322**(21): p. 2068.
86. Mogayzel, P.J., Jr., et al., *Cystic fibrosis pulmonary guidelines. Chronic medications for maintenance of lung health.* Am J Respir Crit Care Med, 2013. **187**(7): p. 680-9.
87. DeSimone, E., et al., *Cystic Fibrosis Update on Treatment Guidelines and New Recommendations.* Us Pharmacist, 2018. **43**(5): p. 16-21.
88. Guichard, M.J., T. Leal, and R. Vanbever, *PEGylation, an approach for improving the pulmonary delivery of biopharmaceuticals.* Current Opinion in Colloid & Interface Science, 2017. **31**: p. 43-50.
89. Klonne, D.R., et al., *Two-week aerosol inhalation study on polyethylene glycol (PEG) 3350 in F-344 rats.* Drug Chem Toxicol, 1989. **12**(1): p. 39-48.
90. Forbes, B., et al., *Challenges for inhaled drug discovery and development: Induced alveolar macrophage responses.* Adv Drug Deliv Rev, 2014. **71**: p. 15-33.
91. Guichard, M.J., *Development of a long-acting version of recombinant human deoxyribonuclease i for the treatment of cystic fibrosis lung disease*, in *Biomedical and Pharmaceutical Sciences*. 2018, Université catholique de Louvain.
92. *European Medicines Agency, ICH guideline M3(R2) on non-clinical safety studies for the conduct of human clinical trials and marketing authorisation for pharmaceuticals.* Int. Conf.Harmon. 3 (2009) 25.
93. Farrell, P.M., *The prevalence of cystic fibrosis in the European Union.* Journal of Cystic Fibrosis, 2008. **7**(5): p. 450-453.
94. Sawicki, G.S., et al., *Randomized trial of efficacy and safety of dornase alfa delivered by eRapid nebulizer in cystic fibrosis patients.* J Cyst Fibros, 2015. **14**(6): p. 777-83.
95. Clark, A.R., C.L. Stevenson, and S.J. Shire, *Formulation of Proteins for Pulmonary Delivery*, in *Protein Formulation and Delivery*, E. McNally and J. Hastedt, Editors. 2008, Boca Raton: CRC Press.
96. Fonceca, A.M., et al., *16 - Drug Administration by Inhalation in Children*, in *Kendig's Disorders of the Respiratory Tract in Children (Ninth Edition)*, R.W. Wilmott, et al., Editors. 2019, Content Repository Only!: Philadelphia. p. 257-271.e3.
97. Chan, H.-K. and I. Gonda, *Solid state characterization of spray-dried powders of recombinant human deoxyribonuclease (RhDNase).* 1998. **87**(5): p. 647-654.

SUPPLEMENTARY MATERIAL

The stability of rhDNase and PEG30-rhDNase was assessed in the presence of commercial porcine lung surfactant Poractant alfa (Curosurf™; Chiesi Farmaceutici SpA, Parma, Italy). Solutions of 1% or 5% (v/v) of Poractant alfa in 150 mM NaCl, 1 mM $CaCl_2$ were spiked with rhDNase or PEG30-rhDNase at 2.7 µM (equivalent to 100 µg/ml of rhDNase). Solutions were transferred to 1.5 ml Eppendorfs, sealed, and incubated at 37 °C for 4, 8, 24, 48, or 96 h in a humid chamber. At the end of the incubation time, samples were stored at -20 °C until analysed by MG assay. For this, samples were diluted to a nominal concentration of 5.4 nM (equivalent to 200 ng/ml of rhDNase) in 96 well plate then the assay proceeded as described in chapters II and III.

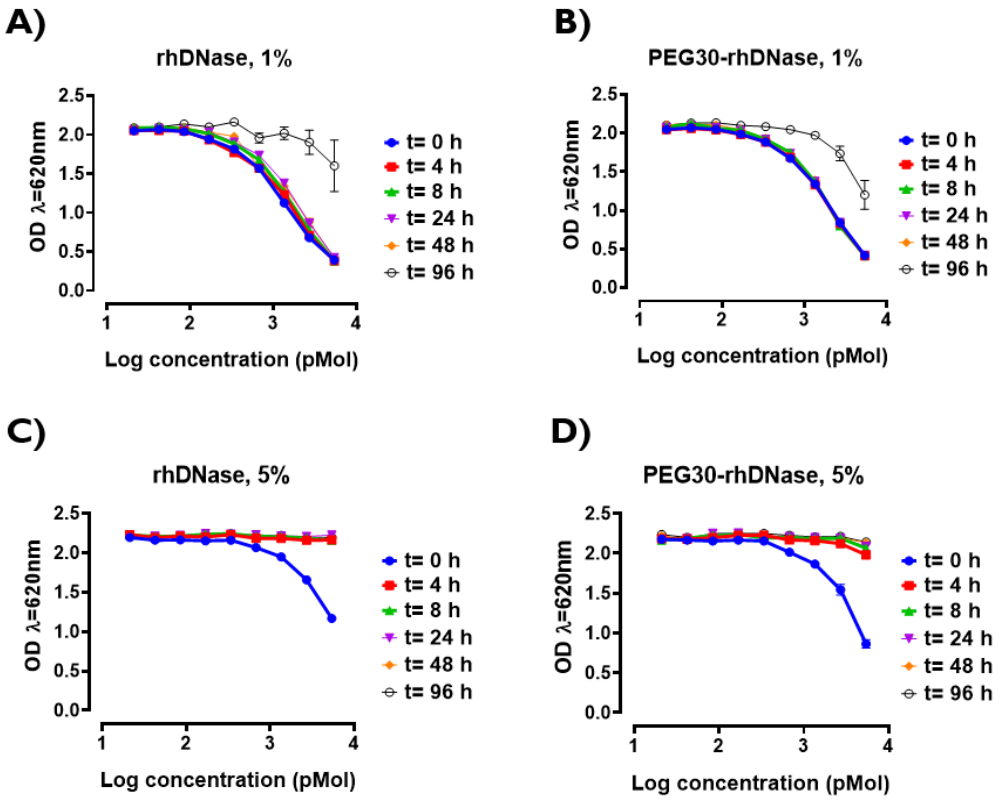

Figure S 1. Stability of rhDNase and PEG30-rhDNase in contact with porcine lung surfactant. rhDNase (A and C) and PEG30-rhDNase (B and D) were incubated for 4, 8, 24, 48, or 96 h at 37 °C in the presence of 1% (A and B) or 5% (C and D) of Poractant alfa (v/v) in 150 mM NaCl, 1 mM $CaCl_2$. The enzymatic activity was assessed by MG assay. Data are expressed as mean ± SEM (n = 3). In the presence of 1% of surfactant, the loss of activity of rhDNase and PEG30-rhDNase was only observed at 96 h and was slightly higher for rhDNase. At 5%, the loss of activity was almost immediate for both rhDNase and PEG30-rhDNase, with this later being slightly less affected at time 0 h. Poractant alfa (Curosurf™) is a modified porcine surfactant preparation; it contains 74 mg/ml of phospholipids, 0.9 mg/ml of low MW hydrophobic proteins, 9 mg /ml of NaCl, and sodium bicarbonate.